Non-Chromate/No VOC Coating System for DoD Applications

WP-1521

Final REPORT

To the SERDP office
by

Naval Air Systems Command, Patuxent River

Army Research Laboratory

University of Connecticut

March 31, 2009

REPORT DOCUMENTATION PAGE

Form Approved
OMB No. 0704-0188

1. REPORT DATE *(DD-MM-YYYY)*	**2. REPORT TYPE**	**3. DATES COVERED** *(From - To)*
03/31/2009	Final Report	01/2005-12/2008

4. TITLE AND SUBTITLE
Non-Chromate/No-VOC Coating System for DOD Applications

5a. CONTRACT NUMBER

5b. GRANT NUMBER

5c. PROGRAM ELEMENT NUMBER

6. AUTHOR(S)
John La Scala
Army Research Laboratory, RDRL-WMM-C
Aberdeen Proving Ground, MD 21005

5d. PROJECT NUMBER
WP-1521

5e. TASK NUMBER

5f. WORK UNIT NUMBER

7. PERFORMING ORGANIZATION NAME(S) AND ADDRESS(ES)
NASC, Patuxent River, ARL,
University of Connecticut

8. PERFORMING ORGANIZATION REPORT NUMBER

9. SPONSORING / MONITORING AGENCY NAME(S) AND ADDRESS(ES)
SERDP
901 N. Stuart Street, Ste 303
Arlington, VA 22203

10. SPONSOR/MONITOR'S ACRONYM(S)

11. SPONSOR/MONITOR'S REPORT NUMBER(S)

12. DISTRIBUTION / AVAILABILITY STATEMENT
Approved for public release.

13. SUPPLEMENTARY NOTES

14. ABSTRACT

15. SUBJECT TERMS

16. SECURITY CLASSIFICATION OF: Unclassified			**17. LIMITATION OF ABSTRACT**	**18. NUMBER OF PAGES**	**19a. NAME OF RESPONSIBLE PERSON** Bruce Sartwell
a. REPORT	**b. ABSTRACT**	**c. THIS PAGE**		208	**19b. TELEPHONE NUMBER** *(include area code)* 703-696-2128

Standard Form 298 (Rev. 8-98)
Prescribed by ANSI Std. Z39.18

Table of Contents

Tables

Figures

List of Acronyms

AAS	atomic absorption spectroscopy
AES	Auger electron spectroscopy
ARL	Army Research Laboratory
CARC	chemical agent resistant coating
CCC	chromate conversion coating
CFP	chromium-free pretreatment
DFT	dry film thickness
DLSME	Defense Land Systems and Miscellaneous Equipment
DMA	dynamic mechanical analysis
DMMP	dimethyl methylphosphonate
DoD	Department of Defense
DSC	differential scanning calorimetry
EDS	energy dispersive spectroscopy
EPA	Environmental Protection Agency
EIS	electrochemical impedance spectroscopy
FIB	focused ion beam
FESEM	field effect scanning electron microscopy
FTIR	Fourier transform infrared (spectroscopy)
HAP	hazardous air pollutant
HBP	hyper-branched polymer
HATE	hydraulic adhesion test equipment
IVD	ion vapor deposition
LC	less corroded
MC	more corroded
NAVAIR	Naval Air Systems Command
NESHAP	National Emissions Standards for Hazardous Air Pollutants
NMR	nuclear magnetic resonance
NSF	neutral salt fog
NSS	neutral salt spray
OCP	open circuit potential
OEM	original equipment manufacturer
OSHA	Occupational Health and Safety Administration
ORR	oxygen reduction reaction
PAA	phosphoric acid anodizing
PEI	polyethyleneimine
PMMA	polymethylmethacrylate
QPL	qualified products list
RRAD	Red River Army Depot
ROI	return-on-investment
SEM	scanning electron microscopy
SERDP	Strategic Environmental Research and Development Program
TCP	trivalent chromium pretreatment
TEA	triethylamine
TGA	thermogravimetric analysis

UHV	ultra-high vacuum
VOC	volatile organic compound
VTR	vapor transfer rate
WTA	wet tape adhesion
XPS	X-ray photoelectron spectroscopy

Executive Summary

This document reports the results of a three year program funded by the Strategic Environmental Research and Development Program (SERDP) to research, develop, and demonstrate military coatings systems that are hexavalent chromium free and use primers and topcoats with ultra low volatile organic compound (VOC) content while maintaining high protection against corrosion and the environment, high durability, high performance, and low cost.

Military coatings systems typically combine a pretreatment system applied directly to the substrate to protect against corrosion and enhance primer adhesion, an organic primer to further protect against corrosion and improve topcoat adhesion, and an organic topcoat to meet survivability and environmental durability requirements. Hexavalent chromium is typically used in the pretreatment or primer of military coatings. OSHA has reduced occupational exposure to hexavalent chromium from 52 $\mu g/m^3$ to 5 $\mu g/m^3$ by 2006 [1], which makes the application, and especially the removal of hexavalent chromium based coatings, extremely costly. Current primers and topcoats typically contain ~1.5-3.5 lbs/gal volatile organic compounds (VOCs). The EPA's Defense Land Systems and Miscellaneous Equipment (DLSME) National Emission Standard will further regulate hazardous air pollutants. As such, it is imperative to reduce VOC contents to nearly zero so that the next generation of military coatings not only have excellent performance, yet also meet or exceed current environmental rules and regulations.

The trivalent chromium process (TCP) is the leading candidate to replace hexavalent chromium pretreatments in the military. Work has been done to modify and improve this process to increase performance and function well on a variety of substrates. Research has been done on the application of TCP to aluminum as a pretreatment and steel substrates as a wash primer. Analysis has indicated that this pretreatment functions through the deposition of chromium(III), zirconium, and zinc onto the surface. Analysis of the chromium deposited indicates that it is in the Cr(III) state rather than the carcinogenic and dangerous Cr(VI) state. Experiments showed that this Cr(III) was very stable and did not form Cr(VI) under normal conditions. However, results showed that it may have been possible to generate Cr(VI) under severely corrosive/oxidizing conditions, but the results were unclear because similar testing of the base metal without the TCP coating also produced Cr(VI) which came from oxidation of Cr deposits within the substrate. Chromium free primers have been used with TCP pretreatments. The results indicate that the performance is good, although not as good as that for chromated systems.

Commercially available zero VOC coatings from Deft have proven very effective for NAVAIR applications. Zero VOC coatings were formulated using standard epoxy monomers and solvated using VOC exempt solvents. These coatings performed well relative to standard Army primers. Powder coat epoxies with no volatile solvents have also been approved for military use. The use of water dispersible topcoats for NAVAIR systems has resulted in lower coating system performance, likely due to an increase in hydrophilicity of the topcoat. Zero VOC powder coat topcoats have not been effective for Army application, failing chemical agent resistance testing and weathering performance. On the other hand, new Zero VOC topcoats have been developed with excellent performance all around. The use of fluorinated additives in Army coatings has potential because they do successfully segregate to the surface and reduce the surface energy, but the existing fluorinated polyols do not have enough environmental stability at the moment. Polymeric bead flattening agents have been applied to all Army topcoats to reduce solvent loading and improve weatherability. New low solar loading pigments have been developed and used to produce excellent coatings with improved weathering performance.

Overall, the program has been successful at both identifying critical DoD environmental needs and developing practical solutions to these requirements for reducing VOC emissions and hexavalent chromium content from military coatings systems. Future work must still be done to further develop these new coatings systems and make them widely applicable to DoD weapons platforms.

Synopsis of the Program

Painting, including conversion coating and primer application and de-painting operations are a significant source of hazardous waste and hazardous emissions for the Department of Defense (DoD) (Figure 1). The environmental impact largely results from exposure to released heavy metal compounds, volatile organic compounds (VOC) and hazardous air pollutants (HAP), which are used in conversion coatings, primers, and topcoat formulations. Traditional coating systems contain hexavalent chromium (Cr(VI) or Cr^{6+}) in both the conversion coating and primer, VOCs/HAPs in both the primer and topcoat and several other heavy metals used for corrosion protection and color. It is estimated that the Navy disposes of 2.3 million pounds of waste related to the coating system for aircraft. That number does not account for any of the associated blast media that becomes hazardous waste after it has come in contact with the hexavalent chromium compounds. Additionally, the other services of the military and other DoD agencies dispose of large amounts of coating related waste each year.

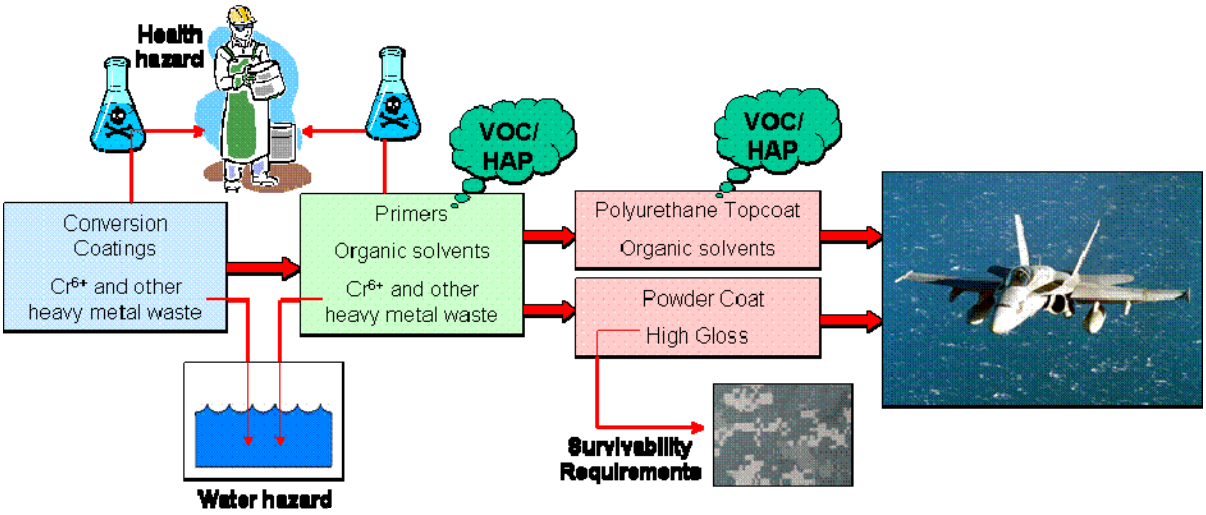

Figure 1: Sources of hazardous waste/emissions in painting operations.

Section 112 of the Clean Air Act allows the Environmental Protection Agency (EPA) to establish emissions limits for specific chemicals through National Emissions Standards for Hazardous Air Pollutants (NESHAP). Furthermore, state agencies have the authority to make these limitations more severe. Section 307 of the Clean Water Act defines a list of 126 priority pollutants for which the EPA must establish water-quality criteria and effluent limitations. OSHA has also proposed to reduce occupational exposure to hexavalent chromium from 52 $\mu g/m^3$ to 5 $\mu g/m^3$ by 2006, which makes the application, and especially the removal of hexavalent chromium based coatings, extremely costly. The high DoD corrosion costs ($10-20 billion annually [2]) are compounded by the pressure to reduce VOC levels to a maximum of 25 g/L for the coating system and the EPA's upcoming Defense Land Systems and Miscellaneous Equipment (DLSME) National Emission Standard to further regulate hazardous air pollutants [3]. It is imperative to maintain and improve the coating systems overall performance, while making it more environmentally friendly. This is especially important since many of the coatings being utilized as chromium and cadmium alternatives depend on enhanced corrosion protection from other coatings in the system.

The technical objectives of this program were to research, develop, and demonstrate chromate-free coating systems with near zero VOC primers and topcoats with high performance to meet new environmental standards as well as meet the high performance required of military coatings. Specifically, the objectives of this program are threefold:

1) Evaluate **combinations of chrome-free conversion coatings and primers** to maintain high corrosion resistance and good physical properties.

2) Develop and evaluate **coatings systems that have near zero VOC (< 25 g/L) and no HAP** emissions by replacing VOC/HAP solvents with chemicals non-listed on the EPA TRI list, while improving performance through the use of nanoparticles and high reflectance pigments to improve barrier properties and durability.

3) Develop and evaluate **environmentally friendly coating alternatives** (laboratory and commercial scale, including in-house and outsourced formulations) ***as a complete system*** with regard to various performance criteria.

As a result, this program researched and developed a number of pretreatments, primers, and topcoat systems that will provide a pallet of high performance, environmentally friendly military coatings systems. To do this, research and development was conducted in a number of areas:

Further development and optimization of the NAVAIR chromium-free process (CFP) and the trivalent chromium process (TCP), which are currently undergoing field-testing on Naval, Marine Corp and Army assets, was performed. Combinations of non-chromate pretreatments and primers were evaluated for performance and corrosion prevention. Additionally, coating characterization was carried out with electrical impedance spectroscopy (EIS) to help predict service life performance of the coating system and correlate the experimental data with data collected from beach front, carrier deck, and accelerated chamber evaluations such as salt fog (cyclic, neutral, and acidified) exposure.

Low VOC primers were formulated using recently exempt solvents, such as t-butyl acetate and were modified to include nanoparticles to enhance barrier properties. A modified urethane primer was also investigated that included nanoparticles to provide longer recoat times with improved barrier properties. Hydroxyl functional urethanes were utilized with water dispersible isocyanates allowing the use of water as a viscosity-reducing solvent. In order to enhance durability, minimize repainting, and reduce solvent emission, a new class of high reflectance pigments was explored. The pigments, which are stable and inert mixed metal oxides, provide excellent near-IR reflection while appearing visibly identical to conventional pigments and providing optimal durability.

Lastly, the chromate-free pretreatment/primer combinations down-selected from the early stage of the project were paired with low VOC, no HAP topcoats developed from this effort and these integrated systems were characterized and evaluated as a whole for performance, corrosion resistance, survivability requirements, and affordability.

In conjunction with efforts to pursue spray technologies meeting the criteria outlined above, alternate technologies to liquid spray coats, including but not limited to powder coats, were explored for suitability to military applications.

Once coating systems were identified, individual components often needed optimization for compatibility with other coating components and performance on specific substrates, which include but are not limited to aluminum and light metal finishing, ferrous alloys, sacrificial coatings, and anodized systems. It is important the environmentally friendly coatings systems not only protect against corrosion, but also can be applied and removed with current equipment, maintain or improve durability, chemical agent resistance, flexibility, environmental resistance, survivability, and reduce or maintain overall cost. Using ARL's and NAVAIR's close relationships with paint companies and respective commodity management authority, successful technologies can be quickly transitioned to benefit the entire DoD community.

These objectives were carried out using the process shown in Figure 2 and Figure 3. The first task was to research, understand, and develop candidate chrome free and near zero VOC, no HAP coatings systems. The second task was to evaluate the performance of the coatings developed in Task 1 relative to commercial paint systems and military specifications. This task served to create a down-select of high performance coating systems for economic evaluation. The third task was to evaluate the potential environmental and cost impact of switching to these candidate systems relative to current commercial systems. This program began with focus mainly on Task 1 and some on Task 2. Tasks 3 and 4 occur intermittently throughout the project.

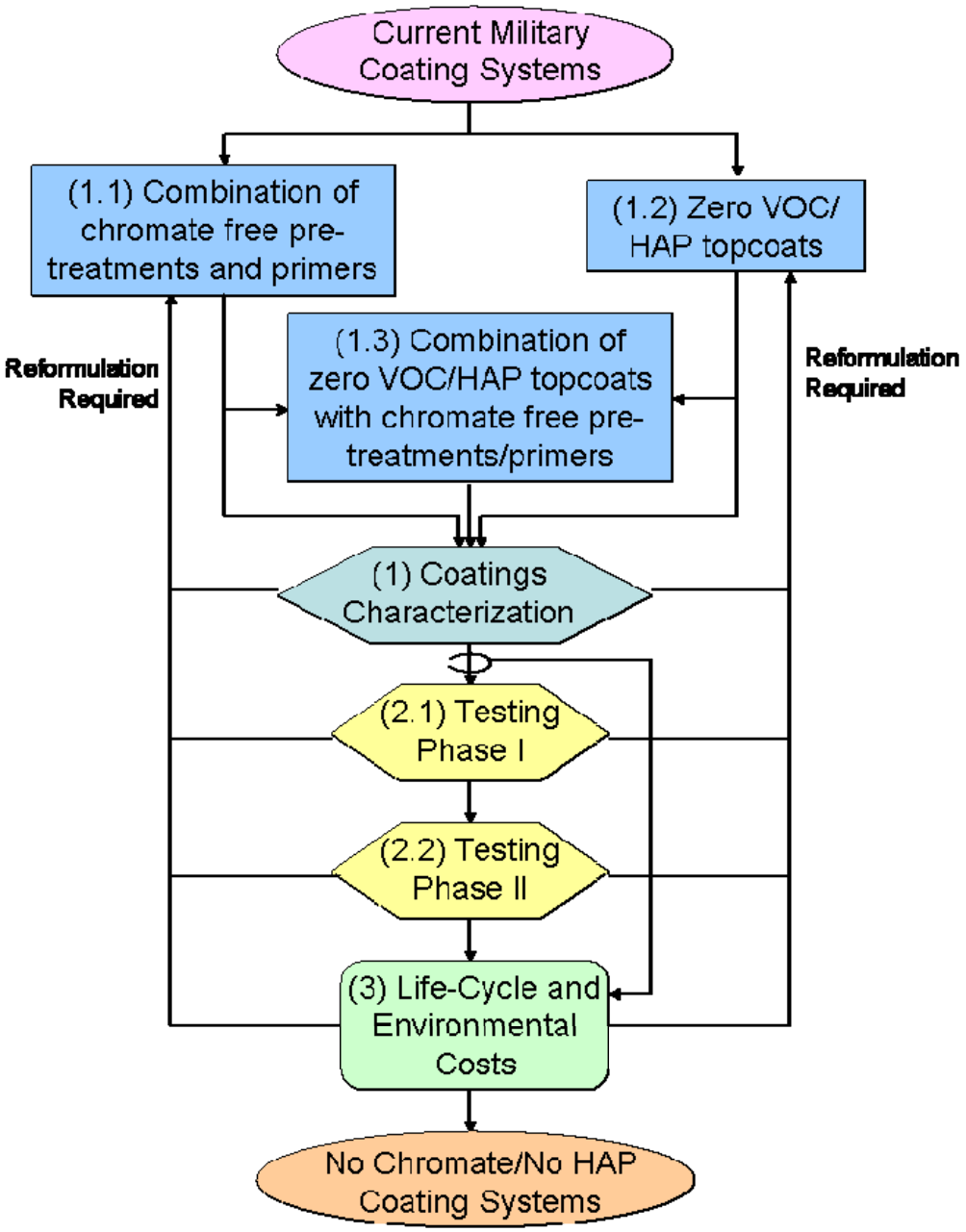

Figure 2: Flow chart of general approach for developing environmental solutions to coatings systems as a complete system. Task 4 - Reporting encompassed all tasks.

Figure 3: Project activities.

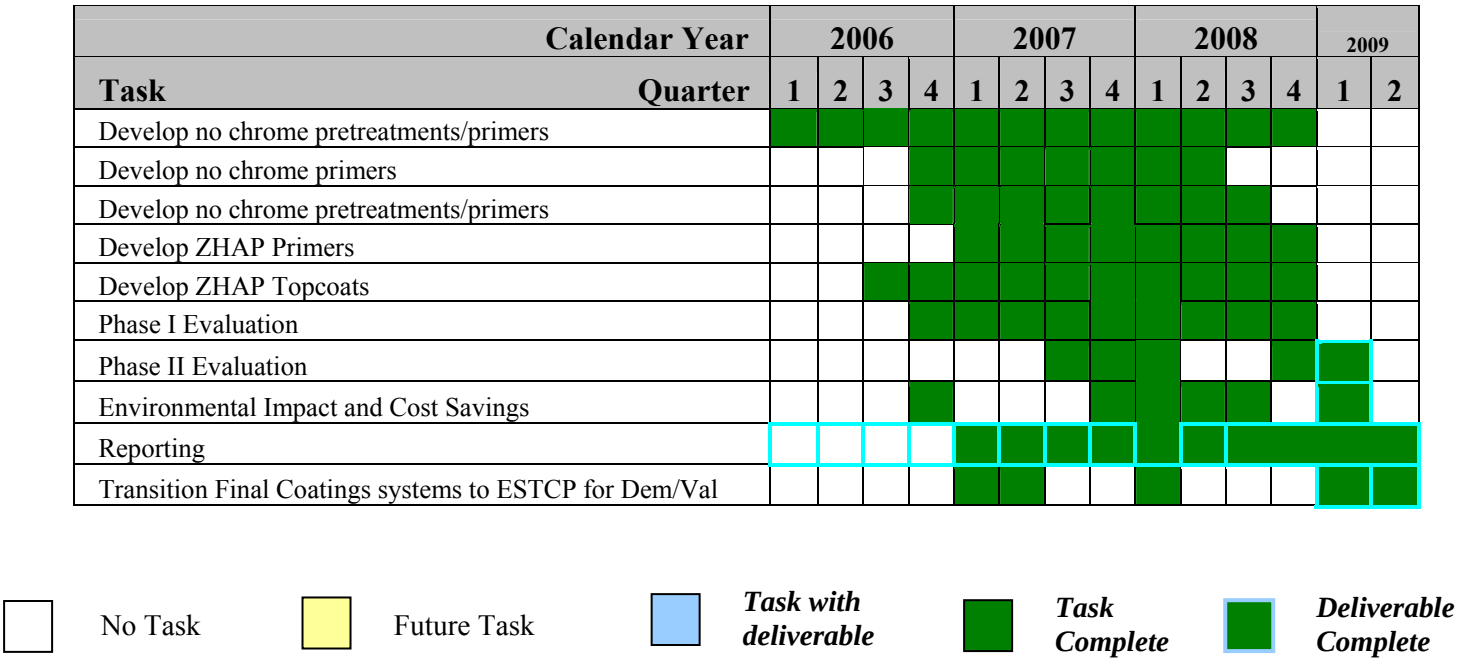

The research team was made up of researchers from government and academia with expertise in pretreatments, coating formulation, coating testing and evaluation, analytical chemistry, polymer science, rheology, cure kinetics, and polymer property testing and evaluation. Table 1 shows the primary team members and contributors to the effort.

Table 1: No Chromate, low VOC coatings team members.

Organization	Team Members	Activities
U. S. Army Research Laboratory (ARL)	John J. La Scala, Ph.D. Chem. Eng. (PI) Felicia Levine, Chemist John A. Escarsega, Coatings Team Leader Brian E. Placzankis, Corrosion Engineer Christopher E. Miller, Corrosion Engineer Kevin Andrews, Chem. Eng. Keith Fahnestock, Drexel COOP Student Faye R. Toulan, Chemist, Adhesion expert Nicholas Nesteruk, Chemist, Formulator	Evaluate low VOC, zero HAP primers and topcoats.
NAVAIR	Bill Nickerson, Materials Engineer Amy Hilgeman, Chemist Julia Barnes, Chemist Craig Price, PhD, Chemist Craig Matzdorf, Senior Corrosion Engineer Rachel Naumann, Graduate Chemistry Student Luwam Hagos, Undergraduate Chemistry Student	Evaluate combinations of Cr(VI) free pretreatments and primers for corrosion protection of various military metal alloys.
University of Connecticut Department of Chemistry	Steven L. Suib, Professor of Chemistry (co-PI) William Willis, Ph.D. Research Professor Zhenxin Liu, graduate student Aparna Iyer, graduate student Samuel Freuh, graduate student Vincent Crisostomo, Postdoc	Employ instrumental analysis to characterize coatings properties.

TECHNICAL PROGRESS

1 Introduction

1.1 Military Coatings Background

Military weapon systems are coated for a variety of reasons. In addition to aesthetic appearance, the coating system must provide countermeasures to satisfy demanding military mission requirements in terms of camouflage, chemical warfare agent resistance, electrical grounding, and electromagnetic shielding. Clearly the most important contribution of the coatings system is protection of these assets from environmental degradation, including corrosion. The annual cost of corrosion in the US and DoD is approximately $250B and $10B, respectively.

A military coating system typically consists of an inorganic pretreatment, an epoxy primer, and a polyurethane topcoat (Figure 4). The pretreatment is applied directly to the substrate to protect against corrosion and provide primer adhesion. An organic primer is used to further protect against corrosion and promote topcoat adhesion. The organic topcoat must meet survivability and environmental durability requirements. The pretreatment is primarily inorganic in nature and on the order of only 0.5 microns thick. Primers are typically slightly less than 1 mil thick, while topcoats are typically ~2.5 mils thick.

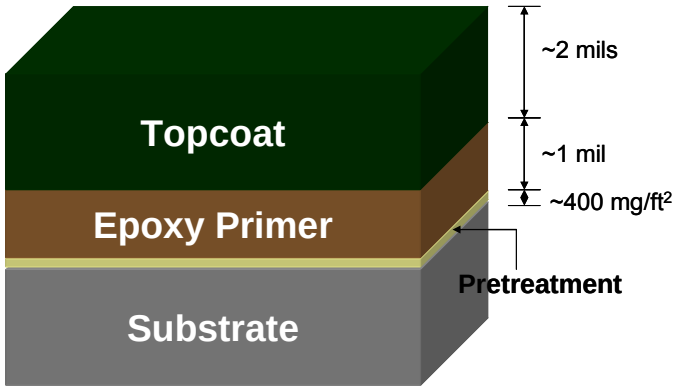

Figure 4: Typical military coatings systems consist of an inorganic pretreatment, an epoxy primer, and a polyurethane topcoat

Table 2 lists specifications for commonly used pretreatments, primers, and topcoats used for military hardware. The goal of the surface pretreatment is to provide corrosion resistance and promote adhesion of the subsequent organic coatings. Epoxy primers are cured with polyamides or amines and formulated with corrosion inhibiting pigments for maximum performance. The primers are designed to wet the surface, provide adhesion, and inhibit corrosion. A high solids polyurethane topcoat is applied to the primer surface for further environmental protection and to provide desired optical properties. The coating system as a whole acts to meet protection and mission requirements.

Table 2: Military coatings specifications.

MIL-SPEC	Ownership	Description
TT-C-490	ARL	Cleaning methods - ferrous surfaces, pretreatments for organic coatings
TT-P-2756	NAVAIR	Polyurethane coating: Self-priming topcoat, low VOC
TT-P-2760	NAVAIR	Primer coating: Polyurethane, elastomeric, high solids
MIL-PRF-23377	NAVAIR	Primer coating: Epoxy, high solids
MIL-P-53022	ARL	Primer coating: Epoxy, corrosion inhibiting, lead and chromate free
MIL-P-53030	ARL	Primer coating: Epoxy, water reducible, lead and chromate free
MIL-PRF-85582	NAVAIR	Primer coating: Epoxy, waterborne
MIL-PRF-22750	NAVAIR	Coating: Epoxy, high solids
MIL-C-46168	ARL	Coating: Aliphatic 2-component Polyurethane, CAR (CANCELED)
MIL-DTL-53039	ARL	Coating: Aliphatic 1-component Polyurethane, CAR
MIL-DTL-64159	ARL	Coating: Aliphatic 2-component Polyurethane, water dispersible, CAR
MIL-PRF-85285	NAVAIR	Coating: Polyurethane, aircraft and support equipment

1.2 Need to Reduce Hexavalent Chromium Content

1.2.1 USES OF HEXAVALENT CHROMIUM

Current conversion coatings utilize hexavalent chromium for corrosion protection. Aluminum alloys such as 2024-T3, 7075-T6, and 6061-T6 are often sprayed, dipped, or wiped with a conversion coating prior to being primed. The conversion coating enhances adhesion as well as provides protection to the metal when the paint system becomes damaged. However, hexavalent chromium is an EPA priority pollutant and a known carcinogen. Cr(VI) is highly soluble and exists in solution as hydrochromate ($HCrO_4^-$), chromate (CrO_4^-), and dichromate ($Cr_2O_7^-$) ions. The goal of remediation schemes is to reduce the carcinogenic, soluble, and mobile Cr(VI) to less toxic and less mobile trivalent Cr(III), which forms insoluble precipitates. Successful removal of Cr(VI) hinges upon the formation and stability of Cr(III) precipitates. Due to its widespread industrial use, Cr(VI) is often found in contaminated groundwater along with complex mixtures of pollutants. OSHA is currently proposing an order of magnitude reduction in the allowable personnel exposure limits [1] thus making the use of Cr(VI) extremely expensive.

From a performance aspect, Cr(VI) provides excellent corrosion protection until it has all been converted to another chromium species, at which point the corrosion protection capabilities suffer. Cr^{6+} is used everywhere that self-healing corrosion protection is required. It is also used to ensure good adhesion for paints and adhesives. For metal finishing (apart from their use in paints and primers) the primary uses for chromates are [4]:

- Chromate conversion coatings for aluminum (Al) and magnesium (Mg) alloys as well as for corrosion-protective coatings [Cadmium (Cd), Al, Zinc-Nickel (ZnNi), phosphate

layers, etc., where the chromate is usually referred to as a sealer or passivation treatment]. This type of coating involves the use of a chromate (sodium dichromate, strontium or zinc chromate) that creates a chemically modified surface region in which the Cr^{6+} remains, forming a self-healing chemistry that re-protects if scratched. Thin (Class 3) chromate conversion layers are electrically conductive, making them suitable for use on electronic hardware. For Class 1A and Class 3 conversion layers, it is important to distinguish between low and high copper alloys. High Cu and Zn alloys are more difficult to protect.

- Chromate primers, sealers, bonding primers, gap fillers, etc., in which the chromate provides corrosion protection by release from a polymer matrix.
- Chromic acid anodization, in which a thick oxide layer is produced at the surface of Al or Mg to protect against corrosion and mechanical damage. Anodization does not leave Cr^{6+} at the surface. However, anodized layers may be sealed with chromate, leaving Cr^{6+} at the surface.
- Chromic acid passivation, which is used for stainless steels. It produces a thin oxide layer that serves the same purpose as the native oxide that is formed on stainless steels over time, namely to inhibit corrosion. Like anodization, passivation leaves no Cr^{6+} at the surface.
- Wash primers prior to painting.
- Chromate conversion coatings also provide color to Al, Zn and Cd surfaces, which makes it obvious that the treatment has been done, as well as showing the degree of protection the coating will provide, from clear (thinnest), through yellow, to olive (thickest).

Chromate conversion of Al is governed by MIL-C-5541. Because there are so many applications for chromates there are different requirements for each type of use [4]:

- Application methods – dip, spray, wipe, brush, full component coating and touch up
- Protection of Al, Mg, Zn, Cd and Cd-alternative coatings
- Protection of surface when scratched, by migrating into the damage region and providing corrosion protection at the exposed metal
- Electrical conduction
- Adhesion of paints and adhesives
- Color Indicator – color varies depending on weight per unit area (and hence on immersion time) – clear (3 $\mu g/cm^2$ on Cd), yellow (40 $\mu g/cm^2$), olive (70 $\mu g/cm^2$). This is not a functional requirement, but is a useful tool proving that the process has been done and how protected the surface is.

1.2.2 POTENTIAL ALTERNATIVES TO HEXAVALENT CHROMIUM

Chromate alternatives generally do not meet all of the requirements listed in 1.2.1, but do meet those critical to specific types of applications. For example, most alternatives do not exhibit the colors of standard chromate layers (and in some cases dyes are added to simulate chromate

colors for ease of identification). Other alternatives are designed only to improve paint adhesion and do not provide corrosion protection, so that they cannot be used on bare metal surfaces. Because the chemistry of chromate alternatives is different from that of Cr^{6+} they do not necessarily work as well on all substrate materials although some alternatives work better than Cr^{6+} on some materials.

There are a large number of Cr^{6+} alternatives for chromate conversion of Al alloys and Zn (Figure 5). Most of these alternatives are based on Cr^{3+} but contain additional corrosion inhibitors such as zirconium or permanganates. Each of these works better on some materials than on others, necessitating the correct choice of alternative for the application. Mg alloys pose one of the most difficult problems because they are so electronegative that they cannot be protected sacrificially. One of the more successful alternatives is a thick anodized layer applied by high voltage spark anodizing. Chromate anodizing is being replaced primarily by thin film sulfuric and boric-sulfuric anodizing.

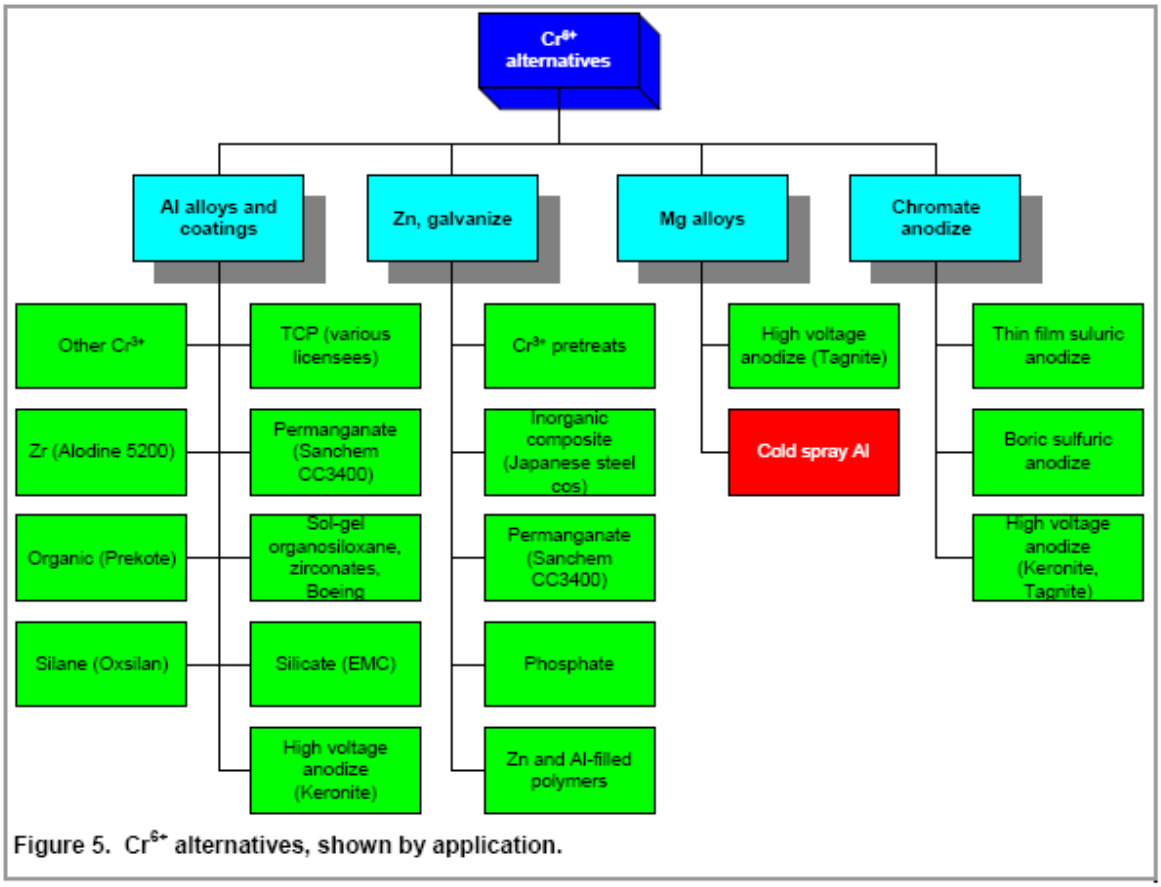

Figure 5. Cr^{6+} alternatives, shown by application.

Figure 5: Cr^{6+} alternatives for various applications [4]

1.2.3 Approach to Reducing Hexavalent Chromium Content

The approach to reducing/eliminating hexavalent chromium from military coatings systems involves using both Cr(VI)-free primers and pretreatments. The primers that are being examined

in this work include MIL-P-53022, MIL-P-85582 N (e.g., Deft 02GN084 and 44GN098), epoxy powder coats, and zeolite primers [5]. Chromate free-pretreatments that are being evaluated include Alodine 5200/5700, TCP, and CFP. In addition, epoxy superprimers [6] that replace the need for separate pretreatments and primers will be studied.

The transition from Cr(VI) to non-chrome alternatives in pretreatments and primers is not feasible at this time due to the overall reduction in performance when chromate is replaced in both the pretreatment and primer [4]. Furthermore, the topcoat can have an effect on the system corrosion performance [4]. Some of these chromium-free coatings have only recently been developed, and have not been fully optimized to deliver high performance on multiple substrates.

The trivalent chromium process (TCP) and chromium-free process (CFP) are NAVAIR developed chemistries that are drop-in replacements for chromated sealers, post-treatments, and conversion coatings. The majority of conversion coating work thus far has focused on the use of TCP and CFP on aluminum alloys, sacrificial coatings, and as a sealant on anodized coatings with extremely promising results. However, further development must be done for use on steels and magnesium alloys where corrosion protection is deeply needed. One of the key advantages to TCP and CFP is that they are drop-in replacements for current technology thus making them favorable alternatives for depots and OEMs. The drop-in replacement eliminates the need for additional training of personnel and large equipment purchases. TCP is based on a fluorozirconate complex with a trivalent chromium salt. TCP contains significantly less total chromium (and no hexavalent chromium) than the current hexavalent chromium conversion coatings. CFP has the added advantage of containing no chromium. The use of TCP and CFP removes personnel exposure to hexavalent chromium. Additionally, it saves time and money by eliminating the need to treat the waste stream for hexavalent chromium.

1.2.4 Issues with Methods for Reducing Hexavalent Chromium Content

There is discussion regarding the adoption of regulations to limit the use of chrome, in general, including trivalent chromium. Metallic chromium is inert and it does not pose a hazard to sustainment personnel except during grinding, when it produces dust. However, the waste chemicals produced during hard chrome plating operations often yield hexavalent chromium [4]. Future regulations regarding hard chrome are therefore justified.

There are arguments that question the use of trivalent chromium. Cr(III) is exceedingly insoluble and therefore cannot migrate to a scribe or corrosion cell without first oxidizing to more mobile Cr(VI), after which it is reduced back to Cr(III) [4]. Some people also argue that the only acceptable method to identify low concentrations of Cr(VI) and Cr(III) together in the same film is via Raman spectroscopy [4]. Also, there is no generally accepted mechanism for Cr(III) protection of aluminum alloys, whereas the mechanism of Cr(VI) activity is understood. Yet, PIs of this work feel that excessive regulation of trivalent chromium is overly cautious and somewhat ignorant.

Hexavalent chromium passivation coatings are based on a thick, gelatinous trivalent chromium layer known as the olation polymer [7]. The first stage in the formation of a hexavalent chromate coating is dissolution. Acidic attack from the aqueous solution results in a pH rise at the zinc surface, releasing both zinc and hydrogen [7]. Cr(VI) is then reduced to Cr(III) and

subsequently precipitates into the Cr-O-Cr olation polymer is [8]. Cr(VI) chromatic acid anions in the olation polymer control color, thickness, and the self-healing property of the film [7].

TCP does not contain any free trivalent chromium and is free of hexavalent chromium. The chemistry being utilized is semi-covalently bonded, similar to an organometallic. The compound forms a polymeric species in aqueous media, so there isn't any ionic dissociation into free trivalent chromium. What results is a multiple-Cr(III) polymer, which is branched by -OH, -O, and -SO_4 groups. The -OH and -O bonds are non-ionic as far as can be determined. So, in order to have conversion, you first need to have a system with enough energy to cleave bonds, plus the proper pH and excess strong oxidizer. This is unlike hexavalent chromium which does contain free Cr(VI) ions. Furthermore, even if free Cr(III) were present, trivalent chromium is an essential nutrient that helps the body use sugar, protein, and fat [9]. Clearly, not all chromium is bad.

Furthermore, TCP has been empirically tested using the old standard hex chrome spot test: 5-diphenylcarbazide is oxidized to 5-diphenylcarbazone by hexavalent chromium (or other strong oxidizers present). The 5-diphenylcarbazone forms a vibrantly purple complex with Cr(III) (which is present after the Cr(VI) is reduced during the redox reaction). The TCP solution was combined with most standard processing chemicals (NaOH, H_3PO_4, alkaline cleaner (pH 8-10), nitric desmutters, etc.) in the presence of 5-diphenylcarbazide and excess oxidizer (benzoyl peroxide, sodium peroxide, potassium hydroxide, etc.) without getting a positive result for the presence of hexavalent chromium. Even if the oxidizer preferentially oxidized the 5-diphenylcarbazide compound and not the trivalent chromium, the 5-diphenylcarbazone species should still give a purple positive if there was ANY free trivalent chromium present.

The only way to get Cr^{3+} to Cr^{6+} conversion was in a highly alkaline solution (pH > 11.0) with excess peroxide while heating the solution to greater than 150°F. So, it is recommended to be cautious with waste streams and strong oxidizers, but there has not been any evidence for the formation of hexavalent chromium in normal operations.

There are numerous epoxy primer military specifications, varying from solvent-based with corrosion inhibiting hexavalent chromium and lead, to water-based primers that are chrome and lead free (Table 2). All epoxy primers are formulated as two component systems that are mixed together to form the coating. The solvent-based primers are usually bisphenol type epoxy resins dissolved in organic solvent. Water dispersible primers (e.g. MIL-P-53030) use water as a co-solvent to reduce VOC content in the primer. The second component is usually a polyamide or aliphatic amine adduct. Both the polyamide and amine adduct are used rather than simple amines to reduce ‘blush’ (simple amines react with carbon dioxide to form carbamates, which hurt surface and interfacial properties of coatings) [10]. MIL-PRF-85582 uses chromate and lead corrosion inhibitors in non-chromate conversion coatings. MIL-P-53022, MIL-P-53030, and MIL-PRF-23377 contain no chromate, lead, or cadmium.

Therefore, there exist high performance pretreatments and primers that contain no hexavalent chromium. However, combinations of hexavalent chromium-free pretreatments and primers have provided poor corrosion protection. In fact, environmentally friendly alternatives without hexavalent chromium are often tested with a chromate “safety.” For example, non-chromate conversion coatings were tested with chromated primers and the non-chromate primers were

tested with chromated conversion coatings. Considering the major environmental benefits associated with reducing water pollution and occupational worker exposure related to heavy metals, it makes sense to combine these two technologies. However, the corrosion, durability, and chemical agent resistance ramifications have not been examined. In addition to the information available regarding traditional coatings, there are also many studies looking at coating systems that do not rely on the multi-layer approach shown in Figure 4.

1.3 The Need to Reduce VOC Content in Primers and Topcoats

Because of the NESHAP requirements, reduced VOC epoxy primers were developed. These primers typically contain no more than 2.5 lbs/gal VOC content. Solvent-based systems use exempt solvents to replace VOC and HAP solvents. Water-dispersible epoxy primers use water as a co-solvent to reduce VOC and HAP content. In water-dispersible epoxies, the epoxy component is usually a bisphenol type epoxy dispersed in water with approximately 30% organic solvents. The hardening agent is again a polyamide or polyamine adduct dispersed almost entirely in water. These water-based formulations have only slightly less VOC than the solvent-based systems, but are less likely to be affected by future regulations, whereby some exempt solvents may no longer be excluded. Unfortunately, MIL-P-53030 clearly has poorer performance relative to solvent-based primers, likely due to its hydrophilic nature, which makes it susceptible to attack by water and ions, leading to corrosion.

The topcoats of chemical agent resistant coatings (CARC) contain polymer binders that provide the required performance attributes of the product, pigments that provide the desired color and gloss, and solvents and additives that control viscosity and aid in film formation [11]. An aliphatic polyurethane binder provides the chemical agent resistance while the camouflage properties are provided by an appropriate selection of tinting pigments for visual color and near-infrared reflectance, plus extender pigments for gloss control. In a typical solvent-based urethane system, polyol reacts with polyisocyanate to form polyurethane. If designed properly, cross-linking (bonds between polymer chains) in this system provides high-performance coatings. CARCs must display resistance to alkali, hydrocarbons, and acids. The coating must also exhibit high flexibility and mar resistance (i.e. high ability to resist damage). Lastly, the coating must have very low gloss for camouflage requirements. This usually requires high pigment contents, which tend to have an adverse effect on the coating's performance.

Traditionally, careful formulation and large-scale empirical testing have provided very durable coatings that meet mission requirements. The camouflage topcoat applied to Army and Marine Corps tactical vehicles and aircraft is a very low-gloss ($60^{o} \leq 1.0$ gloss unit and $85^{o} \leq 3.5$ gloss units), two-component, solvent-based polyurethane (MIL-C-46168 or MIL-DTL-53039). Topcoats for military fixed-wing aircraft used by the Navy and Air Force are aliphatic polyurethanes (MIL-PRF-85285) formulated to meet their demanding requirements. For example, during flight, the coatings are exposed to a wide temperature range (-54 ºC to 177 °C), high mechanical stresses, and rain erosion. Ground and/or carrier conditions can be severely corrosive, so Navy primers are designed to maximize corrosion protection. This research will address both ground and aircraft coatings.

The presence of water is detrimental to the properties of solvent-based polyurethane systems because it participates in a competing reaction with isocyanate to form unstable carbamic acid.

Carbamic acid decomposes to form carbon dioxide and amine, which reacts with isocyanate to yield a urea. These adverse reactions decrease the cross-link density of the polymer, which detrimentally affect the coating properties. These solvent-based topcoats have high VOC/HAP contents (420 g/L) and are limited to using only hydrocarbon solvents due to the unfavorable reaction with water. Therefore, the VOC content can only be decreased a small amount by using exempt solvents.

ARL developed a water-dispersible CARC (MIL-DTL-64159) as a "drop in" replacement for the predecessor solvent-based CARC (MIL-C-46168) that can be applied and stripped using existing equipment [12]. The patented (U.S. patent #5,691,410) water-based system eliminates HAPs and ozone depleting chemicals entirely, along with 4 million lbs/year of VOC emissions, a 50% reduction, thereby meeting the new emissions requirements. In water-dispersible CAR topcoat, water is an integral part of the formulation and enhances physical properties, while reducing VOCs and eliminating the use of HAPs. Unlike solvent-based systems, it is possible to eliminate VOC emissions from water-dispersible topcoats and primers by using exempt organic solvents along with water. **However, no successful near zero VOC topcoats or primers have been developed for military applications.** The binder is still a mixture of polyisocyanates and polyols that cross-link to form polyurethane. While water still competes with polyol to react with isocyanate, the chemical kinetics, raw materials, and an excess of isocyanate to hydroxyl groups (5:1) are used to ensure good coating performance. In addition, polymeric beads are used rather than siliceous flattening agents. This allows for lower pigment content to achieve the same low gloss, while enhancing the coating's mar and UV resistance.

The water-based system was found to be a better CARC than the solvent-based system because of its superior flexibility and durability, and it requires one-third less paint for a given coated area relative to its solvent-based counterpart [12]. This improved performance increases the time between finishing and reduces damage to the structure, resulting in less coating maintenance. Furthermore, the cost per square foot per year of service for the environmentally friendly CARC is actually less than that of the previously used solvent-based system even though the water dispersible CARC costs more per gallon. In addition, dry abrasive blasting has been successful in removing the environmentally friendly CARC, rather than using solvent-based paint removers. For these reasons, the Army has cancelled the old MIL-C-46168 specification to ensure that higher performance topcoats are used.

While many facilities and OEMs will continue using conventional spray applications and implement new coatings as they become available, a key area that can be cultivated for military use is low gloss powder coats for exterior applications. ARL and key cooperating raw material suppliers and vendors have dramatically reduced the gloss levels of powder coats, yet they still exceed (above 5 units for 60° and 85° incidence) the requirement for Army and Marine Corps tactical equipment and support equipment for the aviation community. Powder coats offer significant advantages in many ways; zero emissions, recyclable overspray and controlled film thickness result in an exceptional coating for small parts and components, such as the armor kits being installed on equipment in Iraq and other areas of conflict. Therefore this effort will focus on reducing gloss levels in powder coats to meet the current military requirements for the services. This will be achieved through the use of surface modifiers and novel flattening agents. In addition, powder coats require post-curing to fully react the polymeric binder system, which is

not a standard practice for most DoD coatings operations. Therefore, implementing powder coating would necessitate significant capital investment at the depot level.

Despite considerable reduction in VOC emissions over the past ten years, Naval Aviation Depots (NADEP) typically generate 60,000 lbs of VOCs per year from coating operations. Army hazardous waste generation from coating related operations is even higher at 680 tons of painting waste across 28 locations and a staggering 2,000 tons associated with depainting at 16 locations. The Marine Corps emission of VOCs from primers and topcoats can be estimated at 80 tons annually. Air Force estimates indicate that painting operations cost over $150M per year, and hazardous materials comprise a significant percentage of that amount [3]. In addition, the DLSME NESHAPs will affect the entire coating process in DoD installations [3], not just the coating application itself, further increasing the cost of coatings systems. For this reason, it is important to address environmental concerns with the existing coating systems before environmental regulations come into effect.

1.4 Project Goals

Hazardous ingredients in primers and coatings formulations must be reduced to meet new environmental regulations and protect worker safety. The ultimate goal of this research is to develop environmentally friendly coatings as a complete system that protects DoD assets from the environment in which they operate. In addition to developing "green" coating systems, the new protection scheme must equal or preferably surpass current coating performance. DoD is requiring longer asset service life and less maintenance man-hours than ever before, even with aging fleets. It is these durability requirements that necessitate the need for an ideal and robust coating system. Therefore, this project has determined and developed the best alternatives, combining them to form a complete coating system and optimizing the system based on substrate and application.

The first stage of this project examined the ability of TCP, CFP and other non-chromium pretreatments to protect against corrosion. The University of Connecticut (UConn) characterized the coating systems and assisted in determining how the alternatives differ in the mode of protection when compared to current technology. This helped to determine appropriate formulations to achieve current coating performance without the negative environmental impact. Overall research and development has been done in a number of research areas to develop and understand pretreatments free of hexavalent chromium:

- Improvement of the TCP and CFP to work efficiently on all substrates, provide good coverage and high corrosion resistance.
- Analysis of TCP and CFP coated samples and comparison to other pretreatments to understand coverage uniformity, sample-to-sample differences, and substrate-to-substrate differences.
- Correlation of TCP and CFP analysis with corrosion and performance measurements.
- Prove that hexavalent chromium does not form in the TCP process.
- Evaluation of other non-chromium pretreatments, such as Alodine 5200/5700.

Secondly, the ability of non-chrome primers to work in conjunction with pretreatments that do not use hexavalent chromium is being examined. To do this, research, development, and evaluation of non-chrome pretreatments was done along with Cr(VI)-free pretreatments:

- Evaluate commercial and experimental chromate-free primers applied over hexavalent chromium.
- Evaluate superprimers [6] that potentially replace the need for separate pretreatments and primers.
- Reformulate primers to work efficiently with environmentally friendly pretreatments.

Reduction in VOCs will be accomplished through research and development in the following areas:

- Improvement in water dispersible coatings technology.
- Replacement of VOC solvents with non-listed chemicals on the EPA TRI list.
- Use of mixed-metal oxide high reflectance pigments to reduce solar loading – in progress.
- Use of powder coats with novel non-silica flattening agents to improve barrier properties and durability.
- Use of newly developed polyols to improve durability and reduce solvent loading.

Lastly, the performance of combinations of environmentally friendly pretreatments, primers, and topcoats will be evaluated. The final coating system will be chrome-free and contain near zero VOC and no HAP, making it an environmentally friendly coating system that can be used for years to come.

2 Experimental Techniques

2.1 Pretreatment Preparation and Testing

Test specimens were prepared from aluminum alloy 2024-T3, 7075-T6, 6061-T6, 2219-T87, high-strength steels 4130 and 4340, and stainless steel 316. The panels were prepared by chemical immersion or spray processing. Specimens were hand-wiped with acetone prior to processing. Ambient laboratory temperatures were between 72-79°F and relative humidity levels were between 20-30% during processing and painting operations. The test panels were prepared by a standard immersion process, which included a non-etching, non-silicate alkaline cleaner, an acid-etch deoxidizer/desmutter, followed by immersion in tri-chrome (TCP), non-chrome (CFP and Alodine 5700) or chromate (Alodine 1200S) control solutions. The test specimens were double rinsed in flowing tap water after each step in processing, and given a final rinse in flowing de-ionized (DI) water after the pretreatment was deposited. The panels were then air-dried for 24 hours prior to testing or painting.

Corrosion and adhesion testing were performed on all high-strength steel and aluminum alloys. Flash rust inhibition and adhesion promotion were examined on high-strength steel panels. Class

3 testing (contact electrical resistance per MIL-DTL-81706B) was performed on aluminum alloy 6061-T6 panels. Evaluation of the various surface treatments for use as a post-treatment for sacrificial coatings was performed for cadmium, alkaline zinc nickel, bright zinc nickel, IVD aluminum, and Alumiplate™, over high-strength and stainless steel substrates.

Initial TCP permutations were screened through bare corrosion testing using aluminum alloy 2024-T3. Test panels were then down-selected and the permutations yielding the best results were tested for paint adhesion, painted corrosion testing, and galvanic interface compatibility using both chromated (as a control) and non-chromated primers on the aluminum alloys of interest. The test panels were again down-selected and the final permutations were tested according to MIL-DTL-81706B for Class 1A and Class 3. The permutations were then characterized on additional aircraft substrates such as titanium and anodized aluminum. Selected formulations were further evaluated for corrosion and adhesion performance on steel substrates and as a post-treatment on sacrificial coatings.

Process optimization focused on surface pretreatment compatibility with standard process chemicals using various application methods (immersion, spray, and wipe/brush). These processes were then stacked and evaluated in conjunction with Navy and Army primer and topcoat paint systems.

2.2 Pretreatment Analysis Techniques

2.2.1 Scanning Auger Microscopy and X-Ray Photoelectron Spectroscopy

Elemental analyses of surfaces were achieved using Auger electron spectroscopy and X-ray photoelectron spectroscopy (XPS). Both techniques detect electrons from the surfaces of solids. In both methods, the energies and intensities of electrons emitted from atoms are measured, and the data are displayed as peak intensities versus energies of the emitted electrons. Each element produces a set of peaks with characteristic energies, so the peak energies can be used to identify the elements present. The peak intensities are divided by empirical sensitivity factors to obtain an elemental analysis of the sample surface in units of atom or mole percent. The analyses are semi-quantitative because the relative peak intensities vary somewhat depending on the nature of the matrix in which the emitting atoms are found. The sensitivity factors used were supplied by the instrument manufacturer, and are based on average relative peak intensities from a variety of substances. Concentration errors may be as high as 30% if standard samples are not used to determine an appropriate set of sensitivity factors for a given type of solid matrix. Nevertheless, when the manufacturer's sensitivity factors are used within a series of samples having the same kind of solid matrix, deviations from the average calculated concentrations are often smaller than 10%, provided that the [signal]/[noise] ratios are sufficiently high. When the elemental surface concentrations are compared for some kind of material before and after treatment, this level of deviation often is small enough to gain valuable insights into the effects of a surface treatment, even without a special set of sensitivity factors. It also is useful in evaluating changes in the preparation of different samples in which the general type of solid matrix is not changed.

The most intense photoemission peaks are usually narrower than the most intense Auger peaks. Because the Auger peaks tend to be broader, resolution of raw data peaks in Auger is often only partial. Curve-fitting the Auger raw data peaks would be tedious and very time consuming, therefore it is customary to calculate and display the derivative rather than the raw Auger

spectrum. In contrast to X-ray photoelectron spectroscopy, for which the peak intensity is simply the area, the Auger peak intensity is defined as the peak height (local maximum minus local minimum) of the derivative peak.

Figure 6 is different. It shows a representative plot of the zirconium (Zr) LMM derivative peak with the software label Zr2. Since the derivative peak is used, the peak intensity is defined as the height of the derivative peak, i.e., the intensity at the local maximum minus the intensity at the local minimum. As one examines the plot of this peak, it should be clear that the contribution of noise to the measured peak intensity of the Zr2 peak results in large errors. To minimize the error arising from noise, a cubic polynomial was fitted to the Zr2 derivative peak, and the local maximum and the local minimum of the fitted cubic curve were used to define the peak intensity. This correction was applied to all the Zr2 peaks in this data set. There is a more intense Zr MNN Auger peak with the software label Zr1. It appears at approximately 147 eV, but its shape is much different from that shown for Zr metal in the Handbook of Auger Electron Spectroscopy. Its shape also appears to vary somewhat from sample to sample. For these reasons, the Zr1 peak was not used. Another possible reason to avoid relying on the Zr1 peak is that it is close in energy to the sulfur (S) LMM peak. Of course, if the samples never contain S, this consideration is irrelevant.

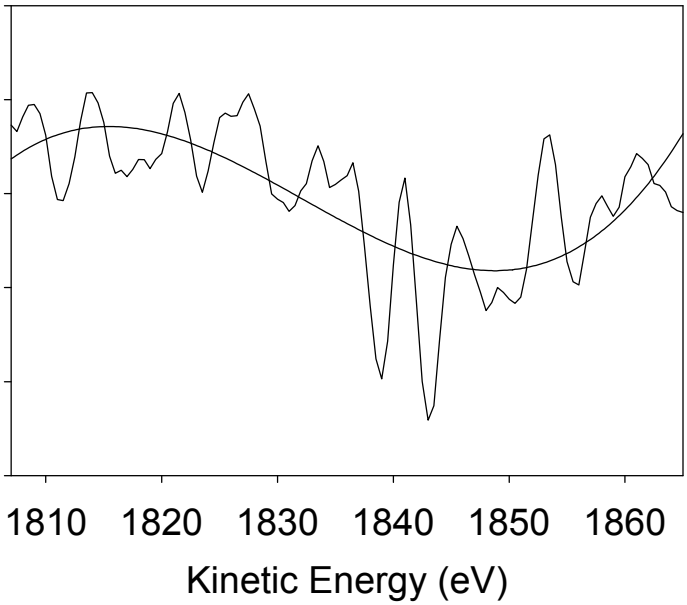

Figure 6: Curve-fitted zirconium peak for Auger electron spectroscopy.

The low intensity of the Zr2 peak causes a low [signal]/[noise] ratio. The local maximum and local minimum of a fitted cubic polynomial were used to correct the error in the peak intensity arising from noise. This correction was applied to all the Zr2 peaks in this data set.

For both Auger electron spectroscopy and X-ray photoelectron spectroscopy, the term *surface* refers to the analytical probe depth rather than to the top monolayer of atoms. The same phenomenon of electron inelastic scattering determines the probe depth in both methods.

Because the range of kinetic energies of the emitted electrons is roughly the same in both methods, the probe depth for both is about the same. For both methods, approximately 99% of the analyte signal intensity arises from the top 50 Å (5 nm) of solid.

In both Auger electron spectroscopy and X-ray photoelectron spectroscopy, the samples are analyzed in ultrahigh vacuum (UHV, i.e., $P \leq 1 \times 10^{-8}$ Torr $\approx 1 \times 10^{-3}$ mPa). Electrons emitted from the solid must pass through the electrostatic field of an electron energy analyzer in order to strike the electron multiplier, which is the detector. Only electrons having energies within a certain narrow energy range are permitted to reach the detector. The energy of the electrons detected is changed as the potential applied to the energy analyzer is changed.

The Auger transition occurs after the creation of an atomic core electron vacancy by the transfer of kinetic or photon energy to an atom. A certain percentage of such excited atoms with core electron vacancies will release energy by fluorescence. Others will release energy by emitting an Auger electron. The details of the physics are omitted here, but the Auger electron kinetic energy is quantized, i.e., it has a specific narrow range of values determined by the energy levels of the emitting atom (the excitation energy is irrelevant, as long as it is large enough to create a core electron vacancy). In this respect, the Auger transition resembles fluorescence.

The Auger data were acquired using a Physical Electronics model PHI 610 scanning Auger microprobe. The Auger transitions are excited using an electron beam of 3 keV and a diameter of approximately 1 μm. To minimize sample charging by the electron beam and backscattering of specular electrons into the energy analyzer, samples were tilted 30°. The instrument has three relative resolution settings: 0.3%, 0.6% and 1.2%, corresponding to high, medium and low energy resolution. All data were acquired using 0.6% relative resolution. The resolution of the energy analyzer is a complex function of the energies of the electrons being detected, i.e., the energy resolution varies from high to low while the energies of electrons detected varies from low to high kinetic energy. Because the energy resolution is not constant, relative rather than absolute resolution is used. The step energy between peak intensity data is 0.5 eV for narrow peaks (Zr, N, O, and chromium (Cr)) and 1.0 eV for broad peaks (C, Zn and Al). The most intense peak (O) required only 2 scans for a satisfactory [signal]/[noise] ratio, whereas weak peaks (e.g., Na, Zn and Zr) required as many as 100 or 200 scans. Survey spectra were acquired in 10 scans in most cases. For each sample, three spots at different locations were analyzed in order to determine the elemental surface concentrations in a more representative manner.

X-Ray Photoelectron Spectroscopy (XPS), more popularly known as Electron Spectroscopy for Chemical analysis (ESCA), is now a widely used analytical technique for investigating the chemical composition of solid surfaces. ESCA is accomplished by irradiating a sample with mono-energetic soft x-rays and analyzing the electron energies emitted. Mg Kα x-rays (1253.6 eV) or Al Kα x-rays (1486.6 eV) are ordinarily used. These photons have limited penetrating power in a solid of 1-10 micrometers. They interact with atoms in the surface region by the photoelectric effect, causing electrons to be emitted. The emitted electrons have kinetic energies give by equation 1:

$$K\,E = h\nu - BE - \Phi_S \qquad (1)$$

where *hv* is the energy of the photon, *BE* is the binding energy of atomic orbital from which the electron originates, and Φ_S is the spectrometer work function. The binding energy may be regarded as the ionization energy of the atom for the particular shell involved. Because there are a variety of possible ions from each type of atom, there is a corresponding variety of kinetic energies of the emitted electrons. For a typical ESCA investigation where the surface composition is unknown, a broad scan survey is necessary to identify the elements present. Once the elemental composition has been determined, narrower detailed scans of selected peaks can be used for more comprehensive picture of the chemical composition.

Chemical analysis was performed on the dendrimer coated samples with a Kratos Axis ULTRA X-ray photoelectron spectroscopy system, equipped with a hemispherical analyzer, which characterized the near surface composition of the thin films. A 100 W monochromatic Al Kα (1486.7 eV) beam irradiated a 1 mm by 0.5 mm spot. All spectra were taken at a 2 x 10^{-9} torr vacuum environment. Survey and elemental high resolution scans for carbon (C) 1s, nitrogen (N) 1s, and oxygen (O) 1s were taken at pass energy = 80 eV for 5 minutes and pass energy = 20 eV for 2 to 8 minutes, depending on S/N, respectively. The photo-emission spectra allow quantitative (surface concentrations) and qualitative (functional group identification) information to be obtained. XPS was able to determine the atomic concentration of elements at the surface of the material.

Data Interpretation

The spectrum is displayed as a plot of electron binding energy versus the number of electrons in a fixed, small energy interval. The position on the kinetic energy scale equal to the photon energy minus the spectrometer work function corresponds to a binding energy of zero with reference to the fermi level. Therefore, binding energy scale beginning at that point and increasing to the left is customarily used. Several types of peaks are observed in ESCA spectra. Photoelectron peaks are more intense and are typically narrowest lines observed in the spectra. Auger lines are more properly groups of lines in rather complex patterns. There are four Auger lines observed in ESCA: KLL, LMM, MNN, and NOO series. X-ray satellites are due to some minor x-rays components at higher photon energies. Energy loss lines, multiplet splitting and x-rays ghost peaks can also be observed in ESCA.

2.2.2 SCANNING ELECTRON MICROSCOPY

Morphologies were obtained using a Zeiss DSM 982 Gemini field emission scanning electron microscope (FESEM) with a Schottky emitter. The sample was mounted on an aluminum stub using carbon tape.

2.2.3 DETERMINATION OF SURFACE HEXAVALENT CHROMIUM ON PRETREATED SAMPLES

A method for determining hexavalent (only) chromium on the surface or as a coating in Al alloys was used. The method is based on the diphenylcarbazide chemistry described above. A solution of diphenylcarbazide was prepared by dissolving 0.50 g of the carbazide in 50 mL acetone and 50 mL of water. Boiling deionized water (25 mL) was added to a set of sample stubs (1.9 x 2.5 cm) placed in a wide-mouth beaker. Typically 16 stubs were used at a time. The beaker was then placed on a hot plate for 5 minutes to keep the water just below boiling point to avoid bumping and sample loss. The stubs were then rinsed with deionized water making sure that the rinsing is conserved in the beaker. The solution was then acidified with 1 mL of ~ 4.5 M H_2SO_4

solution. After cooling down, the solution was transferred to a 50 mL volumetric flask. An aliquot of the diphenylcarbazide (600 μL) was added to the solution and incubated for 2 minutes after which, the reaction between Cr^{6+} and diphenylcarbazide was stopped by the addition of a phosphate buffer solution (55 g $NaH_2PO_4 \cdot H_2O$ in 100 mL deioinized water). The solution was then diluted to the 50 mL mark and the absorbance of the solution at 540 nm was obtained using an HP 8452A Diode Array UV-Vis Spectrophotometer. A calibration curve was obtained by preparing a series of standard $K_2Cr_2O_7$ solutions by the same method and measuring the absorbance of the standard solutions at 540 nm. As a rule, the absorbance of prepared solutions was obtained in less than 30 minutes after final dilution to 50 mL. Results are expressed either as ppm Cr^{6+} or μg Cr^{6+} per area (cm^2) of sample.

Samples were prepared in one of two ways: 1) A known quantity of pretreatment solution (500 μL) was applied to cut Al 2024 panels or stubs (dimensions 1.9 cm x 2.5 cm) and then air-dried. Using this technique, we know exactly how much Cr^{6+} (if any) was put in the stubs so we can verify ISO 3613 Method. 2) This procedure involves dip coating panels or stubs for 5 minutes in a 250 mL solution bath. The panels were then removed and air-dried vertically to allow excess pretreatment to run off the sample.

2.2.4 ISO 3613 Test Method for Determining Hexavalent Chromium

ISO 3613 is a chemical spot-test methodology used to determine the presence and amount of hexavalent chromium in metallic coatings and coating chemistries. This methodology was chosen to evaluate the TCP and CFP coatings as a supplemental analysis to the instrumental techniques. ISO 3613 uses a boiling water extraction, carried out in de-aerated water at a pH of 6.0 for 5 minutes. The vessel containing the test specimen is covered during this time. The resulting leachate is cooled, and acidified with phosphoric or sulfuric acid since the diphenylcarbazide complexing agent only reacts at a low pH. Diphenylcarbazide is then added to the leachate, and a determination is carried out either visually or with a UV-Vis spectrophotometer for the vibrant purple complex indicating the presence of hexavalent chromium. Initial qualitative testing carried out at PAX River on the TCP and CFP solutions indicated no hexavalent chromium species even in the presence of strong oxidizers such as peroxides. Quantitative testing of coated metal specimens was carried out at the University of Connecticut.

Both TCP and CFP show promise as a replacement for chromate pretreatments on zinc and zinc-based sacrificial coatings but further coating characterization and process optimization still need to be carried out. Additional testing with the modified chemistries must also be conducted to characterize corrosion and adhesion performance along with film formation mechanisms. An analysis of the compositional deposits of TCP and CFP on steel substrates as well as phosphated steel surfaces needs to be performed. Additionally, conversion coating and anodized sealing chemistries and processes need to be analyzed and optimized for magnesium substrates.

2.2.5 Determination of Total Chromium using Atomic Absorption Spectroscopy (AAS)

Total Cr content of pretreated and blank Al 2024 was determined. The sample digestion or preparation procedure was adapted from an ICP-AES method for determining Si, Mn, Cr, Ti, Cu, Mg, Ni and Zn in pure Al and Al alloy [13]. Al 2024 samples were cut into smaller pieces or

stubs (1.27 cm x 1.27 cm). The weights of the samples were approximately 0.37 g. A stub was placed in a 50 mL beaker and 10 mL of aqua regia (1:3 HNO_3:HCl) was added. The beaker was then covered with a watch glass and slowly heated until the Al stub dissolved and the solution turned clear. The resulting digestate was then filtered and diluted to 50 mL with deionized water. A blank digestate was also made (no Al stub). Samples were digested in duplicates. A calibration curve was obtained by preparing a series of standard Cr solutions from a stock 1000 ppm $Cr(NO)_3$ solution. The resulting digestates and standard solutions were analyzed for Cr content using a Perkin Elmer Atomic Absorption Spectrometer 3100 and an air-acetylene flame. Results were reported as ppm Cr.

2.2.6 Determination of Hexavalent Chromium Content in Pretreatment Solutions

We determined the hexavalent chromium content of the TCP and Alodine solutions before and after dip coating two Al 2024 panels (3 x 10 in). The method is based on the well-established EPA 7196A method of determining dissolved hexavalent chromium in ground water or industrial wastes [14]. The diphenylcarbazide chemistry is also employed in this method. To an aliquot of the coating solution (97 mL for TCP and TCP-IC and 500 or 100 μL for Alodine 1200S) was added 2 mL of diphenylcarbazide solution (250 mg diphenylcarbazide in 50 mL acetone) and 1 mL of 10% (v/v) H_2SO_4 solution. The solution was then shaken and incubated for 5 – 10 minutes before the absorbance at 540 nm was obtained. When Alodine 1200S was analyzed, an additional 80 mL of water was added and the solution was diluted to 100 mL before obtaining the absorbance because of the considerably higher Cr(VI) content in this pretreatment. As a rule, the absorbance of prepared solutions was obtained in less than 30 minutes after final dilution.

2.2.7 Fourier Transform Infrared Spectroscopy

Fourier transform infrared (FTIR) spectroscopy was used to analyze the chemical composition of pretreated substrates. A Nicolet Magna 560 FTIR spectrometer (IMS, UConn) was used. Measurements were conducted in a reflectance mode using an 80 degree grazing angle accessory for surface analysis of films and submicron coatings. First a blank Al plate (uncoated) was measured in air (RT) as the background signal and then a coated sample was measured (the time interval between background and sample measurements is less than 2 minutes). Each coated sample was measured two times (50 scans each time) to check reproducibility. The scan wavelength range was 4000-600 cm^{-1} with a resolution of 4 cm^{-1} and 50 scans per spectra.

2.2.8 Raman Spectroscopy

Raman spectroscopy was also used to analyze the chemical composition of pretreated substrates. FTIR and Raman are similar techniques, but have the ability to see different stretching bands for various chemicals, such that one technique is often more sensitive than the other in seeing one chemical functionality, but less effective for another functionality. A Renishaw Ramascope Micro-Raman spectrometer was used. The system includes fiber optics, long focal length objectives and a motorized computer controlled sample stage with autofocus for point mapping of specimens. Measurements were conducted at room temperature using the 514 nm laser source with a laser spot size ~ 1 μm. Samples were positioned vertically with respect to the laser beam. To improve the signal/noise ratio for coating samples, 'long' scanning conditions were used. Samples were analyzed in static mode in a wavelength range of 4000-100 cm^{-1} with an exposure

time of 80 s (usually ~10 s for a powder sample, for thin film coatings, it was increased to 80 s to increase signal to noise ratio) and resolution of 1 cm^{-1} and taking 3 scans per spectrum.

2.3 Fundamental Property Measurement and Analysis of Organic Coatings

2.3.1 NUCLEAR MAGNETIC RESONANCE (NMR) ANALYSIS

^{1}H and ^{13}C NMR analysis of the two liquid components (MIL-DTL 64159 Component B and Bayhydrol XP 7110E) used in making clear polyurethane films was done using a Bruker 400 MHz instrument. The goal of this experiment was to see if solid state NMR analysis of the polyurethane films could quantify branching (biuret or allophanate linkages) in the polymer. Performing liquid NMR on the reactants would indicate if it is even possible to identify polyurethane signals from solid state NMR spectra.

2.3.2 FTIR OF FILM FORMULATIONS

Fourier transform infrared (FTIR) spectroscopy was used to analyze the chemical composition of film formulations described below. A Nicolet Magna 750 FTIR spectrometer was used. Each sample was measured twice (200 scans each time) to check reproducibility. The scan wavelength range was 4000- 400 cm^{-1} with a resolution of 4 cm^{-1}.

Given below are the mixing ratios (by weight) for the film formulations.

1). Pigmented MIL-DTL-64159

MIL-DTL-64159 component A	63.56
MIL-DTL-64159 component B	23.28
DI water	13.15

(Add B to A while mixing. Mix for 5 minutes before adding water.)

2). Pigmented MIL-P-53022

MIL-P-53022 component A	63.56
MIL-P-53022 component B	23.28

(Add B to A while mixing.)

3). Clear MIL-DTL-64159 from Bayhydrol XP-7110E

Bayhydrol XP-7110E	9.03
DI water	3.50

(Mix water with XP-7110E thoroughly before adding MIL-DTL-64159 component B.)

MIL-DTL-64159 component B	11.24

(Add slowly to aqueous component while mixing)

DI water	3.50

(Allow component B to mix 5-10 minutes before adding last aliquot of water)

4). Clear MIL-DTL-64159 from centrifuged component A

MIL-DTL-64159 centrifuged component A	37.86
MIL-DTL-64159 component B	23.28
DI water	13.15

(Add B to A while mixing. Mix for 5 minutes before adding water.)

5). Clear MIL-P-53022 from centrifuged component A

MIL-P-53022 centrifuged component A	36.96
MIL-P-53022 component B	11.45

(Add B to A while mixing.)

2.3.3 FTIR CURE KINETICS

An investigation was undertaken to determine what effect, if any, the addition of hyper-branched polymer (HBP) has on the cure behavior of MIL-P-53022. To this end, the cure kinetics of a simplified epoxy-amine analog system were studied with and without the addition of the commercially available polyethyleneimine (PEI), Lupasol PR 8515, and the functionalized PEI-quat, produced at ARL. Also, gel times were determined for both the MIL-P-53022 and analog systems with and without the addition of Lupasol.

The cure kinetics study involved mixing Epon epoxy resin with Amicure PACM amine-functionalized curing agent in a 2:1 stoichiometric ratio of epoxy and amine functionality, since each amine group is capable of reacting with two epoxy groups. The HBP was added to this system at concentrations of 0.5-2.0 wt % of the total mixture. The system was manually stirred for approximately 2 min., and then FTIR was used to measure the epoxy and amine peaks at 30 second intervals at a temperature of 30°C for approximately 1000 min. The system was then post-cured at 120 °C for approximately 60 min. A Thermo Nicolet Nexus 670 FTIR was used in absorbance mode, taking 16 scans per spectrum with a resolution of 4 cm^{-1}.

From the peak absorption measurements (ABS), conversion, α, can be determined as a function of time, using the equation below and a reference peak unaffected by the reaction, denoted by the subscript 'REF' in equation 2:

$$\alpha = 1 - \left(\frac{ABS(t)}{ABS(t=0)} \right) \left(\frac{ABS(t=0)_{REF}}{ABS(t)_{REF}} \right) \tag{2}$$

The conversion of a given functionality (i.e., as calculated from a given peak) was fit via the method of least-squares to an autocatalytic model equation 3:

$$\frac{d\alpha}{dt} = k\alpha^m (\alpha_u - \alpha)^{2-m} \tag{3}$$

Here, α_u, k, and m represent the ultimate conversion, reaction rate constant, and reaction order, respectively. The peaks of interest in the near infrared (nIR) for epoxy-amine chemistry are the primary amines at 4930 cm^{-1}, secondary and primary amines at 6480 cm^{-1}, and the epoxy peaks at 6066 cm^{-1} and 4530 cm^{-1} (Figure 7). The peaks at 6066 cm^{-1} peak and 4530 cm^{-1} both represent epoxy functionality, but do not give the same results because there are overlapping peaks in the 4530 cm^{-1} range. Therefore, the 6066 cm^{-1} epoxy peak has more validity than the 4530 cm^{-1} peak.

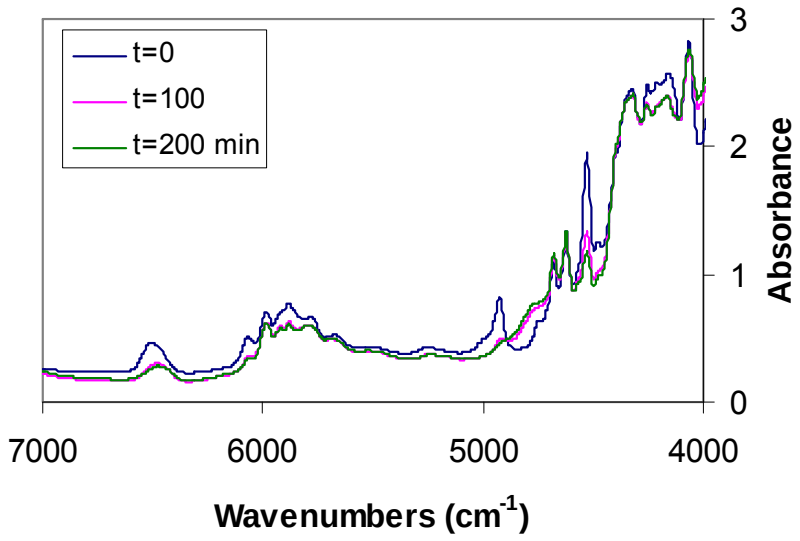

Figure 7: Absorbance as a function of time for the Epon-PACM epoxy-amine system.

2.3.4 CLEAR COAT PREPARATION

Clear (i.e., unpigmented) resin was isolated from pigmented commercial products by centrifugation or prepared from polyurethane reactants based on the Manufacturer's Statement of Composition for Coating Material. Films were made by applying unpigmented liquid resin to clean glass and spreading it to a uniform thickness with a 4 mil stainless steel Byrd applicator. Films were dried at room temperature in the laboratory until no longer tacky to the touch, usually 2-4 days. Films were removed from the glass carefully with a single-edged razor blade. Fully cured films were then stored at ambient laboratory conditions in glass Petri dishes for at least one month before being evaluated by DSC, TGA and DMA to determine resin glass transition temperature (T_g, °C) and molecular weight between cross-links (M_c, g/mol).

2.3.4.1 Clear Resin Film Preparation

This describes the laboratory procedure for isolating the resin binder from commercially manufactured pigmented coatings and making clear cured films from that resin.

1. Agitate the pigmented component A of two-part coatings (or the complete formulation in the case of a one-component formulation such as MIL-DTL-53039B) on a Red Devil paint shaker or equivalent to ensure uniform composition.
2. Pour or pipet the pigmented formulation into disposable polypropylene centrifuge tubes (usually 30-35 ml in a 50 ml tube.)
3. Centrifuge the material until suspended solids are separated and clear resin supernatant can be isolated from the formulation. Frequently, the supernatant will be decanted into a clean tube for subsequent centrifugation. Note that VWR polypropylene 50 ml centrifuge tubes are rated to endure forces up to 12,000 x g. Take care not to exceed the force rating

for the tubes used. Store the clear resin in a glass container with a tightly fitting cap closure.

4. Consult the Manufacturer's Statement of Composition for Coating Material to quantify the weight percentage of the pigments in A. Recalculate the mixing ratios for two-component systems to account for the removal of pigments.
5. Mix the now clear A component and B component with an impeller blade for 5 to 10 minutes.
6. Pipet 1-2 ml of clear resin mixture onto glass cleaned with MEK and spread across the glass with a 4 mil stainless steel drawdown bar (Byrd applicator). It's important to note that the glass used must be free from any fluorocarbon residue. If fluorinated release agent had ever been used on the glass, no amount of MEK will completely remove it and this will lead to de-wetted films or 'crawling'.
7. Allow films to cure at room temperature until no longer tacky to the touch. This usually takes 1 to 2 days for solvent systems and 3-4 days for water dispersible systems. Full curing (solvent evaporation and cross-link development) may take even longer. Film properties should not be tested before 1 month of curing at RT.
8. When the film is no longer tacky, carefully remove it from the glass with a single-edged razor blade. Take care not to nick, tear or puncture the film during removal. Store film in a clean glass Petri dish with a lid.

By using the manufacturer's statement of composition, a formula for clear films of MIL-P-53022 was determined.

Mixing Ratio by Weight for Unpigmented MIL-P-53022

Clear component A	76.45
Component B	23.55

MIL-DTL-53039B is a one-component polyurethane. Clear films were made by direct application of the isolated resin to glass. No mixing with a catalyst or reducing solvent was required.

2.3.4.2 Clear Films of MIL-DTL-64159 from Bayer Raw Materials

MIL-DTL-64159 is supplied as a waterborne two-component polyurethane topcoat. The primary reactants are a water soluble polyol and a water dispersible polyisocyanate. Because water also reacts with isocyanate, the amount of water in the clear mixture will have an effect on the polyurethane reaction kinetics. The full theoretical content of water in the pigmented system exceeds 44% by weight. The pigmented formulation contains this much water to reduce viscosity and promote better mixing of A and B as well as enhance spray application properties. In reality, good quality clear films cannot be made with this much water. Through experimentation, the ideal amount of water and order of addition were determined. Water content ranging from 16.5 to 44.3 percent by weight was explored.

The reaction of concentrated polyol and polyisocyanate species proceeds rapidly and results in unmanageable viscosity build. It is necessary to add some water to the polyol before adding isocyanate. Isocyanate addition should be slow and with adequate mixing to keep the mixture

moving smoothly. Additional water is added after the isocyanate. If too much water is added before the isocyanate, the reaction mixture is very thin and the dispersion of polyurethane becomes non-homogeneous. Some viscosity increase is necessary to provide the shear force needed to reduce dispersion particle size and make even, continuous films.

A well known side reaction of polyol and isocyanate is isocyanate with water to form unstable carbamic acid which quickly decomposes into a primary amine and carbon dioxide (Figure 8).

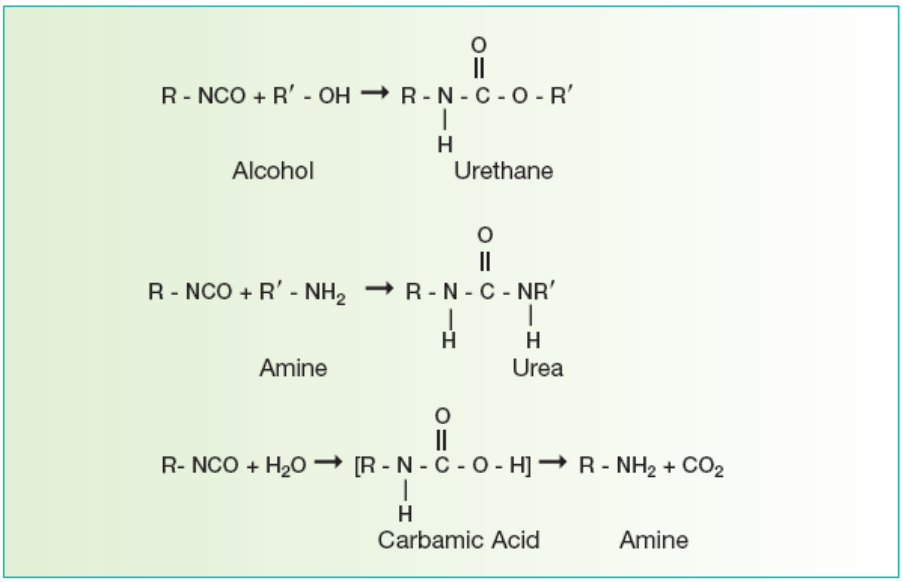

Figure 8: Isocyanate chemistry [15].

This formation of carbon dioxide leads to foaming of the urethane mixture. If the films were deposited in 4 mil wet layers that dried quickly, the formation of foam was minimized. If the wet film viscosity was too thick and water had difficulty escaping, leading to longer dry times, foam was more likely to form.

2.3.5 Fluoropolymer Additive in Clear Coats

The effect of adding a small portion of fluoropolymer to the binder system of MIL-DTL-64159 was studied. For simplicity, clear films were made of the water dispersible two-component polyurethane from Bayer raw materials. The commercially available fluoropolymer emulsion Lumiflon FE-4400 from AGC Chemicals was used to replace a portion of the Bayer polyol. In this way, formula indexing (i.e., the ratio of isocyanate to polyol functionality) remained constant. Cured films were evaluated for thermal and thermo-mechanical properties. Films were also studied with x-ray photoelectron spectroscopy to determine how much fluorine functionality migrated from the film bulk to the film surface.

2.3.5.1 Lumiflon FE-4400

For years fluorinated polymers have been successfully incorporated into more durable high performance coatings for bridges, buildings, aircraft and automobiles. Fluorine functionality in the binder improves water resistance, weatherability and color and gloss retention [16]. The Air Force uses a high performance fluoropolymer coating meeting specification MIL-PRF-85285 D,

Type I for aircraft application. The polyol component of the polyurethane binder is Lumiflon FE-4400. Lumiflon FE-4400 is an aqueous emulsion which incorporates easily into water-borne coatings. AGC Chemicals provided a simplified structure of Lumiflon FE-4400 (Figure 9).

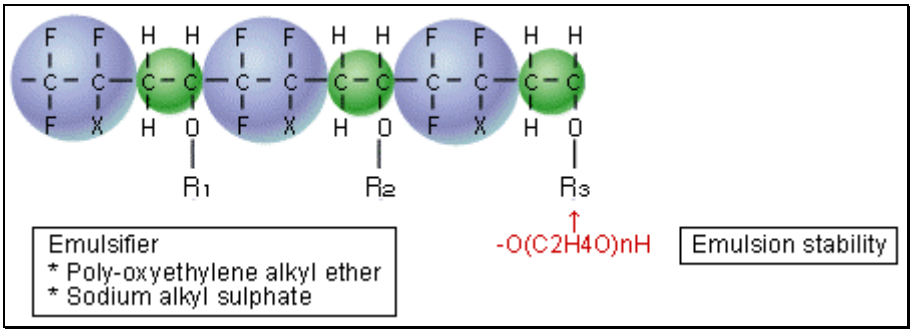

Figure 9: Structure of Lumiflon FE-4400 [16].

In order utilize the benefits of this technology while minimizing cost, the effect of small additions of this emulsion to the water-borne binder system of MIL-DTL-64159 was studied. The working hypothesis being that the natural migration of hydrophobic fluorine to the air interface of the coating while it cures will enable large surface benefits from relatively small additions of fluoropolymer.

The formulae tested in this study are described in the table below (Table 3). Films containing Lumiflon FE-4400 are referred to as 1%, 5%, 10% and 100% because 1%, 5%, 10% or 100% of the polyol solids were replaced by the fluoropolymer emulsion. The weight percent of Lumiflon in the complete wet clear binder formula is 0.4%, 1.9%, 3.8% and 37.6% respectively. Lumiflon FE-4400 was blended with Bayhydrol XP-7110E and some water before reacting the system with isocyanate.

Table 3: Formula grid for Lumiflon study.

(notebook reference)	Control, 27.2% added water (117-1)	1% Lumiflon FE-4400, 28.0% added water (54-007)	5% Lumiflon FE-4400, 27.4% added water (117-3)	10% Lumiflon FE-4400, 28.7% added water (119-2)	100% Lumiflon FE-4400, 27.1% added water (54-009)
Bayhydrol XP-7110E	36.9	36.8	35.8	33.2	0
Lumiflon FE-4400	0	0.4	1.9	3.8	37.6
DI water	14.3	12.4	14.7	10.3	0
Bayhydur 303	36.0	34.8	34.9	34.4	35.2
DI water	12.9	15.6	12.7	18.4	27.1
Defoamer (BYK-023)	0	0	0	0	0.1

2.3.6 CONTACT ANGLE

The advancing and receding contact angles of water on substrates were measured. A water drop was placed on the substrate and the shape of the droplet on the surface was captured using a magnifying lens and a camera. The angle with the substrate was then measured to determine the contact angle. The receding angle was measured by removing water from the droplet until the droplet begins to contract at the substrate surface. Again, the image of the droplet was recorded. The measured contact angle was the receding angle. The receding angle is generally lower than the advancing angle, because it measures the contact angle of the substrate that already was allowed to come to equilibrium with the water environment.

2.3.7 DYNAMIC MECHANICAL ANALYSIS

DMA was performed on a TA Instruments Model 2930 supported by Thermal Advantage software version 1.1A (1999). Samples were mounted to a tension film clamp and run at a single frequency (1 Hz) through a temperature ramp from -20 to 200°C at 2°C/minute with a preload force of 0.10 N and force track at 150%. The amplitude of oscillation was nominally selected to be 1/500 of the sample's length which was determined by the distance between the clamp grips. Storage modulus (E') and loss modulus (E") were graphed as a function of time. From these data values were determined for glass transition temperature (T_g), represented by the maximum value of the loss modulus and molecular weight between cross-links (M_c) by using rubber elasticity theory and the modulus in the rubbery region ($T>T_g$):

$$E = 3RT\rho/M_c = 3RT\nu \quad (4)$$

where E is the rubbery modulus, R is the ideal gas constant, T is the absolute temperature, ρ is the sample density (assumed to be 1 g/mol for all samples), M_c is the molecular weight between cross-links, and ν is the cross-link density.

2.3.8 Differential Scanning Calorimetry

DSC of clear resin films was done in a TA Instruments 2920 MDSC. Samples were in sealed crimped aluminum pans under nitrogen atmosphere and experienced a heat/cool/heat cycle starting at RT to 200°C at 10°C/minute, cooling at 5°C/minute to -20°C and then heating back up to 200°C at 10°C/minute. Generally the first heating/cooling cycle data was ignored to mitigate variations in thermal history of the samples and possible trapped residual solvent. The second heating ramp of each sample was analyzed to determine the midpoint glass transition temperature.

2.3.9 Thermogravimetric Analysis

Cured resin films were analyzed with a TA Instruments High Res TGA 2950 supported by Thermal Advantage software version 1.1A (1999). Samples were heated to 800°C at 10°C/minute in an air cooled furnace. Sample weight loss vs. temperature and derivative weight loss were measured.

2.3.10 Tensile Strength

A method was developed for measuring film tensile strength, elongation at break, elastic modulus at room temperature and film toughness using the DMA. Typically, materials are tested on an Instron or Tinius Olsen type testing machine but it is difficult finding grips and load cells appropriate for thin polymer films. A tension film clamp (the same one used for DMA analysis) was used in controlled force test mode offered in the Thermal Advantage software. In this mode, samples held in tension have a force ramp (linearly increasing stress) applied and the resulting displacement (strain) is measured to generate stress-strain data curves. This is somewhat different from traditional test methods in which sample grips separate at a constant speed inducing a constant rate of strain on the sample and the stress response of the sample material is measured by a load cell mounted in the crosshead of the testing machine. In order to make meaningful comparisons between materials, sample dimensions must be consistent. Rectangular strips 5.0 mm wide were cut with a razor blade and straight edge [17]. Sample length is defined by the distance between the grips and was maintained at 15.0 ± 0.2 mm. Film thickness was measured with a micrometer, accurate to 0.002 mm. A preload force of 0.001 N was applied to the samples and a force ramp rate of 10.0 N/min. was applied to a maximum applied force of 18.0 N. At least five replicates for each sample were measured.

When evaluating the stress-strain data plot, the elastic modulus is determined by the slope of the linear portion of the graph before plastic deformation begins. These data correlate to the storage modulus determined by DMA at room temperature. Tensile strength is marked by the highest stress force endured before film rupture occurred. Strain to failure or elongation at break is the percent strain the sample endured before failure. Material toughness can be quantified by calculating the total area under the stress-strain curve. The magnitude of this area represents the amount of kinetic energy the film can absorb at a given rate of strain before experiencing mechanical failure.

2.3.11 FILM PERMEABILITY AND SOLUBILITY MEASUREMENTS

A key incentive for using fluoropolymers in a coating is to increase that coating's hydrophobicity. Assuming comparable film morphology, one would expect water vapor to penetrate a fluoropolymer film more slowly than a similar non-fluorinated film. It is similarly desirable for the Army to use coatings which are resistant to the absorption of chemical agents. Experiments were run to measure the solubility and vapor transmission rate of water and dimethyl methylphosphonate (DMMP) for the test films. DMMP is a chemical simulant for the nerve agent Sarin.

The solubility, S, of water and DMMP in the test films was determined by submerging a known mass of film completely in the liquid media in closed 20 ml vials held at a constant 35 °C in an oven. Vials were removed from the oven and the film was removed from the liquid media, patted dry with lint free absorbent wipes and weighed. Weight checks continued for a number of days until the film weight remained relatively constant. Equilibrium solubility was calculated as the final percent weight gain of the film.

Vapor permeation experiments were performed according to Napadensky and Elabd [18] using 20 ml vials with septum caps which had been cored to leave a 14 mm circular hole in the septum. The test films were cut into 22 mm circular membranes and were placed between the open septum and cap to form an air tight seal and to allow the test films to act as the barrier between the evaporating liquid in the vial and the external atmosphere. Sample vials were filled with 10–15 ml of liquid (water or DMMP) and were placed in a temperature-controlled oven at 35 °C with nitrogen gas purge passing through a glass column packed with desiccant. Aluminum trays with desiccant were also placed inside the oven to maintain low relative humidity (~10%). A dead weight micrometer accurate to 0.0005 in. was used to measure each film thickness and an analytical balance (precision = ± 0.0001 g) was used to measure weight loss of the vial. Vapor permeation experiments were conducted based on ASTM E 96/E 96M-05 Standard Test Methods for Vapor Transmission of Materials. Vial weights and oven temperatures were recorded over a period of days until sufficient data were collected to determine the steady state weight loss for each vial. RH remained constant at 10% throughout the duration of the experiment. When using water as the volatile test liquid, the conditions were 100% RH (41.854 or mm Hg) on one side of the membrane (inside the vial) and 10% RH on the other side (outside the vial). The concentration gradient provided the driving force for vapor transport. Experiments with DMMP vapor transmission were at 100% DMMP saturation (6.77 mm Hg) on the inside of the membrane and 0% DMMP on the outside the vial. Three sample vials were prepared for each membrane, and the values calculated for each membrane are the average and standard deviation of those experiments.

Vapor transfer rate (*VTR*) is defined as steady state *VTR* per unit area and can be expressed as follows:

$$VTR = G/(t \cdot A) \tag{5}$$

where G is the weight of liquid lost from the vial, t is time, and A is cross-sectional area of the test membrane. For this experiment, the cross-sectional area is 0.000154 m² because septum core diameter is 14 mm. G/t can be determined by the slope of the line drawn through the steady-state (linear) portion of the weight loss *vs*. time data plot. After calculating G/t from the data,

VTR can be obtained using equation 3. *VTR* provides transport rate for a given vapor through a membrane. However, *VTR* does not account for the thickness of the membrane through which the vapor travels. More specifically, *VTR* will have different values for the same material at different thicknesses. To accurately compare materials independent of the processing thickness, permeability must be calculated. Permeability (*P*) can be expressed as:

$$P = (L \cdot VTR) \cdot P_{atm}/P_{sat} \cdot (\Delta p) \quad (6)$$

where L is the sample thickness (m), P_{atm} is atmospheric pressure (mm Hg), P_{sat} is the saturation vapor pressure at the test temperature (mm Hg), and Δp is the difference in partial pressure on the challenge side and the exit side of the membrane. Saturation vapor pressure for water at 35 °C is 41.854 mm Hg and for DMMP at 35 °C, it is 6.77 mm Hg. The DMMP vapor pressure was determined by interpolating from known values at 25 and 65 °C.

2.3.12 PHASE CONTRAST MICROSCOPY

Morphology of clear polyurethane films was studied using an Olympus BX51 phase contrast microscope with Spot Advance software. This optical microscopy technique is useful when studying nearly transparent materials which do not reflect much light. The microscope employs a condenser annulus with a polarizing lens to focus the source light it receives in such a way to make the photons in-phase and parallel. As this in-phase light encounters the sample, it either passes straight through unaltered, or is diffracted by structures and compositional gradients in the sample. Diffracted light is bent away from a straight line trajectory through the sample and this slightly longer pathway results in a phase difference from light that passes straight through. This small phase difference is not visible to the human eye; however, a phase plate on the microscope converts this phase difference into an amplitude difference that is transmitted as an enhanced contrast image to the rear focal plane. These amplitude differences appear to the observer as a proportional change in image brightness [19]. An integrated digital camera was used to capture and store these images.

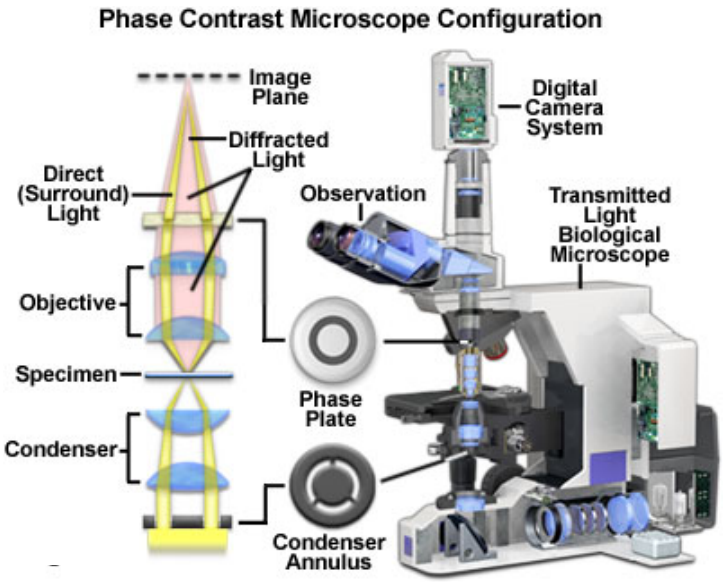

Figure 10: Phase contrast microscope schematic

2.4 Performance Testing of Coatings

2.4.1 PANEL PREPARATION

Test specimens were chemically prepared prior to being painted. Test specimens for corrosion and adhesion testing requiring a subsequent organic coating were prepared using industry standard HVLP paint guns and painting guidelines within 72-hours of surface finishing. Primer coatings were applied to achieve a dry film thickness (DFT) of 0.6-0.9 mils and topcoats were applied to achieve a DFT of 1.7-2.3 mils within 24-hours of primer application. All painted specimens were allowed to cure at ambient laboratory conditions for 14 days before testing. All test specimens were painted with either chromated control or leading non-chromated coating systems. Accelerated paint adhesion panels were primed only. In addition, to evaluate the impact of topcoats on corrosion resistance, subsets of accelerated corrosion panels were primed only or both primed and topcoated.

2.4.2 CONTACT ELECTRICAL RESISTANCE

The electrical resistance of Class 3 test panels, aluminum alloy 6061, was measured under an applied electrode pressure of 200 pounds per square inch (psi). The electrical resistance was measured on a set of test panels 24 hours after the conversion coating was applied and on a set of test panels 24 hours after 168 hour salt spray exposure. Ten measurements were taken on each panel in accordance with MIL-DTL-81706B, Section 4.5.5. Test panels with readings less than 5,000 micro-ohms psi (as applied) and 10,000 micro-ohms psi (after salt spray exposure) were considered acceptable.

2.4.3 ELECTROCHEMICAL TESTING

Electrochemical impedance spectroscopy (EIS) measurements were conducted with a Z-Plot™-controlled Solartron Instruments Model 1287 electrochemical interface, coupled to a Solartron Instruments Model 1260 impedance/gain-phase analyzer. The impedance spectra were collected at frequencies from 1 MHz to 0.1 Hz using alternating current (AC) with an amplitude of $\pm$10 mV at the direct current (DC) open circuit potential. The open circuit potential (OCP) was measured for 60-seconds before each EIS scan. A 0.05 M NaCl solution with a volume of 50 ml was used as the electrolyte. The cell was a glass cylinder clamped and O-ring sealed to the sample surface. The seal exposed 7.75 cm^2 of sample surface area to the salt solution. The reference electrode was a saturated calomel electrode (SCE) and a platinum wire/disk assembly served as the counter electrode. The test specimen was the working electrode. Measurements were made each hour until 12 hours, then every 2 hours until 24 hours, then every 4 hours until 4 days, then at 7, 14, and 21 days. A schematic diagram of the apparatus is shown in Figure 11.

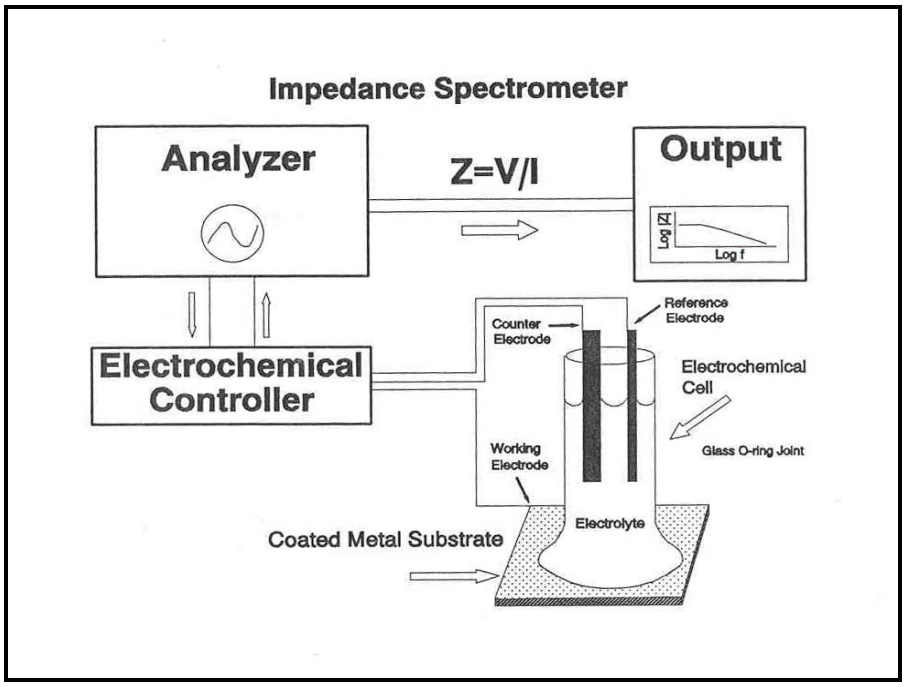

Figure 11: EIS apparatus

OCP and DC linear polarization measurements were performed on the panels with a CorrWare™-controlled Solartron Instruments Model 1287 electrochemical interface coupled to a Solartron Instruments Model 1260 impedance/gain-phase analyzer. The corrosion test cell used was a Princeton Applied Research Model K0235 flat cell. The linear polarization resistance (Rp) was performed from 15 mV below to 15 mV above the OCP with an immersion time of 60 minute in quiescent 0.05 M NaCl. All measurements were conducted in triplicate.

2.4.4 SCANNING ELECTRON MICROSCOPY

High magnification imaging was performed with a JEOL 6460LV scanning electron microscope (SEM). Images were acquired in the backscattered electron mode in order to accentuate compositional (density) differences in the material. Elemental analysis was performed with an Oxford Inca energy dispersive X-ray spectrometer (EDS) attached to the SEM. EDS spectra were acquired for 200 seconds using a primary beam voltage of 15 keV. The EDS analysis was conducted on a horizontally mounted specimen, so that the beam was in a perpendicular position and compositional determination was conducted through the TCP coating. SEM scans of the surface and cross-sectioned coatings were used to determine surface morphology (cracks, voids, etc.) and coating thickness (especially to determine the uniformity of the coating across higher density areas and inter-metallics).

2.4.5 CORROSION TESTING

Neutral Salt Fog (NSF) testing was conducted in accordance with ASTM B 117. Salt spray (5% NaCl) resistance is widely used by the paint industry as a quality control test and is not necessarily indicative of long-term performance of a coating. Three panels per test combination were prepared. Prior to exposure, one of the three specimens had an "X" incision manually scribed through the test coupon coating using a carbide tip scribe per ASTM D 1654, making sure that the coating was scribed all the way through and into the substrate. The smaller angle of

the "X" was 30 to 45 degrees and each line of the "X" was approximately 4 inches long. Scribed and un-scribed test specimens were racked at 15° and placed in the test chamber. Test specimens were visually inspected for corrosion at 500-hour intervals. Sulfur Dioxide Acidified Salt Spray (SO_2) testing was conducted in accordance with ASTM G85 Annex 4 only for painted test panels. The panels were scribed, racked, and placed in test in the same manner as the NSF panels. The SO_2 panels were visually inspected for corrosion at 168-hour intervals. Both NSF and SO_2 corrosion test specimens were rated according to ASTM D 1654 and electronically scanned at each inspection interval.

GM9540P [20] is an accelerated cyclic corrosion test that was developed by the automotive industry to better replicate long-term outdoor performance of coatings. Scribed panels are exposed to multiple cycles of salt mist (0.9% NaCl, 0.1% $CaC1_2$, and 0.25% $NaHCO_3$), high-temperature drying, and ambient rest followed by a cycle of humidity exposure, high-temperature drying, and ambient soak. Standardized calibration coupons are run concurrently to ensure compliance with specified tolerances. The previously described process repeated 80 times is informally claimed by industry to represent 10 years of field exposure in South Florida.

The Prohesion test is another cyclic corrosion test developed by the paint industry to improve correlation between actual environmental exposure and accelerated tests. The test is performed according to ASTM G85 annex A5.13. Specimens are alternatively exposed to 1-hr intervals of salt fog followed by dry off. The solution for the salt fog is 0.05% NaCl and 0.35% ammonium sulfate. The test must be run for a minimum of 336 hours at which point specimens are evaluated and a decision is made about continuing the test. The data generated by this test will be compared to the exposure test data.

Because the failure modes in accelerated corrosion are varied, the panels are evaluated using a combination of three specifications. ASTM D 610 is used when corrosion products bleed through the coating at active corrosion sites. ASTM D 714 is used when corrosion products and water form a blister between the coating and the substrate. ASTM D 1654 is used to assess performance of the coating in the vicinity of a scribe through the coating system. All three standards use a 10-point scale for a rating system, and a score below 5 constitutes failure.

2.4.6 ADHESION TESTING

Painted adhesion testing was conducted by the tape adhesion method, in accordance with Method 6301 of FED-STD-141, and ASTM D 3359, Method A. This test method describes a procedure for evaluating the inter-coat and surface adhesion of an organic coating after water immersion, by applying pressure sensitive tape over a scribed area of the coating. In essence the test also provides a qualitative measure of the coating's ability to resist penetration by water. Coatings were evaluated after immersion in deionized water at room temperature for 24 hours, 120º F for 96 hours, and 150º F for 168 hours. Coupons are not disturbed for the duration of immersion. Two parallel lines were then scribed approximately one inch apart, making sure that the coating was scribed all the way through and into the substrate. Two angled "X" incisions were scribed through the coating across the parallel lines to create an "X" so that the smaller angle of the "X" was 30 to 45 degrees, making sure that the coating was scribed all the way through and into the substrate. Each line of the "X" was approximately 1.5 inches long. A piece of tape was immediately placed over the incisions parallel to the parallel scribe lines, and smoothing the tape with one pass of a 3-lb roller. The tape was then removed rapidly by hand at approximately a

180-degree angle. The incision area was then inspected for damage and rated according to ASTM D 3359.

Pull-off adhesion measurements will be performed in accordance with ASTM D 4541 using an Elcometer Model 108 Hydraulic Adhesion Test Equipment (HATE). In addition to being a more quantitative adhesion test method, pull-off adhesion, especially the hydraulic based devices, is also less prone to human bias in testing such as variations in pressure applied during scribing as well as interpretation and perception of results. For the pull-off adhesion test, a loading fixture commonly referred to as a "dolly" is secured normal to the coating surface using an adhesive. After allowing the adhesive to cure for 24 hours at ambient conditions, the attached dolly is inserted into the test apparatus. The load applied by the apparatus is gradually increased and monitored on the gauge until a plug of coating detaches. The failure value (in psi) and the failure mode is then characterized and recorded. For the pull-off test to be valid, the specimen must be of sufficient thickness to ensure that the coaxial load applied during the removal stage does not distort the substrate material and cause a bulging or "trampolining" effect. On a thin specimen, the resultant bulge causes the coating to radially peel away outwards from the center instead of uniformly pulling away in pure tension and thus results in significantly lower readings than for identically prepared thick specimens. The minimum substrate thicknesses allowable would be 3/16" and 1/8" for aluminum and ferrous substrates respectively. An adhesion measurement sampling of at least 30 for each coating type is recommended for obtaining the optimum data.

2.4.7 MILITARY SPECIFICATION TESTING OF CARC FORMULATIONS

Cold rolled steel panels and tin plated steel Q panels were coated with ~1 mil primer (typically MIL-P-53022) followed by ~2 mil topcoat (typically MIL-DTL-53039 or MIL-DTL-64159). Panels were tested according to military specifications to ensure compliance of coating formulations using experimental additives. Specular reflectance (gloss) measurements were made in accordance with ASTM D 523 using BYK Gardner GB4606 Haze-Gloss Reflectometer. Measurements were taken at 60° and 85° incidence. Spectral reflectance (color) measurements were performed using a Cary 5000 UV-Vis-NIR spectrophotometer with an integrated sphere. Dry film thickness was measured according to ASTM D 1005 using an Elcometer coating thickness gauge. The adhesion of coating to the metal substrate was tested using ASTM D 3359. Solvent resistance was determined according to ASTM D 5402 by MEK double rub. A QUV cabinet was used to test for UV resistance of the coating film, and the testing cycle was UV-A lamp exposure at 60°C for 8 hours and 4 hours condensate at 50°C. ASTM D 1308 involves exposing an organic coating to a reagent to determine adverse affects. The coated panels were immersed halfway in de-ionized water or JP-8 fuel at room temperature (23 ± 5°C) for 7 days. The panels were examined for any defects, such as blistering, loss of adhesion, color and gloss change immediately upon removal and after a 24-hour recovery period. The Mandrel Bend Test was performed on all coatings in accordance with ASTM D 522. The purpose of this test is to rate each coating's flexibility and resistance to cracking. The standard test for resistance to deformation (impact), ASTM D 2794 was performed using an Impact Tester on the reverse side of the painted panel.

2.4.8 CHEMICAL AGENT TESTING

Select chemistries were subjected to chemical agent resistance testing (specifically Mustard and Nerve agents). The test evaluates the ability of the coating to resist absorption of live agent and

the effectiveness of subsequent decontamination with Super Tropical Bleach (STB). The pass/fail limits are 180 μg/cm^2 and 40 μg/cm^2 respectively. Testing protocol is provided.

Army Chemical Agent Resistance Test Protocol

Test Procedure: Place a 5 cm^2 circular template on the area of the test panel to be contaminated with agent. Use a grease pencil to mark a circle around the template; the grease mark serves to keep the agent from spreading out of the designated area. Place 50 microliters of agent HD or GD on the test area. Place a glass cover slip (microscope slide) over the test area to minimize evaporation of the agent. After 30 minutes remove the cover slip, rinse the agent from the panel with isopropanol and allow to air dry for approximately 45 seconds. Place the panel in the test cell, which has been maintained at 25 °C (77 °F), with the coated area positioned such that the nitrogen stream shall pass across the contaminated area. Nitrogen is used instead of air to eliminate the possibility of reaction of the desorbed agent over the time of the test, which is 22 hours. Pass the nitrogen through an impinger containing the appropriate solvent, n-decane for HD and iso-octane (2, 2, 4-trimethylpentane) for GD. The flow of nitrogen shall be maintained at 0.252 grams/minute across each sample. Terminate the test at the end of 22 hours.

Analysis: Transfer the contents of each impinger to a 25 ml volumetric flask. Rinse the impinger twice with the same solvent and add the rinse to the flask. Bring the volume up to the mark with solvent and mix well. Transfer a 1 ml portion to a GC vial for analysis. Perform the analysis on a Finnigan-MAT GQC ion-trap mass spectrometer equipped with a 25 m MS-5 capillary column, using helium as the carrier gas. Standardize the mass spectrometer by serial dilutions of an agent solution in the appropriate solvent, analyzed in the same conditions. The instrument conditions are as follows: introduce the samples from as AST 2000 auto-sampler, volume of 1 microliter onto the GC column in splitless mode; injector temperature of 280 °C (536 °F). Temperature program the column from an initial temperature of 50 °C to 120 °C (122 °F to 248 °F) at a rate of 10°/minute; followed by an increase of 25 °C/minute (77 °F/minute) to a final temperature of 200 °C (392 °F). Acquire mass spectra in electron impact mode over the mass rage of 50-150 for HD and 50-200 for GD. Under these conditions, HD has a retention time of 8.15 minutes. Integrate the peak areas of the relevant portion of the reconstructed ion chromatograms for the ion at m/z 109. Under the cited conditions GD elutes as a pair of completely resolved diastereomeric enantiomers with retention times of 9.56 and 10.04 minutes. Integrate peak areas of the relevant portion of the reconstructed ion chromatograms for the ion at m/z 99. Construct the standard response curve for HD and GD using the integrated area on the y axis and concentration (μg/ml) on the x axis. Use the linear regression analysis function of an Excel spreadsheet, which shall calculate the slope, intercept, and correlation coefficient of the standard response curve. The slope and intercept of the standard response curve are used to calculate concentration of agent HD or GD in the impinger solutions. Calculate the total amount of agent (in micrograms) that outgassed from the CARC panel by multiplying the concentration of agent in the impinger solution (micrograms per milliliter read from the standard curve) by volume of the impinger solution (25 ml).

3 Results & Discussion

3.1 Trivalent Chromium Process and Non-Chromium Process

TCP and CFP are NAVAIR developed chemistries that are replacements for chromated sealers, post-treatments, and conversion coatings. The majority of conversion coating work thus far has focused on the use of TCP and CFP on aluminum alloys, sacrificial coatings, and as a sealant on anodized coatings with extremely promising results. However, further development must be done for use on steels, magnesium alloys, and phosphated surfaces where corrosion protection is deeply needed. One of the key advantages to TCP and CFP is that the processing and maintenance requirements are similar to currently used technologies, thus making them favorable alternatives for depots and OEMs. This transition eliminates the need for additional training of personnel and large equipment purchases. TCP is based on a fluorozirconate complex with a trivalent chromium salt. TCP contains significantly less total chromium than the current hexavalent chromium conversion coatings and has no hexavalent chromium. CFP has the added advantage of containing no chromium. The use of TCP and CFP eliminates personnel exposure to hexavalent chromium saving labor and reporting costs associated with PPE and worker safety regulations. Additionally, it saves time and money by eliminating the need to treat the waste stream for hexavalent chromium.

Baseline TCP is designated as TCP-S. This is self-buffering (hence –S for stabilized) chemistry based on two anionic complex fluorometallates (K_2ZrF_6, KBF_4), and a semi-covalently bound trivalent chromium basic (hydroxide ligand branched) sulfate species (BCS). Through our efforts, and reference electrochemical analyses, we believe that the TCP-S forms a mostly zirconium oxide/fluoride, chromium oxide conversion coating with the aluminum alloy surface. Previous work has been conducted on hexavalent chromium films, suggesting a film backbone consisting of polymerized trivalent chromium hydroxide species, with a loosely hydrogen-bonded active chromate inhibitor species. Chromate films tend to be very thin over precipitates and inter-metallics, only releasing the inhibitor species after the film has broken down and substrate metal is exposed. Electrochemical evidence suggests that the TCP forms a much more uniform film thickness across these inter-metallic sites, with improved barrier coating properties from the denser zirconium oxide, and localized corrosion inhibition through the ability of the trivalent chromium species to bind up attacking anions, such as chloride.

Selected additives were characterized for aqueous solubility by dissolving serial additions in de-ionized water at ambient laboratory temperatures by mechanical stirring. The necessary mixing times for particulates to fully disperse and for subsequent solution clarity were recorded. Solubility limits were determined by dissolving serial additions of the additives in 150 $^{\circ}$F de-ionized water until visible particulates would not disperse after mixing overnight, then allowed to cool to room temperature. The undissolved solid was then collected, dried and weighed to determine the weight/volume concentration at the solubility limit. Multiple solutions of modified TCP and CFP are then prepared at various concentrations of the additive and then evaluated for constituent reaction, precipitation, storage and light stability, and compatibility with mixed-metal substrates. Test specimens are then coated with the modified solutions to characterize the speed and uniformity of the film formation and reaction by-products. Coated specimens are visually evaluated for color, uniform coating deposition, and pitting or substrate corrosion during surface finishing. Different combinations of promising additives are then evaluated for synergistic or detrimental effects on solution and film formation properties.

Modified chemistries are then characterized for corrosion and adhesion performance of the deposited coatings. Cationic transition and refractory metal salts were evaluated for improved corrosion performance to the baseline TCP or for novel CFP chemistries. These additives included cationic zinc, cerium, cobalt, hafnium, and iron compounds. Complex anionic species based on molybdates, tungstates, borates, silicates, phosphates, manganates, and titanates were also evaluated individually and for synergistic effect with the fluorozirconate and fluoroborate species. Additional efforts were made to synthesize basic metallic sulfate and nitrate compounds to mimic the coordination chemistry of the organometallic trivalent chromium species used in the TCP.

Two modifications have been made to the TCP chemistry, one that incorporates a visible color in the film in the form of a cationic zinc compound, and a second that incorporates an organic inhibitor species. The best results to date for corrosion protection have come either from the use of the organic inhibitor species in conjunction with the baseline TCP-S (this modified coating has been labeled TCP-I), or from the use of the organic inhibitor in conjunction with the zinc color additive (this coating has been labeled TCP-IC). Initial formulation of the TCP-C in 2003 yielded a mottled bluish-purple coating that had improved bare corrosion performance as a conversion coating on aluminum alloys versus the baseline TCP. Since then, additional immersion and spray processing evaluations have been unsuccessful in validating these performance gains. The TCP-C became an option only for lower corrosion risk alloys such as 5000-seies and 6000-series aluminum or for post-treatment and sealing applications. The trade-off for conversion coatings became reduced corrosion performance to gain visible color change for quality control benefits. The TCP-C yielded improved performance over the baseline TCP as a seal for phosphoric acid anodizing (PAA). PAA sealed with TCP-C for 10 minutes at 150 °F yielded 1,000 hour B 117 performance. This was hypothesized to be due to zinc phosphate formation. Combining the TCP-C with the "I" additive yielded dramatically improved bare corrosion performance for conversion coating aluminum alloys, however the processing conditions had to be controlled very precisely.

Recent studies conducted jointly with SurTec International (International TCP licensee) have begun revalidating the initial 2003 test results. All of the subsequent work since then overlooked a supposed "optimization" made to the bath make up procedures to impart uniform color change to the surface of the as-deposited coating. The modification was made to the order of addition in mixing procedures causing the color change film to have a uniform brown-purple coloration. It was not noted until recently that this change could be directly linked to the lowered corrosion performance. It is now believed that it is critical for the fluorometallate species to have adequate time to complex with the hydrated basic chromium sulfate before addition of the color and inhibitor species. Returning to the original mixing procedures has once again yielded mottled bluish-purple coatings with improved bare corrosion performance.

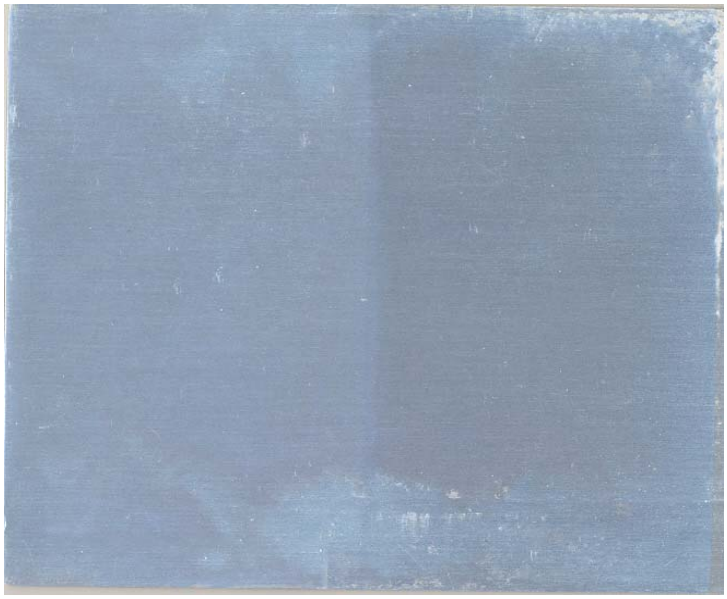

Figure 12: Improved corrosion protection of TCP-C AA2024-T3 panel after 500 hrs. ASTM B 117

This is especially important as the observed bare corrosion improvement is not as sensitive to process conditions in terms of etching and deoxidizing when compared to the baseline TCP or the TCP-I/IC. As reported by Buchheit [21], release or presence of Zn^{2+} has been shown to suppress the cathodic reaction kinetics in the oxygen reduction reaction (ORR) during corrosion. The cathodic inhibition is not nearly as potent as that afforded by chromates but can provide secondary corrosion protection when added in such a way that it does not affect the proper formation of the baseline TCP film.

Potential additives were identified and screened for functionality in solution stabilization, surface activity, film coloration, corrosion inhibition and adhesion promotion. Performance properties were tested for the following surface treatments: Alodine 1200S, Alodine 5700, CFP, CFP-I, TCP, TCP-I, and TCP-IC. These coatings were tested bare and in conjunction with low and zero VOC epoxy and polyurethane paint systems. See

Table 4 for a description of the surface treatments evaluated.

Table 4: Surface treatments evaluated

Process Chemical	**Description**
Alodine 1200S	Chromated conversion coating for aluminum and its alloys
Alodine 5700	Chromium-free, titanium-based conversion
CFP	Zirconium and zinc conversion coating
CFP-I	Zirconium and zinc conversion coating containing an organic corrosion inhibitor additive and color change additive
CFP-Z	Based around the barrier properties of zirconium oxide films, no heavy metals
CFP-A	Aluminum-based conversion coating
TCP-S	Trivalent chromium and zirconium conversion coating
TCP-I	Trivalent chromium and zirconium conversion coating containing an organic corrosion inhibitor additive
TCP-IC	Trivalent chromium and zirconium conversion containing an organic corrosion inhibitor and a cationic zinc color change additive

The baseline CFP formulation is in the process of transitioning to a commercially available product for anodize sealing and post-treatment of aluminum and zinc-based sacrificial coatings. However, the baseline CFP does not currently provide adequate performance for Class 1A or Class 3 conversion coating on aluminum alloys. Additionally, the TCP formulations still yield improved head-to-head performance across the gamut of metal finishing applications.

Newer CFP chemistries have been developed in an attempt to improve overall corrosion resistance and in particular conversion coated aluminum applications. Work in 2007 focused on refractory metal chemistry and corrosion inhibiting organic acids. CFP-Z is a formulation based around the barrier properties of zirconium oxide films. It contains no heavy metals, but does not require any of the special application concerns associated with organic surface preparations. CFP-Z has yielded greater than 720 hours of B117 bare corrosion testing on AA6061-T6, however has limited protection on AA2024-T3. Incremental improvements have been realized for conversion coating 2024 compared to baseline CFP.

Figure 13: Corrosion protection of CFP-Sal (left), CFP-Z (center), and CFP (right) on AA2024-T3 after 48 hrs. ASTM B 117

Figure 14: Improved corrosion protection of CFP-Z on AA6061-T6 after 672 hrs. ASTM B 117

To date, CFP-A, an aluminum-based conversion coating, has been unsuccessful due to bath stability issues. Work is currently underway with several surfactants to create lipophilic-in-hydrophilic emulsions for organic and organometallic inhibitors to address this issue. Current efforts are focusing on inhibiting the ORR at secondary phase inter-metallic particles.

Organic inhibitor evaluations have focused on short chain carboxylic inhibitors but have proved un-successful in acid form. The resulting chemistry primarily forms an etchant solution, with little to no coating deposition. Current efforts are focusing on producing organometallic salts from these acids.

3.2 Pretreatment Testing

3.2.1 ALUMINUM SUBSTRATES

The TCP-I and TCP-IC were evaluated in B 117 salt fog testing for painted corrosion performance under MIL-SPEC qualified solvent and water-reducible chromated and non-chromated epoxy primers, with and without a standard solvent-reducible, high-gloss polyurethane topcoat, on AA2024T3. Both the baseline TCP and a standard chromated conversion coating were used as controls. The TCP-I and TCP-IC were also evaluated in ASTM G 85 Annex 4 (sulfur dioxide acidified salt fog) testing for painted corrosion performance. Traditionally, SO_2 testing is conducted for 500 hours, as it is a much more aggressive environment than the neutral salt fog test. However, previous work by NAVAIR has shown that fully non-chromated coating systems, i.e., no Cr(VI) in either the pretreatment or the primer, often exhibit significant field blistering at 700-800 hours of exposure. This effect is not seen when some chromate is present in the system. Painted corrosion specimens were visually evaluated for scribe creep, blistering, peeling, and corrosion product in the scribe at 500 or 1,000 hr intervals. Specimens were run to failure against chromated and baseline TCP controls.

The chromate control coating performed slightly better than the baseline TCP control, but both coatings performed similarly well across all the painted corrosion tests, i.e., ASTM B 117 or ASTM G 85 Annex 4, whether they were topcoated or not.

Figure 15 shows the relative performance of the TCP under chromated and non-chromated MIL-PRF-23377 primers on AA2024-T3 after 3,000 hours.

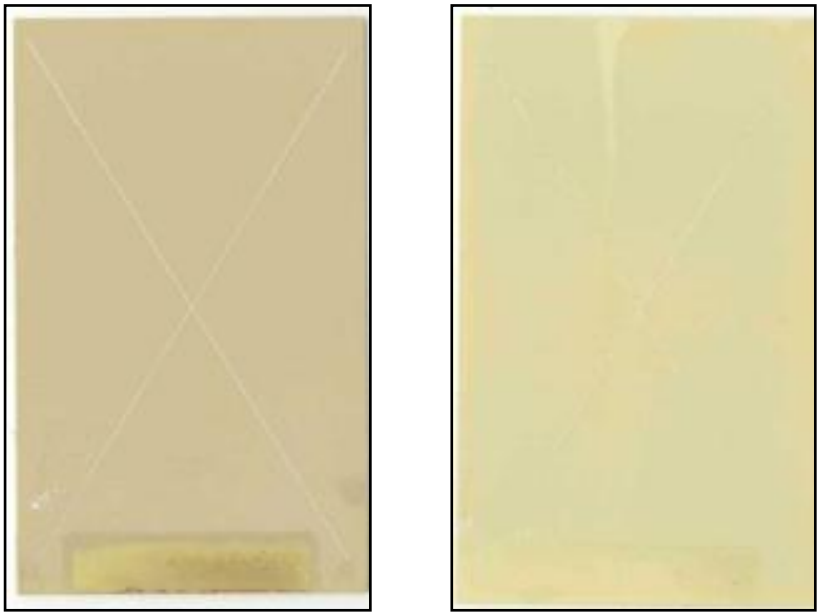

Figure 15: AA2024-T3 TCP with Hentzen MIL-PRF-23377 Class C2 (left) and Class N (right)

These systems were tested in conjunction with MIL-PRF-85285, Type I, Class H polyurethane topcoats. The fully non-chromated system performed well in extended B 117 testing but did not perform equivalently to the chromated systems. Figure 16 shows AA2024-T3 with fully, partially, and non-chromated systems after 5,000 hours B 117 exposure.

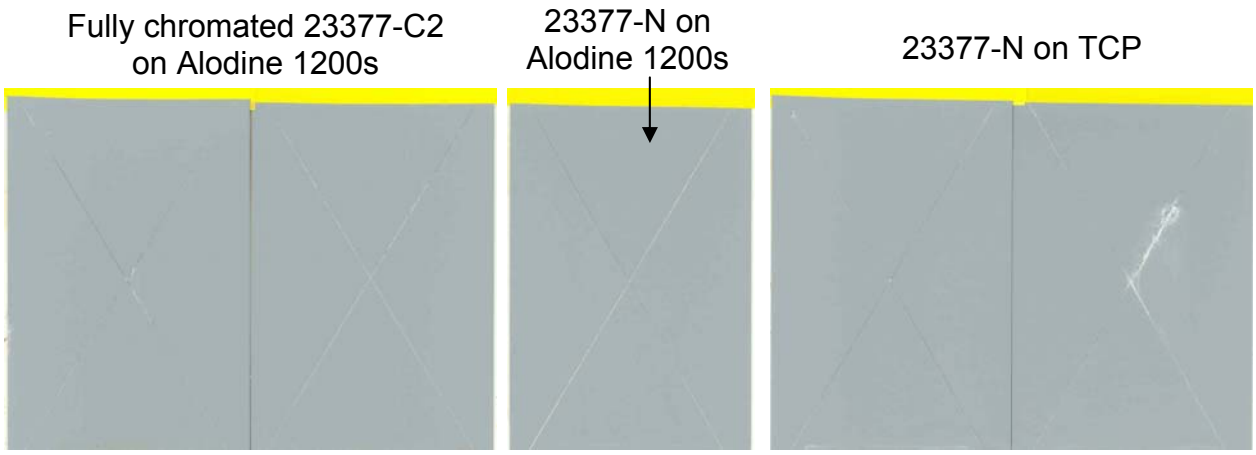

Figure 16: AA2024-T3 with MIL-PRF-23377 and MIL-PRF-85285

3.2.2 STEEL AND ZINC-COATED STEEL

Spray-applied zinc phosphate pretreatment typically results in good corrosion performance for most Army equipment/platforms. However, in a number of cases (for example the MRAP and Stryker, which use high hard steel (MIL-A-46100) and have no pretreatment) the corrosion performance is poor. In these cases where better corrosion performance is desired, a number of promising coatings have been assessed in the laboratory. The following systems require additional demonstration and validation on Army and Navy systems before they can be implemented:

1) Phosphated steel which is "rinsed" or post-treated with trivalent chromium (TCP) or the chromium free process (CFP).
2) Steel which is pretreated directly with TCP or CFP.
3) Aluminum which is pretreated with TCP or CFP.
4) Anodized aluminum which has been sealed with TCP or CFP.

Each of the above systems will be tested with non-chromated low or ZVOC primer and topcoated with low or ZVOC topcoat

Legacy efforts have focused on optimizing the baseline TCP process for use on zinc-based sacrificial coatings for steel alloys. This work was conducted as part of NAVAIR's Y0817 Environmental Program. The TCP post-treatment performed better than the industrial tri-chrome process recommended by the automotive industry for bright zinc plating but still not equivalently to the chromate post-treatment. Figure 17 shows 4130 steel specimens with bright zinc plating

that have been post-treated with the automotive tri-chrome process, the TCP, and a standard dichromate process.

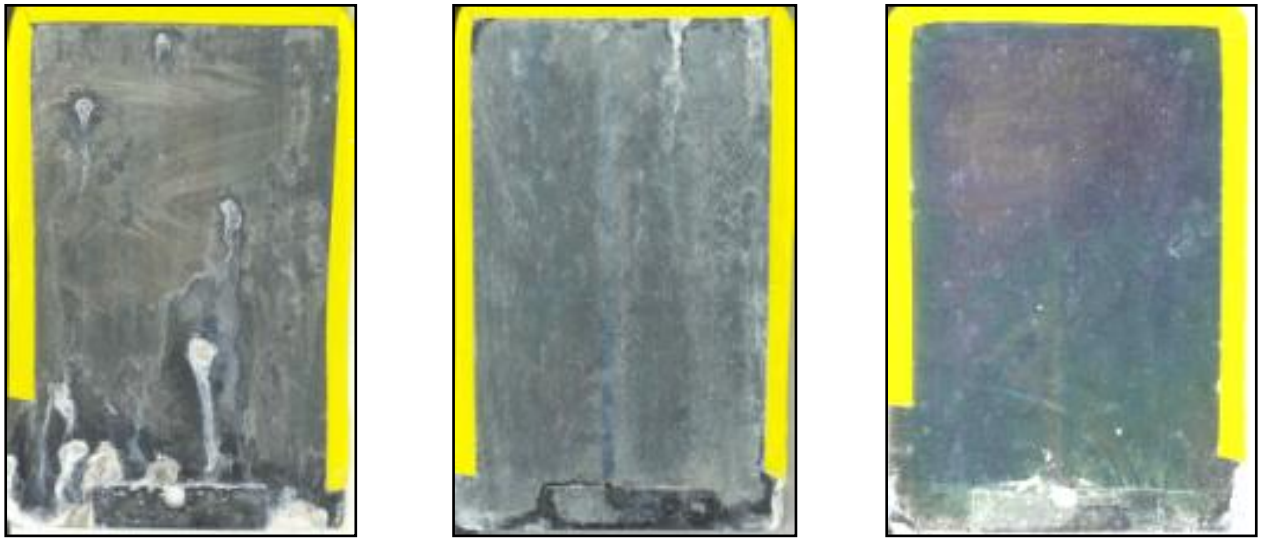

Figure 17: Bright zinc-plate 26 days B 117 exposure with automotive tri-chrome, TCP, and dichromate post-treatment (left to right)

The TCP exhibited more surface staining and some white corrosion product while the dichromate post-treatment had a few discrete white corrosion areas. The specification requirement was for 96 hours B 117 no white rust and 168 hours no red rust. Although all three post-treatments far exceed the specification requirement, the TCP and the dichromate are clearly superior to the automotive tri-chrome process. Additional optimization of the process and characterization of modified chemistries are needed for the TCP to meet equivalence with the dichromate post-treatment.

Additionally, the TCP and CFP formulations have shown good promise for Cd/Cr^{6+} free systems, when used over ZnNi and Zn-phosphate coatings. The TCP and CFP formulas are used to post-treat the ZnNi plating in lieu of standard chromate post-finish. Performance is generally equivalent to chromate rinsing for both corrosion and adhesion testing.

More recent work with NAVSEA and CTC Inc. has shown excellent promise for using TCP and CFP in lieu of chromates for phosphate rinsing [22]. TCP was applied over a zinc-phosphate coating for use on steel and plated steel surfaces. Coating stack-ups were then evaluated for corrosion and paint adhesion performance. TCP adhered well to the phosphated surface yielding excellent adhesion and torque values. Additional work is underway to optimize TCP and CFP for rinsing phosphate coatings directly applied to steel substrates. Current results have led to the implementation of TCP-rinsed phosphated ZnNi plating on steel actuator devices for NAVSEA. The adhesion testing shows the TCP rinse to be equivalent to chromate rinsing on phosphates. However, follow-up bare corrosion testing must still be conducted to compare TCP and CFP to chromate rinsing on zinc and manganese phosphates. This unique coating stack-up was implemented as a direct replacement for chromate post-treated cadmium plating since TCP post-treated ZnNi on steel did not yield equivalent performance to chromate post-treated cadmium plated steel in bare corrosion testing. However, chromate post-treated ZnNi on steel also does

not yield equivalent performance to chromate post-treated cadmium on steel. This coating stack-up provides a completely environmentally preferred coating system with equivalent or better corrosion and adhesion performance when compared with the Cd/Cr^{6+} control system. Previous NAVSEA testing showed good head-to-head performance for TCP post-treated ZnNi versus chromate post-treated ZnNi under neutral salt fog accelerated corrosion testing (Table 5).

Table 5: Time (hours) before failure (red rust visible) under neutral salt fog accelerated corrosion testing

	Sample	#1	#2	#3	Avg
Scribed	None	48-72	72-192	72-192	64
	Alodine 1200S	72-192	72-192	192-216	112
	TCP w/color	720-768	768-840	840-936	776
	TCP w/color 2	600-672	720-768	768-840	696
	CFP	216-288	216-288	288-336	240

It should however be noted that these evaluations were conducted as add-ons to IVD aluminum testing and therefore did not utilize chromate post-treatment chemistry optimized for zinc-based coatings. Field evaluations are currently underway for ZnNi and TCP post-treated ZnNi, therefore additional evaluation is not planned as part of this effort.

Work has been done to develop the TCP and CFP formulas for conversion coating directly to steel substrates. This is a novel application as there is currently no conversion coating analog for steel surfaces as there is for pretreating aluminum surfaces. The intent of the TCP or CFP conversion coating on steel is to provide flash-rust inhibition for steel substrates between surface preparation and painting operations. Currently an organic-based temporary coating is applied to prepared steel surfaces that must be removed prior to primer application. The TCP or CFP provides a permanent surface conversion that functions to inhibit flash-rusting while promoting subsequent adhesion of organic coatings, thus eliminating the additional production step. The as-deposited coatings range in color from dark grey to bluish purple depending on surface morphology and pre-conversion surface preparation. As seen in Figure 18 through Figure 20, both CFP and TCP provide a visibly colored protective coating against flash-rusting. Test specimens were prepared either by solvent wiping with acetone or grit-blasting with alumina and either force-dried using compressed air or allowed to dry at ambient conditions. Rusting is apparent on the uncoated portions of the test specimens that were allowed to dry at ambient laboratory conditions following processing. Some rusting is also apparent on the uncoated portion of the grit-blasted panel that was force-dried with compressed air.

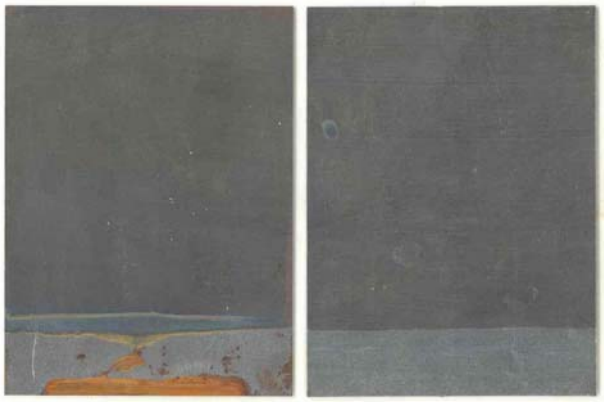

Figure 18: CFP on acetone wiped 4130 steel – air-dried (left) and force-dried (right)

Figure 19: CFP on alumina-blasted 4130 steel – air-dried (left) and force-dried (right)

Figure 20: TCP on alumina-blasted 4130 steel – air-dried (left) and force-dried (right)

Forced air-drying helped protect the uncoated portions from rusting but reduced the visible color change of the deposited coating. No noticeable differences were seen between the two drying methods for subsequent flash-rust inhibition of the coated specimen area.

Paint adhesion and painted corrosion test specimens were prepared in the same manner. Control panels were prepared by solvent wiping or blasting followed by direct-to-metal primer application. Test specimens were painted with a Sherwin-Williams primer conforming to MIL-P-53022 at 1 mil DFT and allowed to cure for 14 days at ambient conditions. Painted corrosion panels were scribed and racked at 15 degrees from the perpendicular and placed in ASTM B 117 neutral salt fog for 168 hrs. Figure 21 through Figure 23 show the relative performance of TCP and CFP coated surfaces compared to solvent-wiped and grit-blasted direct-to-metal controls.

Figure 21: Grit-blasted 4130 steel with TCP/MIL-P-53022 – 168 hrs. B 117

Figure 22: Grit-blasted 4130 steel with CFP/MIL-P-53022 – 168 hrs. B 117

Figure 23: Grit-blasted (left) and acetone-wiped (right) 4130 steel control with MIL-P-53022 – 168 hrs. B 117

Seven-day wet tape adhesion (WTA) tests were performed at 66°C in accordance with ASTM D 3359. Figure X shows the relative performance of TCP coated surfaces compared to solvent-wiped and grit-blasted direct-to-metal controls.

Figure 24: 7-day WTA testing of Acetone-Wipe (left), Grit-Blast (center), and Grit-Blast/TCP (right) on 4340 with MIL-DTL-53022 Type I

Both the TCP and CFP conversion coated surfaces performed better in corrosion testing than the mechanically prepped surfaces alone. Further coating composition analysis and process optimization is needed to understand the film-formation and corrosion protection mechanisms of these coatings on steel alloys. Formulation modifications incorporating phosphate and phospho-functional anionic inhibitor species is planned for CFP and TCP coatings on steel.

Follow up efforts to optimize TCP for conversion coating steel did not yield any additional performance improvements. Addition of phosphate and phosphonate functional inhibitors destabilized the bath chemistry so that a cascading precipitation reaction was set off during processing.

Conversion Coating Optimization of 4130 Steel with TCP and CFP

TCP and CFP conversion coatings were examined on 4130 steel panels for possible improvement over currently used grit blast only method. The test panels were processed using the various methods listed in Table 6.

Table 6: Process Variations for Conversion Coating 4130 Steel Panels

Processing Variation Number	**Processing Variation Description**
1	Acetone wipe only
2	HTC only
3	Acetone wipe/HTC
4	Acetone wipe/HTC/10% Sulfuric Acid Etch
5	Grit Blast only
6	Grit blast/Acetone wipe
7	Grit blast/Acetone wipe/HTC
8	Grit blast/Acetone wipe/HTC/10% Sulfuric Acid Etch

A 25% SurTec 650 solution was used for TCP. Test panels were evaluated for in neutral salt fog (ASTM B 117), humidity testing, and flash rusting. The neutral salt fog and humidity panels were exposed within the test chamber for one hour. The TCP flash rust panels were exposed to ambient laboratory environmental conditions for 7 months and the CFP for 7.5 months. Figure 25-Figure 30 show the best and worst test panels from neutral salt fog, humidity, and flash rust testing.

Figure 25: CFP on 4130 Steel after 1 Hour Humidity Testing – Best Processing Variation (#2 – left) and Worst Processing Variation (#4 – right).

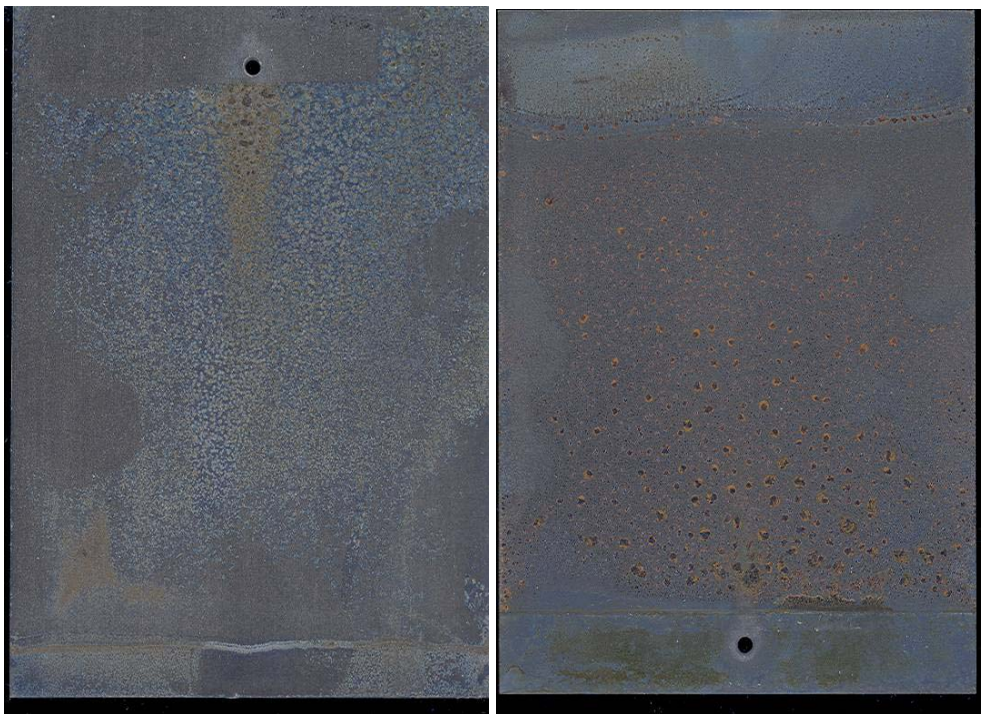

Figure 26: TCP on 4130 Steel after 1 Hour Humidity Testing – Best Processing Variation (#1 – left) and Worst Processing Variation (#8 – right).

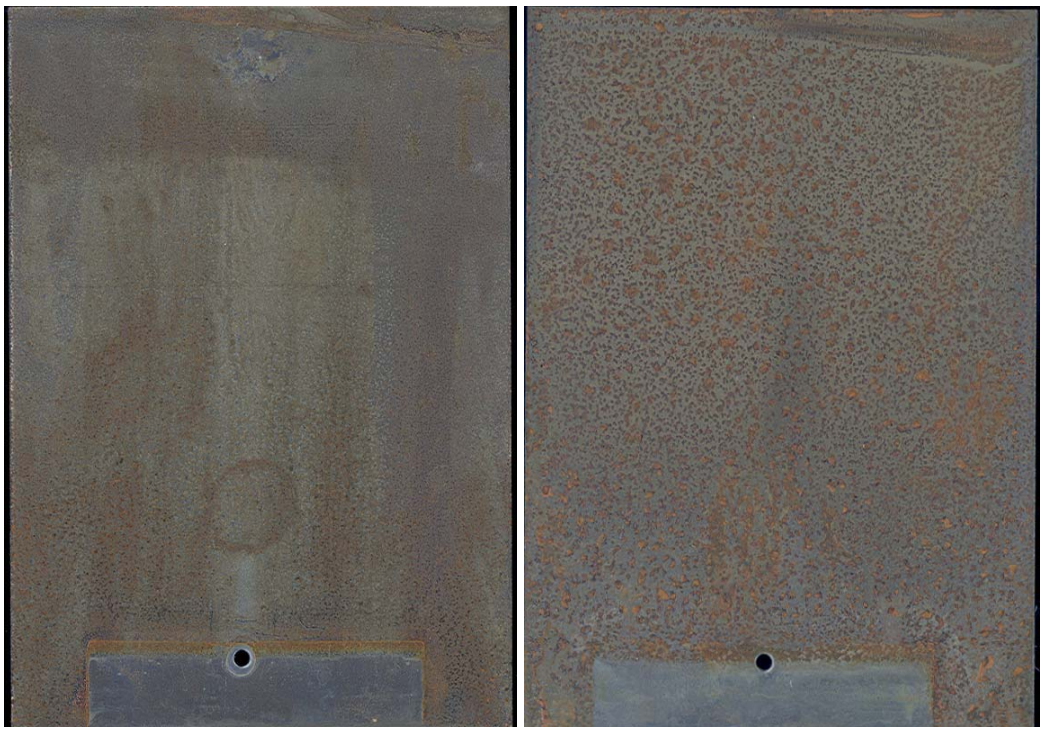

Figure 27: CFP on 4130 Steel after 1 Hour ASTM B 117 Testing – Best Processing Variation (#1 – left) and Worst Processing Variation (#4 – right).

Figure 28: TCP on 4130 Steel after 1 Hour ASTM B 117 Testing - Best Processing Variation (#3 – left) and Worst Processing Variation (#4 – right).

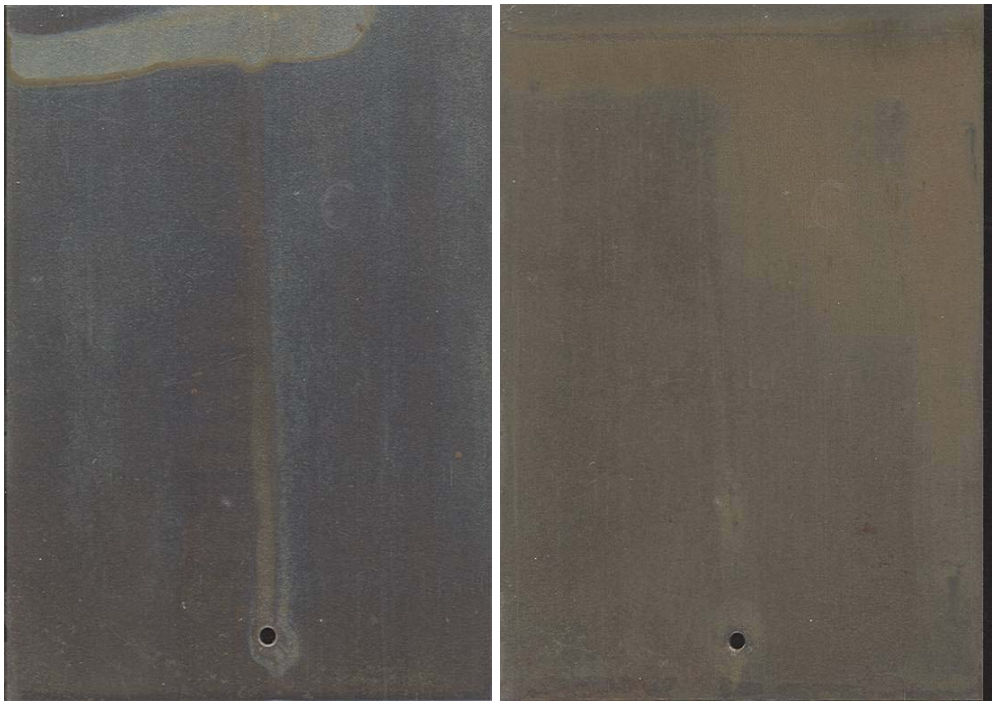

Figure 29: CFP on 4130 Steel after 4344 Hours Flash Rust Testing – Best Processing Variation (#3 – left) and Worst Processing Variation (#2 – right).

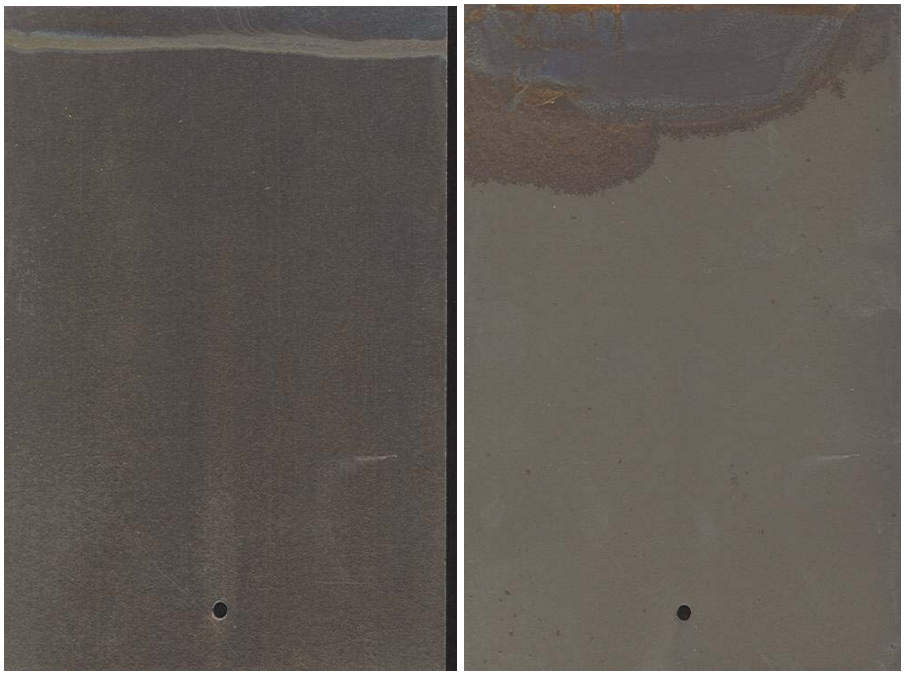

Figure 30: TCP on 4130 Steel after 3864 Hours Flash Rust Testing – Best Processing Variation (#3 – left) and Worst Processing Variation (#5 – right)

Test results are shown in Table 7. Each color-coded block represents a test panel with green indicating the best performance, yellow indicating moderate panel performance, and red indicating the worst performance.

Table 7: Unpainted TCP and CFP Results for ASTM B 117, Humidity, and Flash Rust Testing

Process Method Number	CFP B117		CFP Flash Rust		CFP Humidity		TCP B117		TCP Flash Rust		TCP Humidity	
1												
2												
3												
4												
5												
6												
7												
8												

The best processing variations for non-painted TCP and CFP on steel were:

- Acetone Wipe
- Grit Blast

Additional test panels were processed in accordance with Table 8 to determine which variation performed best in combination with the use of primer.

Table 8: Process Variations for Conversion Coating 4130 Steel Panels with Primer

Processing Variation Number	Processing Variation Description
1	Grit Blast only
2	Grit Blast/ Acetone Wipe
3	Grit Blast/HTC
4	Grit Blast/ 10% Sulfuric Acid Etch
5	Grit Blast/ HTC/ 10% Sulfuric Acid Etch
6	Grit blast/Acetone wipe/ HTC
7	Grit blast/Acetone wipe/10% Sulfuric Acid Etch
8	Grit blast/Acetone wipe/HTC/10% Sulfuric Acid Etch

The 4130 steel panels were primed with MIL-PRF-23377, Class N by Deft at a 1.5 mil thickness. Half of the test panels were put into neutral salt fog, and half were used for 4-day wet tape adhesion (WTA) testing in accordance with ASTM D 3359. Figure 31 and Figure 32 show the best and worst test panels from neutral salt fog testing.

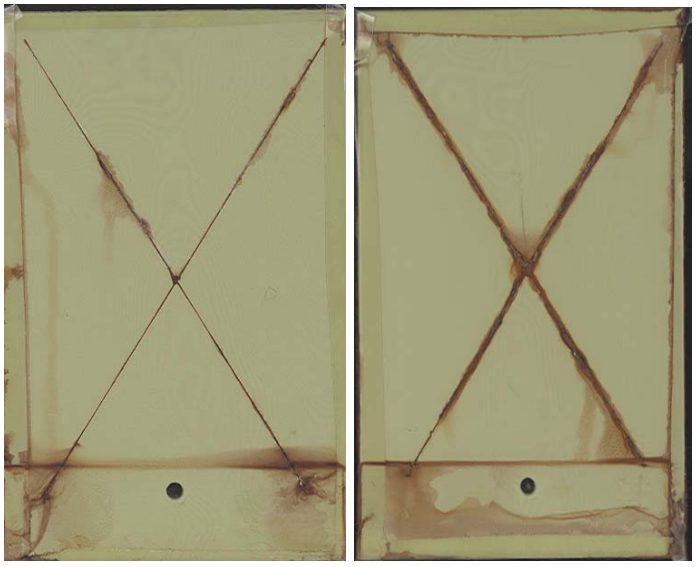

Figure 31: CFP on 4130 Steel with MIL-PRF-23377, Class N after 168 Hours Neutral Salt Fog Testing – Best Processing Variation (#1 – left) and Worst Processing Variation (#3 – right).

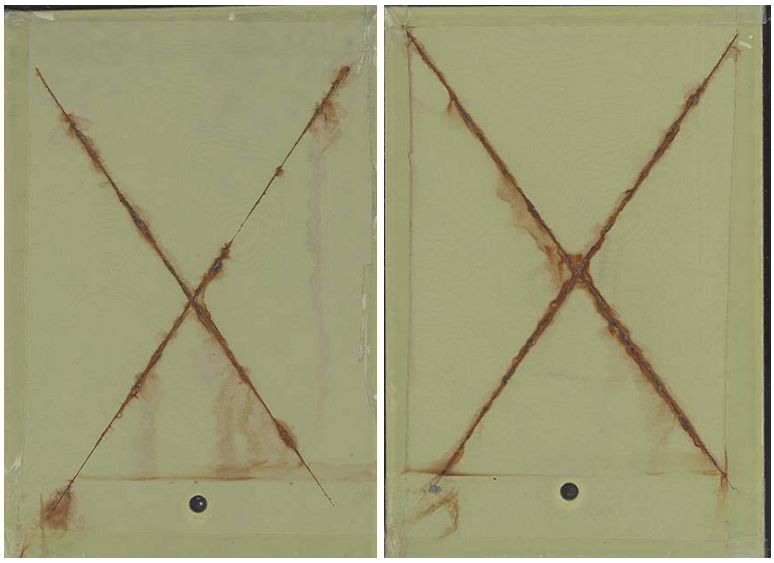

Figure 32: TCP on 4130 Steel with MIL-PRF-23377, Class N after 72 Hours Neutral Salt Fog Testing – Best Processing Variation (#7 – left) and Worst Processing Variation (#2 – right).

Results are shown in Table 9. Once again, each color-coded block represents a test panel with green indicating the best performance, yellow indicating moderate panel performance, and red indicating the worst performance.

Table 9: TCP and CFP with MIL-PRF-23377, Class N Results for ASTM B 117 and Wet Tape Adhesion Testing

Process Method Number	TCP 4-Day WTA		TCP B117 (72 hr)		CFP 4-Day WTA		CFP B117 (168 hr)	
1								
2								
3								
4								
5								
6								
7								
8								

The best processing variations for TCP and CFP on steel in conjunction with a primer were:

- Grit Blast, HTC
- Grit Blast, HTC, 10% Sulfuric Acid
- Grit Blast, Acetone Wipe, HTC
- Grit Blast, Acetone Wipe, 10% Sulfuric Acid

SurTec 617 Tri-Cationic Phosphating Solution Optimization of 1020 Steel

SurTec 617 is a tri-cationic phosphating solution containing zinc, calcium, and manganese that was examined using 1020 steel for performance in conjunction with various seals. SurTec 650 (TCP), CFP, and SurTec 580 were selected for use as corrosion protection post-treatment seals. SurTec 580 (ChromiPhos is a trivalent chromium passivation solution commonly used as a post-treatment for phosphating prior to painting. The use of a grain refiner was also evaluated. SurTec 610V is a grain refiner used prior to zinc phosphating that produces uniform and well adherent zinc phosphate layers.

All 1020 steel test panels went through the following degreasing method:

a. PD-680 Immersion & Brush Scrubbing
b. Isopropyl Alcohol Wipe
c. Acetone Wipe
d. Grit Blast

Test panels were then processed using the conditions outlined in Process Sequence A (Table 10):

1. 15% Potassium Hydroxide (104 – 176F) – 5 minutes
2. DI Water Rinse (ambient)
3. SurTec 610V (ambient) – 2 minutes
4. SurTec 617 (113 – 131F) – 5 minutes
5. SurTec 580/SurTec 650/ CFP-2 (68 – 104F) – 1 minute
6. DI Water Rinse (ambient)

Table 10: Process Sequence A Variations for Phospating 1020 Steel Panels

Process Sequence A Variations	**Process Sequence A Variation Descriptions**
1	Grit blast, 15% KOH, SurTec 617
2	Grit blast, 15% KOH, SurTec 610V, SurTec 617
3	Grit blast, 15% KOH, SurTec 617, SurTec 580
4	Grit blast, 15% KOH, SurTec 610V, SurTec 617, SurTec 580
5	Grit blast, 15% KOH, SurTec 617, SurTec 650
6	Grit blast, 15% KOH, SurTec 610V, SurTec 617, SurTec 650
7	Grit blast, 15% KOH, SurTec 617, CFP-2
8	Grit blast, 15% KOH, SurTec 610V, SurTec 617, CFP-2

The majority of the test panels from Sequence A formed a white residue and brown coloration on the panel surface immediately following processing. Sequence B was also included to determine if process variations could eliminate the white residue and brown coloration. Sequence B added a warm DI water rinse after the use of SurTec 617 and altered the initial DI water rinse step following KOH to be warm water. Decreased immersion time to comply with TDS recommendation and check time difference impact on results.

Sequence B varied from Sequence A as follows:

- DI water rinse after 15% KOH step changed from ambient to 80 – 95F.
- Warm DI water rinse (80 – 95F) added after the SurTec 617 step.

- Decrease in the immersion time of SurTec 580, SurTec 650, and CFP from 1 minute to 20 seconds.

Test panels were then processed using the conditions outlined in Process Sequence B:

1. 15% Potassium Hydroxide (104 – 176F) – 5 minutes
2. DI Water Rinse (80 – 95F)
3. SurTec 610V (ambient) – 2 minutes
4. SurTec 617 (113 – 131F) – 5 minutes
5. DI Water Rinse (80 – 95F)
6. SurTec 580/SurTec 650/ CFP-2 (68 – 104F) – 20 seconds
7. DI Water Rinse (ambient)

Results are shown in Table 11. Each color-coded block represents a test panel with green indicating the best performance, yellow indicating moderate panel performance, and red indicating the worst performance.

Table 11: Flash Rust Performance for Process Sequence A & B Variations

Process Sequence Variation	Sequence A			Sequence B		
1						
2						
3						
4						
5						
6						
7						
8						

Although most steel panels from Sequence A formed white residue and some brown coloration, there was no formation of rust. White residue was found on the test panels that did not use either the grain refiner or a post-treatment seal. The white residue and brown colorations were not limited to any specific process sequence variation as they were found across the board.

The best performing process sequence variations for Sequence A are:

- Grit blast, 15% KOH, SurTec 610V, SurTec 617, SurTec 580
- Grit blast, 15% KOH, SurTec 610V, SurTec 617, SurTec 650
- Grit blast, 15% KOH, SurTec 610V, SurTec 617, CFP

Most of the Sequence B test panels rusted along the bottom edge where the water had gathered while drying in the rack. The panels without the use of grain refiner and no post-treatment seal exhibited no evidence of rust. With the exception of one, all test panels with the use of grain refiner and no post-treatment seal showed no evidence of rust.

The best performing process sequence variations for Sequence B are:

- Grit blast, 15% KOH, SurTec 617
- Grit blast, 15% KOH, SurTec 610V, SurTec 617

The best performing variations from process sequences A and B will be further evaluated for corrosion and adhesion performance as part of an ESTCP project.

It was determined that the potassium hydroxide solution was playing a part in the formation of white residue on the test panels. In order to eliminate this residue from forming, a third process sequence was designed involving the addition of an alkaline steel cleaning solution (Turco HTC). The TCP and CFP seals were removed from this sequence due to lower performance in comparison to SurTec 580 during Sequence B testing.

Test panels were then processed using the conditions outlined in Process Sequence C (Table 12):

1. Solvent wipe
2. Grit blast
3. Turco HTC (120 – 140F) – 5 minutes
4. SurTec 610V (ambient) – 2 minutes
5. SurTec 617 (113 – 131F) – 5 minutes
6. DI Water Rinse (80 – 95F)
7. SurTec 580 (68 – 104F) – 1 minute
8. DI Water Rinse (ambient)

Table 12: Process Sequence C Variations for Use of Turco HTC on 1020 Steel Panels

Processing Sequence Variations	**Processing Sequence Variation Descriptions**
1	Grit blast, SurTec 617, SurTec 580
2	Grit blast, SurTec 610V, SurTec 617, SurTec 580
3	Grit blast, Turco HTC, SurTec 617, SurTec 580
4	Grit blast, Turco HTC, SurTec 610V, SurTec 617, SurTec 580

Results are shown in Table 13. Once again, each color-coded block represents a test panel with green indicating the best performance, yellow indicating moderate panel performance, and red indicating the worst performance.

Table 13: Flash Rust Performance for Process Sequence C Variations

Process Sequence Variation	**Sequence C**					
1						
2						
3						
4						

None of the test panels in Sequence C exhibited any evidence of rust. However, several panels throughout all variations did form a brown coloration on the surface of the test panel. The only variation that did exhibit a brown coloration was processing sequence variation 4.

A number of chromate-free wash primers are also being evaluated that are not using TCP or CFP. These include coatings from NCP Coatings, Sherwin-Williams, Spectrum, and PPG (resulting from SERDP effort). All are HAP-free and chromate-free. The NCP coating is a solvent-based system that has 2.5 lbs/gal VOC, and contains phosphoric acid, epoxy, and polyvinylbutyrate. Two solvent-based Sherwin Williams systems are being evaluated. The first has a vinyl ester binder and contains 6.3 lbs/gal VOC, while the second uses a polyurethane binder and contains 1.14 lbs/gal VOC. The Spectrum wash primer contains 3.14 lbs/gal VOC and uses phenolic modified polyvinylbutyrate as the binder and phosphoric acid. The PPG wash primer is low VOC and uses ZrO_x.

These coatings are currently under evaluation. After application of wash primer, the coatings will be primed using standard primers and topcoats. The testing being performed includes the following: MEK double rub, hardness wet & dry, adhesion wet & dry, pull-off adhesion ASTM D 4541-05, QUV, GM9540P-B, ASTM B 117 salt fog, and Arizona Emmaqua Exposure. These will be tested on Carbon Steel 4130, CRS Steel SAE 1008/1010, Galvanized Steel E60 EZG, Stainless Steel SS 304 or 316, Aluminum 2024-T3 Bare, and Aluminum 7075-T6 Bare. The coatings will be applied by robotic application.

The goal of this work will be to continue evaluation of compliant pretreatments and reformulation of non-compliant material. In addition, we will test, evaluate, and review compliant materials to ensure performance requirements stated are met. Lastly, we will continue reformulation efforts for alternative viable replacements. Overall, this should allow us to qualify materials through acceptance testing, reformulate alternative replacements for critical pretreatments, demonstrate selected material on actual equipment, and revise mil specification.

3.2.3 ELECTROCHEMICAL IMPEDANCE SPECTROSCOPY

Samples of AA2024-T3 coated with TCP (labeled TCP-S in figures), TCP-I, and TCP-IC were monitored using electrochemical impedance spectroscopy (EIS) for three weeks to evaluate their barrier properties. There was a decrease of the impedance in the lower frequency range (<1Hz) of the TCP in the 1 to 7 day interval, and an increase of the TCP-I and TCP-IC. The decrease is attributed to the gradual breakdown of the barrier properties, and the increase may be a consequence of the formation of a more continuous oxide layer or localized corrosion inhibition by trivalent chromium species. This is an indication of increasing barrier properties of the TCP-I and TCP-IC. All of the samples exhibited a decrease in impedance in both the 1 to 2 week and 2 to 3 week periods (Figure 33 and Figure 34). However, the TCP-I and TCP-IC samples have impedance values near an order of magnitude greater than the TCP in all intervals of 1 week or greater, indicating sustained barrier and corrosion resistance properties. The TCP-IC exhibited the highest overall coating resistance, followed by the TCP-I and finally the TCP. The electrochemical analysis correlates with the bare NSF results; i.e., TCP < TCP-I < TCP-IC.

After one day the TCP exhibited the most negative (nearest –90°) phase angle response, followed by TCP-I and subsequently TCP-IC. This is an indication of the greater corrosion resistance of

the TCP-IC and to a lesser extent the TCP-I in comparison to the TCP. Between one day and one week the TCP exhibited the most pronounced downward phase-angle shift, while the TCP-I exhibited less of a shift and the TCP-IC was unchanged. The TCP-I and TCP barrier properties are more quickly degrading while the TCP-IC is maintaining its barrier integrity. This is an indication of the greater corrosion resistance of the TCP-IC, which exhibits more resistance to early breakdown of the coatings barrier layer than the TCP or TCP-I. In the one- to two-week interval all coatings show a decreasing phase-angle shift, indicating breakdown of the barrier layer. The coatings showed little change at three weeks compared to the two-week EIS scans. The TCP-IC exhibited the highest overall barrier properties, followed by the TCP-I and finally the TCP. The overall barrier properties also correlate with the bare NSF results; i.e., TCP < TCP-I < TCP-IC.

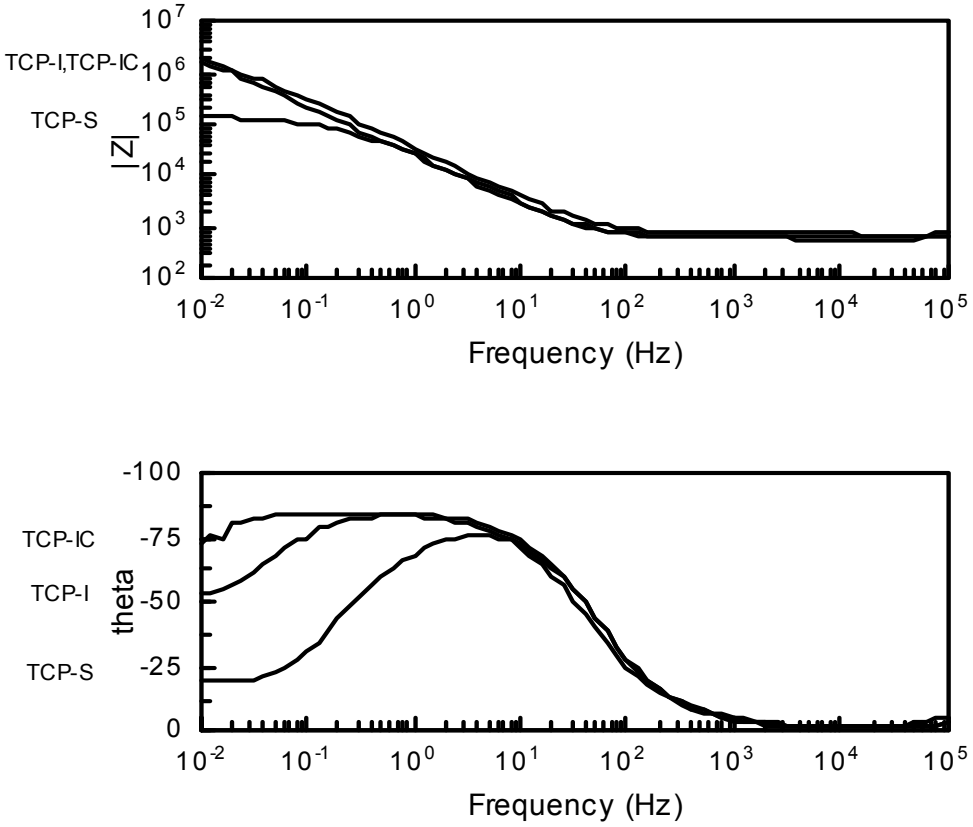

Figure 33: One-week impedance and phase angle plots

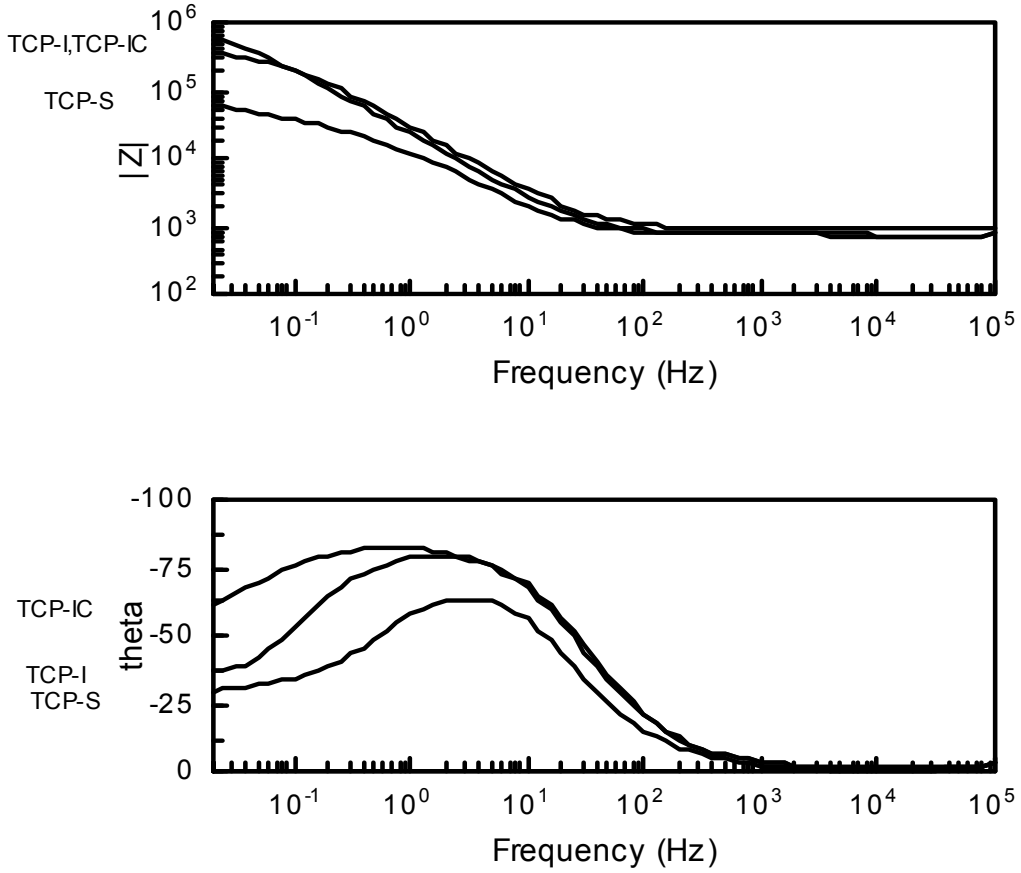

Figure 34: Three-week impedance and phase angle plots

3.2.4 DC LINEAR POLARIZATION

The polarization resistance is the ratio of the applied potential and the resulting current response. This factor is inversely related to the theoretical uniform corrosion rate. The TCP-IC and TCP-I have similar polarization resistances, which are much greater than the baseline TCP. This indicates greater corrosion resistance in the TCP-IC and TCP-I samples. Table 21 shows the measured polarization resistance values, and their corresponding corrosion current densities. Table 14 shows the 3-measurement averages for coating polarization resistance (Rp), corrosion potential (Ecorr), and the corresponding corrosion current density (I Corr) for each TCP coating. Both the TCP-I and TCP-IC coatings exhibit 2 orders-of-magnitude decrease in the corrosion current density, compared to TCP control. This is indicative of a longer coating life in corrosive chloride environments and correlates with the TCP-I and TCP-IC coatings performance in NSF over the first 14 to 21 days. Future evaluations will investigate the effect of exposure of TCP coatings to NSF on the polarization results, to see if changes in the Icorr correlate to the increased performance of TCP-IC over TCP-I after 21 days in NSF. This will be investigated by measuring the DC linear polarization resistance and corrosion current density on TCP and modified TCP coatings after various exposure intervals to NSF.

Table 14: Linear polarization results

Sample	ECorr_(V)	Rp_(Ω*cm2)	ICorr_(A/cm2)
TCP-I	-6.60E-01	6.36E+06	4.09E-09
TCP-IC	-8.08E-01	5.42E+06	4.79E-09
TCP	-6.39E-01	6.14E+04	4.23E-07

3.3 Leveraged Pretreatment Technologies

3.3.1 ANODIZE SEALING

TCP and CFP formulations have also been evaluated for post-anodize sealing of aluminum. Both sealing processes have yielded excellent performance relative to chromic acid sealing with respect to bare and painted corrosion resistance. Further testing is planned with the modified chemistries that performed well as conversion coatings. Figure 35 and Figure 36 show extended B 117 testing on MIL-A-8625F, Type IIB Thin Film Sulfuric Acid Anodize (TFSAA).

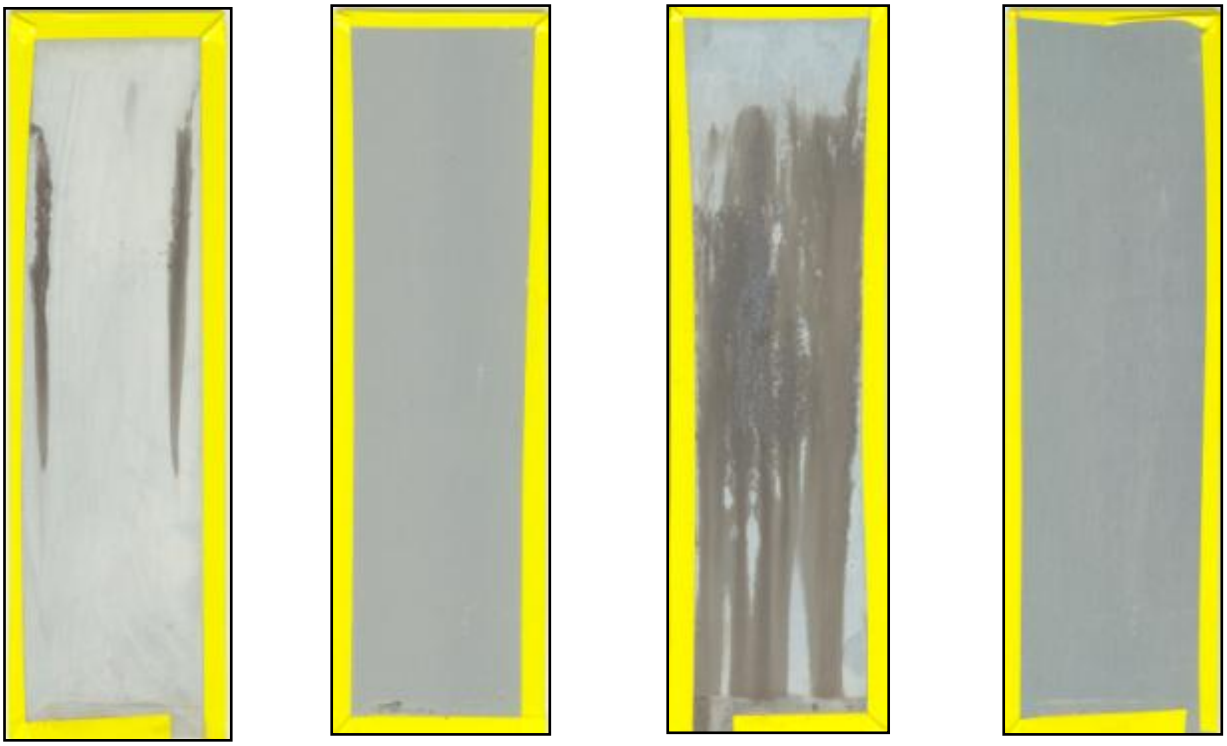

2024 Cr(VI) 190ºF, 25 min | 2024 TCP RT, 10 min | 7075 Cr(VI) 190ºF, 25 min 1680 hrs | 7075 TCP RT, 10 min

Figure 35: Tri-chrome seal for TFSAA after 2,184 hrs B 117 exposure

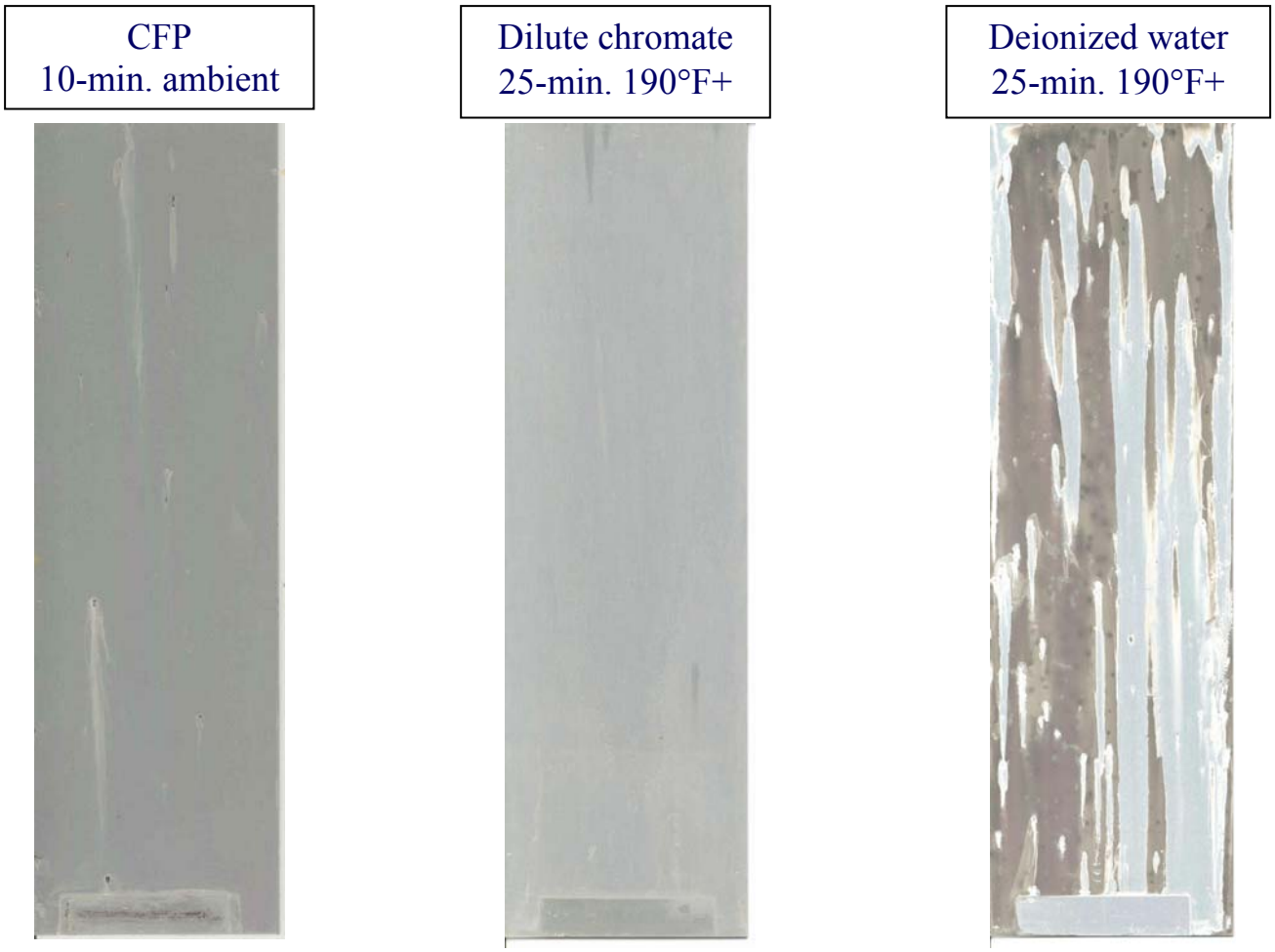

Figure 36: CFP seal for TFSAA on AA2024 in comparison to chromate and DI water controls

Figure 37 shows poor corrosion resistance of Phosphoric Acid Anodize (PAA) film on AA2024-T3 with TCP seal while Figure 38 shows improved corrosion resistance of PAA film with TCP-C seal.

Figure 37: Poor corrosion resistance of PAA film with No Seal (left), TCP – 10 min. ambient (center), and TCP – 20 min. 100F (right) on AA2024-T3 after 72 hrs. ASTM B 117

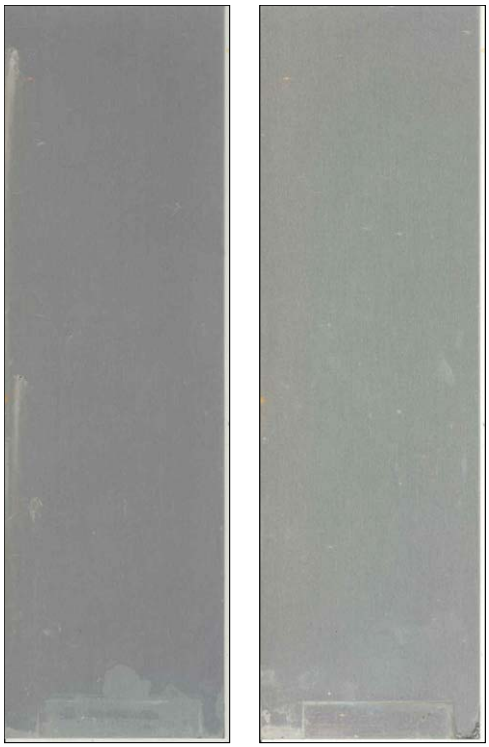

Figure 38: Improved corrosion resistance of PAA film with TCP-C – 40 min. ambient (left), and TCP-C – 10 min. 100°F (right) on AA2024-T3 after 1,000 hrs. ASTM B 117

3.3.2 ALUMINUM SACRIFICIAL COATINGS

TCP and CFP formulations have also been evaluated for post-treatment of IVD and electroplated aluminum on steel substrates. Both sealing processes have yielded excellent performance relative to chromate conversion with respect to bare and painted corrosion resistance. Further testing is planned with the modified chemistries that performed well as conversion coatings. Figure 39 and Figure 40 show extended B 117 testing on Alumiplate™ coated S4130.

Figure 39: Alumiplate™ on 4130 steel – post-treated with CFP 6. After 4,200 hours ASTM B 117 (left) and as deposited (right)

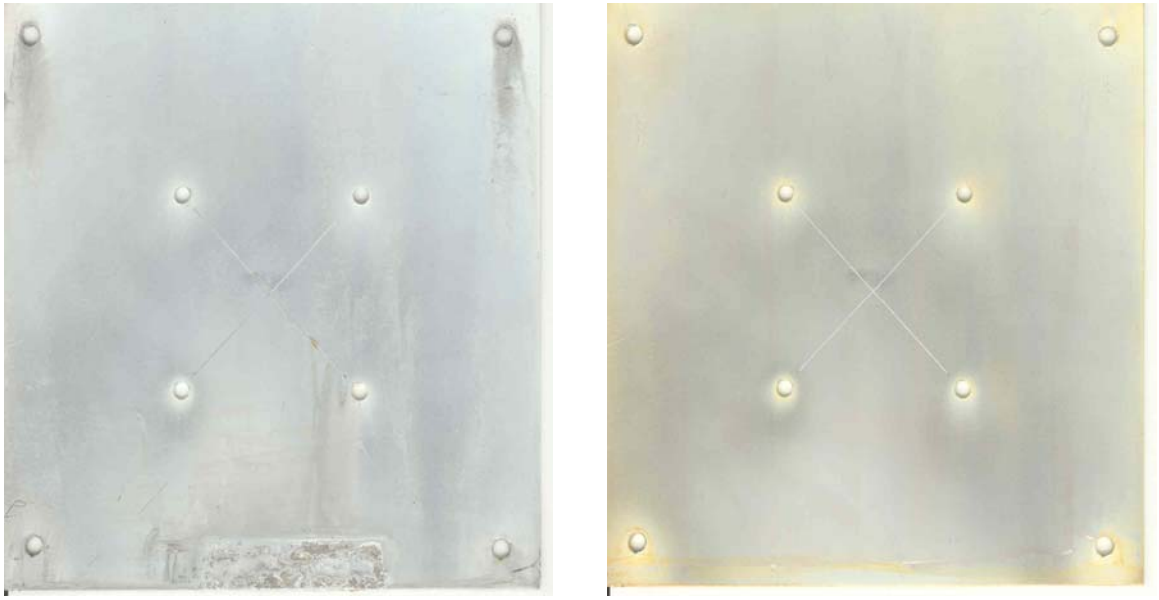

Figure 40: Alumiplate™ on 4130 steel – post-treated with Alodine™ 1200S. After 4,200 hours ASTM B 117 (left) and as deposited (right)

The IVD conversion was evaluated at CTC Johnstown, PA. The test results indicated that TCP-C improved the performance of the IVD with respect to corrosion resistance more than all of the pretreatments, including the chromate conversion coating and the baseline TCP. NDCEE personnel performed observations for signs of red rust every 24 hours up to 96 hours of exposure and then the panels were evaluated every 48 hours until failure. The appearance of white corrosion products during the test period was not considered a failure. Table 15 shows the results of the corrosion test for the IVD panels. The range notes the hours when red rust became visible. For example, "288-336" indicates that no red rust was visible after 288 hours but at 336 hours, some red rust was visible; therefore, the corrosion occurred during this time interval.

Table 15: Corrosion test results for IVD panels

IVD Treatment	Post Treatment Scenario		First Signs of Red Rust (hours)			
	Glass Bead Peen	Conversion Coating				
Conventional	X	None	288-336	336-384	336-384	336-384
Conventional		None	384-432	600-672	600-672	672-720
Conventional	X	Alodine 1200S	432-552	672-720	840-888	888-936
Conventional		Alodine 1200S	552-600	672-720	840-888	840-888
Conventional	X	Alodine 2600	672-720	768-840	840-888	938-1008
Conventional		Alodine 2600	600-672	600-672	720-768	1008-1056
Conventional	X	TCP	552-600	552-600	768-840	1200-1248
Conventional		TCP	768-840	888-936	936-1008	936-1008
Conventional	X	TCP - Color	672-720	1056-1104	1392-1440	1392-1440
Conventional		TCP - Color	840-888	1392-1440	1392-1440	1392-1440

3.4 Pre-treatment Analysis

During pretreatments, substrates are exposed to a liquid solution of organic and inorganic species. In successful pretreatment solutions, these organic and inorganic species adsorb to the substrate surface. These adsorbed species then protect against corrosion on the surface. However, the concentration of adsorbed species need not match the concentration of species in the pretreatment solution. Through analysis of the substrate surface, we can determine which species are attached to the substrate surface. Then through determination of the corrosion protection provided by various pretreatment solutions with various concentrations of species at the surface, we can determine which species are crucial to corrosion protection.

3.4.1 SCANNING ELECTRON MICROSCOPY

Conversion coatings on aluminum alloys are very thin films, and the TCP coatings are generally on the order of 0.5 μm thickness or less. As such, the underlying alloy surface morphology and grain structure shows through the coating, which exhibits micro-cracks and voids. No difference was observed in the coatings' surface structure due to the variations in the TCP formulations.

Electron dispersive spectroscopy (EDS) analysis through thin films picks up much of the underlying alloy composition, and as the chemical composition of the alloy is not uniform across its surface, due to inter-metallic sites, the weight and atomic percentages obtained during compositional analysis cannot be reported as absolute values. However, the EDS analysis does show the presence of zirconium and chromium in approximately the same ratio for both the baseline TCP and both modified formulas. Additional oxygen is also present on the TCP coated surfaces relative to uncoated AA2024T3, most likely from the formation of zirconium and chromium oxides/hydroxides during coating deposition. Figure 41 shows representative EDS results for uncoated AA2024-T3 in comparison to the baseline TCP (Figure 42) and TCP-IC (Figure 43) on AA2024-T3.

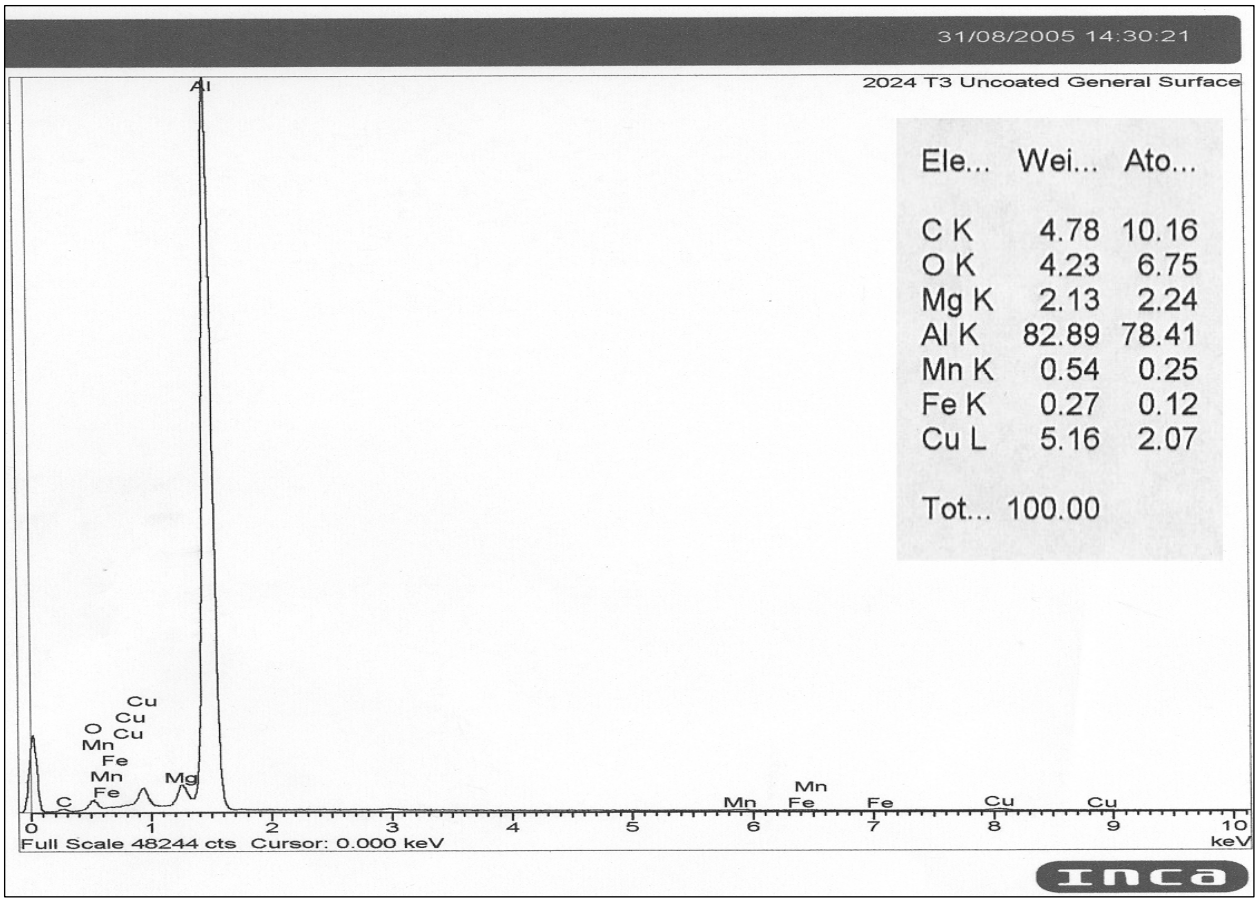

Figure 41: Bare AA2024-T3

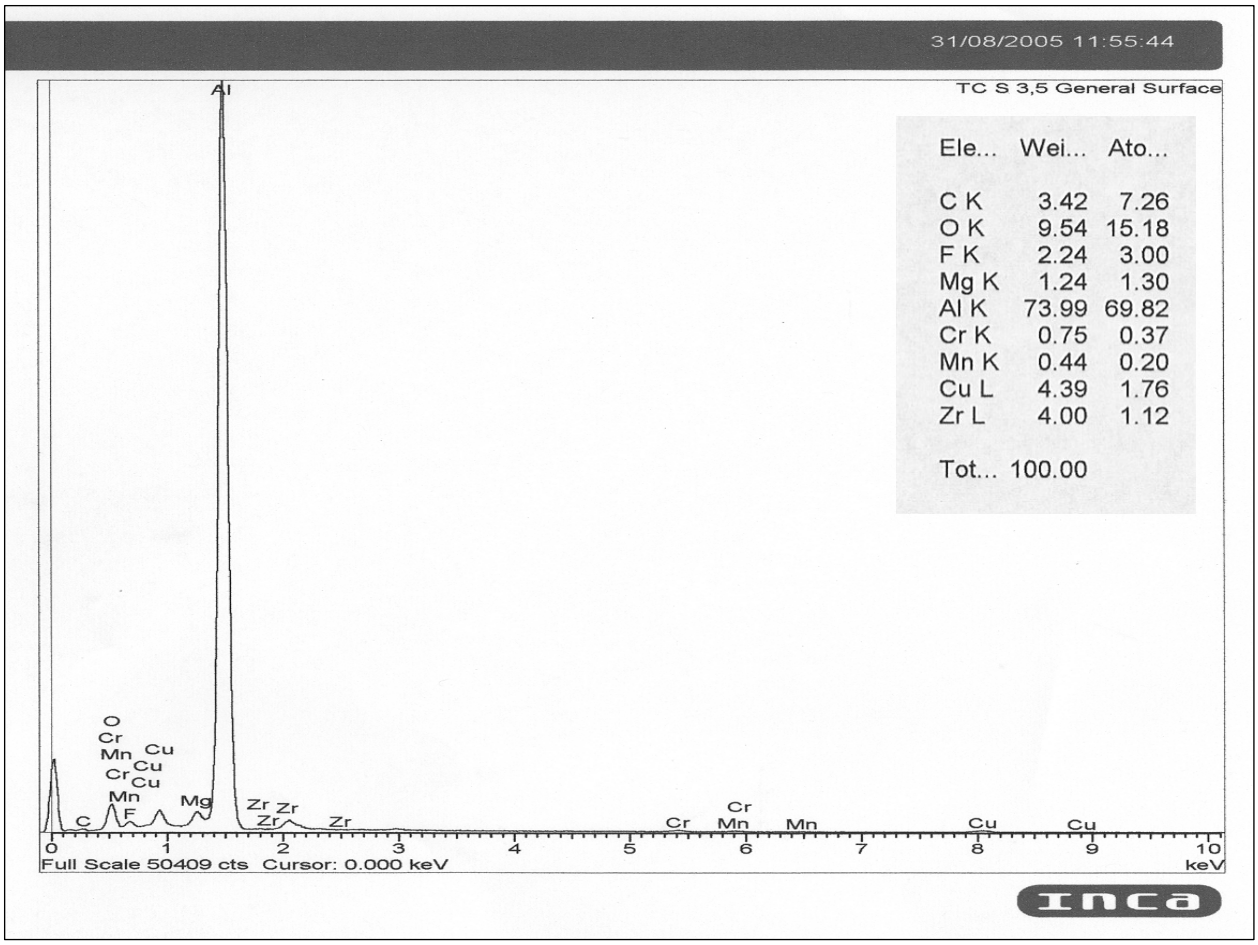

Figure 42: TCP-S on AA2024-T3

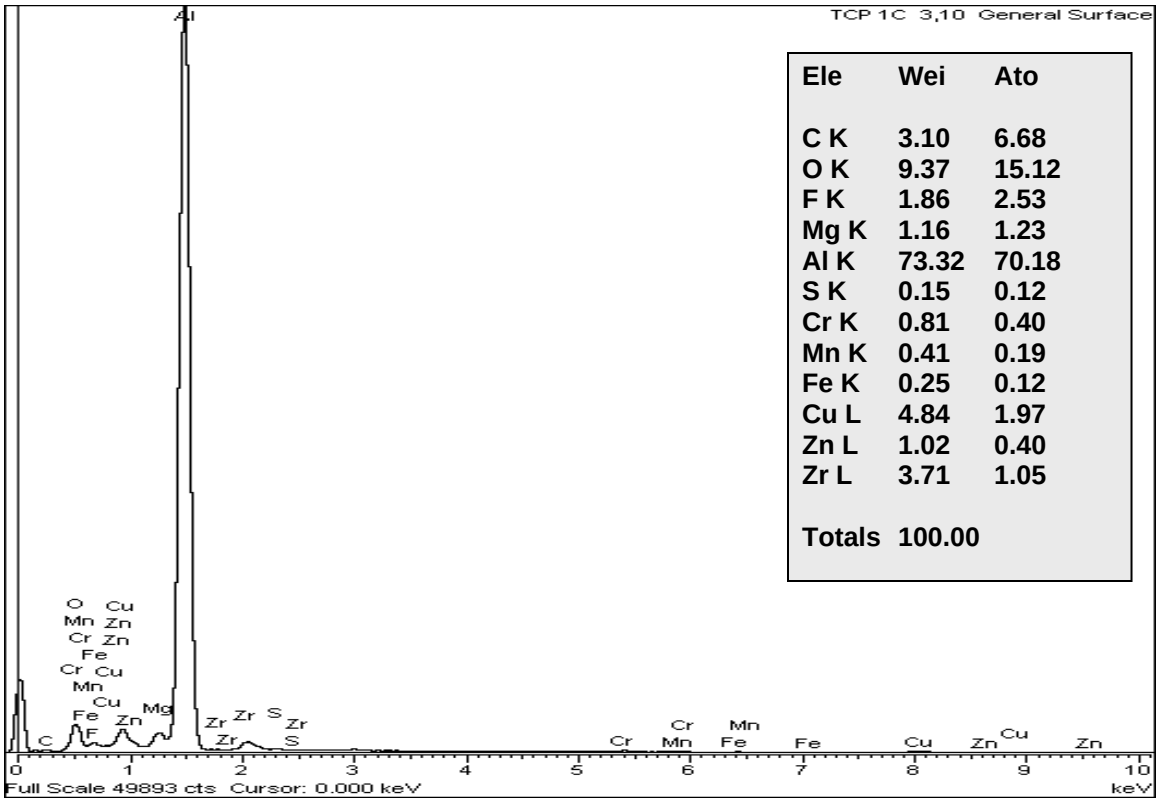

Figure 43: TCP-S on AA2024-T3

The compositional analysis indicated the presence of additional zinc species in the as-deposited coating from the color-change additive. The analysis was inconclusive as to the presence of additional species from the organic corrosion inhibitor additive; however, this is not surprising as C is rather too light of an element to be determined accurately by EDS.

These results imply that the chemistry modifications may not be significantly altering the basic TCP coating composition formation, but instead may either be adding some additional species into the coating, or altering the coating deposition process. EDS analysis of the cross-sectioned coatings looked for relative ratios of Cr, Zr, O and fluorine (F) in the general coating, and the presence/relative amounts of Zn and extra O to help determine how the coating is formed, and what effect the additives are having on the coating composition.

Additional surface imaging analysis is currently being conducted in conjunction with the United Technologies Research Center using ion beam imaging SEM. This effort is to gather data on coating thickness and reaction over secondary inter-metallic particles. Coated specimens are cross-sectioned and imaged. These results are preliminary, but show good resolution of coating across the aluminum matrix phase, with coating thicknesses in the 100 nm range for the baseline TCP and the TCP-IC. Initial results show that the coating is difficult to resolve on the secondary inter-metallic particles, and will need further analysis.

Figure 44 shows the backscatter FIB image of the TCP on aluminum matrix phase AA2024-T3 and Figure 45 shows the backscatter image of the TCP-IC on AA2024-T3 through a secondary inter-metallic particle. The TCP-IC image shows a granular surface morphology to the coating

over the aluminum matrix. The secondary inter-metallic particle image indicates lower density regions on the surface of the particle consistent with a very thin oxide or organic species. Efforts will focus on determination of the formation of mono-molecular organic, zinc-organo-metallic species on the secondary phase particles, as has been hypothesized previously.

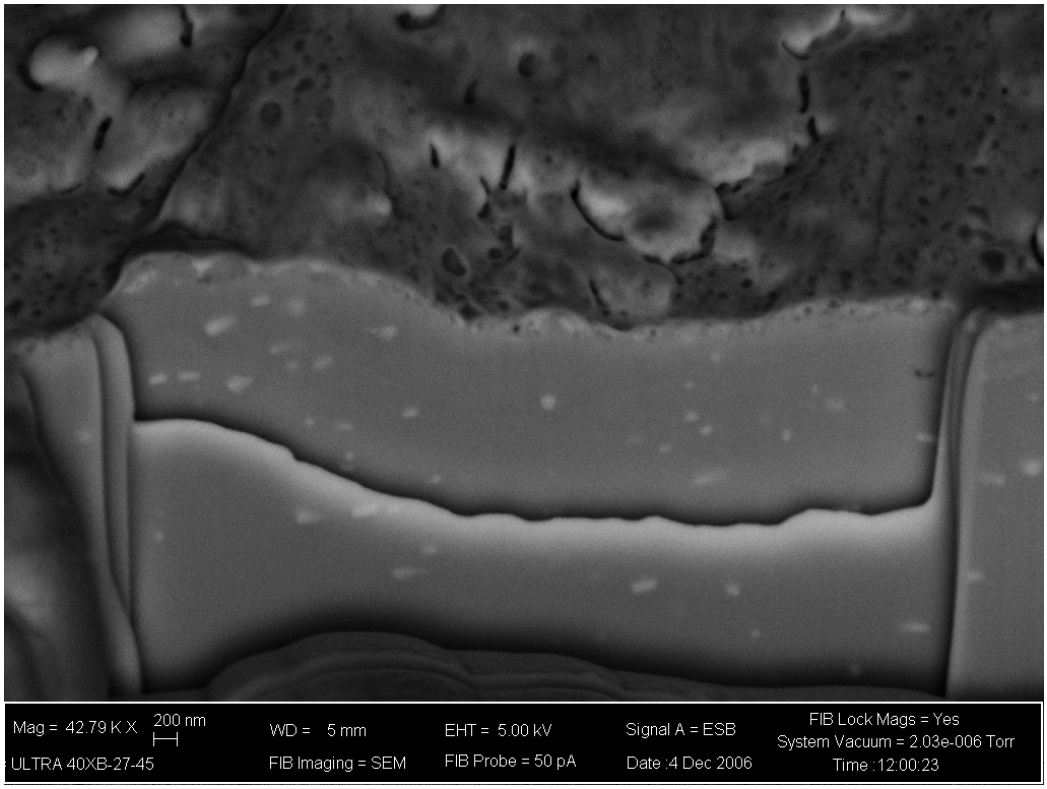

Figure 44: Backscatter FIB image of TCP on AA2024-T3

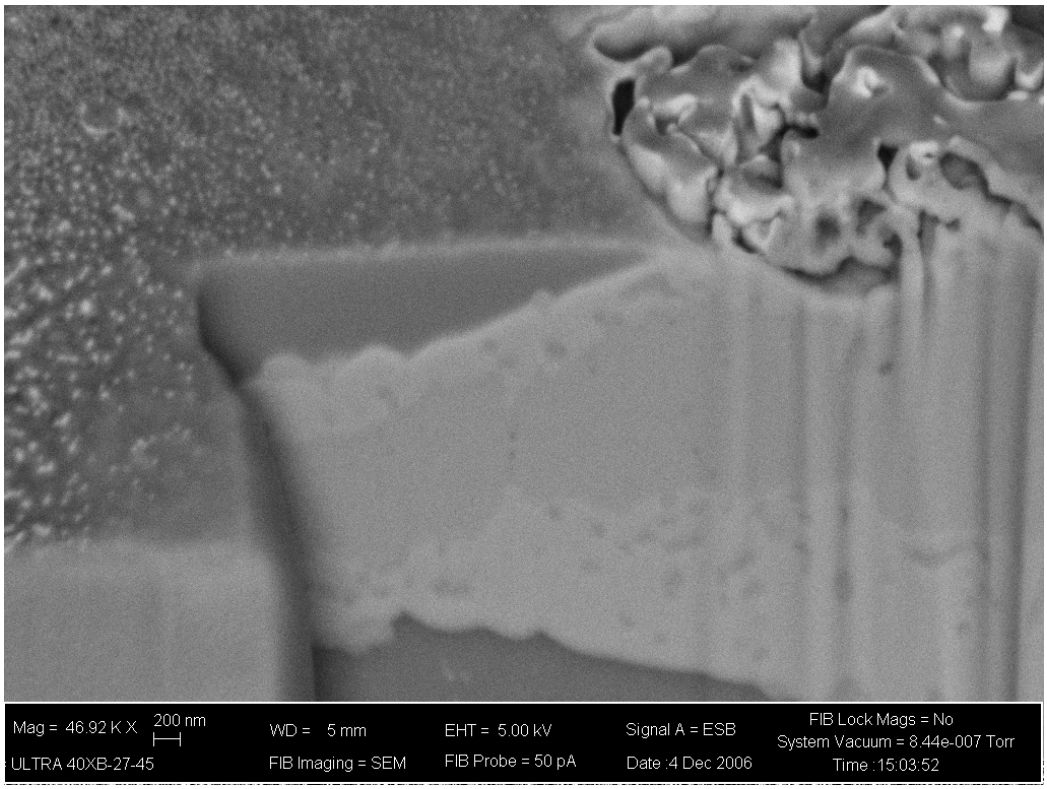

Figure 45: Backscatter FIB image of TCP-IC on AA2024T3 showing aluminum matrix and secondary-phase intermetallic

3.4.2 FTIR AND RAMAN

The purpose of performing FTIR and Raman was to identify any organic components on the pre-treated surface, and especially the chelating corrosion inhibitor added to the 'I' formulations of TCP and CFP. The FTIR and Raman spectra of this organic species are well known [23,24].

The groups of interest in FTIR and Raman are:

Aromatic ring:	~3000 cm^{-1}: unsaturated CH
	1700-2000 cm^{-1}: overtone pattern
	730 cm^{-1} out of plane stretch
	690 cm^{-1} out of plane ring bend
Ether linkage	~ 1240 cm^{-1}: C-O-C
Aromatic C-S stretch	~ 1133 cm^{-1}: C(aromatic)-S:
Ether linkage (Raman)	~ 860 cm^{-1}: C-O-C

Pretreatments are very thin coatings of chemical species on the surface, so it is difficult to obtain spectra that look like the representative ones for FTIR and Raman. The signal to noise ratio is far lower for the pretreated substrates. Figure 46 shows the FTIR spectra of the pretreatments on

Al 2024. Peaks were observed at ~3300 cm^{-1} (unsaturated C-H), 1645 cm^{-1}, 1556 cm^{-1}, and 1430 cm^{-1} (in-plane stretch), 1130 cm^{-1} (C-S) and 930 cm^{-1}. Similar absorption bands were visible on TCP pretreated Al 7075 substrates (Figure 47): ~3300 cm^{-1} (unsaturated C-H), 1645 cm^{-1}, 1556 cm^{-1}, and 1430 cm^{-1} (in-plane stretch), 1130 cm^{-1} (C-S) and 850 cm^{-1} (C-O-C). The peak positions were slightly different for CFP pretreated Al 7075 (Figure 50): ~3300 cm^{-1} (unsaturated C-H), 1680 cm^{-1} and 1520 cm^{-1} (in-plane stretch), 1300 cm^{-1}, 1200 cm^{-1}, 1140 cm^{-1} (C-S) and 960 cm^{-1}. Similar results were observed for the 5083 and 6061 series as shown in Figure 48 and Figure 49.

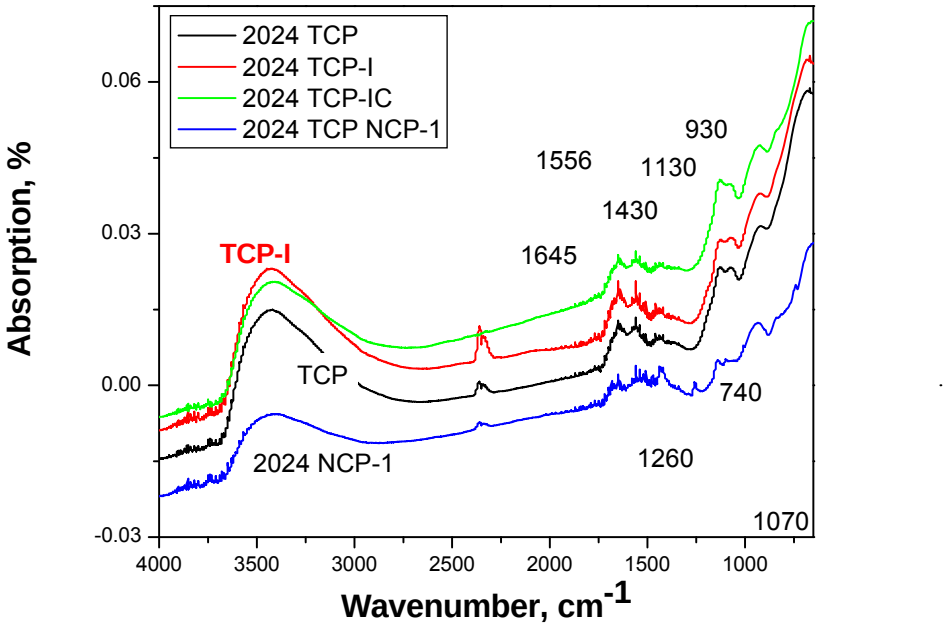

Figure 46: FTIR spectra of pretreated Al 2024 substrates

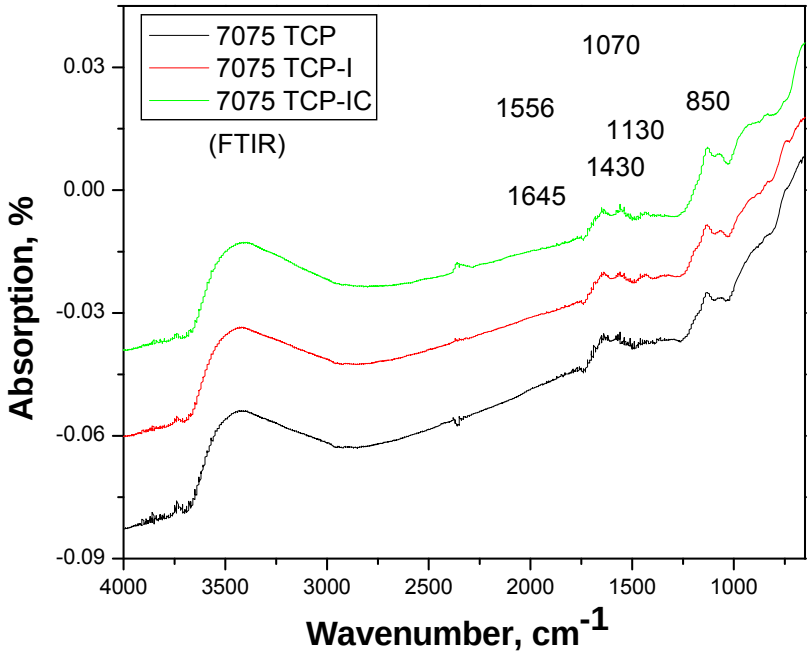

Figure 47: FTIR spectra of TCP pretreated Al 7075 substrates

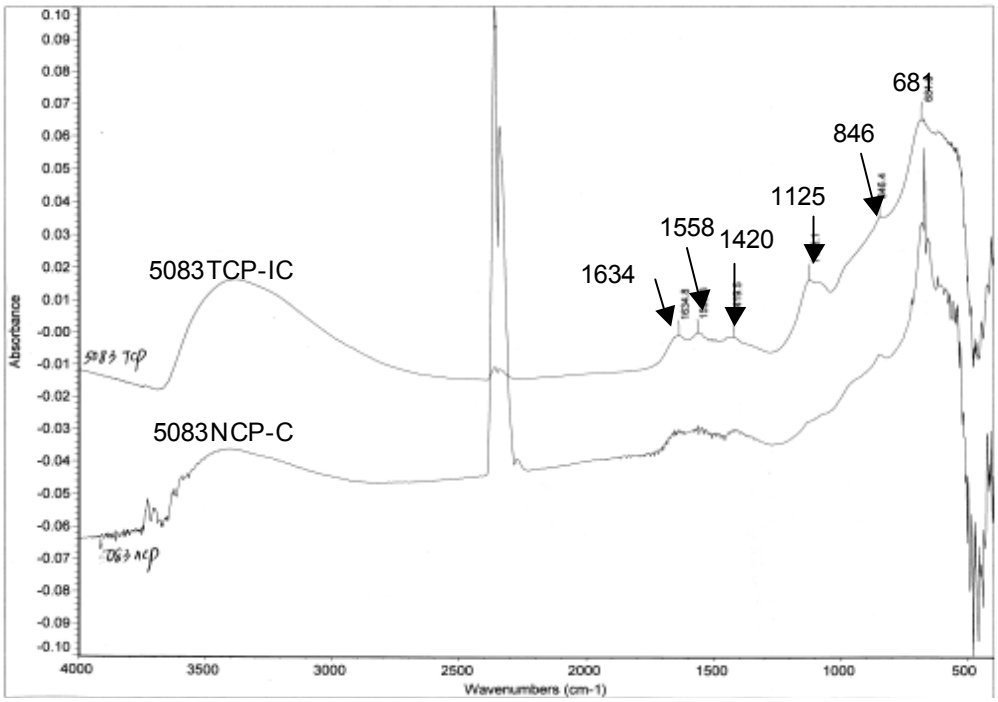

Figure 48: FTIR spectra of 5083 series

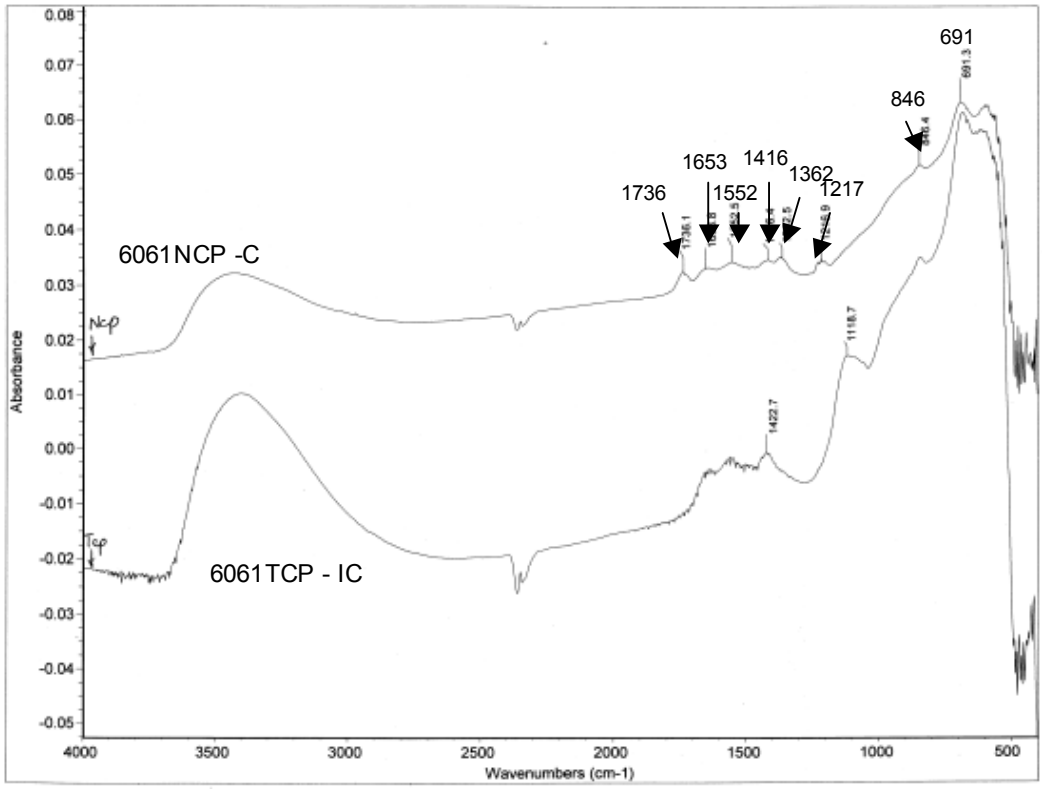

Figure 49: FTIR spectra of 6061 series

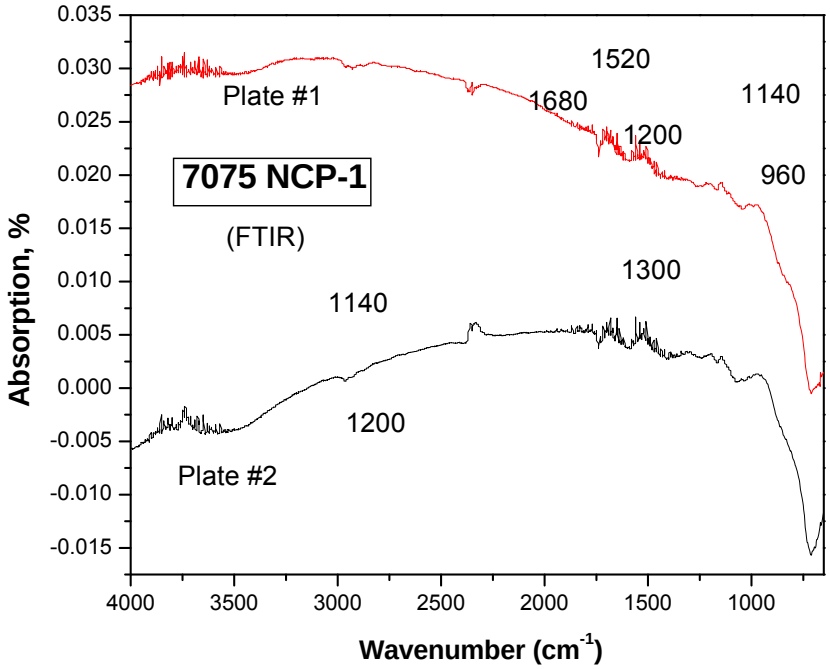

Figure 50: FTIR spectra of CFP pretreated Al 7075 substrates

The Raman spectra of TCP on Al 7075 are shown in Figure 51. Three peaks are clearly visible: 3077 cm^{-1} (=C-H), 1125 cm^{-1} (C-S), and 864 cm^{-1} (C-O-C). The spots where the spectra were measured are significantly different, and also result in Raman spectra with different Raman intensities. Therefore, Figure 51 shows that the TCP pretreatment is not uniform Al 7075. Figure 52 shows an enlargement of the Raman spectra that detected the presence of other functionality: 2550-2600 cm^{-1} (-S-H), 2000-2200 cm^{-1} (C=N:), 2800-3000 cm^{-1} (-C-H). These results were observed in general for the other TCP and CFP pretreatments on both Al 7075 and Al 2024. The Raman spectra of 5083 series and 6061 series are shown in Figure 53. Generally, in 5083 TCP and 6061 TCP samples, 5 peaks are observed: peaks around 3077 cm^{-1} (unsaturated CH), 1125 cm^{-1} (C-S), 2166cm^{-1} (C=N:), 2103cm^{-1} (C=N:) and 959 cm^{-1}. In 5083 TCP and 6061 CFP samples, only 4 peaks are observed: peaks around 3077 cm^{-1} (unsaturated CH), 1125 cm^{-1} (C-S), 2166cm^{-1} (C=N:), 2103cm^{-1} (C=N:). There is no 959 cm^{-1} peak in CFP samples.

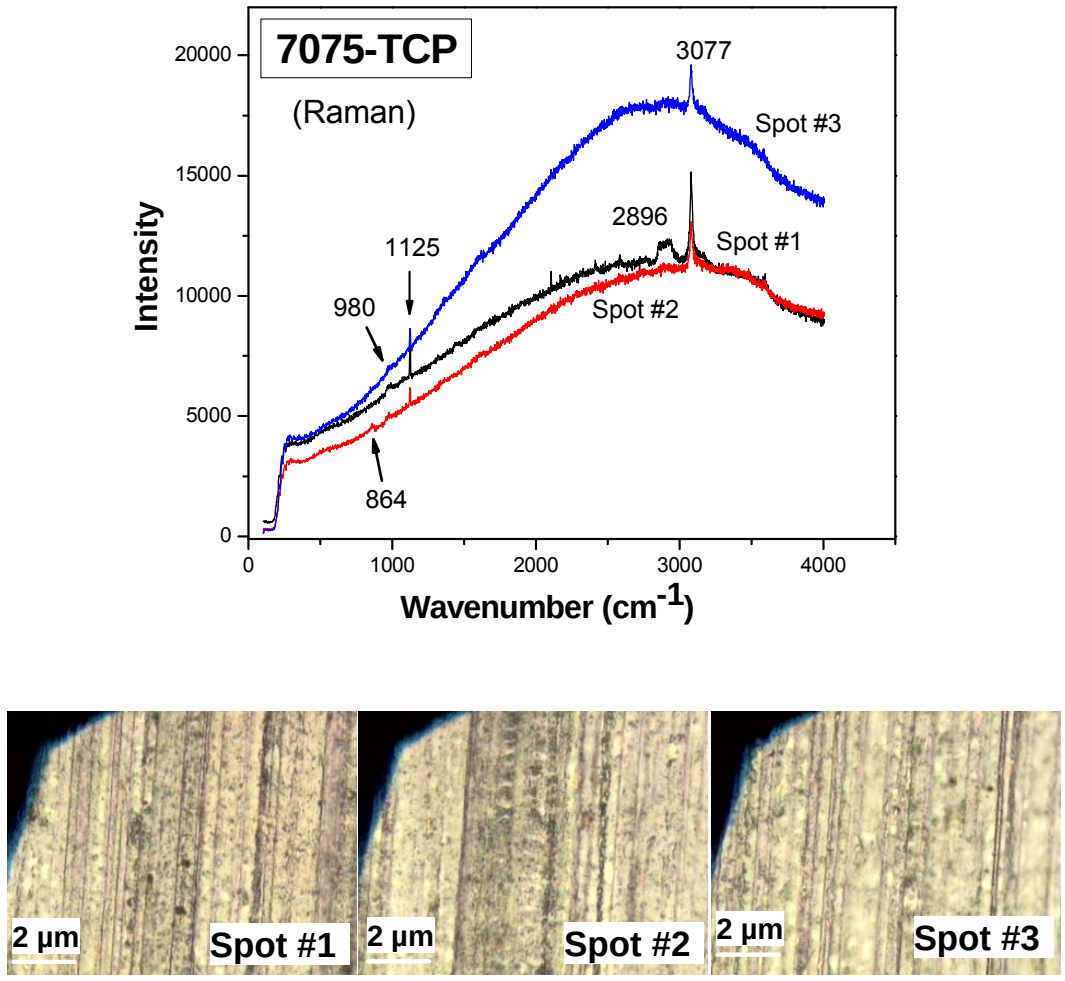

Figure 51: The Raman spectra of TCP pretreated Al 7075 and 2 µm images of the spot on the substrate where the spectra were measured.

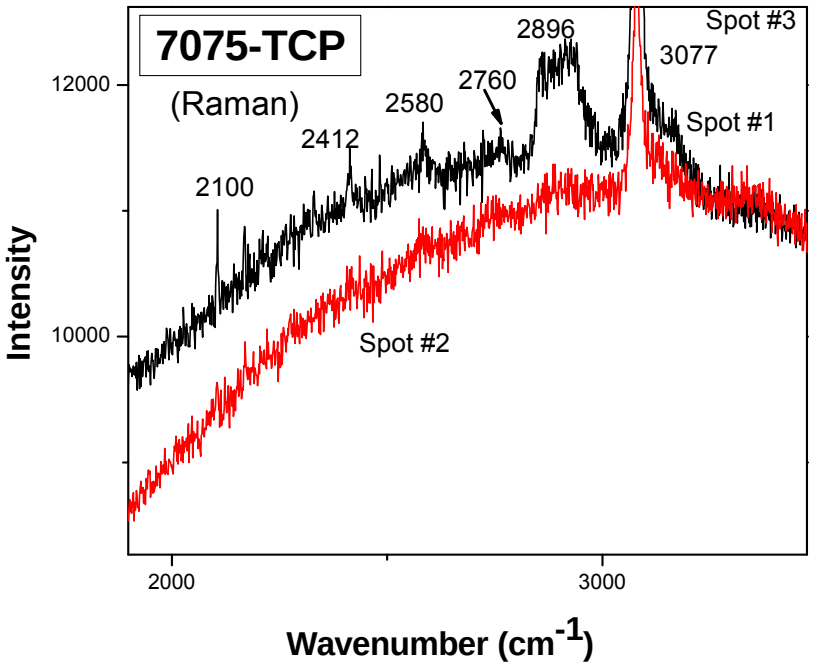

Figure 52: Enlargement of the Raman spectra of TCP pretreated Al 7075

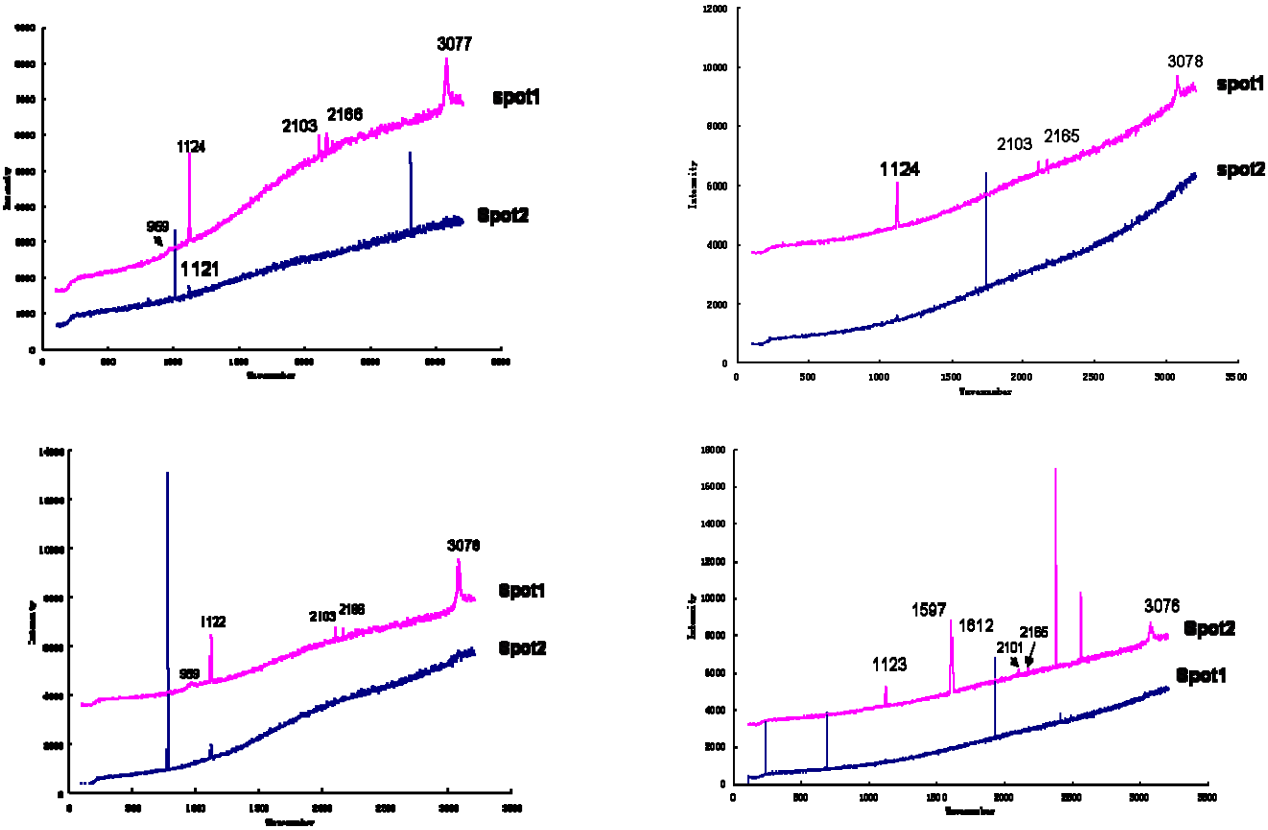

Figure 53: Raman spectra of (A) 5083 TCP-IC, (B) 5083 CFP-C, (C) 6061 TCP-IC and (D) 6061 CFP-C

Glazing angle FTIR and Raman studies were performed on pre-treated substrates (Figure 54). Glazing angle is likely to observe chemical functionality on the substrates because the path length through the pre-treatment is longer. The spectra had peaks at ~3000 cm^{-1} (unsaturated CH), 1700-2000 cm^{-1} (overtone pattern), 1450 cm^{-1}, 1500 cm^{-1}, and 1600 cm^{-1} (in-plane ring stretch), 1240 cm^{-1} (C-O-C), 730 cm^{-1} (out of plane stretch), and 690 cm^{-1} (out of plane ring bend). Overall, these results indicate the presence of the organic corrosion inhibitor on TCP-I, TCP-IC, and CFP-I. The 690 cm^{-1} band shows that the bond strength of the organic inhibitor to the substrate is: TCP-I> TCP-IC (CFP does not show this band). CFP sample did not show peaks below 930 cm^{-1}, which might indicate the absence of out-of-plane stretch and ring bend.

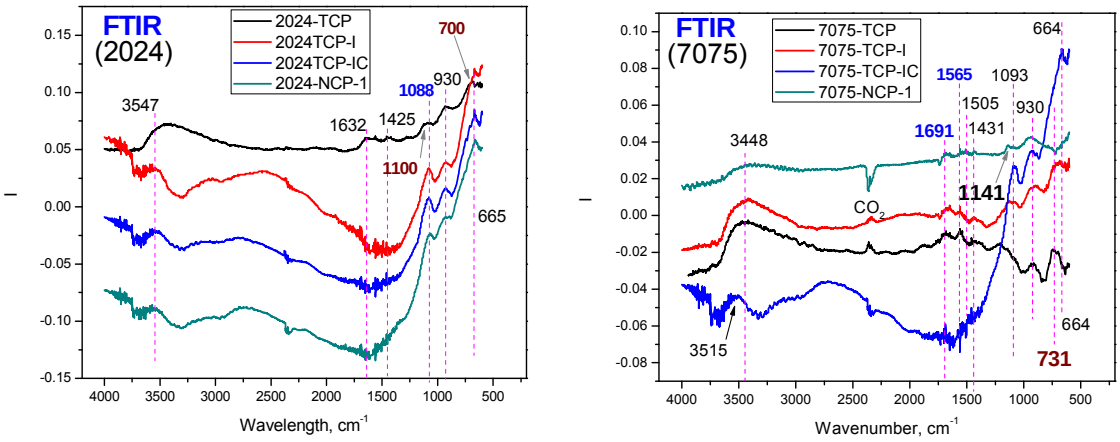

Figure 54: Glazing FTIR spectra of pretreatments on Al 2024 and Al 7075.

The glazing Raman spectra are shown in Figure 55. Both spectra show functional groups at 3077 cm^{-1} (=C-H), 1125 cm^{-1} (C-S), and 864 cm^{-1} (C-O-C). TCP-I and CFP show the presence of the organic corrosion inhibitor molecules, while TCP-IC on Al 2024 did not show the corrosion inhibitor. This could be because the film is too thin because the inhibitor was observed using FTIR. Only CFP samples showed a clear peak at ~1600 cm^{-1}. Interestingly, TCP-IC has more signals observed compared to others on Al 7075 likely due to a thicker TCP-IC film. No clear 866 cm^{-1} peak was observed for TCP, CFP, and TCP-IC samples. This peak was only present in TCP-I.

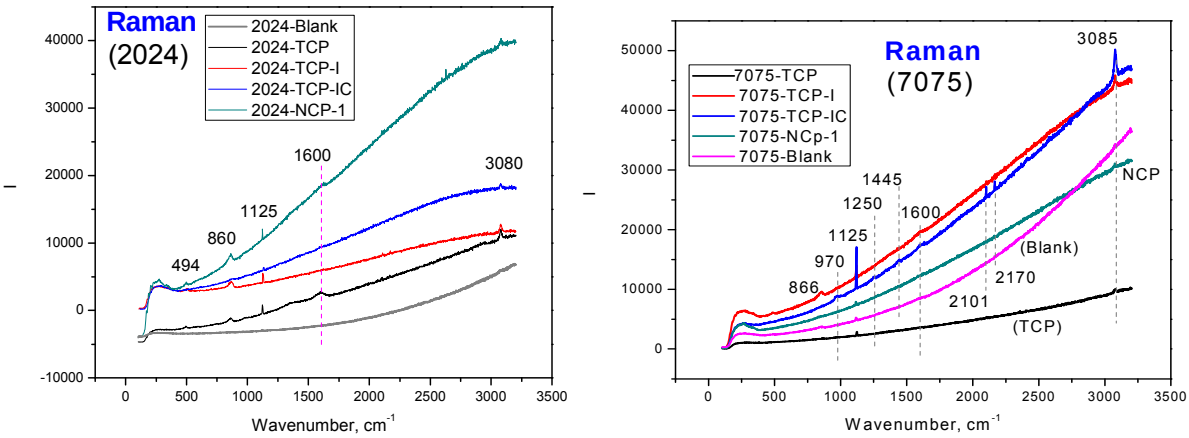

Figure 55: Glazing Raman spectra of pretreatments on Al 2024 and Al 7075.

Raman spectroscopy has also been used to distinguish Cr(VI) oxide from Cr(III) oxide and Cr(III) hydroxide.[25] Figure 56 gives Raman spectra of Cr(III) and Cr(VI) oxide powders. Cr(VI) oxide has two distinctive bands at around 1000 and 500 cm^{-1}, but Cr(III) has no bands around these regions. Instead, Cr(III) oxide has two distinctive bands around 600 and 300 cm^{-1}. The Raman spectra of electroplating and chromium conversion coating (CCC) films made from Cr(III) and Cr(VI) solutions respectively, as reported by Kikuchi et al. are given in Figure 57 and Figure 58. Each sample in Figure 57 exhibit some peaks between 1200 and 800 cm^{-1} and around 560 cm^{-1}. The bands between 1200 and 800 cm^{-1} correspond to a Cr=O stretching frequency around 1030 – 1000 cm^{-1} and a Cr-O-Cr bending frequency around 880 cm^{-1} in the Cr(VI) oxide species. The band around 560 cm^{-1} agrees well with that of Cr(II) oxide. Therefore, Figure 57 shows that black CCC and electroplating films contained both Cr(VI) and Cr(III) species and the colored CCC films contained mainly Cr(VI) species. None of the Cr(II) films showed any Raman band, as shown in Figure 58. Clearly, Raman Spectroscopy can be a useful tool in determining Cr species in coatings.

Sample 5083 TCP-IC has one more Raman peak than 5083 CFP-C around 959 cm^{-1}. The same is true for 6061 TCP-IC and 6061 CFP-C samples. According to Kikuchi et al., peaks between 1200 and 800 cm^{-1} may correspond to a Cr=O stretching of Cr(VI). Since the peaks are very weak, the 5083TCP-IC and 6061TCP-IC *may* contain trace amounts of Cr(VI) species.

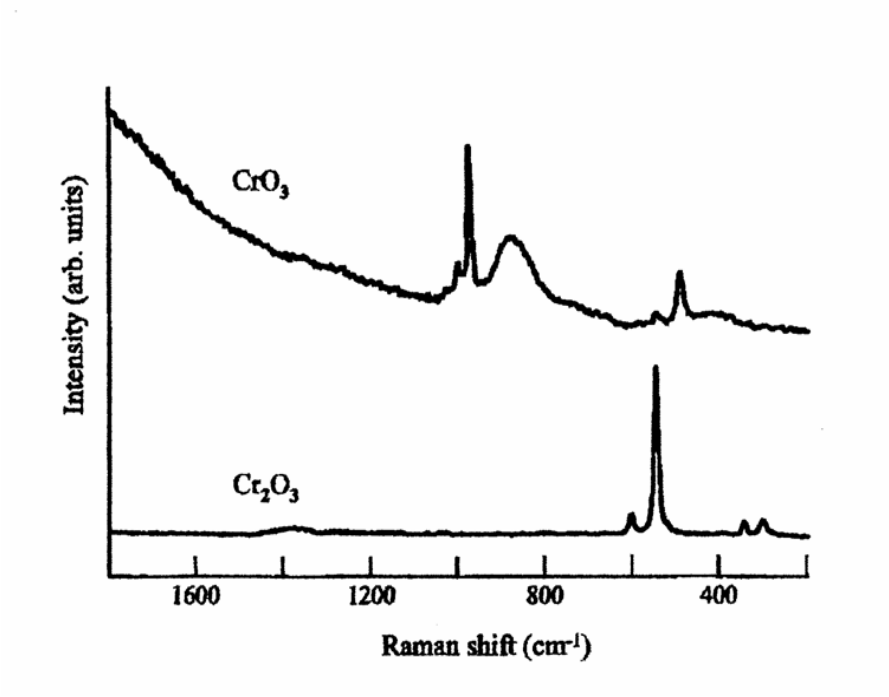

Figure 56: Raman spectra of powders of CrO_3 and Cr_2O_3 [25].

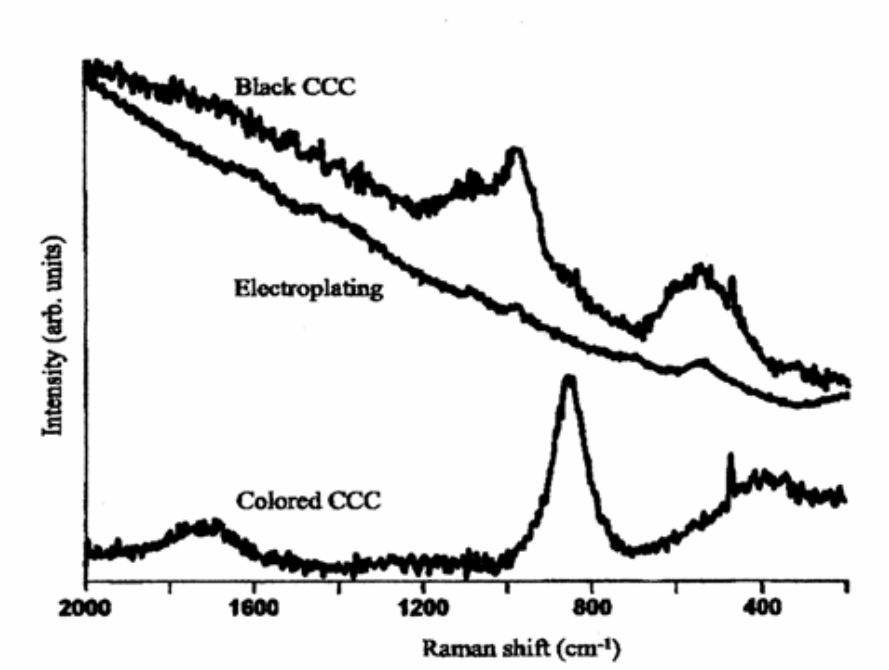

Figure 57: Raman spectra of electroplating and CCC films made from Cr(VI) solutions [25].

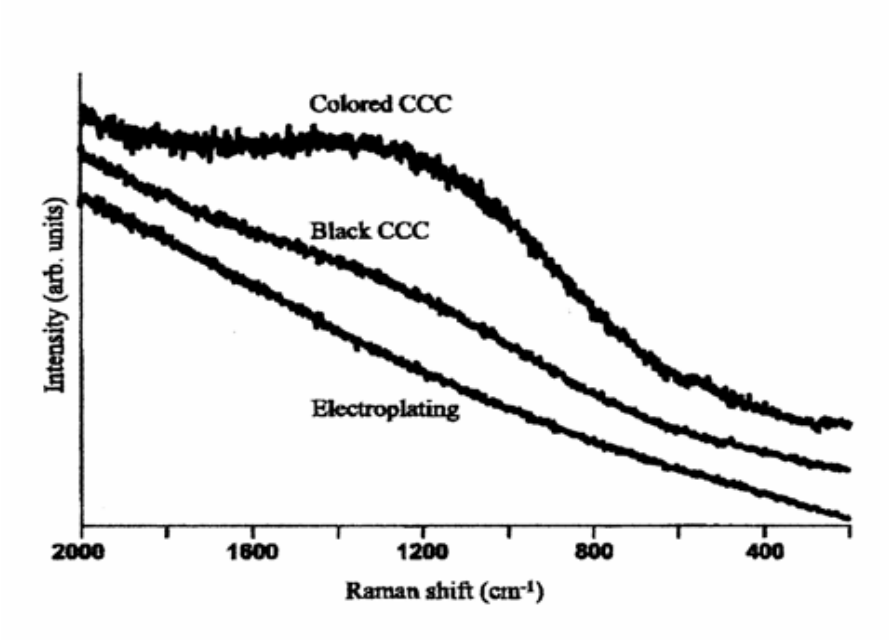

Figure 58: Raman spectra of electroplating and CCC films made from Cr(III) solutions [25].

Overall, both FTIR and Raman positively indicated the presence of the organic corrosion inhibitor on the 'I' varieties of TCP and CFP on coated aluminum surfaces. FTIR and Raman peak positions of the inhibitor on coated Al samples were slightly different from those of the free corrosion inhibitor. This suggests the attachment/bonding of the corrosion inhibitor molecules to the Al surface. Raman results suggested 2024-TCP-IC has less surface coatings compared to the other 2024 samples, while 7075-TCP-IC has more coatings compared to the other 7075 samples. These results and the microscopy results during Raman indicate that the pre-treatments were not uniformly adsorbed to the substrate.

3.4.3 SCANNING AUGER MICROSCOPY

Auger scanning microscopy was run on pretreated samples to make a quick determination of the elemental composition and their relative concentration on the surface. Figure 59 shows the Auger survey results for TCP-IC on Al 2024. From the peaks, it is visible that C, N, O, Cr, Zn, and Zr were adsorbed to the surface, and this was observed in general. Figure 60 shows the adsorbed elements on Al 2024 after CFP pretreatment. C, N, O, F, Zn, Al, and Zr were observed on this coating and on CFP treated aluminum in general.

The spectra show the relative concentrations of elements on the substrate surfaces. The concentration of O is the highest on the surface. The carbon and chromium concentrations are also relatively high. Zinc and zirconium appear in trace quantities. The O and Al (if observed) were detected due to the surface oxide on aluminum substrates. The adsorbed carbon is likely a result on adsorption of organic species, such as the organic corrosion inhibitor. Cr adsorbed due to the ligated trivalent chromium species in the pre-treatment. Zr is adsorbed to the surface because of the fluorozirconate complex used in TCP and CFP. The trace presence on Zn is likely due to contamination of a sort of Zn in TCP. Interestingly, F was not observed on TCP treated surfaces, but was observed in CFP treated surfaces. Both use a fluorozirconate complex so it was expected that F would attach to both surfaces. However, CFP uses a higher concentration of

these species and would be expected to have a higher fluorine concentration. The presence of nitrogen could indicate adsorbed atmospheric nitrogen or may also be a result of adsorbed organic corrosion inhibitor. Note, Auger results do not tell us the oxidation states of the metallic species. As such, the oxidation state of chromium on TCP treated surfaces is unknown. However, based on past results, we expect the chromium to be in the trivalent state with zero hexavalent chromium. Other important results are elements that were not detected on any substrate. Namely, sulfur and chlorine were not detected. Chlorine would likely accelerate corrosion, so lack of its detection increases confidence in these pre-treatments to protect against corrosion. The Zr peak interferes with the sulfur S LMM peak and the high energy S KLL peak at ~2117 eV is too weak to be useful.

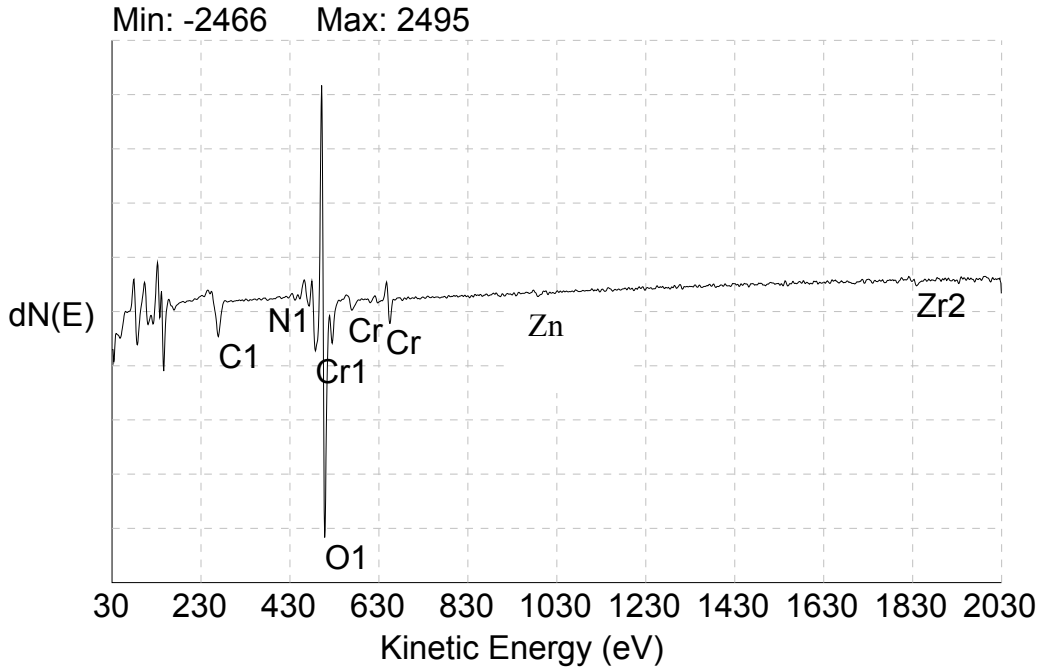

Figure 59: Scanning Auger microscopy Survey results for TCP-IC on 2024

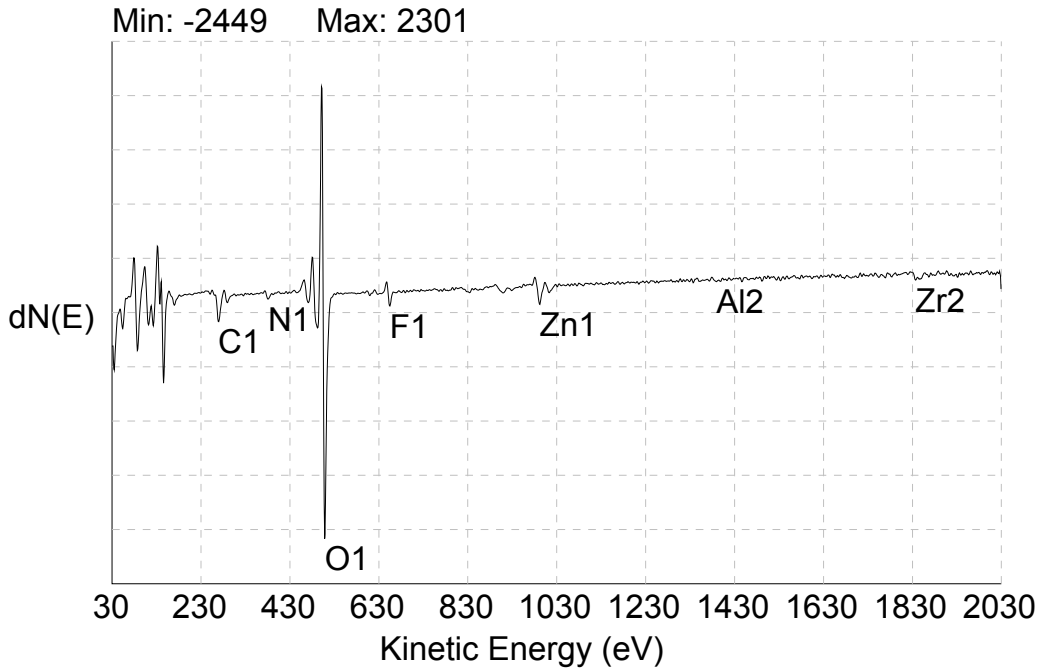

Figure 60: Scanning Auger microscopy survey results for CFP-I on 2024.

3.4.4 AUGER ELECTRONIC SPECTROSCOPY

Scanning Auger electronic spectroscopy results are more accurate than the survey results and allow for better quantification of the elemental composition on the surface. Figure 61 shows a typical plot of measured composition for TCP pretreatments. Note that the surface concentration was measured at three spots on the surface to account for potential thickness and compositional variations. There was some variability from spot to spot, although in general the variance was not large. Figure 62 verifies this compositional thickness. The light microscope image shows large differences from spot to spot that are either a result of compositional differences or thickness variations.

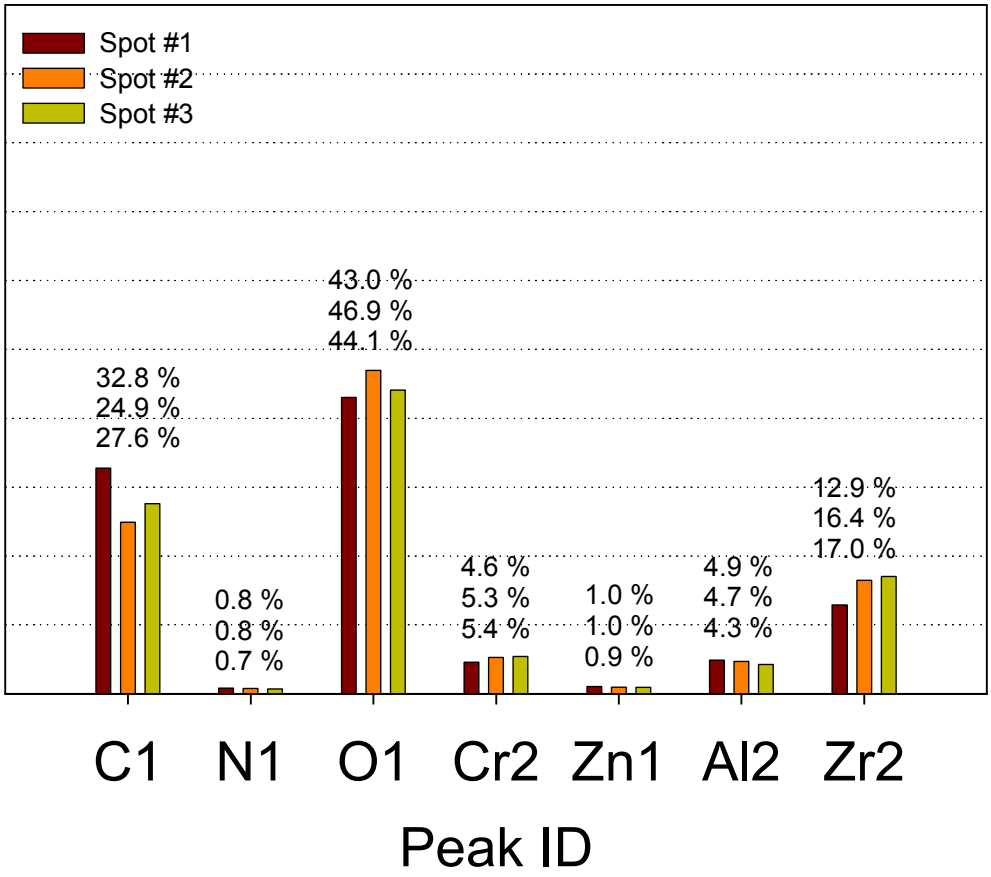

Figure 61: Auger electronic spectroscopy results showing variation in elemental composition from spot to spot for TCP-I on Al 7075.

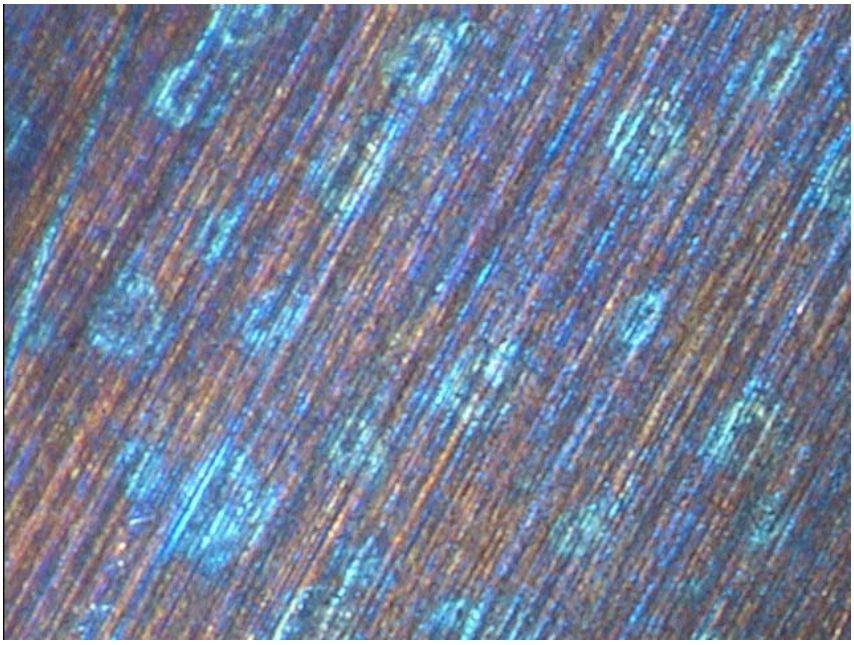

Figure 62: Light microscope image at 500x magnification of TCP on Al 2024 showing compositional or thickness variation on the sample.

The three compositional results were averaged for each surface and plotted for the four different pretreatments analyzed. The composition of TCP and CFP on Al 2024 is shown in Figure 63. In general, the elemental compositions are similar. However, the CFP treated substrate contains no Cr, no Zn, and is the only substrate with F. The higher concentration of the fluorozirconate species in CFP causes this higher F concentration on the surface. CFP uses no Cr, so it was not surprising to see no Cr on the CFP treated surface.

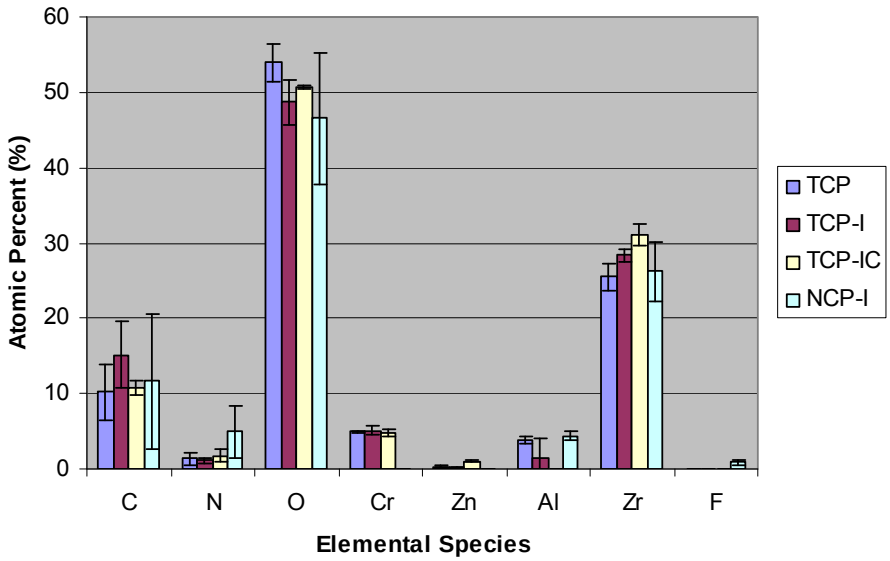

Figure 63: Auger electronic spectroscopy results showing elemental composition for the various Cr(VI) free pretreatments on Al 2024

There were more compositional variations of the pre-treatments on Al 7075 substrates (Figure 64). The carbon composition was highest and the oxygen composition was lower on TCP and TCP-I. This indicates more organic corrosion inhibitor or other organic additive adsorption to the surface on TCP and TCP-I. TCP had the least Cr on the surface of the TCP pre-treatments likely due to competitive adsorption with the organic species. Similarly, TCP and TCP-I had the lowest Zr composition. TCP had the highest Al composition. This was unexpected considering the low oxygen concentration measured for this pre-treatment/substrate. As for Al 2024, there was no Cr on the CFP treated Al 7075 and F was only detected on the CFP treated surface.

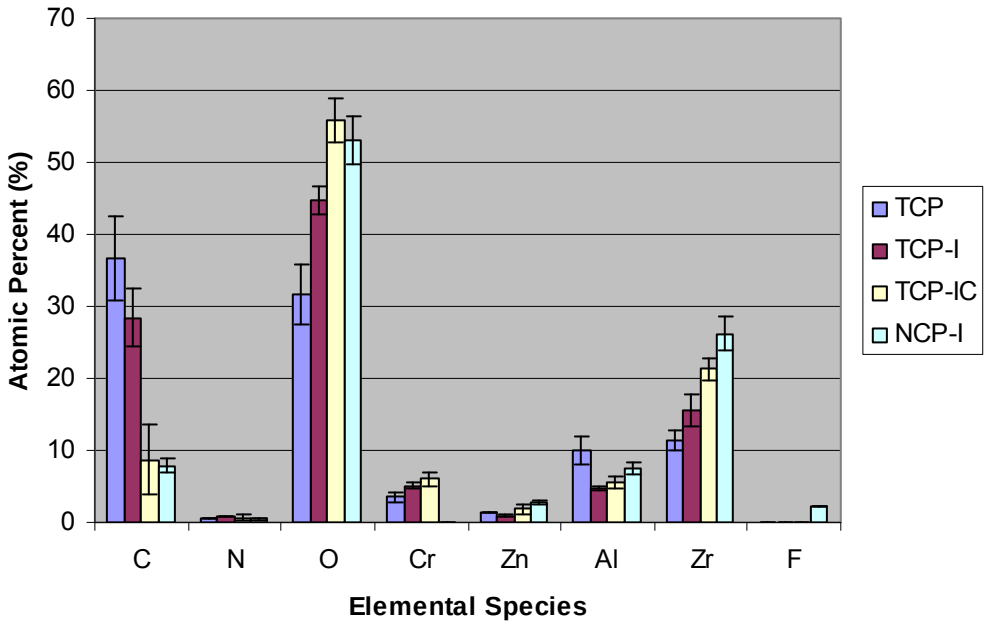

Figure 64: Auger electronic spectroscopy results showing elemental composition for the various Cr(VI) free pretreatments on Al 7075

There are slight compositional variations on how pre-treatments adsorb to different substrates. Figure 65 shows a typical compositional comparison of the pre-treatments on Al 2024 and Al 7075. However, the carbon content on the surface was higher for Al 2024 substrates, indicating greater adsorption of organic corrosion inhibitor. Also, the Al content was higher in 7075 surfaces. These results together possibly indicate a slightly thicker coating layer on Al 2024 substrates. These results indicate that TCP and CFP do not form consistent coatings on substrates regardless of the substrate. Therefore, it is possible that TCP or CFP may be effective on one substrate, but less effective on another. Corrosion results will be correlated with these different compositional variations to elucidate these effects.

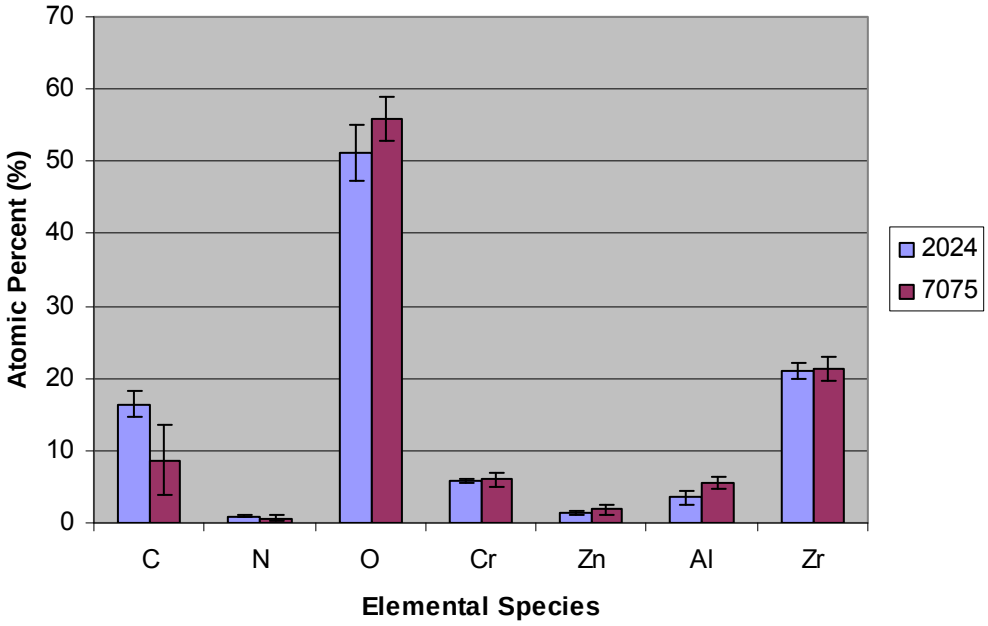

Figure 65: Auger electronic spectroscopy results showing variation in elemental composition for TCP-IC on Al 2024 and 7075.

Two different sets of pretreated samples were analyzed at different times during the year. In general, the compositions were similar for most elemental species. However, the carbon composition was lower and the zirconium composition was higher in the samples measured in January (Figure 66). Thus, compositional differences occur during the same pretreatment step. Therefore, it is possible that slight substrate variations cause these effects. It could also indicate a poorly mixed pretreatment, allowing for compositional variations. More likely, if the same solution was used to treat all substrates, the composition of the solution would be changing with time as a result of adsorption onto the substrate, causing compositional variations on the substrate with time. This indicates that some pretreatments may effectively prevent corrosion while others fail simply due to these variations. Corrosion results will therefore be correlated along with these compositional variations.

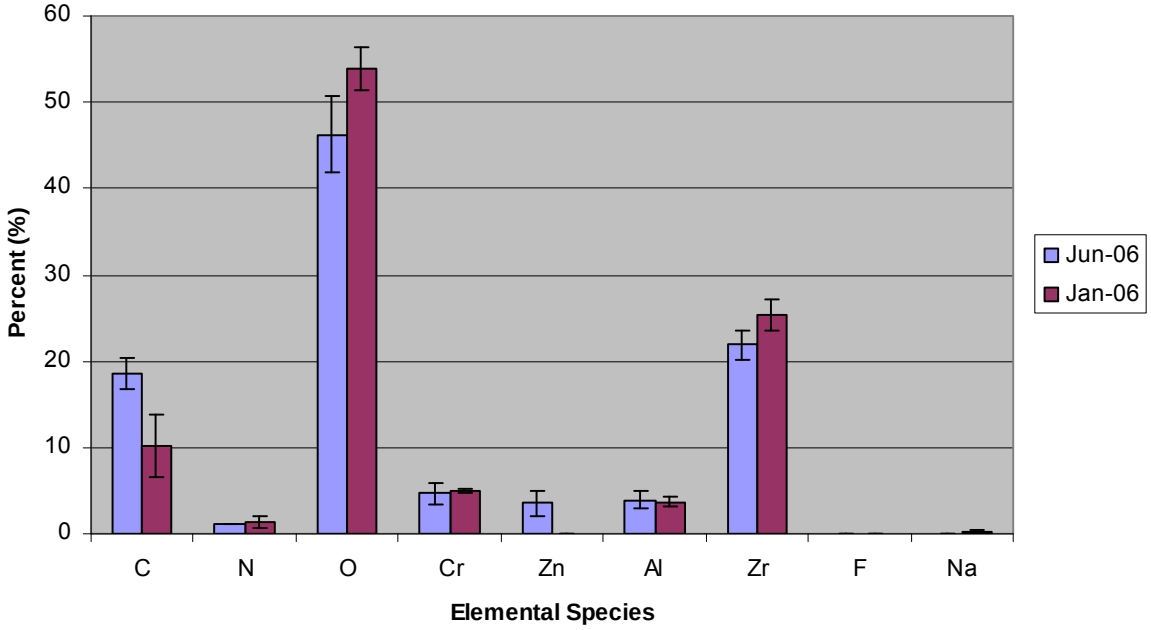

Figure 66: Auger electronic spectroscopy results showing variation in elemental composition for TCP on Al 2024 taken at two different times on samples prepared at different times

TCP/NC vs. Alodine/NC

Figure 67 shows Auger data of (TCP/NC), (Alodine/NC) and (Blank/NC) samples. As mentioned in the experimental section, these are non-corroded (NC) samples. From Fig. 1, (TCP/NC) has a higher concentration of sulfur than the (Alodine/NC) and (Blank/NC). Carbon concentration on (TCP/NC) and (Blank/NC) seem to be much higher than (Alodine/NC). The oxygen content on (Blank/NC) is much less. Obviously, the blank sample has more aluminum on the surface than (TCP/NC) or (Alodine/NC). The (Blank/NC) sample should have a native aluminum oxide film on the surface. Carbon on the surface could be obscuring the oxide on the blank sample. The Mg:Al bulk composition ratio in AA 2024 is 0.015 [26], but the results show a ratio that is much higher (0.08) in (Blank/NC). This could be due to differences in the bulk and surface compositions.

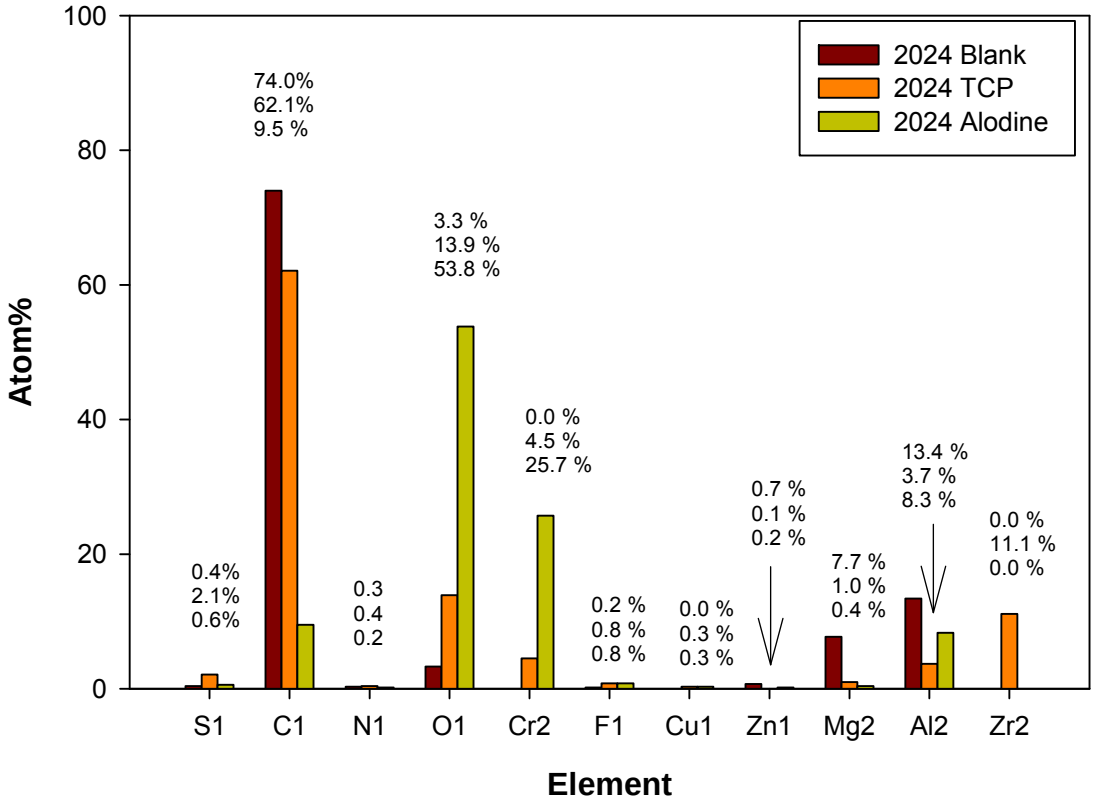

Figure 67: Results of Auger electronic spectroscopy for (TCP/NSS/744hrs) and (Alodine/NSS/744hrs). Both the less corroded (LC) and more corroded (MC) sides are shown. The vertical bars display the average concentration for the elements shown from three spots from each sample.

(Alodine/NC) has higher concentrations of oxygen and chromium (25%) than (TCP/NC) which has only 4% Cr. However, aluminum seems to be more exposed on (Alodine/NC) than (TCP/NC). Images of the coated surfaces show that Alodine coating on 2024 is very porous with cracks compared to TCP (Figure 68). No zirconium was detected in (Alodine/NC).

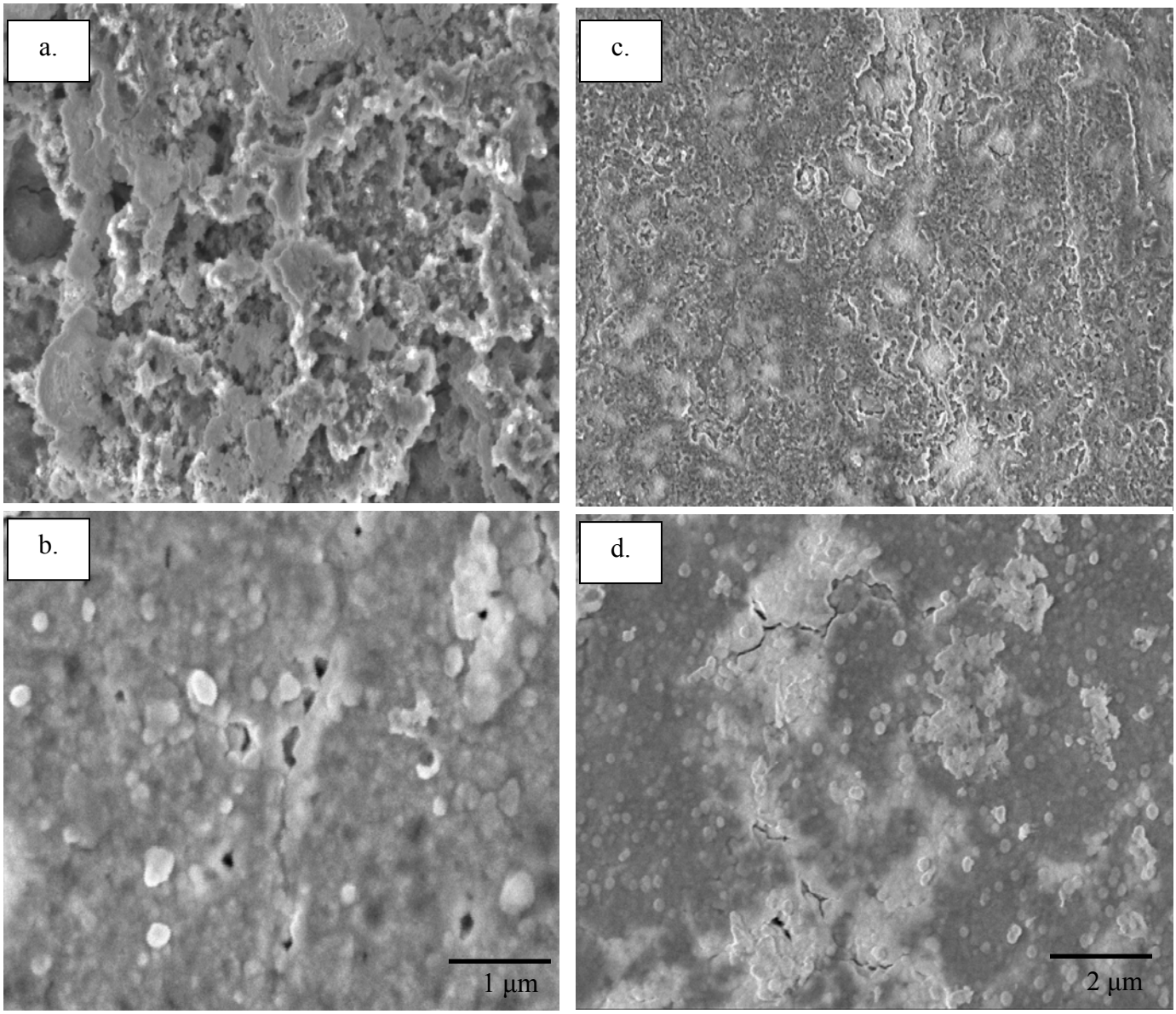

Figure 68: FESEM images of Alodine/NC (a), TCP/NC (b), Alodine/NSS/744hrs/MC (c), and TCP/NSS/744hrs/MC (d).

There is not much fluorine seen on (TCP/NC). The surfaces reveal trace presence of elements like zinc, magnesium, and copper. Overall, Auger confirms the presence of chromium and zirconium as a part of the TCP coating along with sulfur and trace amounts of fluorine.

TCP/NSS/744hrs vs. Alodine/NSS/744hrs

Figure 69 presents surface analysis of 4 samples. These are TCP and Alodine coated samples that have undergone NSS treatment for 744 hours. Each sample has less corroded (LC) and more corroded sides (MC).

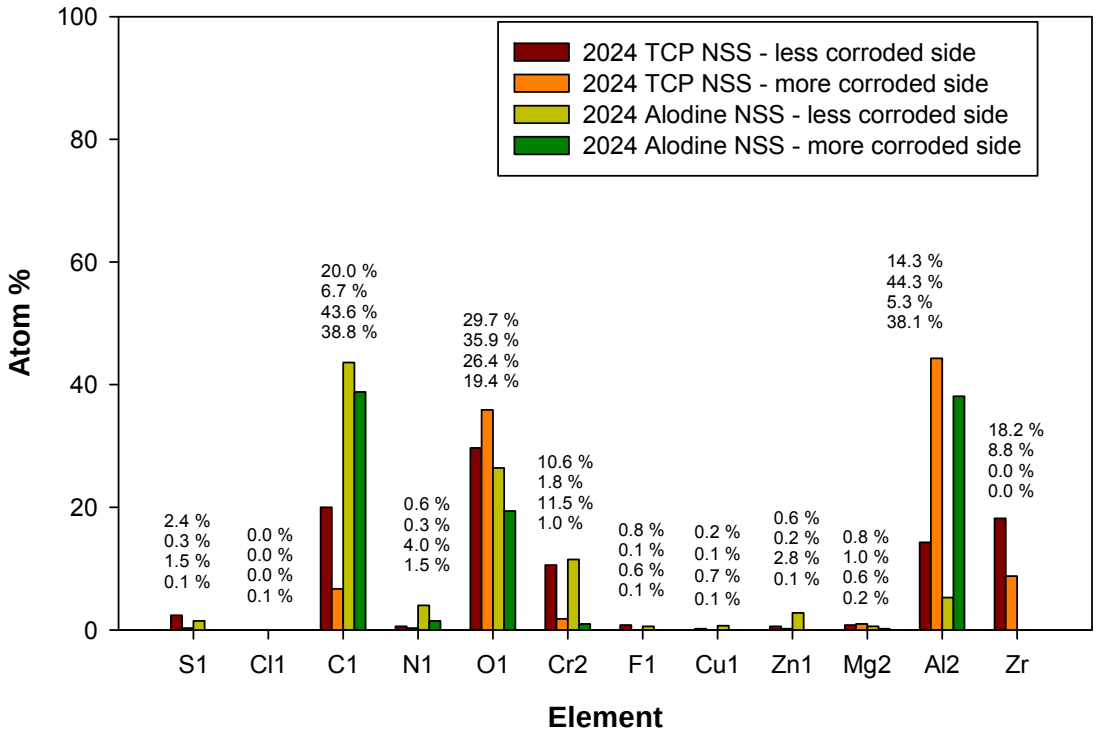

Figure 69: AES data of (TCP/NSS/744hrs) and (Alodine/NSS/744hrs). Both the less corroded (LC) and more corroded (MC) sides are shown. The vertical bars display the average concentration for the elements shown from three spots from each sample.

A comparison of (TCP/NC) in Figure 67 vs. (TCP/NSS/744hrs/LC) in Figure 69 shows that there is an increase in the amount of chromium on the surface. In the case of (Alodine/NC) vs. (Alodine/NSS/744hrs/LC) however, shows that the chromium content has reduced from 25% to 11% after corrosion. On the more corroded side, much less chromium (1-2%) is seen on both (TCP/NSS/744hrs/MC) and (Alodine/NSS/744hrs/MC).

There is more aluminum (~ 14%) exposed on the surface of (TCP/NSS/744hrs/LC) than (Alodine/NSS/744hrs/LC) which has ~ 5%. There is also significant amount of aluminum seen on both the TCP and Alodine more corroded surfaces (~40%).

Comparing (TCP/NC) in Figure 67 vs. (TCP/NSS/744hrs/LC) in Figure 69, there is an increase in zirconium (from 11% to 20%). On all three Auger spots taken for (TCP/NSS/744hrs/LC), the zirconium concentration ranged from 16-20% (Figure 70). Zirconium exists in the TCP coating in the form of hexafluorozirconate species. On the more corroded side i.e. (TCP/NSS/744hrs/MC), the zirconium concentration was not constant on all three Auger spots.

(Fig.4b). A SEM image reveals an uneven surface after corrosion (Figure 68). An increase in aluminum and oxygen was accompanied by a subsequent decrease in zirconium concentration (Figure 70).

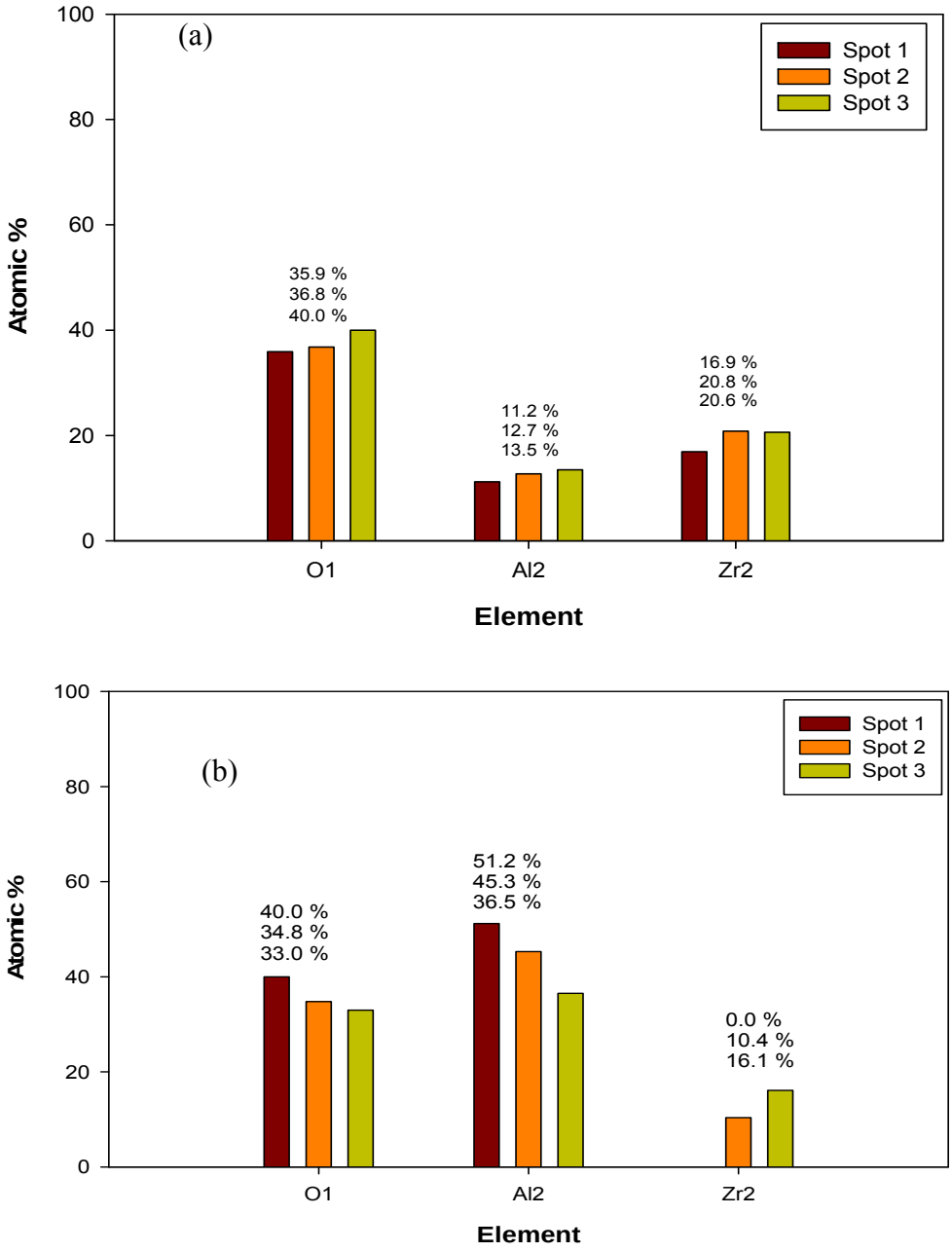

Figure 70: Results of Auger electronic spectroscopy of (a) (TCP/NSS/744/LC) and (b) (TCP/NSS/744/MC). Three spots on the sample surface were taken for collecting Auger data. The surface concentrations of 3 elements are displayed here. Other elements detected on this spot are not shown in this figure.

In (TCP/NC) vs. (TCP/NSS/744hrs) samples, the amount of carbon is decreasing with corrosion. Carbon seen in (Alodine/NC) vs. (Alodine/NSS/744hrs) samples seems to have increased after corrosion. Carbon maybe due to the $K_3[Fe(CN)_6]$ present in Alodine [27].

Other than the elements reported above, metals like copper, zinc, magnesium are present in trace amounts. However, there is no significant increase in metal concentration on the surface before and after corrosion. Also, the presence of Cl and F are not very high on the (TCP/NSS/744hrs) and (Alodine/NSS/744hrs). Sulfur is also detected on these NSS corroded samples.

TCP/SO_2 vs. Alodine/SO_2

Figure 71 and Figure 72 show TCP and Alodine samples that have undergone NSS treatment along with SO_2 mist treatment. Samples have undergone treatment for different exposure times (24 hrs, 72 hrs, 148 hrs). Again each sample has two sides – less corroded (LC) and more corroded (MC). In this section, samples have been referred to as (TCP/SO_2/LC) or (TCP/SO_2/MC) without the exposure time being specifically mentioned in the parentheses. This means that the discussion is applicable to all three exposure times viz. (TCP/SO_2/24hrs/MC), (TCP/SO_2/72hrs/MC), (TCP/SO_2/148hrs/MC). The same nomenclature is followed for (Alodine/SO_2) samples. On each side three spots were chosen for Auger and the average concentration obtained is reported.

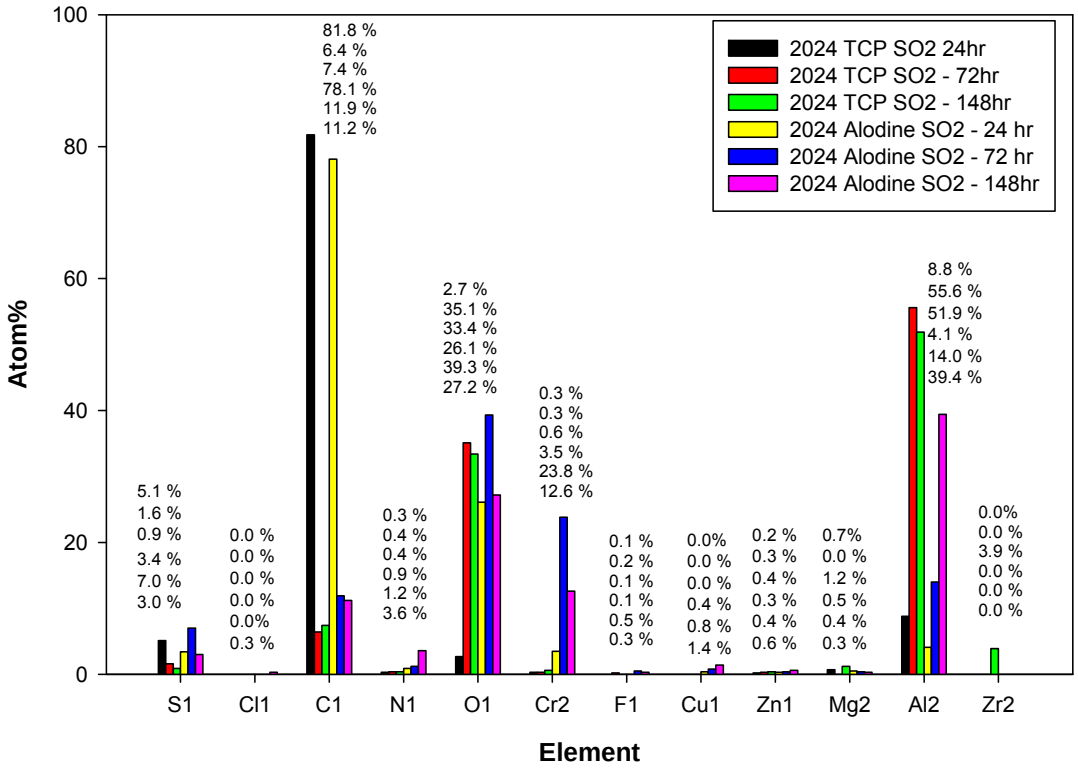

Figure 71: Results of Auger electronic spectroscopy of (TCP/SO_2/LC) and (Alodine/SO_2/LC) samples after different SO_2 exposure times are shown. The vertical bars display the average concentration for the elements shown from three spots from each sample.

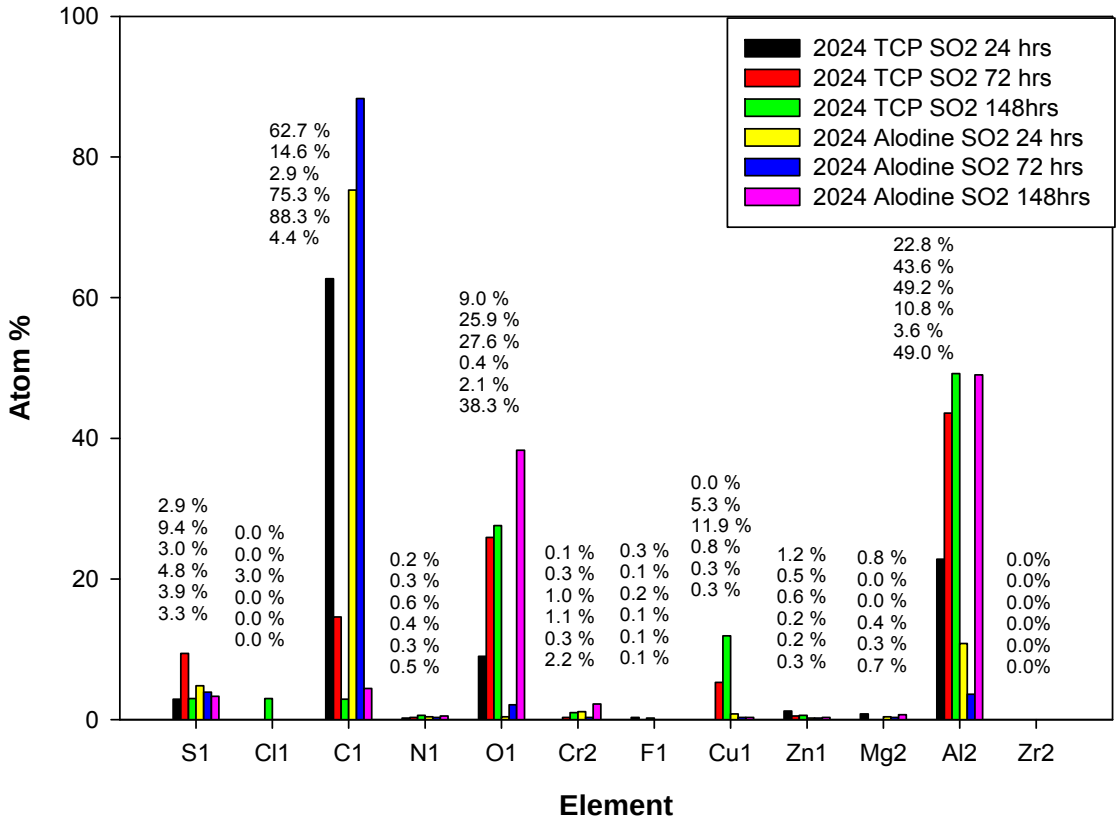

Figure 72: Results of Auger electronic spectroscopy of (TCP/SO2/MC) and (Alodine/SO2/MC) samples after different SO_2 exposure times are shown. The vertical bars display the average concentration for the elements shown from three spots from each sample.

Figure 71 presents the data for the SO_2 treatment less corroded sides (LC). Sulfur concentration has increased on all (TCP/SO_2/LC) and (Alodine/SO_2/LC) samples as compared to Figure 67 (TCP/NC) and (Alodine/NC). The sulfur is part of TCP coating and also could come from adsorption of SO_4^{2-} ions.

Figure 71 also shows clearly that the chromium on (TCP/SO_2/LC) surfaces is much less than on (Alodine/SO_2/LC) surfaces. (Alodine/SO_2/LC) samples also have less aluminum exposed on the surface compared to (TCP/SO_2/LC). This could mean that the Alodine has a better performance against corrosion than the TCP due to the hexachrome based chemistry and migration properties [28].

Zirconium on the coating is not detected in case of all (TCP/SO_2/LC) samples except in (TCP/SO_2/148hrs/LC). Much less chlorine is detected on (Alodine/SO_2/LC) and (TCP/SO_2/LC) samples. Trace amounts of metals like copper, zinc, magnesium are also detected whose concentrations vary between 0 to 2%. A comparison of Figure 67 and Figure 71 shows that there

is no significant difference seen in the surface concentration of copper, zinc and magnesium. This is true for both (TCP/SO_2/LC) and (Alodine/SO_2/LC) samples.

Figure 72 provides Auger data for the (TCP/SO_2/MC) and (Alodine/SO_2/MC) samples. The increase in the presence of sulfur on the surface is obvious and is due to the SO_2 mist treatment. A comparison can be made between Figure 67 and Figure 72. This is seen on both (TCP/SO_2) and (Alodine/SO_2) samples.

The chromium content (~1-2%) on (Alodine/SO_2/MC) and (TCP/SO_2/MC) suggests that the coating is almost gone. The increase in aluminum content from 3.7% in (TCP/NC) in Figure 67 to almost 50% in (TCP/SO_2/MC) in Figure 72 suggests that the coating is washed away after corrosion. Zirconium was not detected on (TCP/SO_2/MC) samples.

For the (TCP/SO_2/MC) samples, carbon content decreases with corrosion time. However, on the (Alodine/SO_2/MC) samples, there seems to be no specific trend between treatment time and carbon content on the surface. Especially for sample marked as (Alodine/SO_2/72hrs/MC), the surface appears to be very rich in carbon. In order to verify the results obtained for carbon concentration, three additional spots were chosen (not shown here). In all the 6 spots evaluated, the carbon content was the same. We do not know the exact reason as to why the surface was so rich in carbon. In both (Alodine/SO_2/24hrs/MC) and (Alodine/SO_2/72hrs/MC), the carbon on the surface is affecting the percentage of other elements like aluminum and oxygen detected.

The copper content on the (TCP/SO_2/MC) samples in Figure 72 is much more than on the (TCP/NC) in Figure 67. An increase from 0.3% to almost 12% is seen (compare Figure 67 and Figure 72). This increase in copper is not seen in (Alodine/NC) vs. (Alodine/SO_2/MC) samples (compare Figure 67 and Figure 72). Chlorine at 3% was detected on (TCP/SO_2/148hrs/MC) whereas the Alodine counterpart (Alodine/SO_2/148hrs/MC) shows 0% chlorine on the surface.

3.4.5 SURFACE HEXAVALENT CHROMIUM ON PRETREATED SAMPLES

Figure 73 gives the calibration curve for the analysis of hexavalent chromium on pretreated samples as described above. Table 16 lists the exposure and measured Cr(VI) content for various pretreated samples on Al 2024. Some samples were analyzed after pretreatment without accelerated corrosion exposure, while other samples were exposed to neutral salt fog (NSF) or a neutral salt spray and SO_2 gas exposure for different times. No Cr^{6+} was detected for the acetone-wiped blank, the TCP-S, and TCP-IC, regardless of accelerated corrosion exposure (Table 16). Alodine 1200S and 1600S are commercially available Cr^{6+}-based chromate conversion coating solution. Chrome (VI) levels of 0.81 and 3.6 μg Cr^{6+}/cm^2 were obtained for 2024 Alodine 1200S and 1600S respectively for samples not exposed to accelerated weathering. This proves that the TCP and TCP-IC pretreatments indeed are non-hexavalent producing ones.

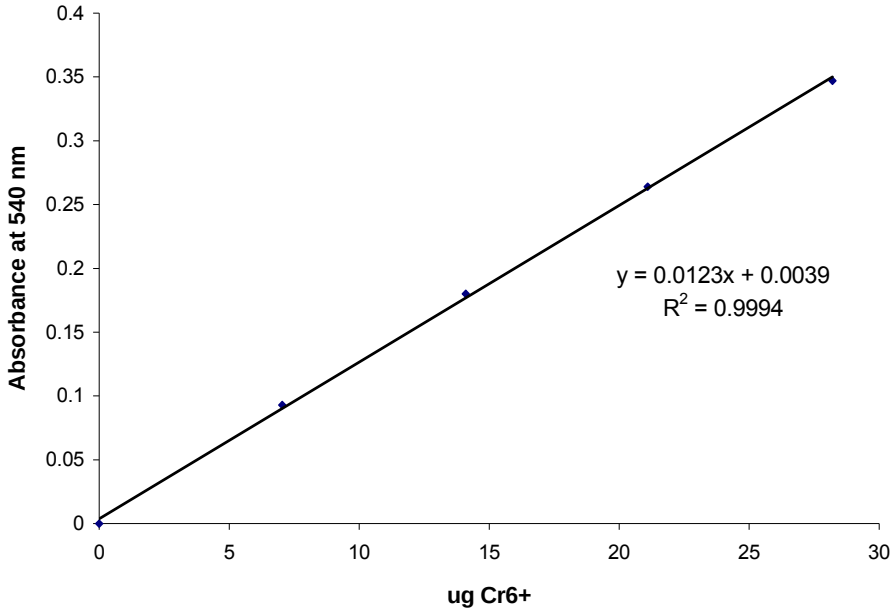

Figure 73: Calibration curve for the hexavalent chromium analysis on pretreated samples.

Table 16: The measured Cr(VI) content for various pretreatments and exposure conditions on Al 2024.

Pretreatment	Exposure	Cr^{6+} Level ($\mu g/cm^2$)
Acetone Wiped (blank)	None	0
TCP-S	None	0
TCP-S	NSF 744 hrs	0
TCP-S	SO_2 24 hrs	0
TCP-S	SO_2 72 hrs	0
TCP-S	SO_2 148 hrs	0
TCP-IC	None	0
Alodine 1200S	None	0.81
Alodine 1200S	NSF 744 hrs	0.09
Alodine 1200S	SO_2 24 hrs	0
Alodine 1200S	SO_2 72 hrs	0
Alodine 1200S	SO_2 148 hrs	0.03
Alodine 1600S	None	3.6

Note that even in Alodine 1200S-coated samples, after SO_2 corrosion treatment for 24 and 72 hours, no hexavalent chromium was detected. This could be explained by the very likely possibility that the coatings in samples during corrosion treatment might have been stripped or dissolved by the mist of salt spray solution. Yet, Alodine 1200S samples exposed to NSF with SO_2 for 148 hours and NSF for 744 hours, gave Cr^{6+} levels of 0.03 and 0.09 μg Cr^{6+}/cm^2, respectively. Comparing these levels from the original Cr^{6+} level of 0.81 μgCr^{6+}/cm^2 mentioned above, we can see that a significant decrease is observed. Again, this is likely due to dissolution or stripping during the corrosion treatments. Also, the Cr^{6+} being detected here could be due to

the oxidation of Al 2024 alloy-content chromium since it seems that the hexavalent chromium has already been stripped as early as 24 hours of corrosion treatment as can be seen from the results of the hexavalent analysis on samples 2024 Alodine 1200S SO_2 24 and 72 hrs.

To verify the method we used to detect hexavalent chromium, 500 µL each of TCP, TCP-IC and Alodine 1200S solutions was spiked onto the surface of a piece of Al 2024 blank stubs (1.9 x 2.5 cm). The stubs were then air-dried. Using this technique, we know exactly how much Cr^{6+} (if any) was put on the surface so we can test the method validity. No Cr^{6+} was detected for the stubs coated with TCP and TCP-IC solutions. This is in agreement with the results described below where the solutions of TCP and TCP-IC were tested for Cr^{6+} content. This means that the method we used for determining surface Cr^{6+} causes no oxidation of any Cr^{3+} that might be present in the surface or coating. A level of 238 µg Cr^{6+} was detected in the Alodine 1200s coated stub. From the determination of hexavalent chromium in the Alodine 1200S solution, we expect that there should be 839 µg Cr^{6+} that was coated on the stub. We can see from the results that the detected Cr^{6+} is much lower than the expected level. This can be accounted for the fact that not all of the coating in this method was extracted during the immersion in hot water step of the analysis (Figure 74). However, this clearly **verifies the validity of the method we used for determining Cr^{6+} in pretreated samples.**

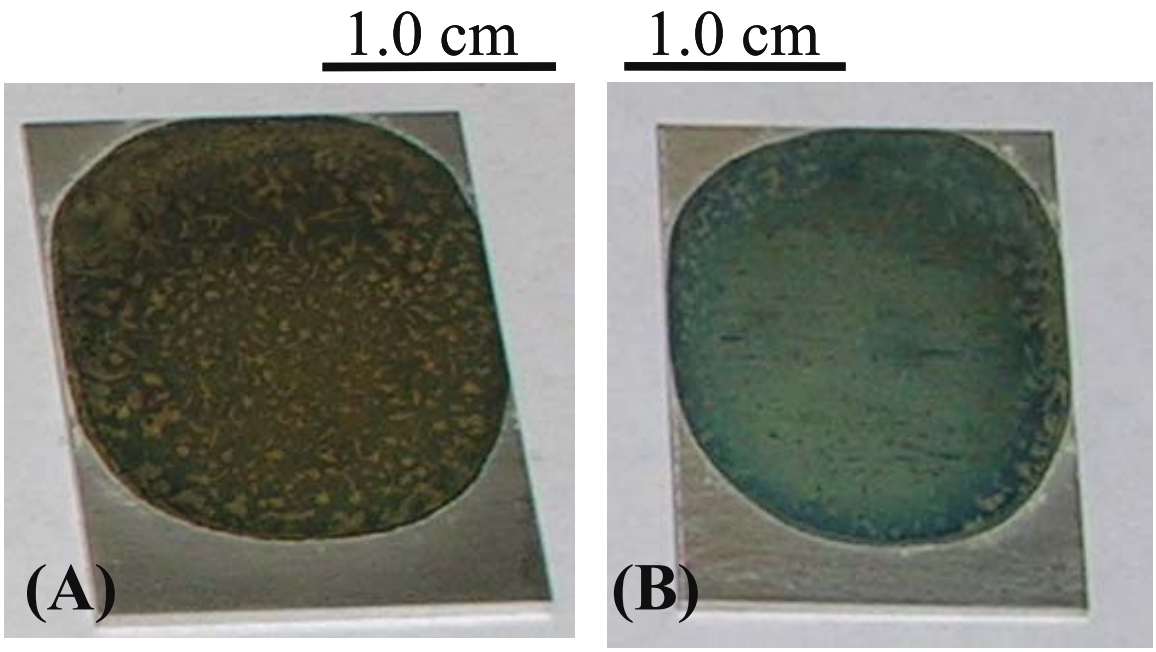

Figure 74: Alodine 1200S-coated stubs (A) before and (B) after analysis. It is evident from B that during the analysis, not all of the coating was extracted; the coating was too thick.

Initial results did indicate low levels of hexavalent chromium from the TCP films at quantities less than 0.1µg/cm^3 (Table 17). However, these have not been duplicated. It is believed that contamination from the Alodine 1600 samples which were shipped along with the TCP-pretreated samples for analysis at the University of Connecticut caused this false positive.

Table 17: Quantitative analysis of hexavalent chromium in various metal coatings

	μg Cr^{6+}/cm^2	ppm Cr^{6+}	Cr^{6+}/Total Cr
2024 TCP	0.073	0.65	0.001
2024 Alodine 1600S	3.6	8.3	0.005
7075 TCP	0.049	0.44	0.001
7075 Alodine 1600S	2.9	6.4	0.07

3.4.6 TOTAL CHROMIUM USING ATOMIC ABSORPTION SPECTROSCOPY (AAS)

Figure 75 gives the calibration curve for the total Cr analysis using AAS. Samples 2024 Blank and TCP-IC and 7075 Blank and TCP-IC were analyzed for total chromium content. Levels of 480 ppm and 540 ppm Cr were obtained for samples 2024 Blank and TCP-IC respectively. For samples 7075 Blank and TCP-IC, levels of 3085 and 3401 ppm Cr were obtained. As expected TCP-IC levels are higher than the blank ones. Using this method of determining total Cr, the different Cr uptake upon pretreatment between different types of Al alloys can be assessed.

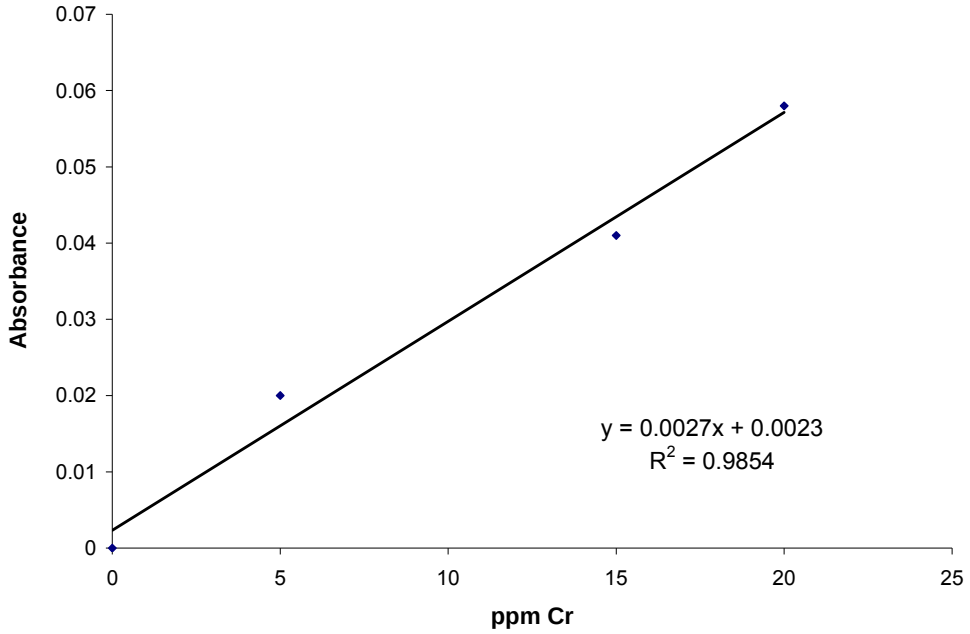

Figure 75: Calibration curve for the total Cr analysis using AAS

3.4.7 HEXAVALENT CHROMIUM CONTENT IN PRETREATMENT SOLUTIONS

Figure 76 gives the calibration curve for the Cr^{6+} analysis on pretreatment solutions before and after coating two Al 2024 panels with dimensions of 3 x 10 inches. No Cr^{6+} was detected in the TCP and TCP-IC pretreatment solutions before and after coating the panels. This shows that there is no oxidation of Cr^{3+} to Cr^{6+} occurring during the pretreatment. Also, the "IC" additive on TCP does not induce any oxidation of Cr^{3+} to Cr^{6+}. For the unused Alodine 1200S, a level of 1678 ppm Cr^{6+} was obtained while a level of 960 ppm was obtained on the used Alodine 1200S

pretreatment solution. The decrease in Cr^{6+} content here is due to coating onto the Al panel. Approximately 180 mg of Cr^{6+} was coated on two Al 2024 panels using a dip coating of 5 minutes each and a bath volume of 250 mL.

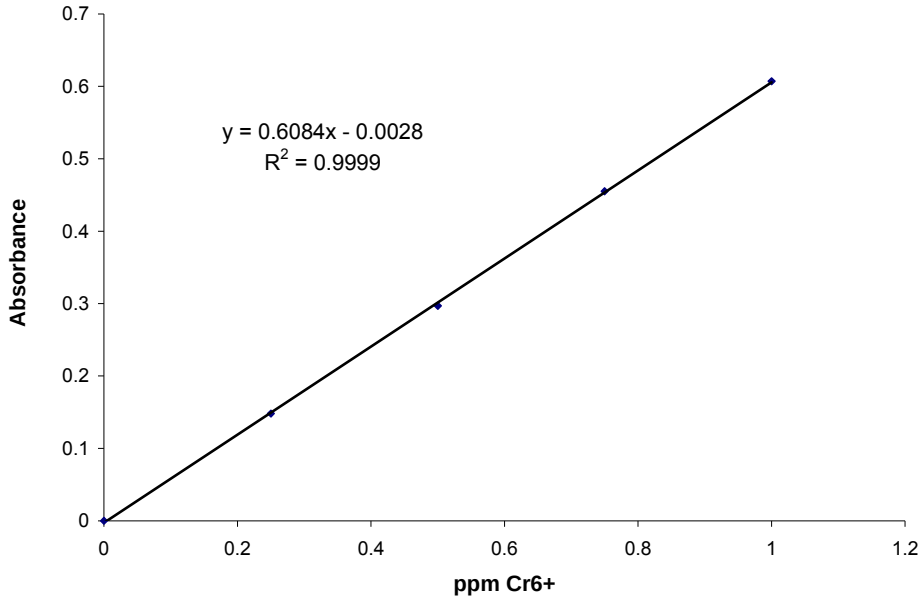

Figure 76: Calibration curve for the Cr^{6+} analysis of pretreatment solutions

The concentration of Cr(VI) before and after pretreatment can be used to predict the amount of Cr(VI) on a pretreated panel. Table 18 lists the measured Cr(VI) content using four different methods for TCP-S, TCP-IC, and Alodine 1200S pretreatments. As before, no Cr(VI) was measured for the TCP pretreatments or pretreated panels. On the Alodine 1200S, the ISO method conducted on the 1.9 cm x 2.5 cm stubs (Figure 74) revealed a measurement of 50 $\mu g/cm^2$. Based on the concentration change of Cr(VI) in the solution, the amount of Cr(VI) expected on the panel should be 177 $\mu g/cm^2$. Efforts were taken to ensure that the pretreatment solution did not run off the stub and both sides of the stub. The reason for this difference is then likely due to the fact that not all of the pretreatment coating was removed from the substrate for analysis (Figure 74) and could also be due to instability of the Cr(VI). Some of the Cr(VI) on the panel was likely reduced back to Cr(III). This number agrees well with the EPA 7196A analysis method (232 $\mu g/cm^2$) of the pretreatment solution before and after pretreatment. The stubs had far more Cr(VI) on them than the pretreated panels (0.81 $\mu g/cm^2$) because the pretreated panels were only contained in the pretreatment bath for 5 minutes and the excess solution was allowed to drip off the surfaces as the panels air-dried. Therefore, the use of a known mass of pretreatment on a given substrate with a known surface area allows for a magnification of the concentration of components deposited onto the substrate. This is even further proof that no Cr(VI) is formed in TCP pretreatment solutions and pretreated panels.

Table 18: Cr(VI) content as measured using a variety of techniques.

Test Method	TCP-S $\mu g/cm^2$	TCP-IC $\mu g/cm^2$	Alodine 1200S $\mu g/cm^2$
ISO 3613 on stub - measured	0	0	50
ISO 3613 on stub - expected	0	0	177
EPA 7196A back calculation for Cr(VI) on panel	0	0	232
ISO 3613 on pretreated panels	0	0	0.81

3.4.8 DISCUSSION OF CR(VI) CONTENT IN PRETREATMENTS

AA 2024 contains 4.5% copper in the alloy [26] and because copper is prone to corrosion, this alloy is hard to protect. There are two types of corrosion that aluminum alloys can undergo – anodic and cathodic. Anodic corrosion is a result of anions like Cl^- adsorbing on the aluminum surface and forming complexes with aluminum [29] whereas cathodic corrosion is a result of oxygen reduction catalyzed by copper rich alloy surfaces. Surface copper enrichment results from the dissolution of the alloy and re-deposition on the alloy surface [30].

Corrosion of a metal surface forms a barrier layer that can inhibit both oxygen adsorption on re-deposited copper and chlorine adsorption to aluminum [31]. Hence, detection of chlorine and copper on the corroded surface suggests that the coating may be able to act as an efficient barrier against further corrosion. We used AES to detect chlorine and copper.

As mentioned in the introduction, the TCP coating mainly consists of trivalent chromium, a hexafluorozirconate complex, sulfur compounds and additives. Alodine 1200S consists of 50-60% CrO_3, KBF_4, $K_3[Fe(CN)_6]$, K_2ZrF_6, NaF [27].

AES surface analysis of elements suggests us that in all (TCP/SO_2) and (TCP/NSS/744hrs) samples, chlorine was not detected in significant amounts on the surface. However, there was one exception. In case of (TCP/SO_2/148hrs/MC) (Figure 72), 3% chlorine was detected. Otherwise, the results are comparable to the (Alodine/SO_2) samples (Figure 71 and Figure 72). Even though very less chromium (~1%) was present on the (TCP/SO_2) corroded surfaces and zirconium was absent, there is negligible chloride adsorption. Even a thin layer of TCP coating seems to provide sufficient protection against chloride ion adsorption. Sulfur compounds are a part of the TCP coating [32] and they too might play a key role in the inhibition process. TCP forms a barrier on the alloy that is able to resist anodic attack by blocking adsorption of chloride ions.

Cathodic corrosion catalyzed by copper containing intermetallics is also a possibility. Copper rich surfaces come from the de-alloying of inter-metallic phases especially the S-phase (Al_2CuMg) and re-deposition of copper on the alloy surface. Dimitrov et al. studied the redistribution of copper on the aluminum alloy surface after corrosion. These reactions are enhanced under acidic conditions [30]. Copper is a good catalytic site for oxygen reduction. In (TCP/NSS/744hrs/LC) and (TCP/NSS/744hrs/MC) the percentages of copper and other alloying elements have not increased even after 744 hours of corrosion (Figure 69) so there seems to be less alteration in the surface composition of the alloy. This analysis indicates that under NSS conditions the performance of TCP and Alodine 1200S coatings is almost equal. Chromium and

zirconium are still present on the (TCP/NSS/744hrs/LC). Significant amount of zirconium seen on (TCP/NSS/744hrs/MC) is proof that the coating is still present on the surface after 744 hours of treatment. The SEM image also shows that the coating is still present on the alloy (Figure 68) along with signs of corrosion.

However, in the SO_2 treated samples, there is an increase in copper content on (TCP/SO_2/MC) samples (Figure 72) from 0% up to 11% as corrosion time increases. The (Alodine/SO_2/MC) counterpart does not show increase in copper content on the surface. This indicates that under acidic conditions the TCP coating is more susceptible to corrosion. Copper deposits on the surface indicate that the coating is washed out. The performance of TCP coating is not as good as the hexavalent Alodine 1200S coating under acidic pH. A build-up of aluminum oxide is seen on both (Alodine/SO_2/MC) and (TCP/SO_2/MC). There is more aluminum oxide on TCP corroded surfaces than on Alodine 1200S corroded surfaces.

Further, the objective of a trivalent chromium based coating is to ensure the absence of residual hexavalent chromium. TCP coatings have the major advantage as they do not contain any residual hexavalent chromium. All tests (Table 16-Table 18) lead to this conclusion. Alodine 1200S coatings contain residual hexchrome [29,33]. Diphenylcarbazide test on (TCP/NC), (TCP/NSS/744hrs) and (TCP/SO_2) (Table 16) proved that no hexachrome is present in the TCP samples. (Alodine/NC) has 0.81 μg/cm^2 of Cr^{6+} and (Alodine/NSS/744hrs) has 0.09μg/cm^2 of hexavalent chromium. In comparison (TCP/SO_2) and (TCP/NSS/744hrs) samples have no hexchrome. From the hexavalent chromium analysis, TCP coated and corroded panels did not show any Cr^{6+} (Table 16) as expected [4].

We decided to check TCP coating for hexavalent chromium not only after coating on AA 2024 substrate but also during the coating process and in TCP solutions. For the sake of comparison Alodine 1200S was also subjected to the same tests. Table 17 discusses the various values of hexchrome obtained from different experiments. Treatment solutions tested before and after coating of the panels did not contain any Cr^{6+}. This means that no oxidation of Cr^{3+} to Cr^{6+} occurred during any time of the coating process. Hexchrome analysis of the TCP solution spiked coupon (Table 17) did not show any Cr^{6+} because no hexavalent species are used in the preparation of the TCP solutions unlike Alodine 1200S [33]. A significant level of Cr^{6+} was detected in Alodine 1200S solution (Table 17). This proves that the method we used for determining Cr^{6+} did not cause oxidation of any Cr^{3+}. All chromium detected in TCP samples by AES is trivalent chromium. Total chromium level of Alodine 1200S coating (Alodine/NC) is twice that of a TCP coating (TCP/NC).

In conventional chromate conversion coatings like Alodine 1200S the coating solution contains hexchrome which is converted to an insoluble Cr^{3+} oxide layer after coating on the substrate. But the coating still contains residual Cr^{6+} [34]. This is also proven by the diphenylcarbazide tests (Table 18). The coating formed on the surface is a mixture of Cr^{3+} and Cr^{6+} oxides [34]. Exposure to electrolytes like NSS and SO_2 causes significant decrease in chromium levels because the hexchrome is a very labile species [26].

Unlike the above case of Alodine 1200S, a trivalent chromium based coating like TCP does not have hexchrome in the treatment solution to begin with. Even though the exact mechanism of film formation is not clear, a Cr^{3+} polymer may form on the alloy surface which is branched by -

OH, -O, and -SO_4 groups. The -OH and -O bonds are non-ionic as far as can be determined. Film formation may be due to the hydrolysis of a trivalent chromium compound like chromium sulfate at basic pH. The coordinated complex may polymerize and form an insoluble layer or film on the surface. The probable structure of the film which has chromium chloride is shown in Figure 77. Analogous compounds are formed with sulfates [35].

$$[Cr(H_2O)_6]Cl_3 \longrightarrow [Cr(OH)(H_2O)_5]Cl_2 + HCl$$

$$[Cr(OH)(H_2O)_5]Cl_2 \longrightarrow [Cr(OH)_2(H_2O)_4]Cl_2 + HCl$$

$$[Cr(OH)_2(H_2O)_4]Cl_2 \longrightarrow [Cr(OH)_3(H_2O)_3]Cl_2 + HCl$$

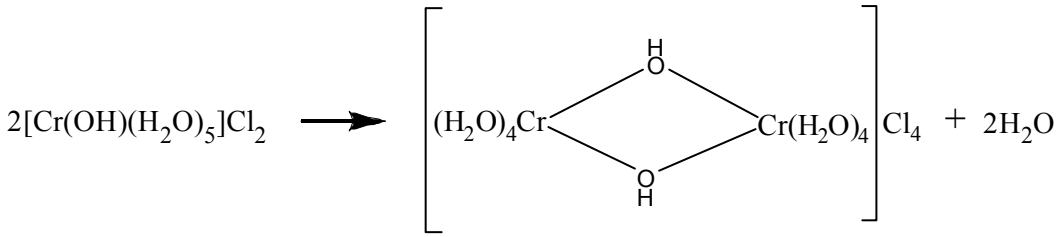

Figure 77: Suggested hydrolysis products of trivalent chromium [32]

Because the reaction is associated with the release of acid, it is likely that under acidic conditions the reaction is reversed and the branched film formed on the surface of the alloy is not stable. This relates to the poor performance of TCP coatings under acidic conditions. Hence, a highly acidic pH is required to cleave the bonds [9]. Our analysis shows that under NSS treatment, the performance of TCP coatings is equal to Alodine 1200S coatings. Furthermore, free trivalent chromium is not toxic and is considered an essential nutrient [9].

3.4.9 Effect of Highly Corrosive Environments on Cr(VI) generation in Pretreatments

3.4.9.1 Experiment

The following tests were done on TCP and Alodine samples to examine the effect of highly corrosive conditions:

- Drop of 4M H_2SO_4 TCP and Alodine 2024 samples.
- Drop of 4M HNO_3 on TCP and Alodine 2024 samples.
- Effect of 4.6M H_2SO_4 on TCP 2024 samples.
- Test on TCP and Alodine solutions in conc. H_2SO_4 and conc. HNO_3
- Effect of 1M H_2SO_4 and 1M NaCl on Alodine.

A drop of acid was placed on 1 coupon and placed in a glass vessel. The sample was covered with vinyl film and allowed to age. After a specific amount of time, the acid on the surface was extracted. A drop of DPC was spiked on the residues left on the 2024 surface. The surface was checked for pink color formation indicative of Cr^{6+}. The residues along with DPC are analyzed using ISO 3613: 2000(E). The results are expressed in $\mu g/cm^2$. For TCP sample size was (1.27cm x 1.27 cm) and Alodine (2.5cm x 2.5cm). This is because we did not have much TCP coated 2024 samples at this point.

3.4.9.2 Results and Discussion

Table 19 shows the results of 4M sulfuric acid on the pretreatment coatings. No pink color was visible on the surface for TCP pretreatments, indicating that no Cr(VI) was formed. On the other hand, the pink color was visible for Alodine pretreatments, as expected. No Cr(VI) was measured using UV-Vis because the Alodine coating was not sufficiently removed from the substrate (Figure 78).

Table 19: 2024 TCP and Alodine treated with 4M H_2SO_4

Sample	Treat-ment time	Visual obs. on surface before spiking with DPC	Visual obs. on surface after spiking with DPC	Cr(VI) ($\mu g/cm^2$) by UV-Vis
TCP	3 hrs	Black surface. Residue comes off easily.	No pink color formn. Forms a brown colored soln.	n.d
Alodine	3 hrs	Black surface. No residues form.	Pink spot obtained. After few mins. Pink color intensifies. Film formn.	n.d
TCP	6 hrs	Black surface. Coating come out easily.	No pink color forms. After 5 mins. a very light pink color forms. No film. formation.	n.d
Alodine	6 hrs	Black surface. Residues not easy to remove from the surface.	No pink color forms initially. After removing the black surface and spiking again with DPC, pink color forms. Film formation. after a few mins.	n.d

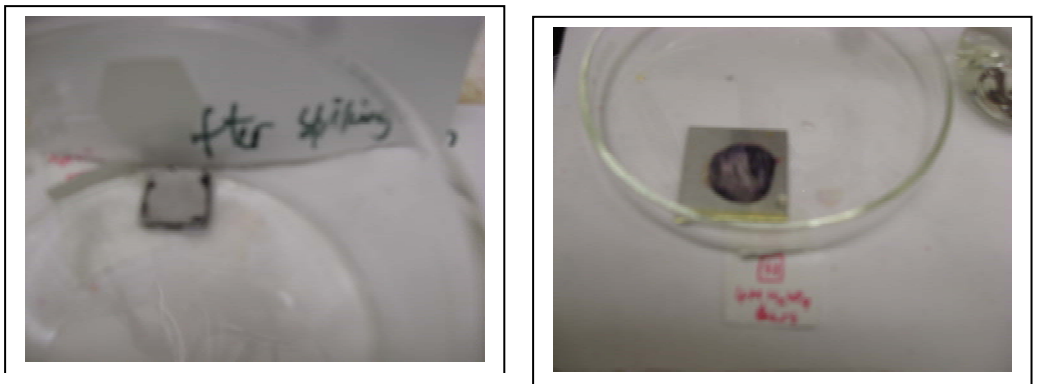

Figure 78: The TCP coating (left) is easily dissolved using the ISO procedure while the Alodine coating (right) is not after exposure to 4M sulfuric acid.

Table 20 shows the effect of 4.6M sulfuric acid over time in a separate experiment. These results indicated that Cr(VI) did form after only 20 minutes and clearly is still present after 120 minutes of exposure.

Table 20: 2024 TCP treated with 4.6M H_2SO_4 as a function of time

Treatment time	**Cr^{6+} ($\mu g/cm^2$)**	**Visual observations after corrosion**
10 min	n.d.	No change on surface of the stubs.
20 min	0.08	Gray layer forms on the stubs.
60 min	0.14	Before spiking with DPC pinkish gray layer forms on the stubs, which is a black residue on wiping off. A brown colored solution is obtained on combining with DPC.
120 min	n.d	Pinkish gray layer forms on the stubs, which is a black residue on wiping off. A brown colored solution is obtained on combining with DPC.

Table 21 shows the effect of 1M sulfuric acid on 2024/TCP. A small amount of Cr(VI) is observed after 6 hrs using UV-Vis, and a pink residue is observed after 1 day. Table 22 shows the effect of 1 M sulfuric acid on 2024/Alodine. Cr(VI) is detected in 3 hrs using UV-VIS, and the coating shows a pink color after 6 hrs. This indicates that Cr(VI) is detected sooner for Alodine samples, as we would expect.

Table 23 examines the effect of 1 M sulfuric acid on TCP/7075. No Cr(VI) was detected using either method at any time.

Table 21: 2024 TCP treated with 1M H_2SO_4

Treatment time	Cr^{6+} ($\mu g/cm^2$)	Visual observations on surface after corrosion
1 hr	n.d.*	No change on surface of stubs.
3 hrs	n.d	No change on surface of stubs.
6 hrs	0.12	No change on surface of stubs. Solution contained some small floating particles.
1 day	n.d.	Uniform pinkish gray layer forms on the stubs. A brown colored solution forms on combining with DPC.

Table 22: 2024 Alodine treated with 1M H_2SO_4

Treatment time	Cr^{6+} ($\mu g/cm^2$)	Visual observations after corrosion
1 hr	n.d.	No change on surface.
3 hrs	0.14	No change on surface.
6 hrs	0.31	No change on surface. Spiking with DPC gives small pink spots.
1 day	n.d.	No change on surface.
2 days	0.37	Coating comes off. Pinkish grey residues on the surface just like TCP.

Table 23: 7075 TCP treated with 1M H_2SO_4

Treatment time	Cr^{6+} ($\mu g/cm^2$)	Visual observations after corrosion
1 hr	n.d.	No change on surface.
3 hrs	n.d.	No change on surface.
6 hrs	n.d	No change on surface.
1 day	n.d.	A very thin grey layer forms. Not uniform.
2 days	n.d.	Dark maroon chunky residues floated in the solution. The surface didn't have any layer formation which was seen in 2024 TCP. Surface showed some pink gray pits. The surface on wiping off didn't give any black residue which was seen in 2024 TCP.No brown solution formed on combining with DPC. No pink complex with DPC formed.

The effect of 1 M NaCl was examined. Table 24 shows that only very low amounts of Cr(VI) were detected using UV-Vis, but not observed using the DCP test. Therefore, it is possible that the Cr(VI) detected using UV-Vis is not real, but if it is, the amount of Cr(VI) formed is likely very low. Table 25 shows that Cr(VI) was not detected using UV-Vis until 2 days, and pink spots were only observed at the 6 hr mark, and not afterwards. Again, this indicates that Cr(VI) is likely not formed from exposure to NaCl, but if it is, the concentration is very low. Table 26 shows that only low amounts of Cr(VI) are observed after 2 days using DCP. These results indicate that no more than very low amounts of Cr(VI) are formed in TCP and Alodine coatings as a result of NaCl exposure.

Table 24: 2024 TCP treated with 1M NaCl

Treatment time	**Cr^{6+} ($\mu g/cm^2$)**	**Visual observations after corrosion**
1 hr	n.d.	No change on surface.
2 hrs	0.14	No change on surface.
3 hrs	0.11	No change on surface.
1 day	0.07	No change on surface.
2 days	n.d.	No change on surface.

Table 25: 2024 Alodine treated with 1M NaCl.

Treatment time	**Cr^{6+} ($\mu g/cm^2$)**	**Visual observations after corrosion**
1 hr	n.d.	No change on surface.
3 hrs	n.d.	No change on surface.
6 hrs	n.d.	No change on surface. Spiking with DPC gives small pink spots.
1 day	n.d.	No change on surface.
2 days	0.2	No change on surface.

Table 26: 7075 TCP treated with 1M NaCl

Treatment time	**Cr^{6+} ($\mu g/cm^2$)**	**Visual observations after corrosion**
1 hr	n.d	No change on surface.
2 hrs	n.d	No change on surface.
3 hrs	n.d.	No change on surface.
1 day	n.d.	No change on surface.
2 days	0.25	No change on surface. A light pink solution forms with DPC, showing the presence of Cr^{6+}.

Table 27 shows the effect of 4M nitric acid. Alodine again shows a pink color on the surface, and is detected after 3 hrs of exposure. Beyond 3 hours, no Cr(VI) is detected likely because the Cr(VI) content is probably below the detection limits or was not extracted using the ISO method. For TCP, no pink color was observed after 3 hrs, but a slight pink color was observed after 6 hrs. No Cr(VI) was observed, indicating the amount of Cr(VI) generated was small or was not properly extracted using the ISO procedure (Figure 79).

Table 27: 2024 TCP and Alodine treated with 4M HNO_3.

Sample	Treat-ment time	Visual obs. on surface before spiking with DPC	Visual obs. on surface after spiking with DPC	Cr6+ (µg/cm2)
TCP	3 hrs	Not much change on surface.	No pink color formn. No film formn.	n.d
Alodine	3 hrs	Not much change on surface.	Slight pink color formed.	0.11
TCP	6 hrs	White surface forms. Residues present on surface.	PINK color forms with DPC. No film formn.	n.d.
Alodine	6 hrs	White surface. No residues.	Pink color forms with DPC. Intensifies with time. Film formn.	n.d.

Figure 79: The TCP coating (left) is easily dissolved using the ISO procedure while the Alodine coating (right) is not after exposure to 4M nitric acid.

To determine whether the Cr(VI) observed is due to the pretreatment or substrate, the bare substrate was tested similarly. Aluminum alloys were not pretreated nor acetone washed prior to use. Test coupons (1" x 1") of either 2024 or 7075 aluminum alloys were placed in a Nalgene® beaker and immersed in 25-40 mL of the appropriate aqueous solution. The coupons remained immersed in the solution for 16 hours. After 16 hours visual observations about the condition of the coupon and the color of the solution were recorded (Table 28). Aliquots of each solution were tested for the presence of Cr(VI) with DPC solution (Table 29). Coupons were then removed from the solution with Parafilm® covered forceps, and the surface of the coupon was tested for the presence of Cr(VI) by placing three to five drops of DPC solution on the surface of

the coupon (Table 30, Figure 80-Figure 82). Deionized water, 1 M H_2SO_4, 4M H_2SO_4, concentrated H_2SO_4, 4M HNO_3, concentrated HNO_3, and 1M NaCl did not test positive for Cr(VI) with the DPC solution. Note: It was found that mixing HNO_3 with a positive DPC test for Cr(VI) turned the solution from pink (positive) to brown, thus masking the results for a positive test.

The results are shown in Table 28-Table 30 and Figure 80-Figure 82. Tests of the solutions reveal that Cr(VI) is liberated from both 7075 and 2024 aluminum alloys when the alloys are immersed in H_2SO_4. Due to the masking effect of HNO_3 on the DPC solution test the results of those solution tests are inconclusive. Cr(VI) is not liberated into solution from either alloy in 1M NaCl.

Table 28: Initial observations of 1" x 1" aluminum alloy test coupons and solutions after 16 hours of immersion

Aluminum Alloy	**1 M H_2SO_4**	**4 M H_2SO_4**	**Conc. H_2SO_4**	**4 M HNO_3**	**Conc. HNO_3**	**1 M NaCl**
2024	Slight darkening of coupon; solution clear	Complete blackening both sides of coupon; solution clear	Brown flakes on coupon and surface of solution; thin dense milky layer at bottom of solution; solution yellow	No apparent effect on coupon; solution clear	No apparent effect on coupon; solution yellow	Some black spotting on bottom of coupon; solution clear
7075	Slight darkening of coupon, solution clear	Complete blackening top of coupon; solution clear	Brown flakes on coupon and surface of solution; thin dense milky layer at bottom of solution; solution yellow	No apparent effect on coupon; solution clear	No apparent effect on coupon; solution yellow	Some black spotting on bottom of coupon; solution clear

Table 29: Results of diphenylcarbazide test for Cr(VI) for solutions with 1" x 1" aluminum alloy coupons immersed in them for 16 hours (decanted off coupon for test)

Aluminum Alloy	1 M H_2SO_4	4 M H_2SO_4	Conc. H_2SO_4	4 M HNO_3	Conc. HNO_3	1 M NaCl
2024	Possible Positive	Positive	Positive	Negative*	Negative*	Negative
7075	Possible Positive	Positive	Positive	Negative*	Negative*	Negative

*Blank tests show that HNO_3 can mask the results of a positive test for Cr(VI).

Table 30: Results of diphenylcarbazide test for Cr(VI) conducted upon the surface of aluminum alloy coupons following their removal from a 16 hour immersion in solution

Aluminum Alloy	1 M H_2SO_4	4 M H_2SO_4	Conc. H_2SO_4	4 M HNO_3	Conc. HNO_3	1 M NaCl
2024	Positive	Negative*	Negative	Negative	Positive	Positive
7075	Positive	Negative*	Negative	Negative	Positive	Positive

*The black layer on the test coupons may have masked a positive result for the test.

Figure 80: AA2024 after 16 hr in 1M sulfuric acid

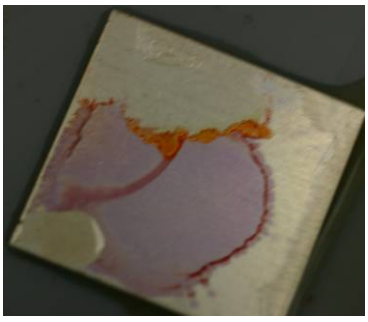

Figure 81: AA2024 after 16 hr in concentrated nitric acid

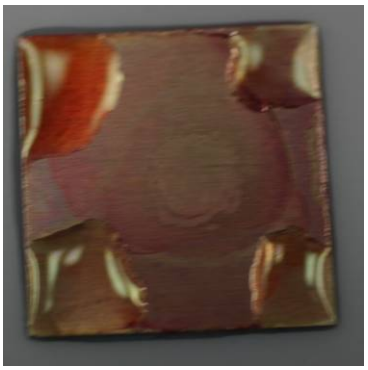

Figure 82: AA7075 after 16 hr in 1M sodium chloride solution

Surface tests of the coupons reveal that Cr(VI) is present at the surface of both 7075 and 2024 aluminum alloy coupons that have been immersed in 1M H_2SO_4. Coupons of both alloys immersed in concentrated HNO_3 also tested positive for Cr(VI) at the surface of the coupon. Surprisingly, even coupons immersed in 1M NaCl for 16 hours tested positive for the presence of Cr(VI).

These experiments have shown that Cr(VI) can be formed or liberated from both 7075 and 2024 aluminum alloys when exposed to acid or salt solutions. Thus, it is possible that the source of the Cr(VI) detected by UConn researchers investigating TCP may be the test coupons and not the TCP conversion coating. It is therefore not clear whether the Cr(VI) detected in coating tests was liberated from the TCP coating, the base aluminum alloy, or both.

The TCP and Alodine pretreatment solutions spiked with nitric acid and sulfuric acid were analyzed for Cr(VI) content (Table 31). A drop of conc. acid (H_2SO_4/ HNO_3) was placed in a vol. flask containing 0.5ml Alodine/TCP. 300 µL of DPC was added. After 2 minutes, 5 mL of phosphate buffer is added to stop the reaction. The solution was diluted to 100mL and UV-vis spectra were taken. Results are expressed in µg/100mL. The results clearly show that the Alodine pretreatment solution contains Cr(VI), while the TCP pretreatment solution does not (Figure 83). This indicates that the chromium within the TCP solution is not succeptable to oxidation from nitric or sulfuric acid. This lends creedance to the hypothesis that Cr(VI) generated during exposure to sulfuric or nitric acid on aluminum is due to the aluminum itself.

Table 31: Tests on TCP and Alodine coating solutions in concentrated acids

Sample i.d.	Observation after adding DPC	Cr^{6+} ppm
TCP + conc. H_2SO_4	No pink color formation	0
Alodine + conc. H_2SO_4	DARK pink color forms	55
TCP + conc. HNO_3	No pink color formation	0
Alodine + conc. HNO_3	DARK pink color forms	76

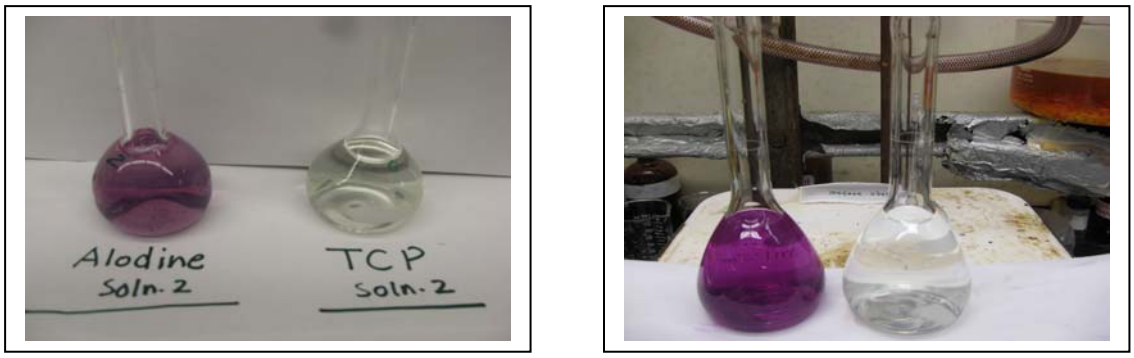

Figure 83: TCP and Alodine solutions exposed to sulfuric acid (left) and nitric acid (right) where the pink sample is the Alodine solution, while th eclear solution in the TCP solution.

3.4.10 Discussion of Cr(VI) Under Severely Corrosive Conditions

It is possible for Cr(III) to oxidize if ISO Method 3613 is not followed carefully. The boiling water and acid treatments in preparing the samples are energetic enough to cleave bonds and generate some Cr(VI) from the Cr(III) film.

There are many analytical and volumetric techniques being proposed for determining the presence of hexavalent chromium from trivalent chromium chemistries. Most of these yield drastically different results and conclusions depending on specific coating and test conditions. The important fact is Cr(III) will oxidize to Cr(VI) under certain conditions, which have yet to be clearly identified or established as legitimate environmental conditions. For example, an alkaline medium in an oxidizing atmosphere, such as air or chloride, can trigger the reaction. Additional complications from cobalt species often found in automotive finish applications have been reported. It was found that Co(II) in the passivation layer can oxidize to Co(III) under certain accelerated test conditions, including during the simple boiling water extraction test for Cr(VI). The presence of Co (III) oxidizes Cr(III) to Cr (VI) which can give the reported positive test. Industrial testing has reported when a boiling water extraction test was performed with a Co-free passivation, no Cr(VI) was detected. The more Co was present, the higher the detected level of Cr(VI). While the TCP films are free of cobalt and therefore not subject to this effect, this does highlight the susceptibility of this widely accepted methodology to erroneous conclusions for testing non-chromate coatings. Specifically, the deoxidizer chemical, Turco Smut-Go NC-LT yields false positive results. This is due to iron interference with the complexation reaction. Smut-Go is composed primarily of nitric acid and ferric sulfate. It is possible that some iron contamination remains on the surface of the panels and is included in the passivation layer.

Furthermore, as there have been no positive results for testing the solutions themselves, such as spiking the leachate with Cr(III) or evaluating TCP solution. Thermodynamically, spontaneous conversion to the unstable Cr(VI) state during coating deposition is highly unlikely. One suggestion is that it is much more likely that boiling the metal panel to "extract" the chromium, then acidifying with concentrated acid is causing some conversion. Boiling the panel is going to concentrate a lot more thermal energy into the substrate-coating interface, whereas boiling the solution, you are effectively limited in thermal energy input to the heat capacity of water.

Initial testing to examine this possible effect may be borne out by altering the methodology to show the impact of each step. Aluminum test specimens with Cr(VI) conversion coating were tested this way. Samples tested without the boiling water extraction only performing the acidification and tested with diphenylcarbazide (DPC). Samples were also tested by removing the acidification step and just performing the boiling water extraction. By removing the boiling water step, the amount of the detected Cr(VI) in Alodine 1200S was greatly reduced. Removing the acidification step yielded no detectable Cr(VI) at all, however this portion of the analysis may be invalid since the DPC only complexes within the acidic pH range. Most widely accepted chromate coating models suggest the structure is mostly hydrated Cr(III) hydroxide with loosely bound chromate species on top. It is possible that boiling the panel is converting some of the base trivalent species up to chromate instead of merely extracting it from the coating.

3.4.11 TCP PRETREATMENT ANALYSIS CONCLUSIONS

This study has determined a number of things regarding TCP relative to alodine pretreatments:

- TCP pretreatments are purely trivalent chromium based unlike conventional pretreatments. The results indicate that TCP may produce small amounts of Cr(VI) under highly aggressive conditions.

- Like Alodine 1200S, Cr is a major component of TCP as detected by AES. SEM images show that a TCP coating has better coating uniformity with lesser cracks compared to Alodine 1200S coating. AES also shows that in the NSS tests, both TCP coating and Alodine coating have similar performance. Under SO_2 conditions, Alodine 1200S coated coupons have a better corrosion resistance.

- Analysis of TCP coated AA 2024 panels analyzed by diphenylcarbazide tests show that TCP does not contain any hexavalent chromium.

- Alodine 1200S coated samples that have undergone corrosion produce low amounts of Cr(VI). TCP coated panels that have undergone corrosion may contain very low concentrations of hexavalent chromium. This indicates that it may be possible to generate Cr(VI) from TCP coatings under highly corrosive conditions.

- Blank aluminum samples exposed to the same corrosive conditions also produced very low amounts of Cr(VI) indicating that Cr(VI) generated from TCP treated aluminum is unlikely a result of the TCP and more likely a byproduct of the aluminum substrate.

- Analysis of TCP and Alodine 1200S treatment solutions reveal significant amounts of hexchrome present in Alodine 1200S, while none is present for TCP solutions.

- We hypothesize that TCP forms an insoluble inorganic Cr(III) polymeric barrier on the surface of AA 2024 that protects copper rich surfaces and also prevents adsorption Cl^- ions.

- TCP and CFP pretreatments deposit O, Al, and Zr. CFP contains no Cr, but contains detectable levels of F due to the more active fluoroborate species used.
- Organic corrosion inhibitor is present and detectable on substrates coated with TCP and CFP with the 'I' modification.
- There are compositional variations in the deposited pretreatment that occur from spot-to-spot on a given substrate and from substrate-to-substrate because TCP deposits more heavily over inter-metallic sites.
- Pretreatment process does not cause oxidation of Cr(III) to Cr(VI) on TCP and TCP-IC solutions.

3.4.12 FUTURE WORK IN PRETREATMENTS

The mechanism of corrosion protection for TCP needs to be understood to improve the process and make more robust and effective coatings. This mechanism is being studied through a SERDP effort between NAVAIR and The Ohio State University. Furthermore, these pretreatments must be demonstrated/validated in real time environments. The ESTCP effort that has just begun will do this for various NAVAIR applications.

3.5 Results for Low VOC Primers

Generally speaking, there are two types of water borne epoxy coatings. In one type, the admixed solvent based components are highly viscous and are emulsified by mixing with large amounts of water to reduce the viscosity to a sprayable consistency. In the second type, both components are emulsified waterborne polymers requiring little viscosity reduction with water for spray application. In the last few years there have been claims made by major coating manufacturers that there are emulsion type epoxy systems available equal to the solvent types in performance.

Knowing that various additives play a very important role in defining the performance properties of water borne coatings, the ARL Coatings and Corrosion Team is evaluating the factors that control these properties. These additives include wetting agents, dispersants, defoamers, coalescing agents, adhesion promoters and silicone based modifiers. Incompatibility between any of these powerful additives can lead to formulation instability and coating failure no matter the properties of the binder polymer.

In evaluating industrial quality primers on various substrates, the time to film failure can be many months even using accelerated corrosion protocols. In the current evaluations being carried out by ARL, one aspect that will be studied is the possibility of applying thinner films to predict corrosion resistance in a much shorter time. To that end, zinc phosphate treated steel panels were sprayed to various film thicknesses with three formulations and control samples of MIL-P-53022 and MIL-P-53030 and exposed via GM9540. Exposure will continue to failure and results will be available in future reporting periods.

3.5.1 PANEL TESTING OF NON-CHROMATE PRIMERS

The SERDP Coatings Team worked very closely with leading military paint manufacturers to evaluate and characterize new non-chromium and zero-VOC formulations to current mil-spec performance requirements. Candidate products were tested independently and in conjunction with non-chromate surface preparations to evaluate their properties separately and as part of an overall coating system. This effort focused on both exempt solvent and water-borne resin formulations. Table 32 and Table 33 list the products in testing according to their applicable specifications.

Table 32: MIL-PRF-85582 class N primers

Designation	Manufacturer	Description	Date	Status
65GN015	Deft	La-based inhibitor, emulsion, ZVOC	12/05	Blistering seen in water resistance, wet adhesion and filiform
44GN098	Deft	La-based inhibitor, LVOC	12/06	QPL – Some issues with batch to batch variability have been observed
EWAE118	PPG	Legacy non-chrome, Type II	1996	QPL – Poor performance in on-aircraft flight testing
EWDY048	PPG	Legacy non-chrome, Type I	1995	QPL – Poor performance in on-aircraft flight testing
RW3946	PPG	Improved version of EWDY048 with developmental inhibitor package		In progress

Table 33: MIL-PRF-23377 class N primers

Designation	Manufacturer	Description	Date	Status
16708TEP-16709CEH	Hentzen	Proprietary non-chrome inhibitor	02/04	QPL – Currently in field testing with baseline TCP, exempt solvent ZVOC version in process, evaluating over steel substrates
02GN083	Deft	Proprietary non-chrome inhibitor	12/03	QPL – Currently in field testing with baseline TCP, evaluating over steel substrates
02GN084	Deft	La-based inhibitor, improved version of -083		Filiform and salt fog testing in progress, production issues with long induction time and short recoat window still being worked
RW3899	PPG	Same inhibitor package as RW3946		Qualification testing in progress, only tested with chromated substrates to date
CM0481968	Sherwin-Williams	Proprietary non-chrome inhibitor		Qualification testing in progress, only tested with chromated substrates to date
SicoPoxy 577-630	Sico	Proprietary non-chrome inhibitor		Samples received, no testing to date

The Hentzen 16708TEP, Class N primer from these evaluations has been reformulated with exempt solvents such as t-butyl acetate and OxSol 100. Further characterization is needed for the zero-VOC version for use with improved non-chromated surface treatments.

Non-chrome primers that performed well over the baseline TCP were subsequently tested over the modified conversion coating chemistries. The TCP-I generally performed well in both neutral and acidified salt fog testing, but exhibited slightly more variability with regards to the applied primer coating when compared to the controls. The TCP-IC coating tended to degrade the corrosion performance when used in conjunction with the MIL-PRF-23377J Class N primers, exhibiting noticeably more blistering away from the scribe when compared to the TCP-I and the controls. Figure 84 shows blistering failure of TCP-IC/23377N/85285 after 1,450 hours G 85, Annex 4 exposure.

Figure 84: 1,450 hours SO_2 exposure – Primer MIL-PRF-23377J Class N – Topcoat MIL-PRF-85282D – over TCP, TCP-I, & TCP-IC (left to right)

This effect was greatly minimized when TCP-IC was tested under a chromated primer, but the trend was still evident. This trend was reversed however, when the TCP-IC was tested under the MIL-PRF-85582 Class N product (Deft Finishes 44GN098). This was the only fully non-chromated coating system that performed equivalently or better than the chromated control in this evaluation. However, the 44GN098 product exhibited significantly more corrosion failure when tested in conjunction with the standard polyurethane topcoat. Figure 85 shows the relative performance of the TCP-IC/44GN098 stack-up with and without topcoat on AA2024T3 after 5,000 hours B 117 exposure.

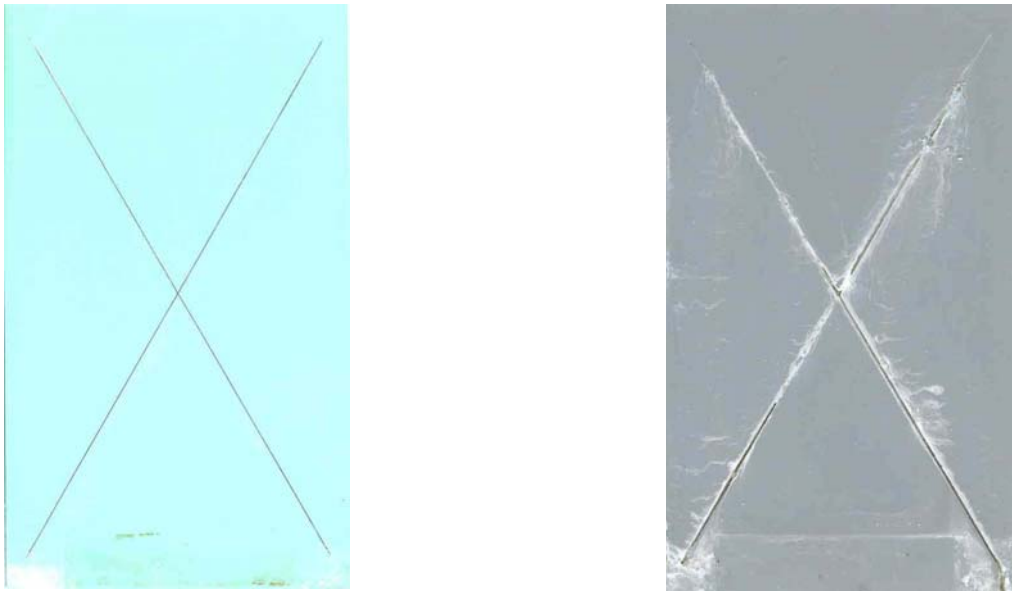

Figure 85: AA2024-T3 TCP-IC/44GN098 (primer only – left) and TCP-IC/44GN098/85285 (right)

Additional work is being conducted in partnership with Boeing - St. Louis to evaluate Deft's 65GN015 zero-VOC non-chrome epoxy primer. This product has the same inhibitor package as the 44GN098 but utilizes a water-emulsified resin. This product has shown promise to perform in a similar fashion over non-chromate surface treatments as the 44GN098. To date, the 65GN015 has exhibited blistering and adhesion issues during water and fluid immersion exposures. This has been attributed to the lack of a solvent package degrading the barrier properties of the coating system. Optimization efforts are ongoing to characterize the TCP-I, IC, and CFP-I in conjunction with these primers.

To date, there is no fully non-chromated system that offers the same corrosion protection of a fully chromated system. However, promising results have been obtained with modified TCP chemistries and new non-chrome primers and further optimization of these systems is planned.

3.5.2 POWDER COAT PRIMERS

The US Army Research Laboratory has great interest and support for the use of powder coat technology. During the testing, evaluation and validation of chemical agent resistant coating (CARC) systems, primer powder coatings for specific substrates were also studied. That effort resulted in a listing of approved primer powder coatings for CARC. The list (Figure 86) retains the company names when the products were originally submitted and approved. This reference will be updated for the Qualified Products List (QPL) as ARL moves toward publishing a powder coat specification for CARC systems. Current efforts have been successful in evaluating several starting formulas for Powder Top Coats. Formulations have passed preliminary live agent testing with either nerve or mustard agents though continue to have higher gloss values than NAVAIR or ARL requires for topcoat formulations. Additionally efforts will continue to down select powder formulations that provide very low gloss, UV protection and for the Army chemical agent resistance.

Powder Coatings Passing Chemical Agent Resistance

Manufacturer	Product	Color	Substrate
Morton	1368-71-2	SF Green	CCCAl
Pratt & Lambert	85-1746	SF Green	CCCAl
Morton	746-3	OD	ZS
PPG	40102	SF Green	CCCAl
International	PK202U02	SF Green	CCCAl
O'Brien	H 175-187-A	SF Green	CCCAl
Morton	675-12	OD	ZS
Morton	17-7006	Gray	ZS
Lilly	908A	Gray	ZS
Morton	10-6062	OD	ZS
Morton	10-1002	White	CCCAl
Morton	10-1013	White	CCCAl
Herberts	047-36-1	White	CCCAl
International	BA004U	White	CCCAl
Spraylat	PEL91307	White	CCCAl
Morton	242-13-1	White	CCCAl
Spraylat	PEL91583	White	CCCAl
Herberts	071-32-5	White	CCCAl
Tiger Drylac	269/10220	White	CCCAl
Pratt & Lambert	85-1942	OD	CCCAl, ZS, SS
Morton	270-04-6	OD	CCCAl, ZS, SS

ZS = Zinc Phosphate Steel SS = Zinc Phosphate Stainless Steel CCCAl = Alodine Aluminum

NOTE: Due to corrosion requirements when used as a substitute for MIL-P-53022, the products are SUBSTRATE DEPENDENT.

Figure 86: Approved powder coat primers for CARC systems

3.5.3 EVALUATION OF EMULSION POLYMERS IN A WATERBORNE EPOXY PRIMER

Reichhold water-borne epoxy components were used to formulate a MIL-DTL-53030 type epoxy coating. The samples were made with the manufacturer recommended formula of 74.3% total solids, 38% pigment volume concentration, and a VOC content of 0.77 lbs/gal.

Before going to a white primer formula, clear coatings were made at the recommended stoichiometry for the Reichhold polymer system with just the addition of a coalescing solvent to evaluate film formation, clarity, curing rate, water resistance and to perform knife ribboning tests. Drawdowns of a 3 mil wet film gave glossy smooth films with just a trace of haze. Dry films made at 6 mil wet film thickness showed moderate haze and orange peel. After 18 hours of air dry and 10 minutes at 70 C, a 2 hour water spot test showed a very slight softening. Films showed very good adhesion to metal panels and the film ribboned when knife tested. After air drying for six days, films immersed for 24 hours in water showed no effect, being hard and ribboning well.

A white primer was formulated using mica, barium sulfate and wollestonite as fillers/anti-corrosive pigments/pigments. Another commercial water borne epoxy primer was also tested. These samples were compared against a MIL-DTL-53030. Substrates sprayed were cold rolled steel and zinc phosphated steel B952. An attempt was made to coat thin and thick films. Panels were air dried for two weeks and exposed to ASTM B 117 for 504 hours and GM9540 up to 80 cycles. Panels were evaluated for rust creepage in the scribed area and for over all blistering. 10 = no change and 0 = most change i.e. most rust or most blistering.

The corrosion results are shown in Table 34. In the salt spray testing the effects on cold rolled steel are more evident than on the zinc phosphated steel panels with the control epoxy showing more rust creep at the scribe but less blistering over all compared to the vendor and the experimental. In the GM9540 the experimental formulation delaminated from the cold rolled steel, yet did well over the zinc phosphated steel. The control epoxy did much better on blister resistance over cold rolled steel than the commercial epoxy and the formulated sample.

Table 34: Corrosion and blistering ratings for water-based primers.

	Cold rolled Steel			Zinc Phosphated Steel		
	MIL-DTL-53030 control	Commercial water-based Primer	White formulated primer	MIL-DTL-53030 control	Commercial water-based Primer	White formulated primer
B117 Salt Spray						
Scribe Rust	0	4	5	7	8	7
Blistering	2	0	0	4	6	0
GM9540 Cyclic Exposure						
Scribe Rust	2	5	0	4	7	6
Blistering	5	1	0	1	4	3

The next experimental formulas will attempt to improve the adhesion and blistering problem with higher pigment volume content and an increase in the flexible polymer. The efforts summarized are results of numerous emulsions evaluated and did not meet or provide the minimum requirement necessary to move toward accelerated chamber testing.

3.5.4 CORROSION TESTING OF LOW-VOC/ZERO-VOC PRIMERS

Two commercial primers and two experimental primer formulations were subjected to ASTM B 117 Salt Fog and GM9540P testing. The control sample was Sherwin Williams MIL-P-53022

(lead and chromate free, solvent based epoxy primer) which contains 2.8 lbs/gal VOC. A solvent substituted sample of the control was another leg of the test. For that formulation, commercial product was thinned with t-butyl acetate and evaporated in a hood until 30% of the initial sample weight had been added and evaporated. Tertiary butyl acetate has a slower evaporation rate than the predominant solvents listed on the manufacturer's label. Therefore, during evaporation, the VOC solvents are leaving the formula more quickly than the t-butyl acetate. By carrying out this process long enough, one can theoretically replace all of the more volatile solvents with t-butyl acetate, a VOC exempt solvent. The other commercial product in this test is a zero-VOC version of MIL-P-85582 by Deft. MIL-PRF-85582 is a water-reducible epoxy primer. A water-based direct-to-metal (meaning no pretreatment of the metal substrate is required for primer adhesion and corrosion protection) epoxy primer was developed by the University of Cincinnati. The exact composition is proprietary but ARL agreed to do some performance testing and characterization of their product. More details of the test design can be seen in Table 35. Each primer was applied to steel panels to produce a dry film thickness of 0.9-1.5 mil. Ten panels for each primer were top coated with a standard commercial product meeting MIL-DTL-64159 two-component water-borne polyurethane. Top coat dry film thickness was maintained at 1.8-2.5 mil across all samples. Ten panels of each primer were tested without topcoat. Five panels for each test combination were subjected to B 117 and five more panels for each test combination experienced GM9540P. Periodic checks were made to evaluate the coating degradation according to ASTM D 1654 Methods A and B. Method A rates the spread of corrosion from the scribe and Method B rates the film integrity (blistering) in the unscribed areas. For both methods a higher number is better performance (scale 0-10). Samples were removed from testing once they failed according to Army standards. Average ratings for the five test panels of each product are summarized in Table 36 and Table 37. Color coding has been added to aide comparison. Ratings of 10-8 are green for good performance. Ratings of 7-6 are yellow to indicate impending failure. Ratings of 5-4 are orange for failure; ratings 3-0 are red for severe failure. The lower of the two ratings for Methods A and B determined the color for the box.

Table 35: Design for low VOC primers corrosion testing

Leg	Primer Formulation	Primer VOC (lbs/gal)	Substrate	Top Coat
1	MIL-P-53022 (control)	2.8	Unpolished cold rolled steel, zinc phospate treated, chrome sealer	None
2	MIL-P-53022, t-butyl acetate solvent replacement	near zero	Unpolished cold rolled steel, zinc phospate treated, chrome sealer	None
3	MIL-PRF-85582	0	Unpolished cold rolled steel, zinc phospate treated, chrome sealer	None
4	University of Cincinnati primer	unknown	Unpolished cold rolled steel	None
5	University of Cincinnati primer	unknown	Unpolished cold rolled steel, zinc phospate treated, chrome sealer	None
6	MIL-P-53022 (control)	2.8	Unpolished cold rolled steel, zinc phospate treated, chrome sealer	MIL-DTL-64159
7	MIL-P-53022, t-butyl acetate solvent replacement	near zero	Unpolished cold rolled steel, zinc phospate treated, chrome sealer	MIL-DTL-64159
8	MIL-PRF-85582	0	Unpolished cold rolled steel, zinc phospate treated, chrome sealer	MIL-DTL-64159
9	University of Cincinnati primer	unknown	Unpolished cold rolled steel	MIL-DTL-64159
10	University of Cincinnati primer	unknown	Unpolished cold rolled steel, zinc phospate treated, chrome sealer	MIL-DTL-64159

Table 36: Average ratings for ASTM B 117 Salt Fog testing

Coating Description	168 hours (Method A / B)	504 hours (Method A / B)	1008 hours (Method A / B)
SW MIL-P-53022 (control)	8.0 / 7.6	7.0 / 7.4	5.2 / 7.0
t-butyl acetate solvent replacement in MIL-P-53022	7.8 / 5.4	6.2 / 4.2	5.2 / 3.6
Deft zero-VOC MIL-PRF-85582	7.8 / 3.0	4.8 / 0.4	n/a
U. Cinci primer on bare steel	3.6 / 4.0	2.0 / 0.6	n/a
U. Cinci primer on phosphate treated steel	1.8 / 3.4	1.4 / 2.4	1.0 / 0
SW MIL-P-53022 (control) with topcoat	8.0 / 9.4	8.0 / 8.6	5.6 / 7.6
t-butyl acetate solvent replacement in MIL-P-53022 with topcoat	8.0 / 8.2	6.2 / 4.6	4.2 / 0.2
Deft zero-VOC MIL-PRF-85582 with topcoat	8.0 / 0.6	5.8 / 0	n/a
U. Cinci primer on bare steel with topcoat	2.4 / 2.6	n/a	n/a
U. Cinci primer on phosphate treated steel with topcoat	4.8 / 7.0	4.6 / 4.8	2.2 / 3.6

Table 37: Average ratings for GM9540P testing

Leg	10 cycles	20 cycles	30 cycles	40 cycles	50 cycles	60 cycles	70 cycles	80 cycles
1	7.6 / 9.6	7.2 / 9.4	7.0 / 9.4	5.4 / 9.2	5.4 / 7.8	5.0 / 7.8	5.0 / 7.8	5.0 / 7.2
2	7.4 / 5.4	6.8 / 4.8	5.8 / 4.8	5.0 / 4.0	4.6 / 3.8	4.0 / 3.8	3.8 / 3.6	3.4 / 3.4
3	7.2 / 0	n/a	n/a	n/a	n/a	n/a	n/a	n/a
4	6.2 / 7.4	5.6 / 7.4	5.6 / 5.2	5.4 / 0.2	n/a	n/a	n/a	n/a
5	6.6 / 8.6	6.2 / 8.6	6.2 / 8.6	5.8 / 7.8	5.6 / 5.2	5.6 / 5.0	5.6 / 4.0	5.4 / 3.2
6	6.6 / 10	5.6 / 10	5.0 / 10	4.6 / 9.8	4.0 / 6.6	4.0 / 5.2	3.8 / 5.2	3.0 / 4.4
7	6.2 / 8.8	5.4 / 7.8	5.0 / 7.6	4.2 / 6.4	2.6 / 4.0	1.4 / 2.5	n/a	n/a
8	5.4 / 3.0	4.4 / 2.0	3.4 / 1.6	2.0 / 1.0	n/a	n/a	n/a	n/a
9	5.0 / 10	4.6 / 10	4.0 / 9.8	1.2 / 6.0	n/a	n/a	n/a	n/a
10	5.2 / 6.4	5.0 / 5.2	4.2 / 4.8	3.2 / 3.2	2.4 / 2.4	1.8 / 1.8	n/a	n/a

Primers for the Army are expected to achieve a rating of at least 8 for corrosion creep and blistering after 338 hours of B 117 exposure. GM 9540 is not a specified test but it is considered by many to be more realistic due to the alternation of wet and dry cycles as well as a more corrosive mixture of salts. While it is difficult to predict actual performance of a coating by corrosion results, these laboratory methods provide a rough comparison of the general robustness of a coating or coating system. From these results, we can conclude:

- The solvent substituted control MIL-P-53022 performed nearly as well as the commercial product with 2.8 lbs/gal VOC suggesting there might be an opportunity to further reduce VOC levels by utilizing t-butyl acetate.

- The Deft zero VOC MIL-PRF-85582 did not meet the minimum performance requirements for corrosion protection. The primer developed an unacceptable number of blisters despite preventing the spread of corrosion from the scribe in B 117 testing.

- The direct to metal primer from the University of Cincinnati failed miserably during B 117 testing on both bare steel and phosphate treated steel. It is interesting to note that the UC primer without topcoat performed better on bare steel than the phosphate treated steel which is more corrosion resistant than untreated steel without coatings.

- It is also important to note that the intercoat adhesion between the UC primer and MIL-DTL-64159 failed after 168 hours of salt spray. More than 50% of the topcoat peeled from the panels starting at the scribe.

- The UC primer on phosphate steel performed much more comparably to the control in GM9540 testing.

- Generally, B 117 performance of most primers was better when protected with a topcoat. Curiously, GM9540 performance of the primers was hampered when a topcoat was added.

3.5.5 FORMULATION OF ZERO-VOC PRIMER

Epon bis-phenol A epoxy resins and Epikure amide curing agents were obtained from Hexion. Zero-VOC primer formulation began with solubility studies of the epoxies in acetone, t-butyl acetate and blends of these two VOC exempt solvents. Solubility results can be seen in Figure 87. For simplicity and uniformity epoxy solutions (50% by weight epoxy) were prepared using a 50/50 blend of acetone/t-butyl acetate. Epon 826 (liquid), Epon 1001 (flake) and Epon 1004 (flake) were selected for formulating primers due to greater solubility and lower viscosity than higher molecular weight resins Epon 1007 and Epon 1009. Curing agents Epikure 3175, Epikure 3155 and Epikure 3192 were made into lower viscosity 50% (wt.) solutions in acetone and t-butyl acetate.

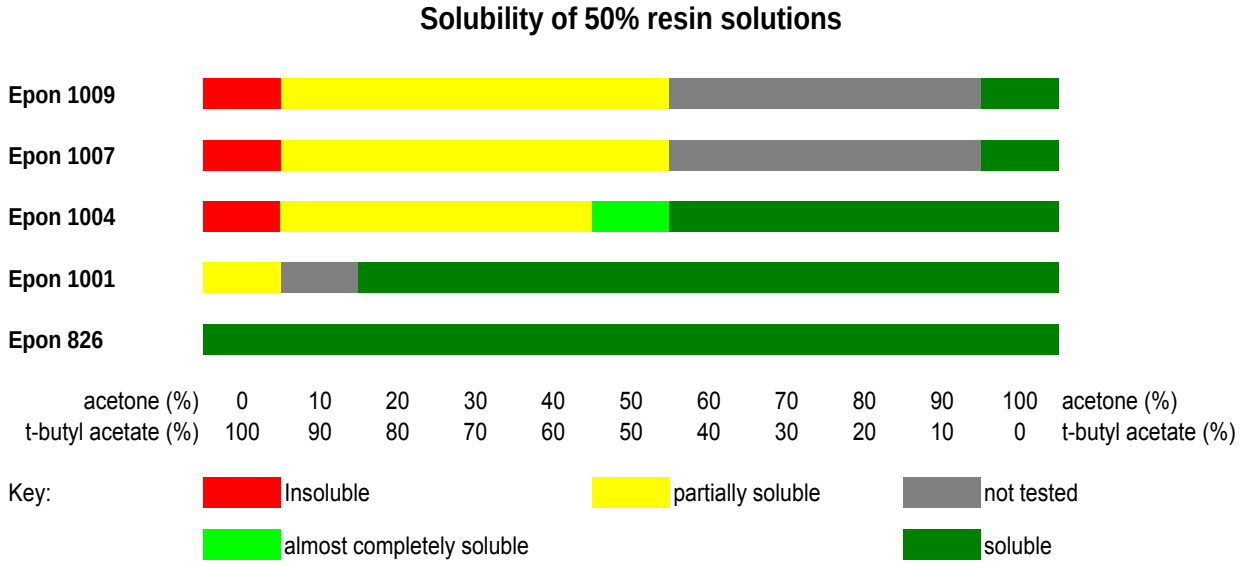

Figure 87: Epoxy resin solubility in acetone and t-buytl acetate

Nine clear films were made by mixing each of the 3 Epon resin solutions with each of the 3 amide curing agents at a 1 to 1 ratio based on equivalent weights (Table 38). Wet films were applied to glass using a 4 mil drawdown bar and cured at ambient conditions for several days. Cured films were removed from the glass with a single-edged razor blade and stored in glass Petri dishes at room temperature for several months before testing any physical properties.

Tensile testing of clear films was used to down-select the epoxy-amide combinations for formulation of pigmented coatings. Results are reported in Table 39. Films made from reacting Epon 826 with Epikure 3192 were very poor quality. This was evident from the rough uneven foamy appearance and flimsy brittle texture. The tensile results illustrate the deficiency numerically.

Table 38: Equivalent weights of epoxy-amide reactants

Epoxy Resin	epoxide equivalent weight		Amide Curing Agent	amine hydrogen equivalent weight
Epon 826	182		Epikure 3175	96.6
Epon 1001	538		Epikure 3155	131.7
Epon 1004	900		Epikure 3192	135.9

Table 39: Tensile testing results for clear zero-VOC epoxy films

	tensile strength (MPa)		adjusted % elongation at break		Elastic Modulus (MPa)		Area (MPa)	
	average	st dev.	average	st dev.	average	st dev.	average	st dev.
826-3175	57.15	1.84	3.09	0.31	2565	115	1.04	0.15
826-3155	56.48	5.12	2.93	0.37	2379	115	0.94	0.22
826-3192	1.79	0.41	0.86	0.11	261	57	0.01	0.00
1001-3175	38.99	1.97	3.97	0.33	1978	88	1.10	0.15
1001-3155	41.56	2.03	3.30	0.40	2041	118	0.87	0.17
1001-3192	44.66	1.80	3.78	0.29	2014	96	1.12	0.15
1004-3175	37.17	2.59	4.40	0.42	1711	233	1.11	0.15
1004-3155	35.85	2.03	5.01	0.27	1697	149	1.30	0.11
1004-3192	43.26	3.00	3.74	0.15	2022	178	1.10	0.11

Tensile testing data from clear epoxy films (excluding 826-3192) suggest that as epoxy equivalent weight increases tensile strength and elastic modulus decrease while elongation at break increases Material toughness was relatively similar across all formulations in light of experimental error. Indentifying trends for the curing agents was more difficult. Epikure 3175 and 3155 produced remarkably similar tensile strength and elastic modulus for each epoxy resin. However, elongation at break and material toughness were more equivalent between Epikure 3175 and 3192. It was decided to select four combinations which would bracket the tensile properties of the clear films to begin pigmented primer formulation.

Pigmented zero-VOC epoxy primer formulation began with Epon 826 and catalysts Epikure 3155 and 3175. Model primer formulations obtained from raw material suppliers and the composition disclosures for Army primers were used to develop a very simple pigmented coating for spray application to steel panels for corrosion testing and other mil-spec tests of interest. Only white formulations were prepared for simplicity of the pigment loading. Titanium dioxide

was the only colorant. Zinc phosphate was incorporated to inhibit corrosion. Micronized silica was added to act as a balancing ingredient to adjust total pigment loading to a specific pigment to binder ratio (P/B). Anti-Terra U is a dispersant from BYK-Chemie. Bentone SD-2 is a clay rheology additive. Several batches were required to fine tune the ingredient levels to a workable formulation. The formulae depicted in were sprayed onto phosphate treated steel panels to await further testing.

Table 40: Zero-VOC primer formulation based on Epon 826 resin.

Part A	**% wt.**	**% wt.**
Epon 826	20.25	20.05
Anti-Terra U	1.10	1.10
t-butyl acetate	14.25	12.00
titanium dioxide	16.00	16.00
zinc phosphate	11.00	11.00
microcrystalline silica	7.50	11.00
Bentone SD-2	0.65	0.65
TOTAL	70.75	71.80
Part B		
Epikure 3155		14.50
Epikure 3175	10.75	
acetone	18.50	13.70
TOTAL	29.25	28.20
total batch	100.00	100.00
epoxy/catalyst (wt.)	1.8837	1.3828
P/B	1.11	1.10
total solvent	32.75	25.70

Learnings from the formulation of Epon 826 primers were applied to formulation of primers based on Epon 1004. Unfortunately, many batches were made without producing a successful formulation. Film properties were not acceptable displaying cratering and pinholing. Many BYK additives were explored to improve coating leveling and drying characteristics. It was determined that the higher viscosity of Epon 1004 would require the addition of more than 50% wt. solvents. For this reason, this resin was eliminated from consideration.

Formulation focus has turned to Epon 1001 and continues at this writing. Follow on efforts are planned to complete an acceptable spray primer and test alongside the Epon 826 formulations.

3.5.6 FTIR Cure Kinetics Results

3.5.6.1 FTIR of Epoxy Coatings

Within the range of concentrations added, there was no observed trend in the variation of these kinetic parameters for either of the added HBPs relative to the baseline system (Figure 88). Furthermore, conversion as a function of time appeared approximately the same in the baseline, PEI-quat, and Lupasol systems (Figure 89). Although it appears that samples with HBP reached higher conversion at faster times than the control samples, the fact that the kinetics parameters are within experimental error indicates that the differences in Figure 89 are likely a result of inconsistencies in FTIR sample preparation time after mixing the reactants. The addition of these HBPs, therefore, had no evident impact on the cure kinetics of this epoxy-amine system. This can be understood by the fact that the hyperbranched polymer is not a catalyst for the epoxy-amine reaction. The amine groups available on the hyperbranched polymer do increase the concentration of available amines, but at the same time decrease the concentration of available epoxy groups. As found, this has little effect on the cure kinetics.

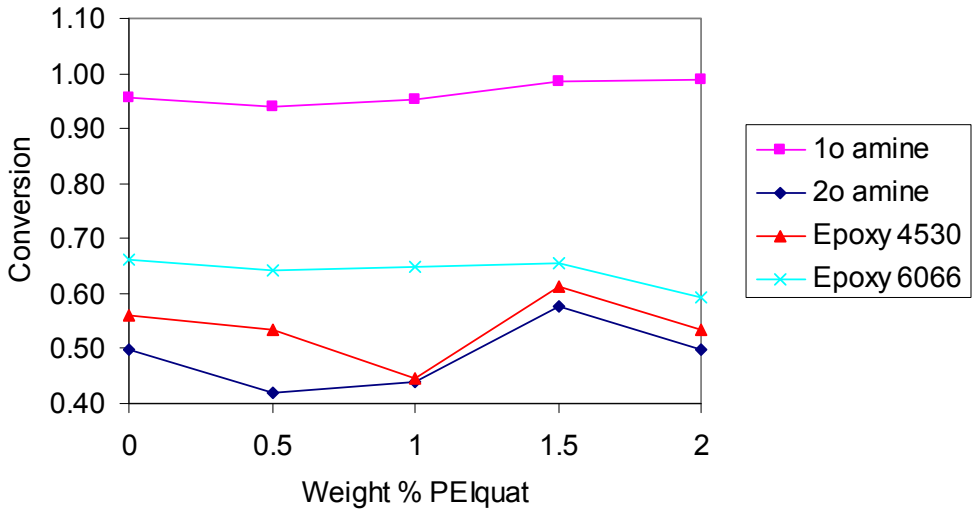

Figure 88: Ultimate conversion as a function of PEIquat concentration of primary amine, secondary amine, and epoxy functional groups. Note that two distinct peaks yielded epoxy kinetics data.

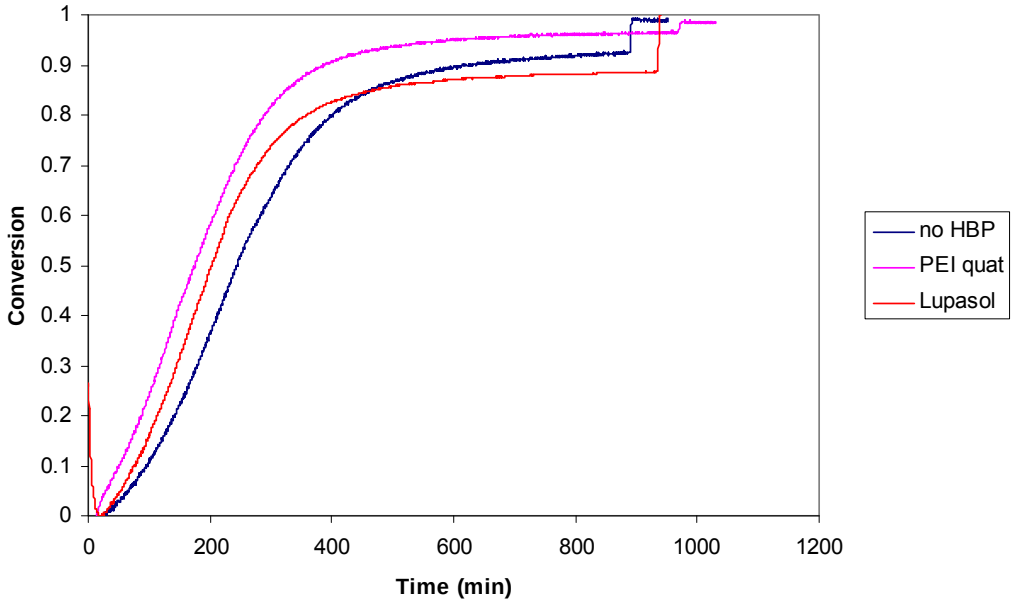

Figure 89: Conversion as a function of time of primary amine groups for the baseline system and 2.0 wt % HBPs

The gel time study involved adding Lupasol to a concentration of 1.0 wt % to MIL-P-53022 and the above mentioned epoxy-amine system during the mixing process. MIL-P-53022 with and without the added Lupasol was cured at a temperature of 50 °C. The analog Epon-PACM system with and without added Lupasol was cured at a temperature of 40 °C. As the systems approached their gel times, as evidenced by increasing viscosity, they were checked approximately every five minutes until definitive gelation was observed.

In the case of MIL-P-53022, the baseline system was observed to gel within approximately 184 min., whereas with 1.0 wt % Lupasol the system gelled within 129 min. The Epon-PACM system with 1.0 wt % Lupasol gelled within 90 min, compared to a baseline gel time of 109 min. Therefore, while the presence of these HBPs does not seem to affect the cure kinetics of these epoxy-amine systems, it does have a noticeable impact on gel time. This occurred because the hyperbranched polymer has multiple amine functionality available for cross-linking the reaction. According to Gel Theory, increasing the concentration of multifunctional cross-linking agents decreases the conversion at which gelation occurs.

3.6 Results for Low VOC and High Performance Topcoat Developments

Figure 90 below highlights the five raw material groups used in the formulation process. Resin, solvent, and pigments each make up approximately 1/3 of the coating composition. Therefore, changes to any of these can create a large change in the cost or performance of the coating. Additives make up a small percent of the coating, but play a large role in optimizing the performance of the coatings.

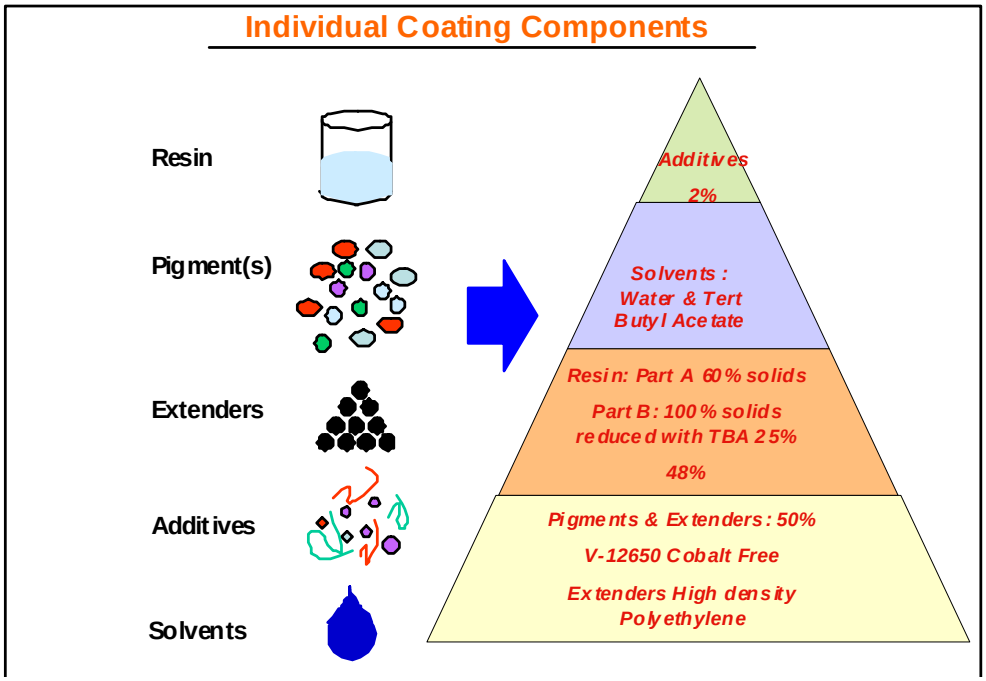

Figure 90: Raw material components used in the formulation of Army topcoats.

3.6.1 Low VOC Topcoats

Research efforts for topcoats have primarily focused on developing near zero VOC formulations by either using water as a co-solvent and lower molecular weight binder systems or using exempt solvents and nontraditional binder chemistries such as non-isocyanate urethane. Commercially available water-dispersible lower molecular weight binders will help minimize formulation viscosity and eliminate the need for organic reducing solvents. A mandatory criterion for any candidate technology is to meet or exceed current CARC durability. In short, performance properties cannot be compromised to achieve lower VOCs. Table 41 lists military specification tests and evaluations used to determine the durability and viability of a coating. Tests highlighted in green were used in Phase I screening of various technologies. Details of these procedures and coating performance criteria can be located in either MIL-DTL-53039 or MIL-DTL-64159.

Table 41: Military specification tests

Item	FED-STD-141 Method	ASTM Method
Color and Spectral Reflectance	**6241**	**E308**
Total Nonvolatile		
Pigment Analysis	4021	
Lead Content		
Chromium, Hexavalent		
Antimony Sulfide		
Solvent Analysis	7360	D3272
Volatile Organic Compounds		
Viscosity		
Krebs Stormer		D562
Hiding Power (contrast ratio)		D2805
Fineness of Grind		D1210
Drying Time	**4061**	
Specular gloss		**D523**
Specular Reflectance		**E167**
Infrared Reflectance		
Camouflage Colors	**6241**	
Noncamouflage Colors	**6242**	
Condition in Container		
Component A	3011	
Component B	4261	
Mixing Properties		
Spraying Properties	**4331/2131**	
Brushing Properties	4321	
Flexibility	6221	
Recoatability		
Water Resistance		**D1308, 6.4**
Hydrocarbon Resistance		**D1308, 6.4**
Acid Resistance		
Accelerated Weathering		**G26 &G154**
STB Resistance		
Chemical Agent Resistance		MIL-DTL-64159 or 53039
Weather Resistance		D1014

3.6.1.1 Polymeric Flattening Agents for Improved Durability

Concurrent efforts are ongoing to qualify manufacturers of MIL-DTL-53039 (one-component moisture cure urea coatings) that replace silica based flattening agents with polymeric flattening agents. Polymeric flattening agents were proven to minimize marring, reduce solvent demands and improve flexibility in the SERDP program 'Low VOC CARC' (PP-1056) which resulted in the creation and DoD implementation of MIL-DTL-64159 (Figure 91). The fact that the

flattening agents are distributed throughout the coating allows for consistent properties regardless of coating weathering and erosion [36]. All formulations for the current SERDP effort will require non-silica flattening agents to support requirements of durability.

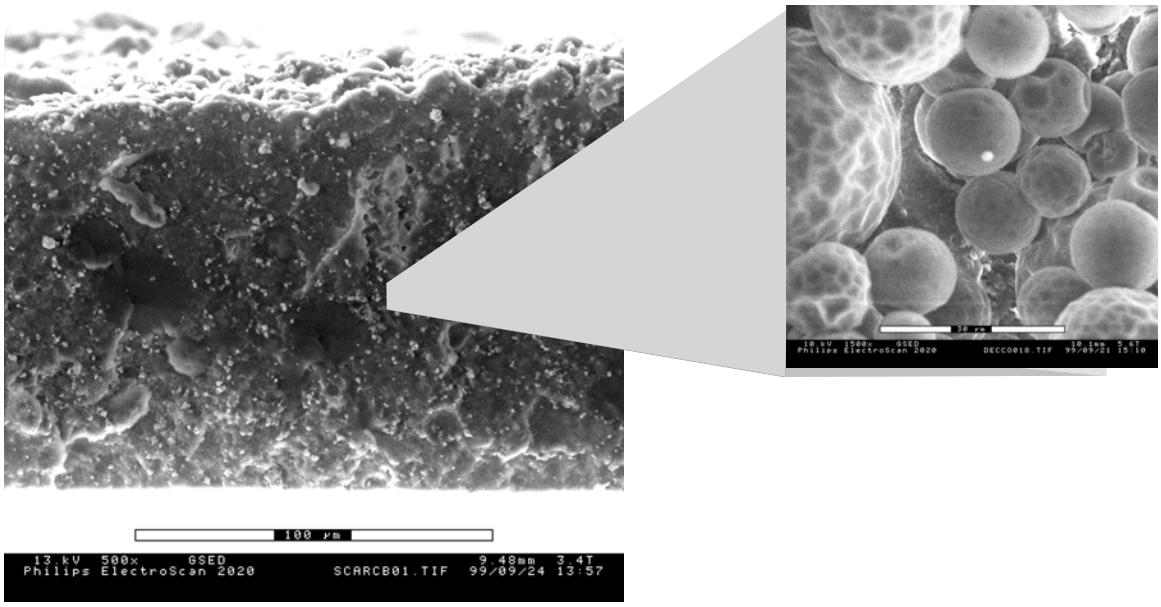

Figure 91: Cross-section of coating with polymeric bead flattening agents. The inset shows the polymeric beads at higher magnication.

3.6.1.2 Non-VOC Thinners for Use with MIL-DTL-53039

RRAD is acting as a pilot facility for the use of ZVOC thinners for solvent-based CARC (MIL-DTL-53039). ARL introduced an exempt solvent blend of OXSOL 100 (Parachlorobenzotrifluoride), PM Acetate and Tert Butyl Acetate as a thinner for this topcoat. This reduced VOCs from 1.5 to 1.0 lbs/gal. Trials at RRAD have proven the effectiveness of this new thinner. ARL has approved this thinner for use on April 9, 2008. ARL will acquire NSNs through GSA and request DoD use for all MIL-DTL-53039.

3.6.1.3 One-Component Moisture-Cure Candidate

ARL is evaluating near zero VOC one-component technology that uses aliphatic urethane chemistry with modifiers to assist in reducing viscosity and eliminating VOCs. Phase I was conducted with satisfactory results (all physical testing listed in green passed and near zero VOC were calculated) and Phase II accelerated weathering in QUV chambers was conducted. The conditions consisted of 12-hour cycles (8 hours of UV irradiation at 60°C followed by 4 hours of condensate at 50°C) with the total time of exposure being 800 hours. The samples demonstrated very poor UV stability and resulted in color change of 9.8 to 10.0 NBS units for three panels exposed (Figure 92). Note the top portions of the panels were covered by the sample holder and provide a "before" exposure view of the samples. The color difference after UV exposure should

not exceed 2.5 NBS units. The chemistries did allow for very low VOCs yet at the expense of durability which is not acceptable for DoD use.

Figure 92: One component near zero VOC coating after 800 hours QUV exposure

3.6.1.4 Water-Dispersible Formulations

The urethane polymer is formed by the reaction of hydroxyl terminated polyol and a diisocyanate as shown in Figure 93. The reaction between water and isocyanate forms an unstable carbamic acid. The carbamic acid quickly decomposes to generate carbon dioxide and amine (Reaction 1) [37,38]. The amine then reacts with additional isocyanate to yield the substituted urea (Reaction 2). In a solvent-borne, two-component system, this reaction inhibits the development of crosslinking that is crucial in providing the film with the integrity and performance commonly associated with two-component polyurethanes. However, these developments, using waterborne polyurethane technology have enabled high-performance coatings to be formulated using water-dispersible polyisocyanates and hydroxyl-functional polyurethane dispersions [39]. While there is a competing reaction occurring with water, the kinetics and raw materials used in the formulations ensure that sufficient crosslink density is established in the film. In two-component waterborne polyurethane coatings, the water-dispersible aliphatic polyisocyanates reacts slowly with water. Thus, an excess of polyisocyanates will preferentially react with the hydroxyl groups of the polyurethane dispersion. Since the polyisocyanates is dispersed and not dissolved in water, it coalesces with the polyol dispersion particles, enabling the isocyanate group to be close enough to the hydroxyl group for cross-linking to occur.

(1) $RNCO + H_20 \rightarrow [RNHCOOH] \rightarrow CO_2(g)\uparrow + RNH_2$

(2) $RNH_2 + RNCO \rightarrow RNHCONHR$

Figure 93: Important polyurethane reactions

The Army has developed two candidate zero VOC chemical agent resistant coating topcoat systems. The first uses alternative Bayer polyols (Bayhydrol XP-2591) instead of the current polyols (Bayhydrol XP-7110). Bayhydrol XP-2591 contains no VOC solvents and allows for complete water dispersibility with the standard isocyanates used in MIL-DTL-64159 (Bayhydur 303). However, the standard isocyanates contain significant amounts of VOCs. This topcoat paint would have a VOC content of ~ 1 lb/gal vs. 1.5 lbs/gal for the current topcoat. The second system makes use of Bayhrol XP-2591 cured with a ZVOC isopheronediisocyanate (IPDE) solution. This solution contains no VOCs or HAPs. The paints were formulated by Sherwin Williams with standard pigment packages or low solar loading pigments and other standard additives. The binders used in these formulations have lower molecular weights relative to the standards, allowing for lower water contents needed for dispersion, thereby decreasing drying time.

Experimental efforts have been on going to evaluate water dispersible formulas. The preliminary stages of development have been successful in using both exempt solvents for viscosity reduction and water for spray application. Currently, prototype formulas have been sprayed and are being evaluated for chemical agent resistance. The prototypes use the identical pigment package as our current and successful formulation MIL-DTL-64159 and have eliminated co-solvents in the polyol component of the formula. The formulas meet gloss and color specifications and have excellent spraying and flow properties.

Table 42: Test results according to MIL-DTL-64159 for experimental ZVOC topcoats.

Property	**Requirement**	**Pass/Fail**
Color		Pass
Gloss 60 º/85º	1.3/1.1	Pass
Dry Film Thickness	3.1-3.6 mil	Pass
ASTM D 3732 MEK Double Rub Test	200+	Pass
ASTM D 2794 Impact resistance, lb-inch, Direct/Reverse	40/20	Pass
ASTM D 3359: Cross Cut Adhesion, WET/DRY	5B/5B	Pass
QUV Cyclic Test (600 hrs)		Pass
Super tropical bleach immersion		Pass
Flexibility		Pass
Water resistance		Pass

In the last quarter of this effort, ARL evaluated the chemical agent resistance of these formulations. Table 43 highlights the average values for two ZVOC formulations. These results clearly show that the new ZVOC topcoat formulations performed extremely well. The slight increase for the 2591/303 sample vs. the control for HD is not considered significant, and is well below the threshold anyway.

Table 43: HD and GD values of ZVOC CARC samples.

NOMENCLATURE	HD-PASS	GD-PASS
Bayhydrol XP-2591/ Bayhydur 303	<16.8	<4.3
Bayhydrol XP-2591/IPDE	<10.3	<4.25

NOTE: PASS/FAIL is 180 μg or less for HD and 40 μg or less for GD.

3.6.1.5 Low Solar Absorbing Coatings/Pigments

The technical gap and stimulus for the development described here originates from several sources. The first information being received from both Iraq and Afghanistan with regard to high ambient temperatures and system failures resulting from heat build up. The second is from a Government Accountability Office (GAO) report to Congress on the cost of corrosion leading to degradation and equipment failure [40]. In this report, the GAO estimates that low and high cost estimate of repair and replacement the Marine Corps and Army range from $10 to 20 billion, and our current war efforts in Iraq and Afghanistan are some of the most severe conditions for materiel. Efforts to minimize coating degradation are paramount from both a readiness issue and ensuring our personnel could function in high temperature environments. This critical need lead to the development and formulation of Low Solar Absorbing Coatings for DoD application.

All camouflage coatings use a mixture of metal oxides to impart color and provide camouflage properties. Our current 383 Camouflage green uses a combination of Chrome Oxide and Cobalt Spinel to both replicate foliage background in the visible (400nm–700nm) and in the near IR spectra (750nm–900nm). Unfortunately, Cobalt Spinel is a foreign imported source with its cost increasing over 300% in recent years and supply is erratic. Additionally, the Environmental Protection Agency has designated cobalt as a hazardous air pollutant when it is in free form. Finally, and most importantly continual reports to Natick Soldier Systems Center from field units indicated that during the summer months, solar radiation was causing the air temperatures inside refrigerated/dry International Standards Organization (ISO) containers to range from 160°F to 180°F. At these temperatures, the heated air in the containers has an “oven effect”, literally baking the products stored within them. The result was rapid food spoilage, degradation to electronics and chemical and biological protective clothing and related equipment. Solar loading will rapidly degrade many products and equipment shipped and stored within ISO containers used in theater. These elevated temperatures have a significant readiness impact on stored

materials and there is a need to preserve the contents stored in refrigerated and dry storage ISO containers currently used by the DOD in hot and arid climates. These reports along with severe temperatures within vehicle compartments prompted an immediate development and formulation effort to minimize or eliminate solar absorption and coating degradation.

Our primary goal was to develop a technical basis to greatly reduce or eliminate solar absorption while maintaining all existing coating requirements. An additional goal was to scale up development to ensure replication by commercial vendors and continue meet or exceed all CARC requirements. In our work, we introduced a new type of novel pigmentation of a mixed metal oxide commercially available though never used for this type of military application with nano-flow additives and surface modifiers to our enhanced low molecular weight polyol and polyisocyanates. The testing and validation included accelerated cyclic corrosion evaluations, outdoor solar determinations, heat absorption, specular and spectral reflectance and degradations. In house formulation using high speed dispersion techniques were made and all samples were evaluated by ARL. The results were superior coatings that specifically overcame the key technical gaps described above. Numerous formulations have been created and vendors have taken our starting formulation and are matching our new IR and color requirements. This effort has been multifaceted and has involved all the major paint companies in the United States and numerous raw suppliers and manufactures who provide the base resins, pigments, extenders, solvents and additives used in coating manufacturing.

Our efforts are enabling the United States to rely on non-imported sources to produce our camouflage coatings. Currently, the Army and Marine Corps are using over two million gallons a year and these volumes have been steadily climbing. Additional efforts are under way with Naval Air Systems Command to use our technical achievements with these coatings on the Navy's Air and Sea equipment. The coating formulation will assist efforts to paint outdoor industrial items, roofing materials and facilities where corrosion and degradation are a persistent problem. One of the new colors developed will be named 808 Green to replace 383 Green which is our standard green camouflage coating used on all military assets. 808 follows the similar naming convention of using the month and year with which the color space and IR spectra was first determined.

Technical Description

The long term stability of camouflage coatings that are also resistant to chemical agents is directly related to the degree of exposure to sunlight, temperature extremes and humidity. The effect of the high temperature that the CARC is subject to on a daily basis in Iraq and Afghanistan results in a shortened coating life cycle due to erosion and formation of micro cracks in the film. While storage of our tactical vehicles in a garage type environment would be a solution, the more practical approach is to lower the solar absorption or solar loading on the vehicles to a significantly lower level. The amount of solar absorption that a surface is subject to is directly related to the reflectivity of the coating system in both the visible and the near IR region of the spectrum, about equally divided. To lower the solar absorption in the non visible IR, pigment and nano additive changes to the color formulations have been developed together with the use of high reflective primers. ARL using commercially available raw materials developed novel CARC formulations and pigment blends which reduces solar loading, eliminates the need for a cobalt spinel inorganic pigment and enhances the UV durability and life cycle of the coating.

Our efforts are based on formulations with isocyanate (NCO) to hydroxyl (OH) ratios between 4:1 and 5:1 to obtain optimum film properties for MIL-DTL-64159. The low solar loading pigments were also incorporated into MIL-DTL-53039 formulations using the same indexing as the current paints. The cobalt free unique pigmentation permits maximum reflectance and enables the same processing and high speed dispersion currently used to formulate CARC combined with nano film stabilizers and additives. The resulting reflectance curves as shown in Figure 94 eliminates any specific IR characteristics and maximizes the reflectance of the IR band from 750 to 2000 nm while the coating is still visually similar to our current 383 Green color number 34094 (RS831-7 Cobalt based formulation).

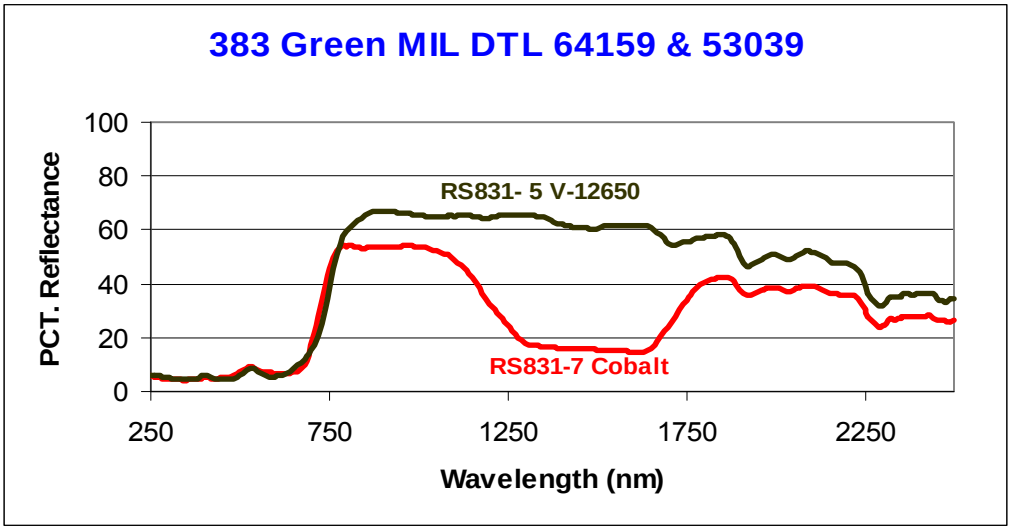

Figure 94: Spectral reflectance curve of cobalt (lower curve) versus novel coating (upper curve); note that in the visible range identical reflectance or appearance is achieved.

MIL-Spec testing was performed on the coatings with low solar loading pigments (Table 44). The performance of the coatings was similar to the baseline. However, the low solar loading samples had less color and gloss change during outdoor weathering, indicating improved performance. Furthermore, CAR testing was performed on these samples, and all samples passed.

Table 44: Test results according to MIL-DTL-64159 and MIL-DTL-53039 for low solar loading pigments in 5:1 indexed polyurethane topcoats.

Property	MIL-DTL-64159	MIL-DTL-53039
	Rating	Pass/Fail
Color	Pass	Pass
Gloss 60 º/85º	Pass	Pass
Dry Film Thickness	Pass	Pass
ASTM D 3732 MEK Double Rub Test	Pass	Pass
ASTMD 2794 Impact resistance, Ib-Inch, Direct/Reverse	Pass	Pass
ASTM D 3359: Cross Cut Adhesion, WET/DRY	Pass	Pass
QUV Cyclic Test (600 hrs)	Pass	Pass
Super tropical bleach immersion	Pass	Pass
Flexibility	Pass	Pass
Water resistance	Pass	Pass
Outdoor weathering	Pass	Pass

3.6.1.6 Powder Coat Alternatives

Powder topcoats are also being investigated. Several vendors have submitted formulations which successfully provide UV protection in low gloss formulas. This is the key advance in powder coat chemistries for the military. Currently several formulations with different binder systems and gloss levels have been prepared to evaluate for live agent resistance. It must be noted that none of the formulas submitted meet the gloss limit values of 1.0 unit maximum at 60° incidence and 3.5 units maximum at 85° incidence. In general, it has been found that lowering gloss in powder coat systems deteriorates the UV and exterior properties. Two new formulations with textured surfaces to assist low gloss application are being evaluated for chemical agent resistance. Our current efforts have been successful in evaluating several starting formulas for Powder Top Coats. Formulations have passed preliminary live agent testing with either nerve or mustard agents though continue to have higher gloss values than NAVAIR or ARL requires for topcoat formulations. Additionally efforts will continue to down select powder formulations that provide very low gloss, UV protection and for the Army, chemical agent resistance. This effort is ongoing is being funded by RDECOM and may be available for an ESTCP evaluation in the near future.

3.6.1.7 Low VOC Topcoat Development Conclusions

Achieving near zero VOCs and meeting military requirements stated above has been extremely difficult. ARL has evaluated several formulations in both the MIL-P-53022 and MIL-P-53030 chemistries with limited success in meeting our SERDP goals. The major obstacle to this goal is acquiring 1,000 hour salt spray performance coupled with cyclic exposures. The best candidates still contain 2 to 2.5 lbs/gal VOCs. Resin systems offering low molecule weight and proper cross link density for corrosion inhibition are limited. Efforts have been successful in using inorganic corrosion inhibitors with good to excellent properties though the availability of a viable binder has been a key hurdle. Future efforts will explore nanoparticle additives to support

the binder system and use silane adhesion promoters to bolster the formulations. The results to date have enabled ARL to approve several formulations that have successfully endured nearly double the hours of corrosion exposure as required by current standards (336 hours to 600 hours salt fog) and reduced VOCs by 30%. These coatings are currently available and will be a benchmark for new DoD requirements as this SERDP effort continues to pursue near zero VOCs.

3.6.2 HIGH PERFORMANCE TOPCOATS USING HYPERBRANCHED POLYMER ADDITIVES

Hyperbranched polymer (HBP) additives were added to CARC systems to alter surface properties while using only a low additive concentration. These HBPs were chemically prepared to enable thermodynamically drive surface-segregation as the coating cures [41]. As such, the surface of the coating can be modified significantly, without significant modification of the bulk coating. These specific hyperbranched polymers were prepared with fluorine functionality to enable surface segregation [41]. Remaining functionality on the hyperbranched polymer (amine or hydroxyl) allows for reaction with the paint and could potentially increase crosslink density, thereby improving barrier properties and possibly chemical agent resistance.

3.6.2.1 XPS Analysis of CARC with HBP Additives

XPS was run on CARC samples with hyperbranched additives. Two base hyperbranched additives were used: Bolton hyperbranched polymer polyester (PE) with hydroxyl functionality (MW~2100 g/mol, ~16 –OH/HBP) [41] and Lupasol polyethyleneimine (PEI) hyperbranched functionality with 1°-3° amine functionality (MW~1000 g/mol, ~8 1° amine, ~6.5 2° amine) [41]. These HBPs were modified by reacting them with fluoro and alkyl functionality. The polyethyleneimine HBPs were reacted with epoxy functional aliphatic character at room temperature to alkyl functionality, and were reacted with methacrylate aliphatic fluoro chains to add fluoro functionality. The polyester HBPs were reacted in the bulk with fatty acids and fluorinated fatty acids to add alkyl and fluoro functionality. These functionalities gave the hyperbranched polymers low surface energy so they thermodynamically segregate to the coating surface. In all cases, some base functionality (alcohol or amine) remained on these HBPs. The purpose of the base functionality was to allow the HBP to react into the paint to prevent leaching with time. The hyperbranched polymer additives were added into MIL-DTL-64159, MIL-C-53039, and MIL-P-53022 in the amount of 1 wt % of the coating solids. The goal of these polymers was to reduce surface tension of CARC paints and to increase the cross-link density at the paint surface to improve CAR.

XPS revealed fluorine concentrations at the surface in excess of the bulk concentration in some coatings, implying that additives with fluorine functionality had effectively surface segregated (Figure 95 and Table 45). This behavior was observed with both PEI and PE additives in each military coating tested. The PE additive had ~0.17 atomic% fluoro functionality, whereas the PEI additive had ~0.025 atomic% fluoro functionality. Based on these numbers, the fluoro or HBP surface enrichment was calculated and listed in Table 45. The results show a surface enrichment of 18-135 times that of the bulk concentration. In the 53022, the PEI HBP was much more effective in surface-segregating than the PE HBP additive. This was unexpected because the PEI HBP should react with the epoxy functionality in the paint, whereas the PE HBP should be unreactive with the paint. In MIL-DTL-64159 and MIL-DTL-53039, both HBPs were of similar effectiveness in segregating to the coating surface.

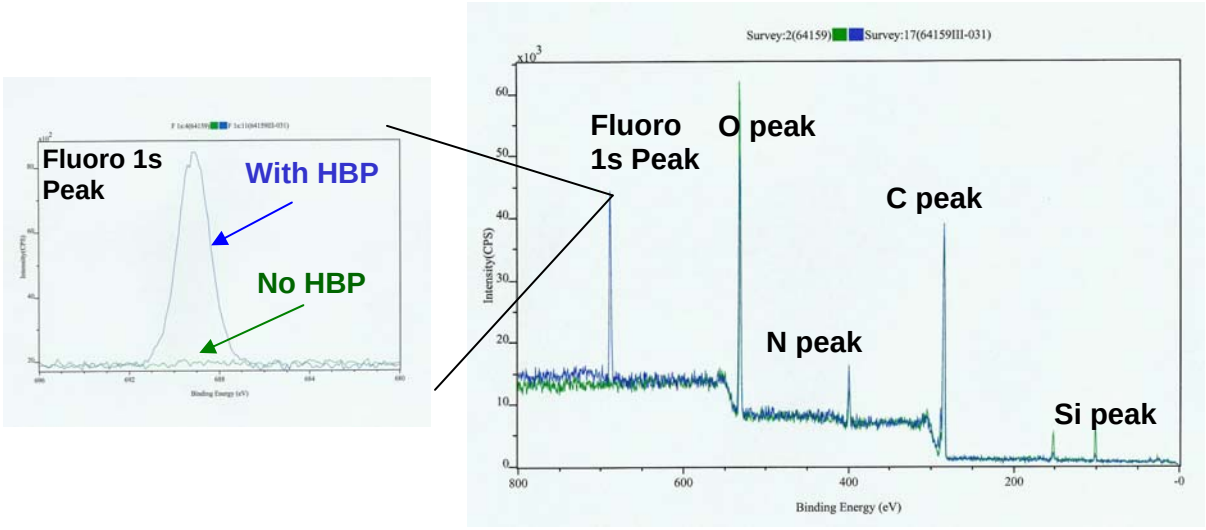

Figure 95: XPS spectra of MIL-DTL-64159 showing samples with and without a fluorinated HBP PEI HBP additive.

Table 45: XPS results showing the elemental atomic percent of chemicals at the surface for the various military coatings with and without HBP.

Sample	Composition - Atomic % C	O	N	F	F Surf Enrich.
MIL-P-53022 Baseline 3-3-06	80.26	16.31	3.08	*0.34*	*0*
MIL-P-53022 Baseline 4-7-06	-	-	-	*ND*	*0*
MIL-P-53022 Baseline 5-2-06	82.05	14.36	3.29	*0.30*	*0*
MIL-P-53022 PEI HBP	74.69	16.37	5.55	**3.39**	**135.60**
MIL-P-53022 PE HBP	77.15	16.12	3.62	**3.11**	**18.29**
MIL-DTL-64159 Baseline 2-16-06*†	72.537	19.946	5.242	*ND*	*0*
MIL-DTL-64159 Baseline 2-23-06*	71.688	19.291	5.065	*ND*	*0*
MIL-DTL-64159 Baseline 4-3-06	72.35	20.95	6.45	*0.26*	*0*
MIL-DTL-64159 Baseline 5-5-06	73.64	20.88	4.99	*0.48*	*0*
MIL-DTL-64159 PEI HBP	67.487	17.992	5.529	**1.247**	**49.88**
MIL-DTL-64159 PE HBP	70.32	16.20	7.04	**6.45**	**37.94**
MIL-C-53039 Baseline 2-16-06*†	78.796	12.278	7.411	*ND*	*0*
MIL-C-53039 Baseline 4-6-06	76.84	16.92	5.62	*0.62*	*0*
MIL-C-53039 Baseline 5-5-06	76.31	17.4	5.96	*0.33*	*0*
MIL-C-53039 PEI HBP	88.951	4.688	3.939	**1.020**	**40.80**
MIL-C-53039 PE HBP	71.53	14.79	5.15	**8.53**	**50.18**

3.6.2.2 Contact Angle of CARC with Hyperbranched Additives

Water droplet contact angle deflection, relative to the baseline, was observed in Army coatings after addition of PEI HBPs (Figure 96 and Figure 97) and PE HBPs (Figure 98 and Figure 99).

There was a significant increase in advancing contact angle through the use of the PEI and PE HBP in MIL-C-53039 and MIL-P-53022. There was also a significant difference in the receding angle for PE and PEI HBPs in MIL-P-53022. Therefore, both HBPs performed similarly. Unfortunately, overall the effect on contact angle was relatively small. It is doubtful that these HBPs would be able to reduce adsorption of chemical agents and improve durability based on the surface energy. However, the cross-link densities of the surfaces of these coatings may be elevated. Further study must be performed to determine this.

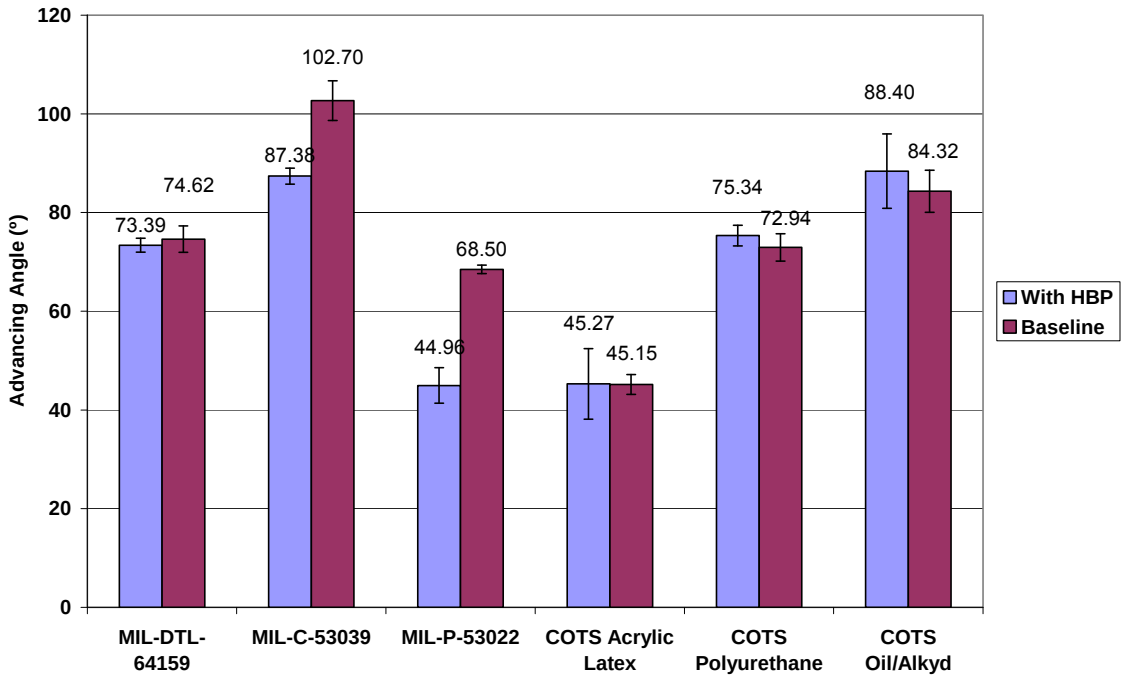

Figure 96: The advancing contact angle for samples with (1 wt %) and without PEI HBPs

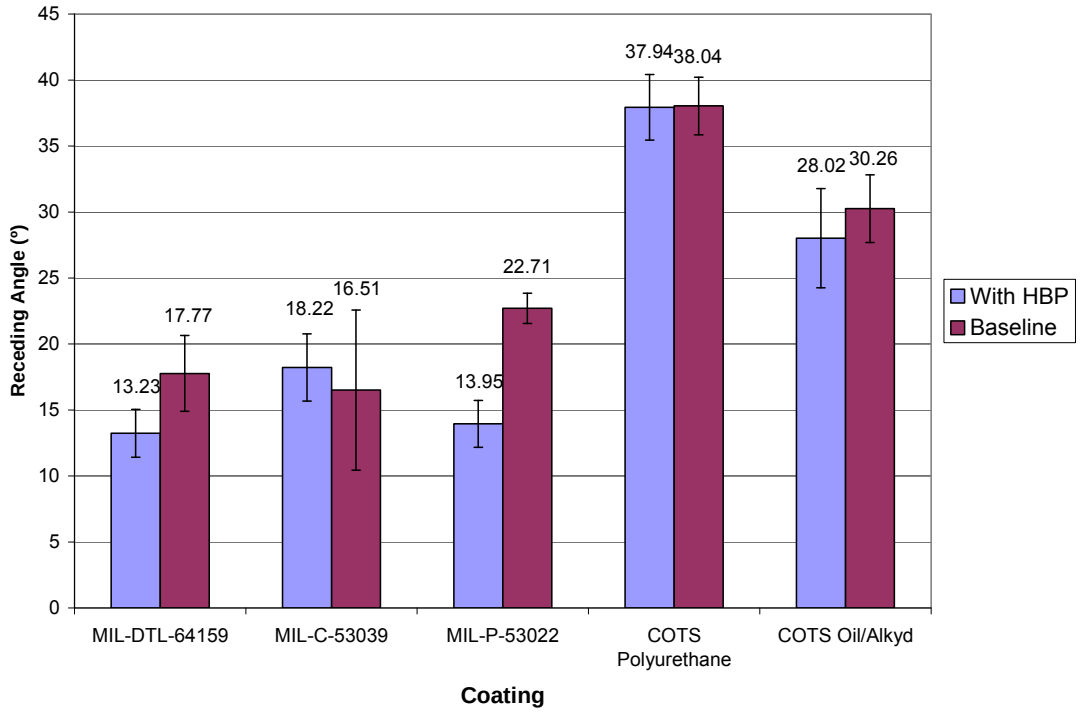

Figure 97: The receding contact angle for samples with (1 wt%) and without PEI HBPs

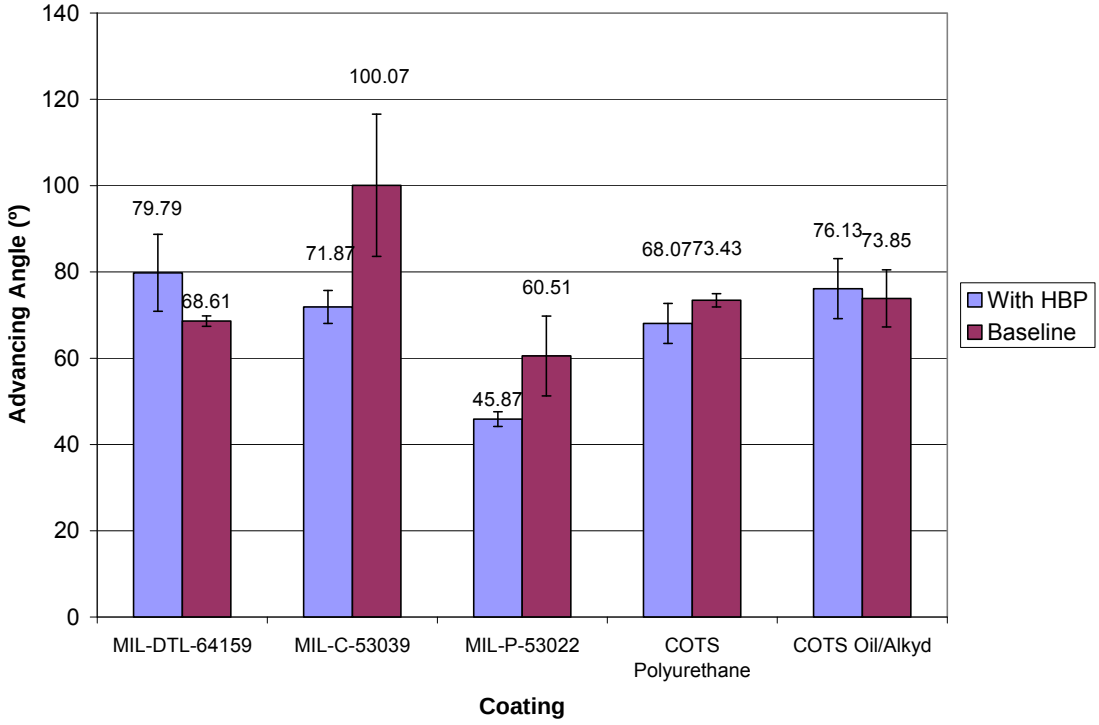

Figure 98: The advancing contact angle for samples with (1 wt%) and without PE HBPs

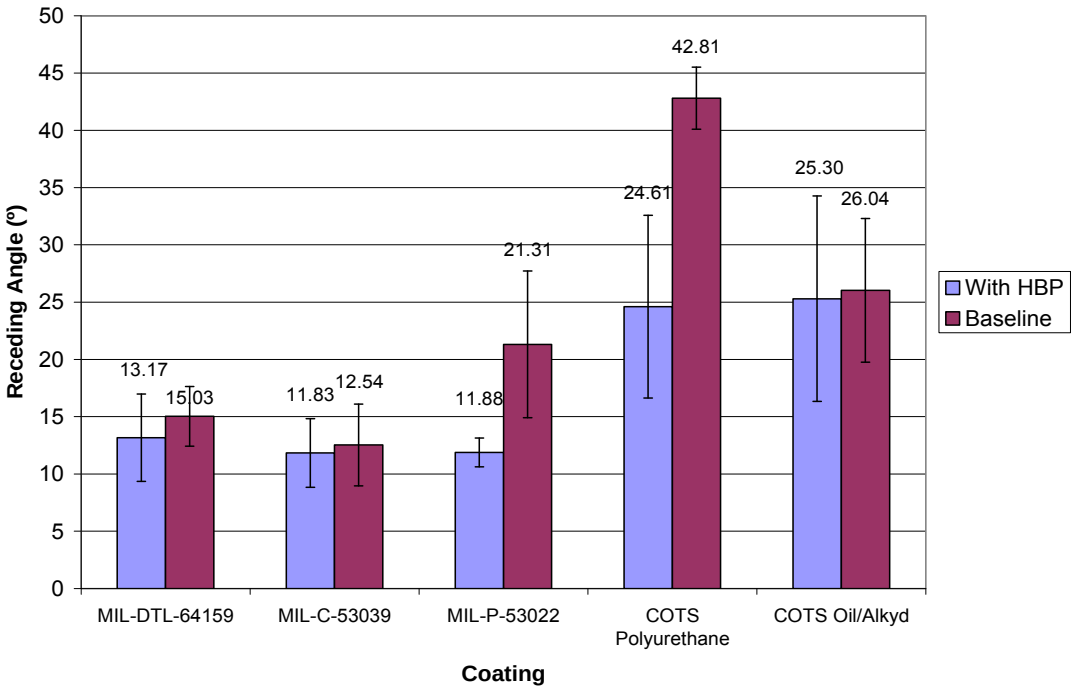

Figure 99: The receding contact angle for samples with (1 wt %) and without PE HBPs.

3.6.2.3 CARC Panel Testing with Hyperbranched Additives

Two hyper-branched polymers that were studied, PE and PEI HBPs, were dissolved into an appropriate solvent and mixed into existing military coatings at 1 % weight of coating solids. Cold rolled steel panels pretreated with zinc phosphate were spray-coated with these modified formulations and subjected to typical military specification testing *vs.* control panels of unaltered commercially sourced product. The results are reported in Table 46 and Table 47. MIL-P-53022 is a two part epoxy primer and MIL-DTL-64159 is a two part water dispersible polyurethane topcoat.

In general, epoxy performance was not adversely affected by the addition of PE or PEI. The only negative result found was a slight decrease in water resistance when PEI was added. Dry adhesion determined by the tape method B in ASTM D 3359-02 was rated at < 5% removal whereas the control and PE HBP panels experienced 0% removal. Wet adhesion after 1 week DI water soak at room temperature declined from 0% removal for the control and PE to 5-15% removal. The urethane topcoat with 1 wt% PE HBP had comparable performance to the control in all tests except for mandrel bend flexibility. The testing should be repeated to ensure an error was not made in surface preparation of the panels.

Table 46: CARC testing results for MIL-P-53022 with HBP additive

Test Description	ASTM	conditions	specification requirements	control	+ 1% wt. PE Quat	+ 1% wt. PEI Quat
Specular Gloss (60°)	D 523 - 89 (99)		10 - 30	**10.1**	**10.9**	n/a
Solvent Resistance (MEK double	D 5402 - 93 (99)		not specified	**some dulling and slight color removal**	**some dulling and slight color removal**	**some dulling and slight color removal**
Flexibility (mandrel bend)	D 522 - 93a (01)		no cracking or flaking	**PASS**	**PASS**	**PASS**
(DI) Water Resistance	D 1308 - 02	*immediate properties:*				
50% submerged		blistering	none	**none**	**none**	**none**
7 days at RT		wrinkling	none	**none**	**none**	**none**
		after 2 hours drying:				
		adhesion	no more than slightly affected	**not affected**	**not affected**	**not affected**
		color	no more than slightly affected	**not affected**	**not affected**	**not affected**
		gloss	no more than slightly affected	**not affected**	**not affected**	**not affected**
		hardness	no more than slightly affected	**not affected**	**not affected**	**not affected**
		after 24 hours of drying:				
		adhesion	no difference from control	**no difference from control**	**no difference from control**	**no difference from control**
		hardness	no difference from control	**no difference from control**	**no difference from control**	**no difference from control**
Adhesion (tape test)	D 3359 - 02, method B	obsolete reference, rate according to TM		**0% removed wet and dry**	**0% removed wet and dry**	**< 5% removed dry, 5-15% removed wet**
Hydrocarbon	D 1308 - 02	*immediate properties:*				
Resistance (JP-8 fuel)		blistering	none	**none**	**none**	**none**
50% submerged		wrinkling	none	**none**	**none**	**none**
7 days at RT		color	no more than slight yellowing	**no change**	**no change**	**no change**
		softening	slight is acceptable	**none**	**none**	**none**
		after 2 hours of drying:				
		hardness	no difference from control	**no difference from control**	**no difference from control**	**no difference from control**
		gloss	no difference from control	**no difference from control**	**no difference from control**	**no difference from control**
Adhesion (tape test)	D 3359 - 02, method B	obsolete reference, rate according to TM		**0% removed wet and dry**	**0% removed wet and dry**	**0% removed wet and dry**
Knife Test	D 6677	difficult to furrow, does not flake, chip or powder		**PASS**	**PASS**	**PASS**
Impact Resistance	D 2794 - 93	not in specification; diameter of paint removal		**4.5 mm**	**4 mm**	**4 mm**
Salt Spray Resistance	B 117		rusting	**none**	**none**	**none**
			blistering	**none**	**none**	**none**

Table 47: CARC testing results for MIL-DTL-64159 with HBP additive

Test Description	ASTM	specific attribute	MIL-DTL-64159 Specification	control	+ 1% wt. PE Quat
Specular Gloss	D 523 - 89 (99)	60° observation angle	Tan 686A ≤ 1.5	1.1	1.0
		85° observation angle	Tan 686A ≤ 3.5	1.4	1.3
Spectral Reflectance	E 308	NBS error	≤ 2.0	1.7	2.0
(COLOR)		Brightness (Tristimulus Y)	36.0 - 40.0	37.9	37.3
% Reflectance from		Chromaticity x, y	0.368, 0.364	Marginal	FAIL
380 - 900 nm		IR average	62.0 - 72.0	67.6	65.9
UV Resistance	G 154 - 05	cracking	none	none	none
1000 hours exposure		chalking	none	none	none
		loss of adhesion	none	none	none
		gloss	meets spec. 60° / 85°	1.2 / 2.1	1.1 / 2.0
		Camouflage Colors	≤ 2.5 N.B.S. units	0.9	1.4
Solvent Resistance	D 5402 - 93 (99)	MEK double rub	not in specification	some color transfer to cloth	some color transfer to cloth
Mandrel Bend	D 522 - 93a (01)	1/4" mandrel, 180° bend	no cracking or flaking	PASS	FAIL
(DI) Water Resistance	D 1308 - 02	*immediate properties:*			
seal uncoated metal		blistering	none	none	none
50% submerged		wrinkling	none	none	none
7 days at RT		discoloration	no more than slight whitening	none	none
		softening	no more than no. 2 pencil difference from	none	none
		after 2 hours drying:			
		adhesion	no difference from control	no difference from control	no difference from control
		color	no difference from control	no difference from control	no difference from control
		gloss	no difference from control	no difference from control	no difference from control
		hardness	no difference from control	no difference from control	no difference from control
Adhesion (tape test)	D 3359 - 02	test wet and dry areas of panel	4B or better	5B wet and dry	5B wet and dry
Hydrocarbon	D 1308 - 02	*immediate properties:*			
Resistance		blistering	none	none	none
JP8 (universal fuel)		wrinkling	none	none	none
50% submerged		*after 2 hours of drying:*			
7 days at RT		softening	not to exceed no. 2 pencil diff. from control	none	none
		whitening	not excessive	none	none
		dulling	not excessive	none	none
		after 24 hours of drying:			
		hardness	no difference from control	no difference from control	no difference from control
		adhesion	no difference from control	no difference from control	no difference from control
		general appearance	no difference from control	no difference from control	no difference from control
Adhesion (tape test)	D 3359 - 02		4B or better	5B wet and dry	5B wet and dry
Knife Test	D 6677		not in specification	very difficult to remove	very difficult to remove
Impact Resistance	D 2794 - 93	10 in-pounds on reverse side	not in specification	cracking radius 6-7 mm	cracking radius 5-6 mm

3.6.3 FUNDAMENTAL PROPERTIES OF CLEAR ORGANIC COATINGS

Military specifications for coatings encompass an array of different binder chemistries. A study was made of some of the physical and mechanical properties of the resin binders in commercially manufactured coatings from the Qualified Products List (QPL) associated with MIL-P-53022B, MIL-DTL-53039B and MIL-DTL-64159. It is believed that a fundamental understanding of the resin properties will enhance our understanding of the pigmented coating performance in military specification testing and possibly lead to improved coating performance characteristics.

3.6.3.1 Liquid ^{1}H and ^{13}C NMR Analysis of Polyurethane Components

2.4.3.1.1 Bayhydrol XP 7110E

Figure 100 through Figure 104 give the ^{1}H, ^{13}C and Correlation NMR spectra for Bayhydrol XP 7110E. This sample contains a polymer that is very similar to block copolymerizations of polymethylmethacrylate (PMMA) and poly(1,4-butylene glutarate) hydroxy terminated. The sample could be co-blended with poly(1,4-butylene adipate). The difference is glutarate is a 5 carbon diester and adipate is a 6 carbon diester. This sample contains substantial amounts of triethylamine (TEA) and with N-methyl-2-pyrrolidone. We have identified these peaks in the ^{13}C and ^{1}H spectra. After subtracting out these peaks, we are left with the broad peaks in the baseline. We obtain a molar ratio for TEA:polymer:N-methyl-2-pyrrolidone of 1:2:4.

The polymer has a molecular weight of above 1000 amu from the NOESY data. This polymer is probably atactic polymethylmethacrylate (PMMA).

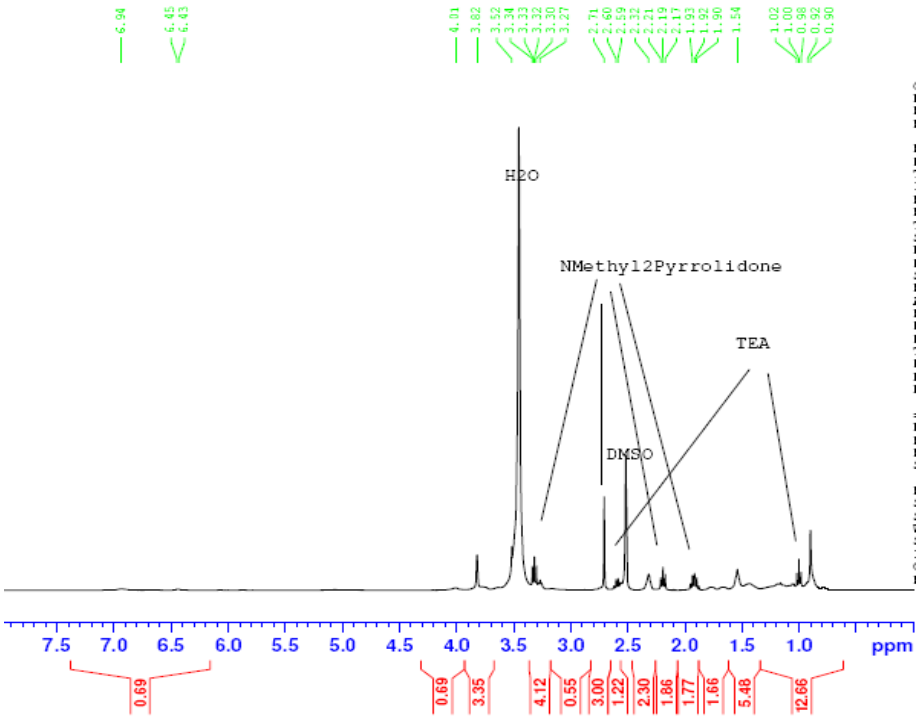

Figure 100: ^{1}H NMR spectra of Bayhydrol XP 7110E

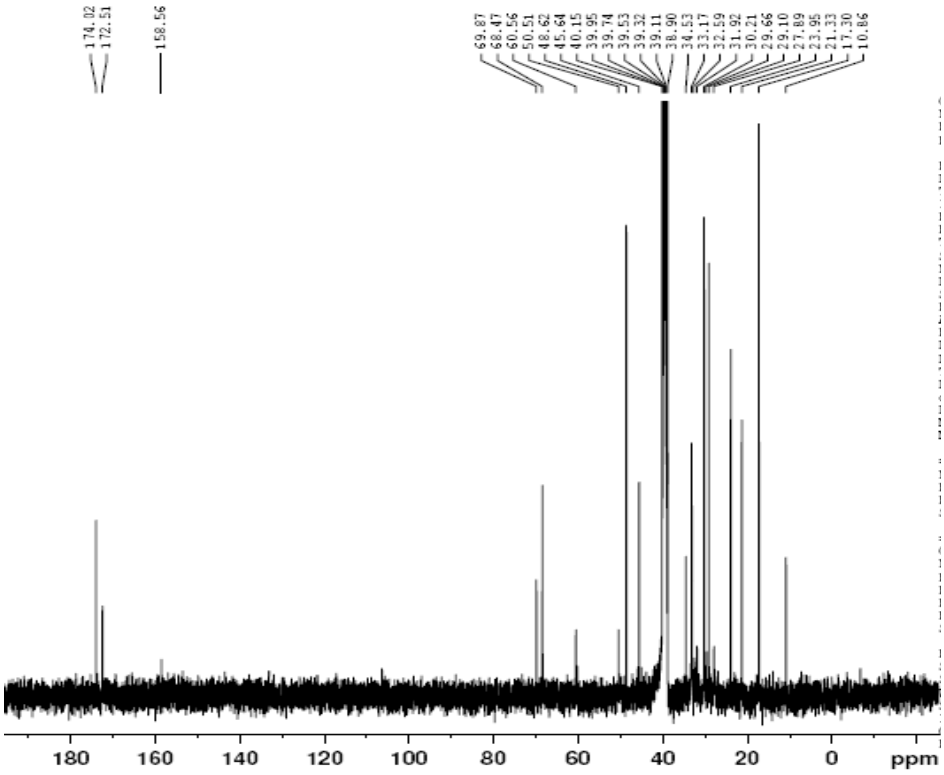

Figure 101: ^{13}C NMR spectra of Bayhydrol XP 7110E

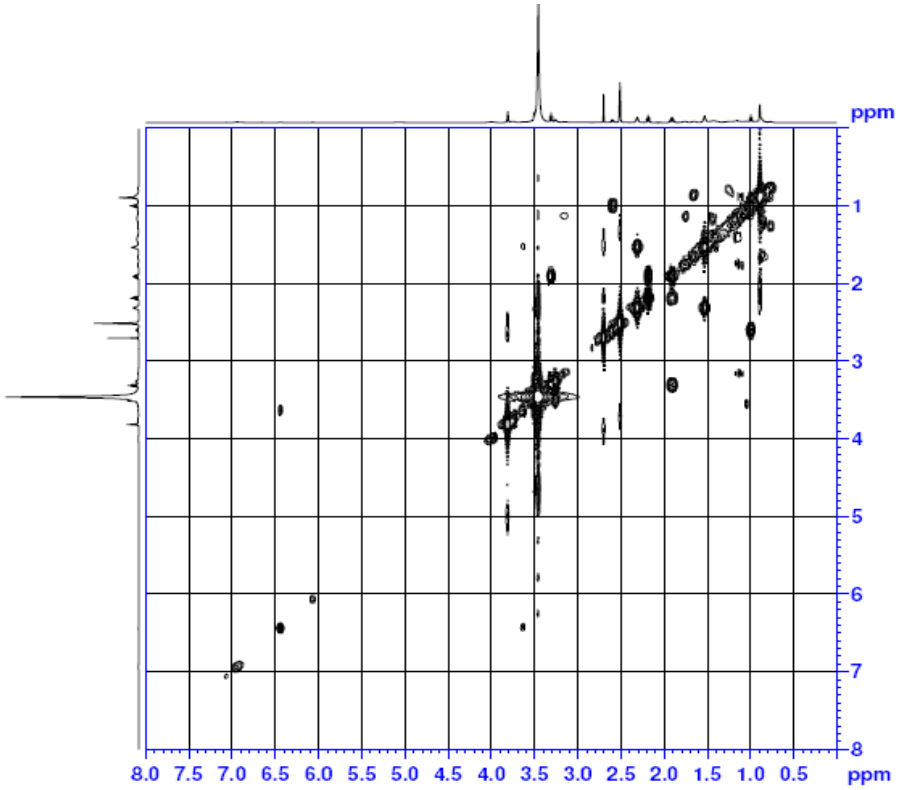

Figure 102: COSY of Bayhydrol XP 7110E

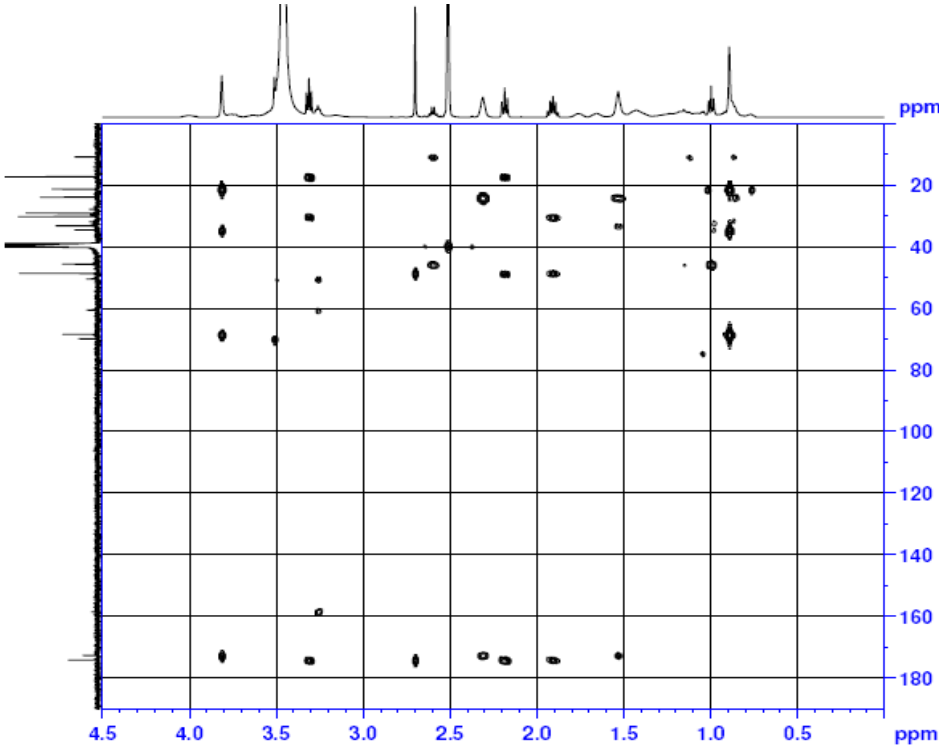

Figure 103: HMBCGP of Bayhydrol XP 7110E

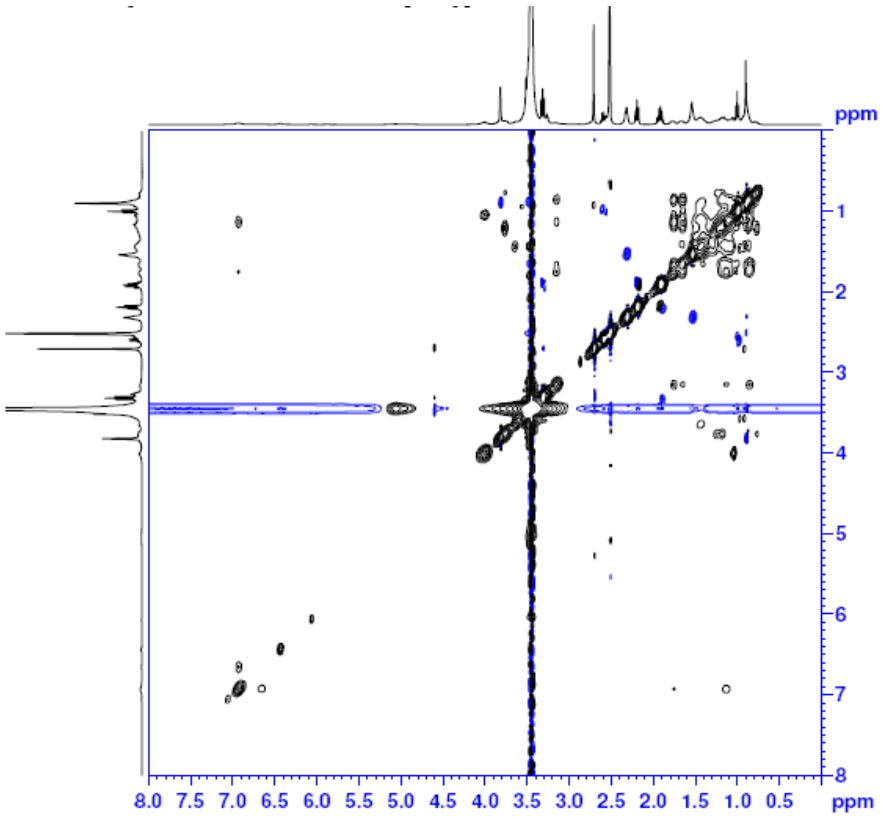

Figure 104: NOESY of Bayhydrol XP 7110E

2.4.3.1.2 MIL-DTL 64159

Figure 105 through Figure 109 give the ^{1}H, ^{13}C and Correlation NMR spectra for MIL-DTL 64159 component B. This sample is supposed to be a diisocyanatohexane. The Aldrich NMR library shows ^{1}H signals at 3.3 ppm (triplet), 1.62 ppm (multiplet) and 1.42 ppm (multiplet). The ^{13}C signals are at 121.9, 42.8, 31.1 and 26.0 ppm. These signals are present in the data sets. Other components that are roughly equimolar with diisocyanatohexane are $CH_3CO_2(CH_2)_6NCO$ and $CH_3(CH_2)_5NCO$. The acetate peaks are at 2.07 and 2.09 ppm for the acetate methyl and the ester carbonyl peak is at 171.2 ppm. All of these molecules overlap at 1.6 and 1.42 ppm in the ^{1}H spectra. This overlap issue makes the assignment of peaks for polyurethane films in the solid state NMR very difficult.

With the amount of impurity in the two starting materials, there will be a huge degree of overlap in the allophanate and biuret type signals. This overlapping of signals prevents quantification of the allophanate and biuret linkages through solid state NMR.

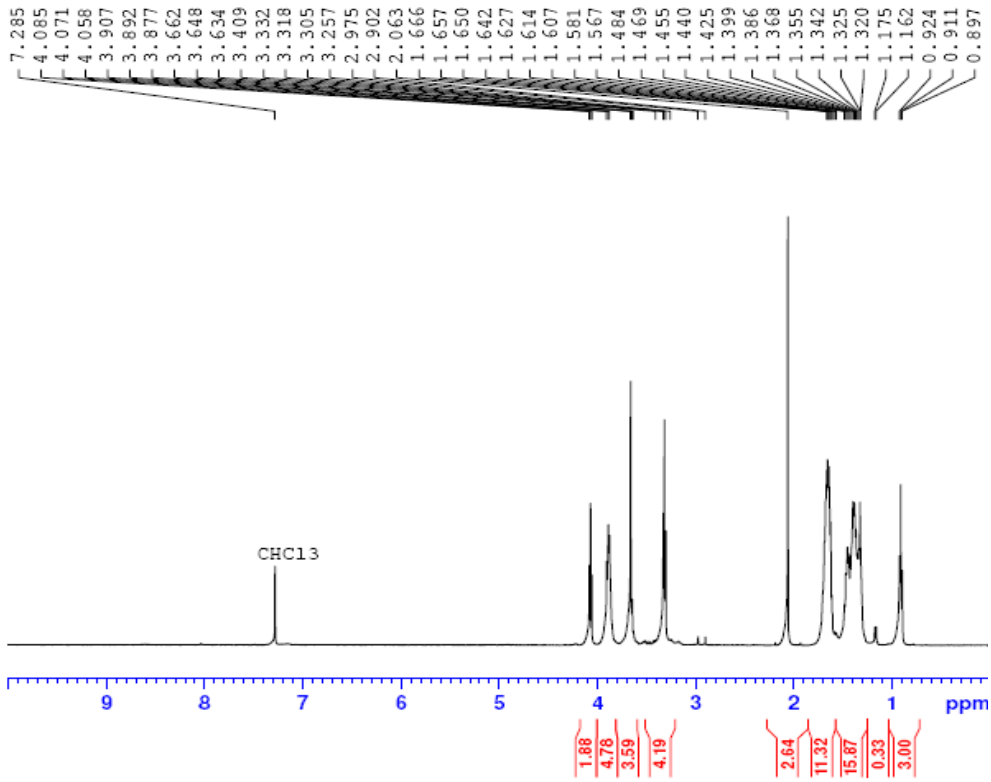

Figure 105: ^{1}H NMR of MIL-DTL-64159 component B

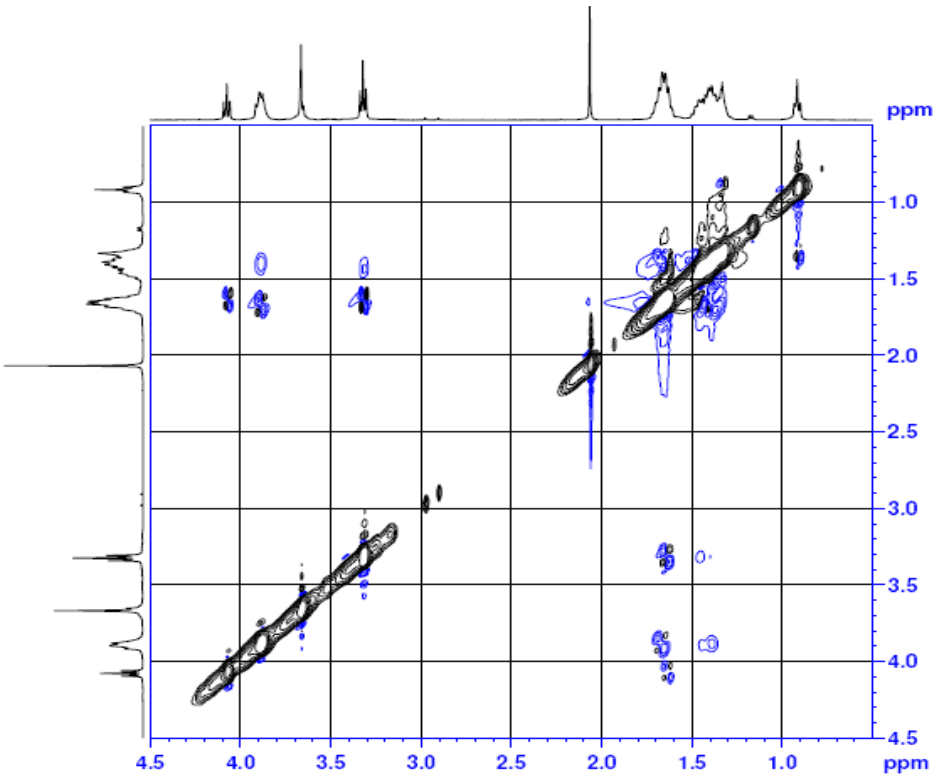

Figure 106: NOESY of MIL-DTL-64159 component B

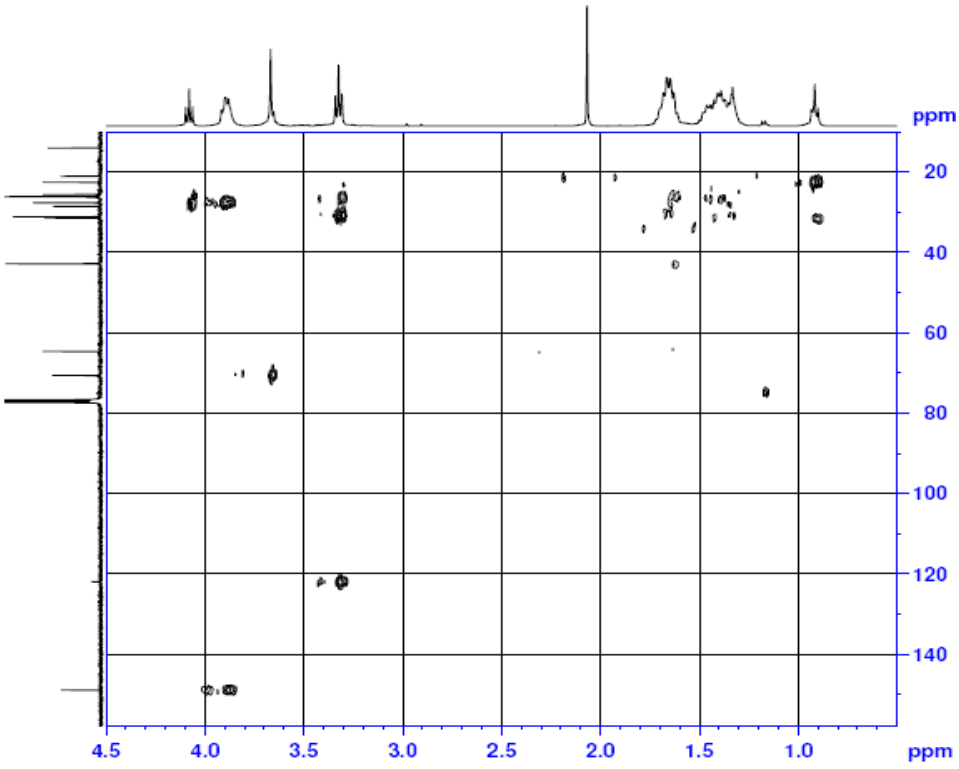

Figure 107: HMBCGP of MIL-DTL-64159 component B

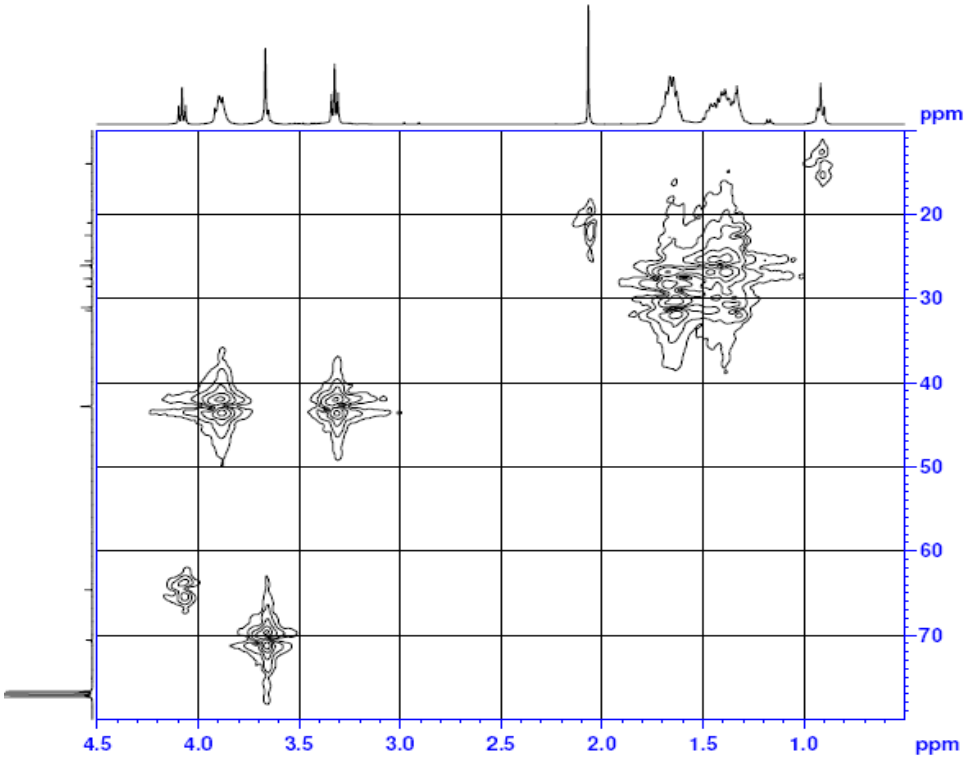

Figure 108: HMQC of MIL-DTL-64159 component B

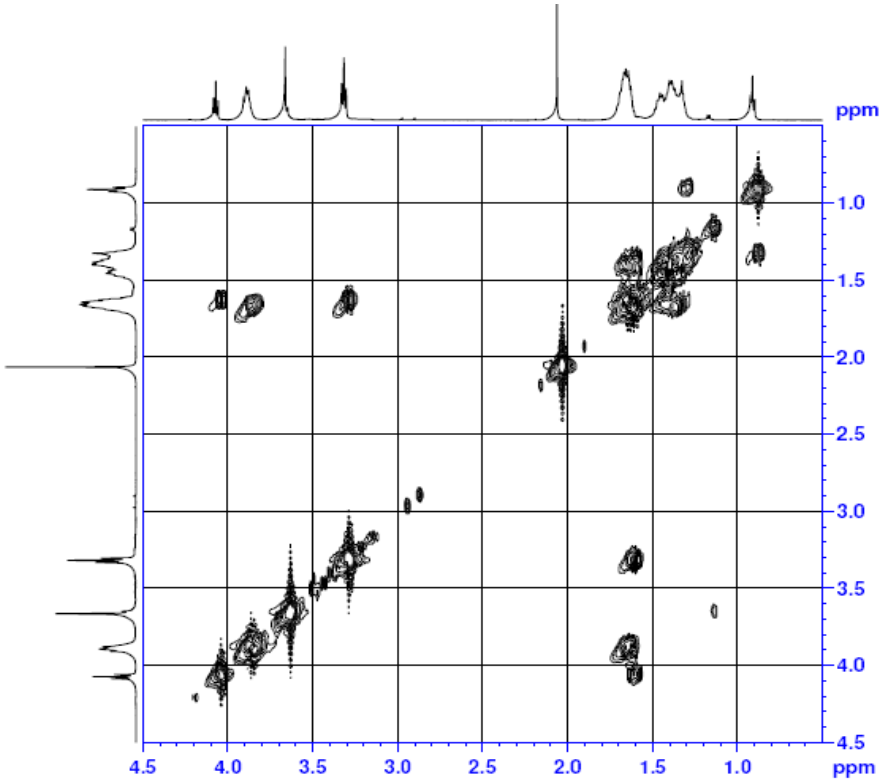

Figure 109: COSY of MIL-DTL-64159 component B

3.6.3.2 FTIR Film Formulations Results

Figure 110 shows the FTIR spectra of pigmented MIL-P-53022. The peaks at around 2920, 2872, 1450 and 1375 cm^{-1} are attributed toCH_3. The peak at 1737 cm^{-1} is attributed to C=O. The peaks at around 3050, 1650-1450 and 910-650 cm^{-1} belong to aromatic rings. Figure 111 shows the FTIR spectra of Clear MIL-P-53022 from centrifuged component A. -CH_3, C=O, and aromatic ring signals were found in this sample.

Figure 112 shows the FTIR spectra of pigmented MIL-DTL-64159. Three functional groups were found: -CH_3 (2920±20; 2872±10; 1450±20; 1375±10 cm^{-1}), -N=C=O (2283 cm^{-1}) and C=O (1737 cm^{-1}). Figure 113 shows the FTIR spectra of Clear MIL-DTL-64159 from Bayhydrol XP-7110E. Three functional groups were found: CH_3 (around 2872, 1450, 1375 cm^{-1}), -N=C=O (2282 cm^{-1}) and C=O (1737 cm^{-1}). Figure 114 shows the FTIR spectra of Clear MIL-DTL-64159 from centrifuged component A. Similarly, -CH_3, -N=C=O, and C=O signals were found in this sample.

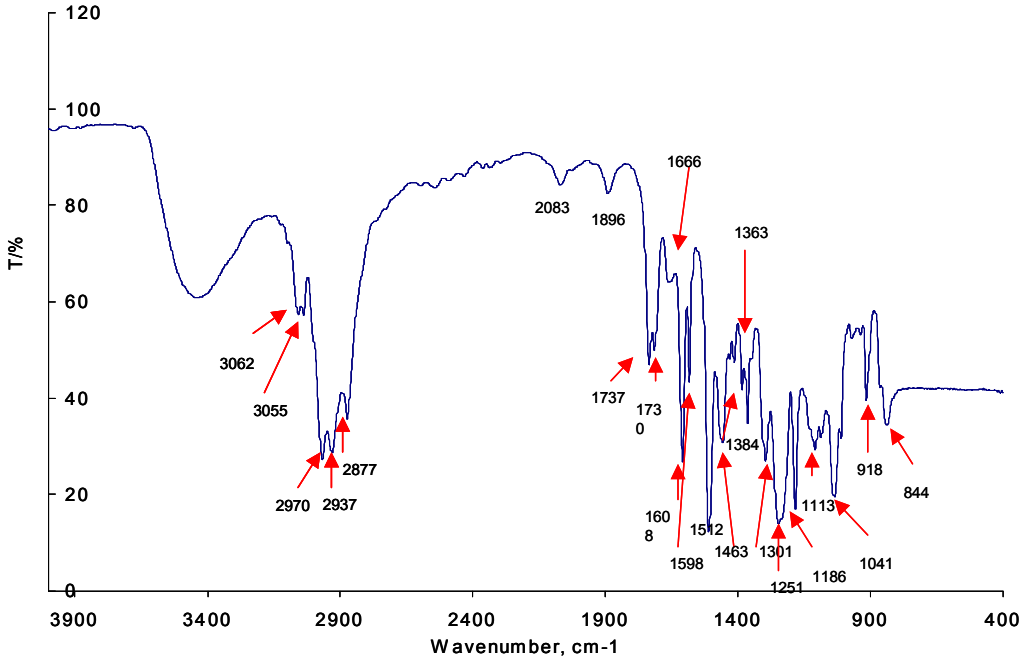

Figure 110: Pigmented MIL-P-53022.

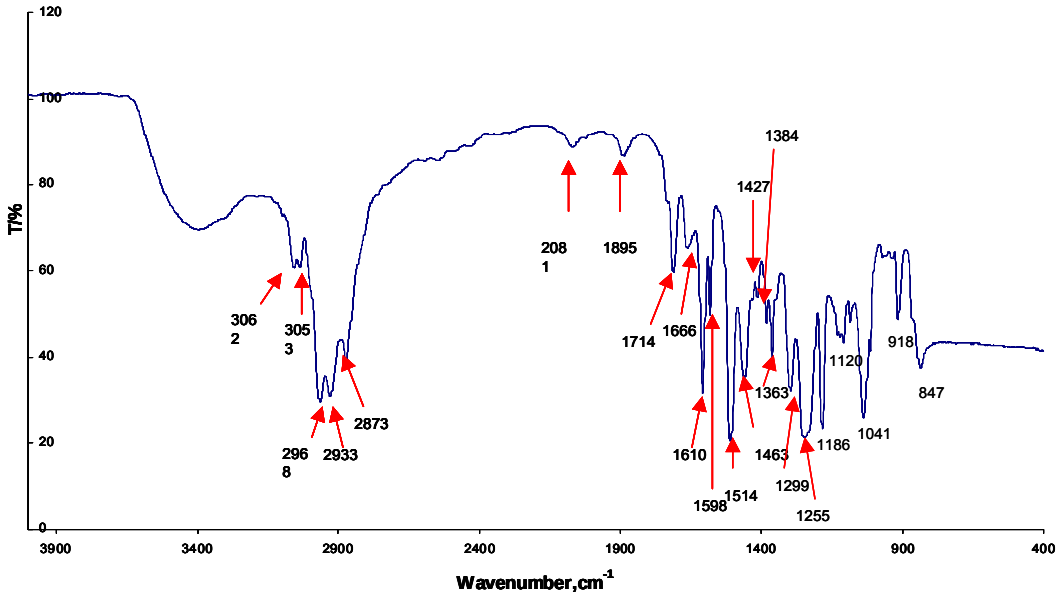

Figure 111: Clear MIL-P-53022 from centrifuged component A.

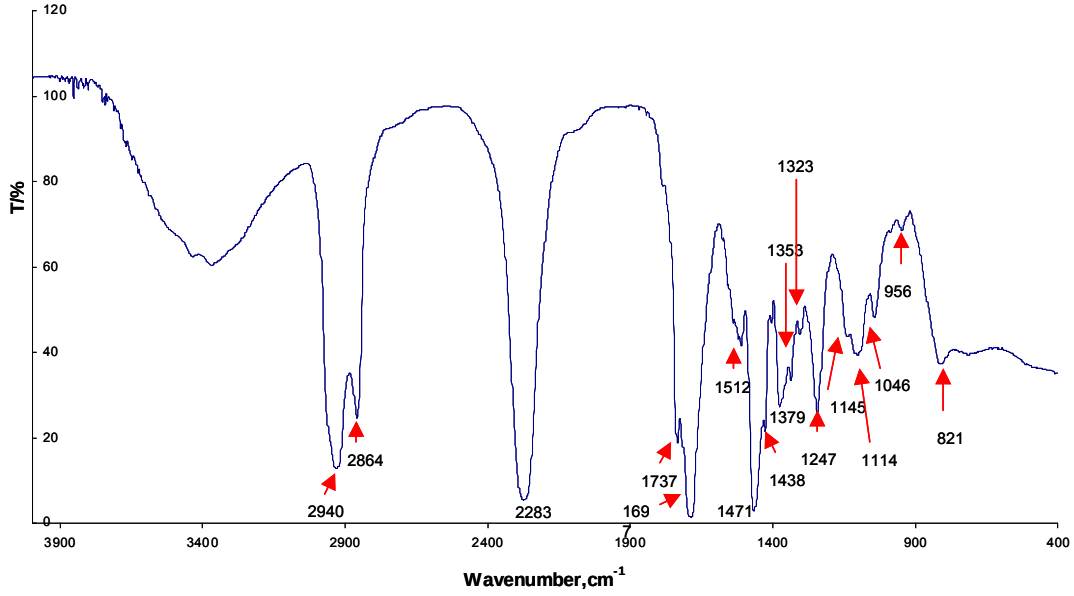

Figure 112: Pigmented MIL-DTL-64159.

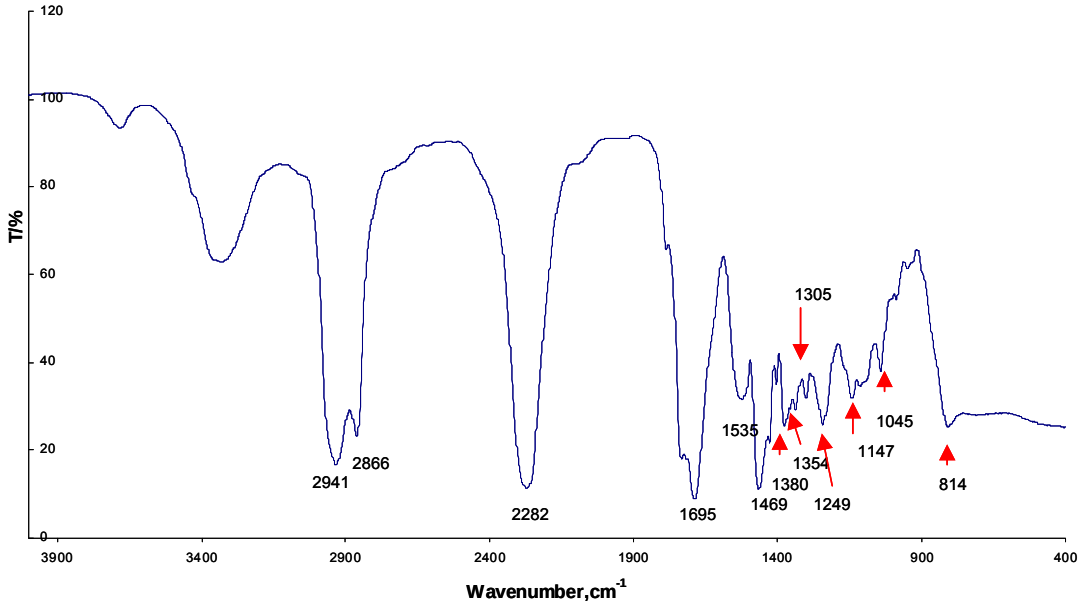

Figure 113: Clear MIL-DTL-64159 from Bayhydrol XP-7110E.

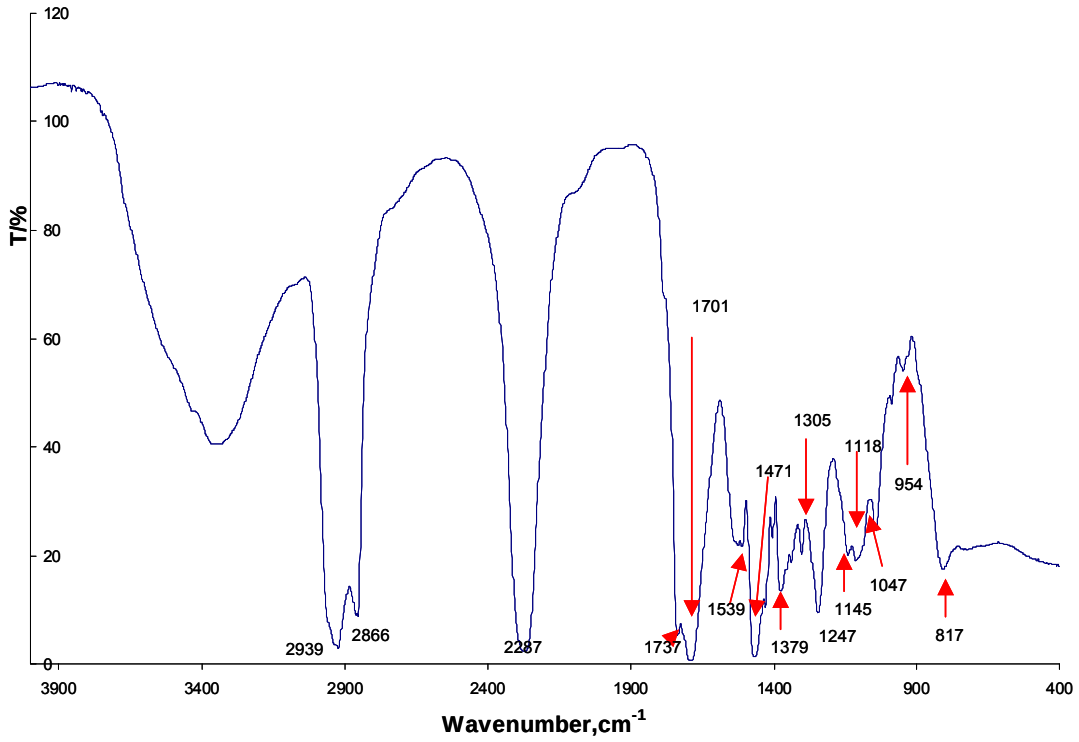

Figure 114: Clear MIL-DTL-64159 from centrifuged component A

Conclusions from FTIR

For MIL-P-53022 formulations, very similar spectra were obtained for the pigmented and the centrifuged formulations. The only difference noticed was in the C=O signal which appeared as a singlet sharp peak at ~1714 cm^{-1} for the centrifuged formulation and a sharp doublet at ~1737 and 1730 cm^{-1} for the pigmented one. This could be due to the residue that was removed from the formulation.

For MIL-DTL-64159 formulations, again, similar IR spectra were obtained for the three formulations (pigmented, centrifuged and Bayhydrol). Since we are interested in the branching of the polyurethane obtained in this formulation, we looked at the C=O peak for possible branching originating from a urea (or allophanate) linkage which is at ~1695-1700 cm^{-1}. We opted to get the peak ratio of said C=O peak to that of the end CH_3 bending band at ~1380 cm^{-1}. In so doing, we *normalize* the comparisons in terms of film thickness. The following transmittance ratios were obtained:

Pigmented = 0.09

Centrifuged = 0.08

Bayhydrol = 0.37 (lower intensity)

Form these ratios we conclude that the use of Bayhydrol could possibly lower the degree of branching because of the lower intensity of urea peak.

3.6.3.3 FTIR of Polyurethane Systems

Polyurethane Cure Kinetics Study

The effects of adding hyperbranched polymers on the cure rate of a polyurethane system were studied using mid-FTIR to resolve the amount of isocyanate in curing systems as a function of time. The binder in 64159 was used as a model polyurethane system. The binder consists of a polyol component, Bayer's water dispersed Bayhydrol XP 7110E, and an isocyanate component, Bayer's Bayhydur 303. The HBPs in Table 48 were dissolved directly in the polyurethane. All HBPs were added at 2 wt % of the dry polyurethane and the polyol/isocyanate was mixed at a ratio of 10:9 by weight, and all experiments were run in KBr salt plate sandwiches at 30 ^{o}C.

Table 48: Description of the HBPs used in the polyurethane cure kinetics study.

Name	PEI or PE	Nominal Alkyl Addition	Nominal Perfluoro Addition	Active Biocidal Functionality	Description
Lupasol G20 WF	PE	0	0	none	Baseline PEI, commercially available.
Boltorn	PEI	0	0	none	Baseline PE, commercially available.
NR4-58	PEI	20	20	none	Modified Lupasol

In order to measure the amount of isocyanate as a function of time, the area of the isocyanate peak centered at 2275 cm^{-1} was measured relative to the area of a reference peak at 1700 cm^{-1} (ester peak), and the conversion was calculated from Equation 2.

Figure 115 shows the isocyanate conversion as a function of time for a baseline system (no additives) and the HBPs mentioned above. It is apparent that, in the baseline polyurethane system, the isocyanate completely reacted into the matrix within 250 minutes, and the addition of 2% hydroxyl functional Boltorn did not appreciably affect the kinetic characteristics of the system. However, the addition of PEI HBPs effected the final conversion of isocyanate; leaving roughly 20% unreacted, although the initial rate of conversion was unperturbed. It is not clear why this is the case; just as –OH on the Boltorn reacts with isocyanate, the reactive amines from the PEI should also react with isocyanate, leaving little or no isocyanate unreacted. It is possible that the PEIs gelled the systems quickly, thus decreasing the molecular mobility, leaving some reactive isocyanate stranded from a hydroxyl or amine with which to react. In coatings applications, the addition of PEI HBPs might not cause isocyanate to remain unreacted because atmospheric moisture can react with isocyanate.

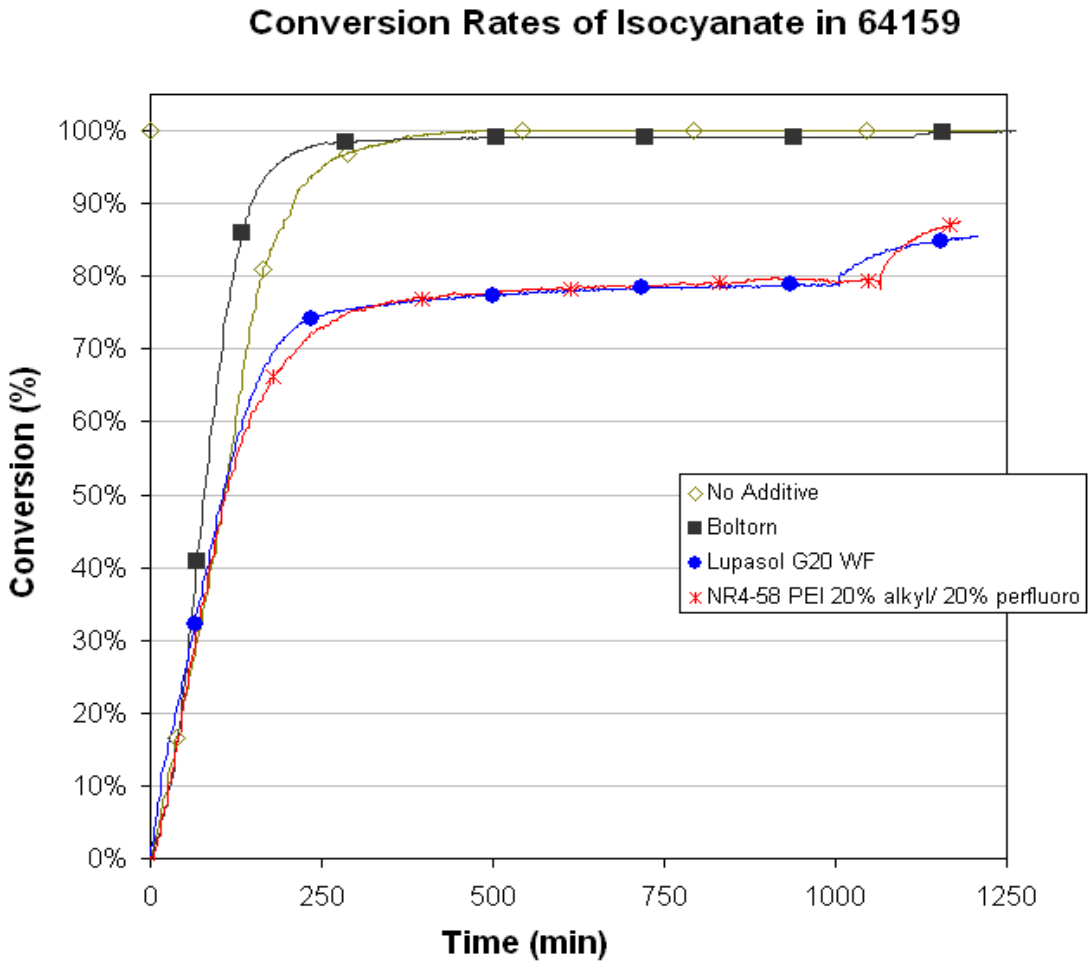

Figure 115: Conversion of isocyanate versus time in a polyurethane system with and without hyperbranched polymer additives

3.6.3.4 A Survey of Military Coatings Resins

The initial study of coatings binder properties began with epoxy primer MIL-DTL-53022, 1K moisture-cure polyurethane topcoat MIL-DTL-53039 and the benchmark technology 2K waterborne polyurethane topcoat MIL-DTL-64159. Centrifugation of commercial product yielded relatively pure resin making from MIL-P-53022 and MIL-DTL-53039 for film characterization. Availability of polyol and isocyanate components from Bayer made it possible to formulate a simple 2K waterborne polyurethane to model MIL-DTL-64159 properties. Much of the experimental work with this formulation was focused on developing and optimizing the gamut of variables explored including amount of water added, order of addition, mixing time, method of film application, substrates, surface preparation and bulk viscosity to name a few. T_g and M_c results calculated from DMA data were used to quickly compare the variations in the film making method.

Of primary interest was the effect of added water during the reaction of the water dispersible polyol and polyisocyanate of MIL-DTL-64159. The data were analyzed to determine if T_g or M_c were dependent on the amount of water added to the primary reactants. This analysis revealed that the amount of water had much less of an effect than the mixing dynamics during reaction, specifically viscosity of the bulk mixture. As discussed in the MIL-DTL-64159 film preparation section, good dispersion of the reactants required sufficient viscosity during mixing to reduce particle size and produce even films. Films made from poor dispersions had a mottled appearance and sometimes contained entrapped air or foam bubbles.

The next phase of the study branched out to include other military coatings. Of particular interest are Army epoxy primer MIL-P-53030, Navy epoxy primers MIL-PRF-23377J and MIL-PRF-85582, and Air Force fluorinated urethane topcoat MIL-PRF-85285. Commercial products were obtained from approved suppliers and resin was isolated from the pigmented portion of the 2 part formulations by centrifugation. Clear films were made on glass with a drawdown bar as before. DSC and TGA were performed to characterize these resins. It was discovered that these binders were considerably more brittle than the binders in MIL-P-53022 and MIL-DTL-53039 in that attempts to remove the films from glass resulted in chipping, flaking and splintering of the coating. Consequently, it was not possible to perform DMA on these samples. New films will be prepared over a release coat or will be peeled before the films become completely brittle.

Dynamic Mechanical Analysis of Clear Resin Films

DMA was used to compare the thermo-mechanical properties of the resin binders in the most common coatings used in the Army (Figure 116 through Figure 118). The storage modulus decreased slowly at low temperatures, decreased rapidly through the glass transition region, and leveled off in the rubbery plateau. The glass transition temperature (T_g) is the temperature at which the maximum in the loss modulus occurs.

The results show that the epoxy primer is more rigid at low temperatures (Figure 116), but less rigid at high temperatures (Figure 117). Loss modulus curves (Figure 118) reveal that the epoxy primer has a lower glass transition temperature and a more narrow glass transition relative to the topcoats. The glass transition temperatures determined by DMA at 2°C/minute for these resin binders (Figure 119) are:

- Clear coat MIL-P-53022 59 - 60°C
- Clear coat MIL-DTL-53039 68 - 70°C
- Clear coat MIL-DTL-64159 71 - 78°C

It is likely that the lower T_g of the epoxy primer was due to less cross-linking (Figure 120), likely due to lower inherent functionality of the paint monomers. T_g of the MIL-DTL-64159-based clear coat is slightly higher than that of the MIL-DTL-53039-based coatings. Furthermore, using a high isocyanate to hydroxyl indexing resulted in a higher T_g (Figure 119) due to an increased cross-link density (Figure 120). This was expected because additional water was added to decrease that indexing, and water results in polymeric chain ends rather than continuous polymeric chains.

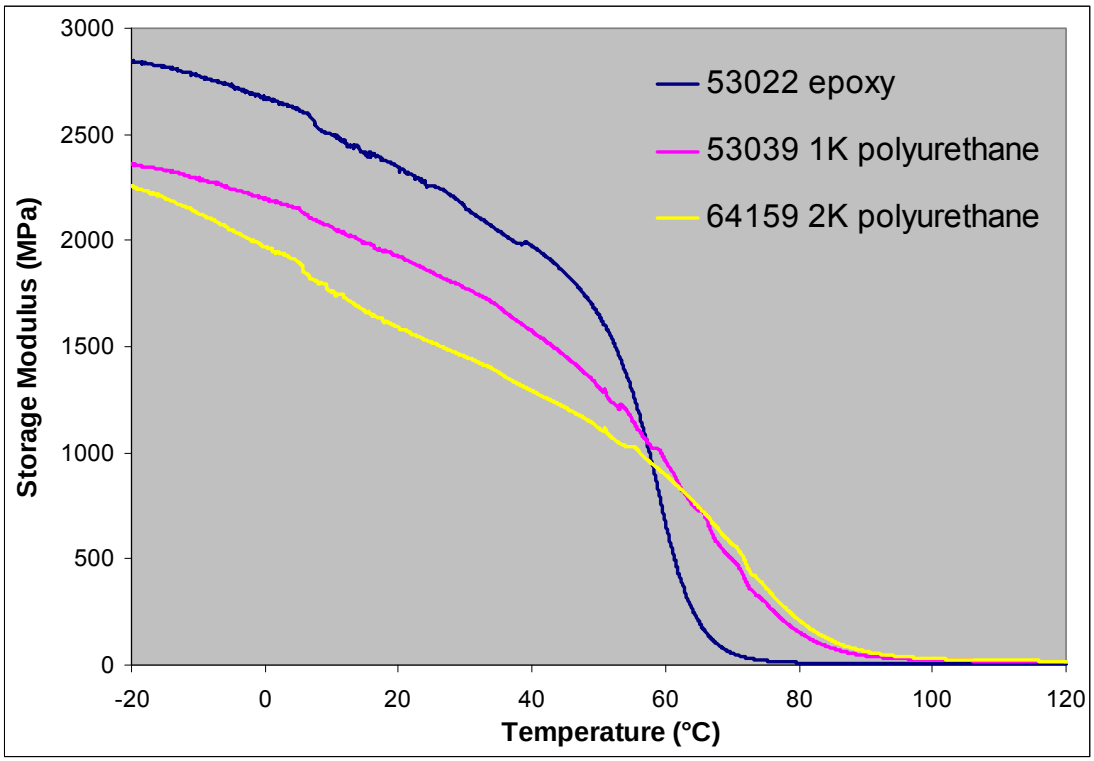

Figure 116: Comparison of storage modulus for various clear film chemistries

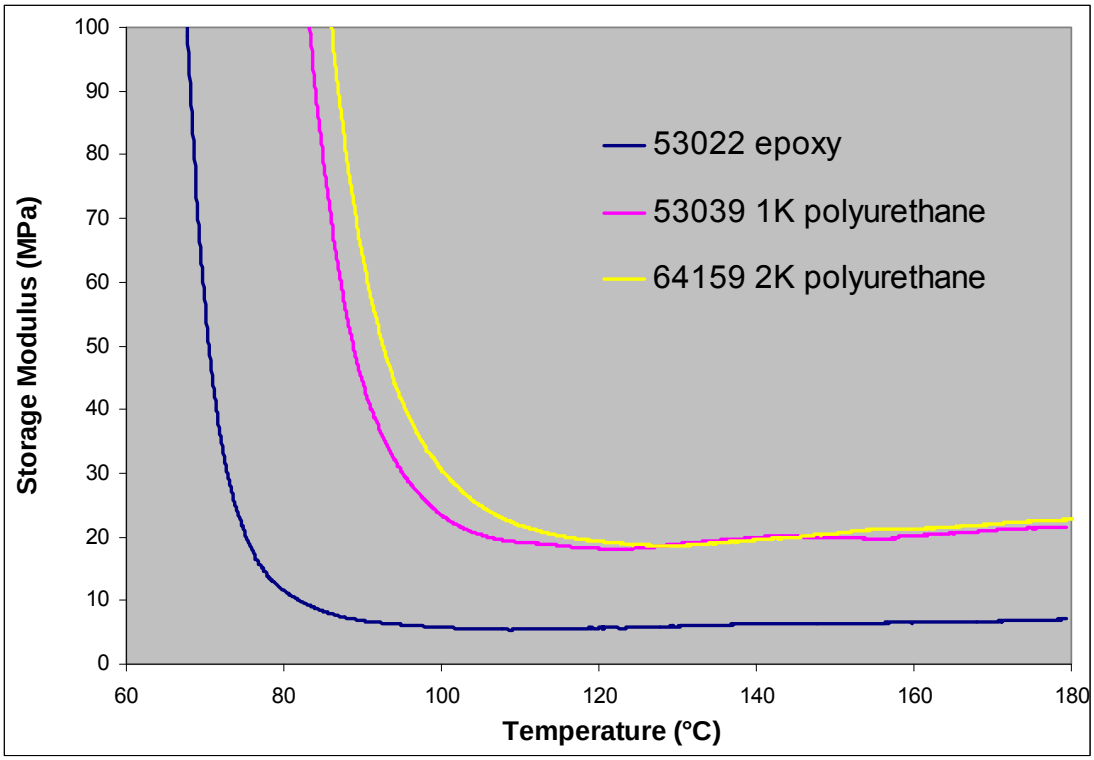

Figure 117: Comparison of storage modulus in the rubbery region for various clear film chemistries

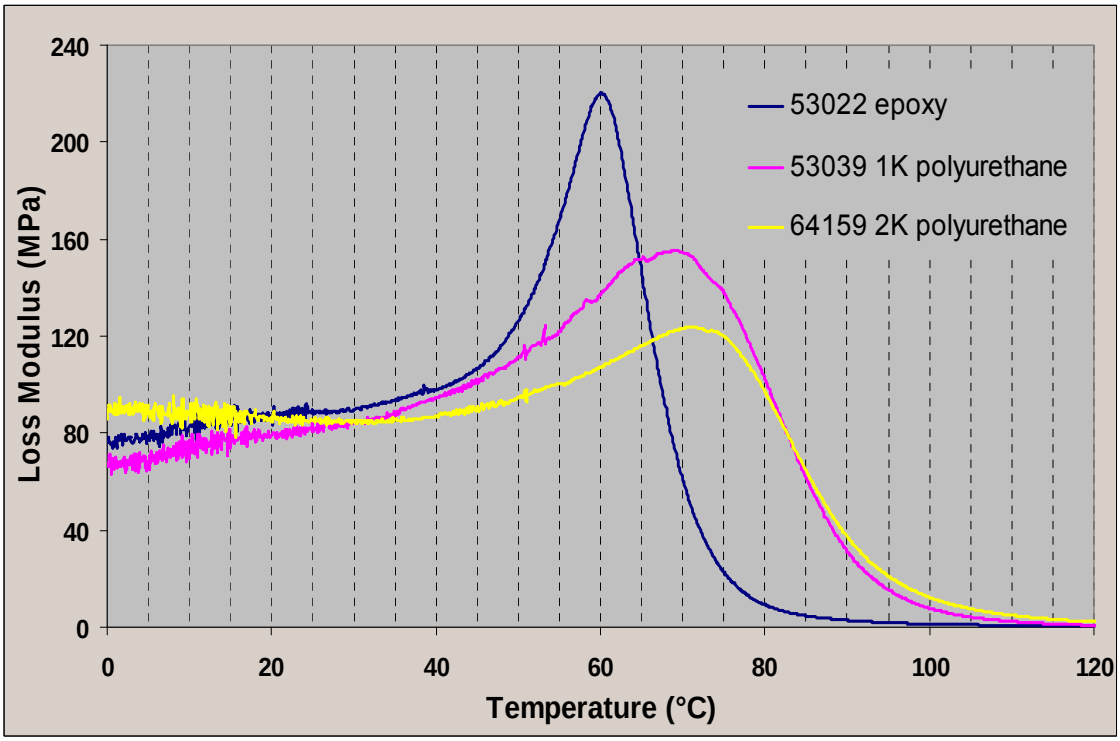

Figure 118: Comparison of loss modulus for various clear film chemistries

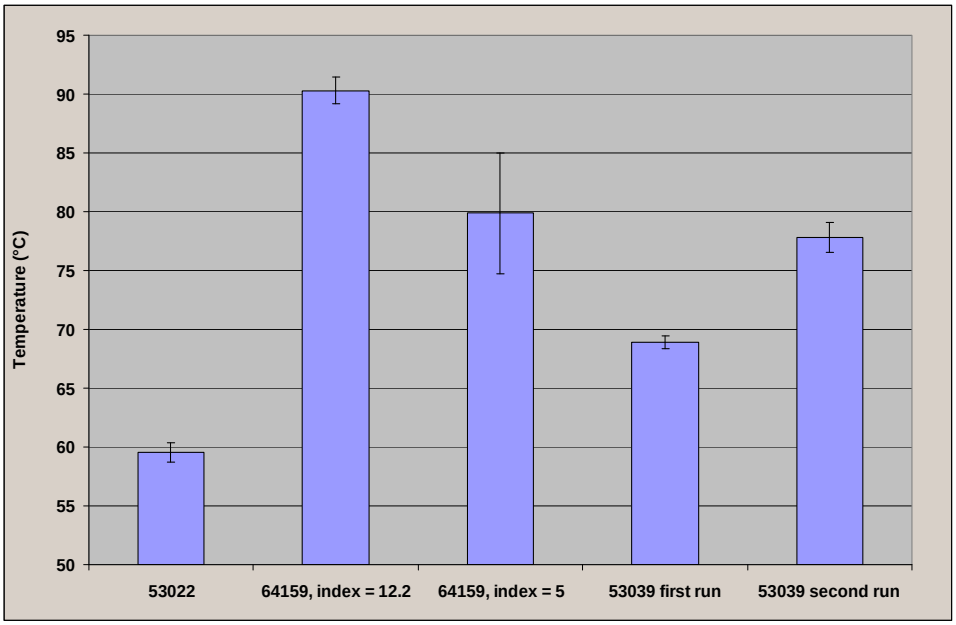

Figure 119: DMA glass transition temperature for coating resins

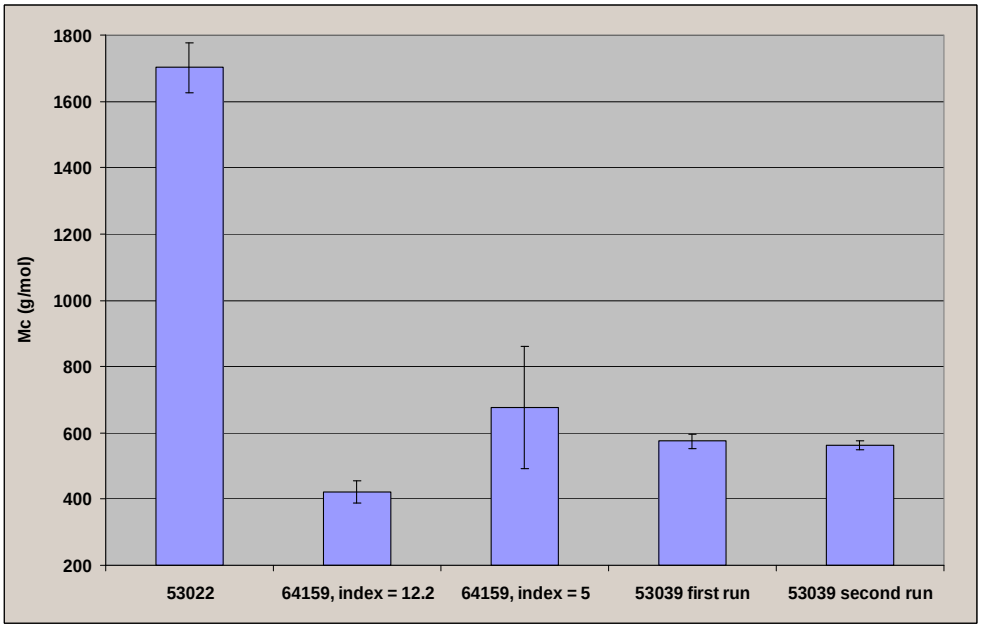

Figure 120: DMA molecular weight between cross-links (g/mol).

Some of the MIL-DTL-53039 clear films were run twice to determine if a higher degree of cross-linking would result from the post-cure heating above the glass transition temperature during the first run. Glass transition temperature increased by 10°C when a sample film was tested a second time (Figure 121). However, cross-link density was unaffected by heating (Figure 120). Therefore, this aging effect can be attributed to solvent evaporation and not additional polymerization, which would result in a change in M_c. Similarly, cross-linking in one-component urethane MIL-DTL-53039 continues after solvent evaporation at room temperature.

A film tested at 24 hours was remarkably under-developed *vs.* a sample from the same film one month later (Figure 122).

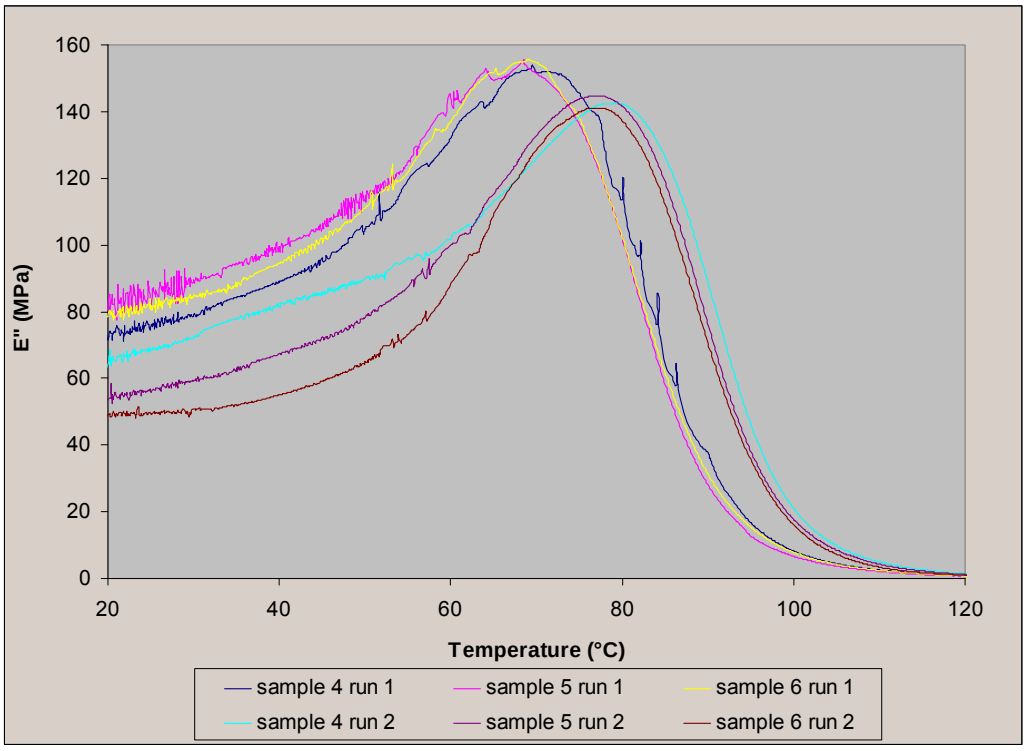

Figure 121: Shift in MIL-DTL-53039 loss modulus after post-cure heating

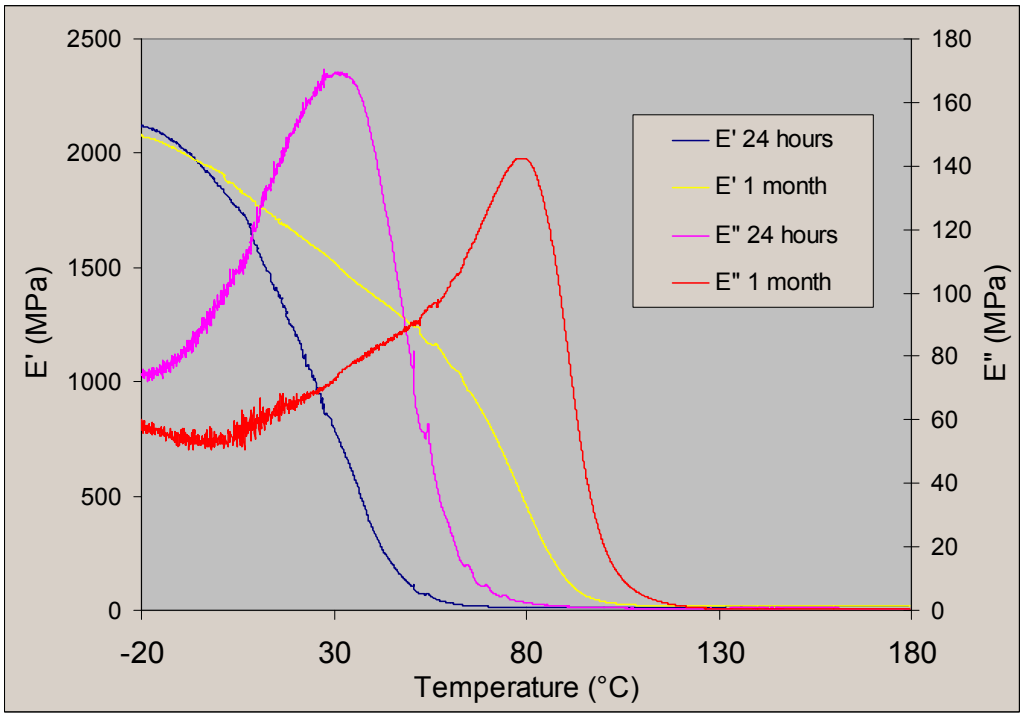

Figure 122: Effect of aging on mechanical properties of moisture-cure urethane film

DMA results alone are not necessarily predictive of coating performance at this point but when paired with other instrumental data and correlated to empirical results to be gathered later in this research we hope to develop a more comprehensive understanding of these coating chemistries and move toward developing reliable screening methods for evaluating new resin chemistries. Some points to glean from the DMA results:

1. Running samples of MIL-DTL-53039 twice resulted in a higher T_g but roughly equivalent M_c, indicating temporal differences were a result of solvent evaporation.
2. Cross-link density of MIL-P-53022 is considerably lower than that of the topcoats, whereas the topcoats have similar cross-link densities
3. Increasing the NCO:OH index from 5 to 12 in two-component MIL-DTL-64159 resulted in a higher glass transition temperature and higher cross-link density, indicated by a lower M_c value.
4. For water reducible two component urethane films, M_c is a better predictor of empirical film quality than T_g. Lower M_c values tended to correlate to the better quality films.
5. Topcoat samples require a considerable amount of time at RT to reach their ultimate properties.

DSC Analysis of Clear Resin Films

All films studied exhibited an endotherm during the first heat ramp which disappeared during the second heat ramp suggesting evaporation of solvent and possibly a continuation of curing or cross-linking occurred. Epoxy MIL-P-53022 had a rather distinct endotherm at 57°C occurring well below the onset of the glass transition. However, since this endotherm did not appear in subsequent cycles for that sample it is assumed to be evaporation of solvent and not a molecular transition (Figure 123). The polyurethane films MIL-DTL-53039 and MIL-DTL-64159 had broader, less distinct endotherms but they were similar to each other (Figure 124).

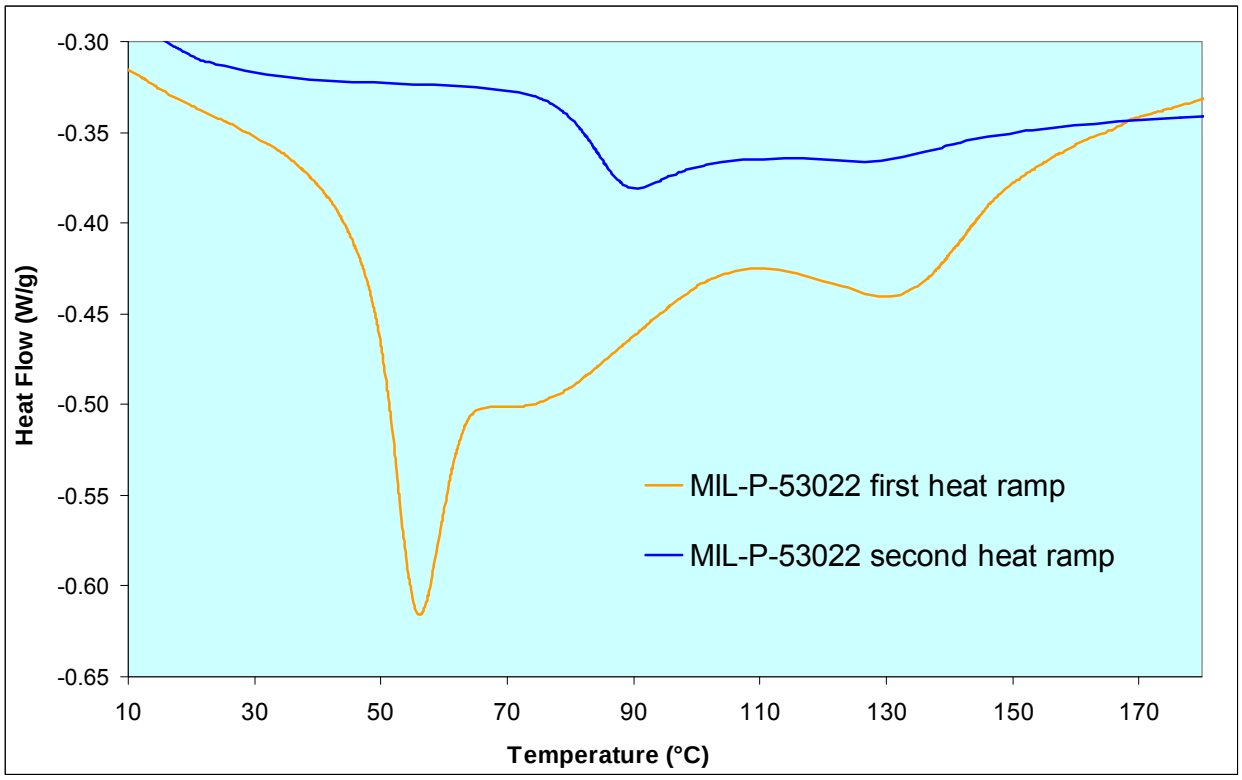

Figure 123: DSC curve for clear epoxy resin film MIL-P-53022

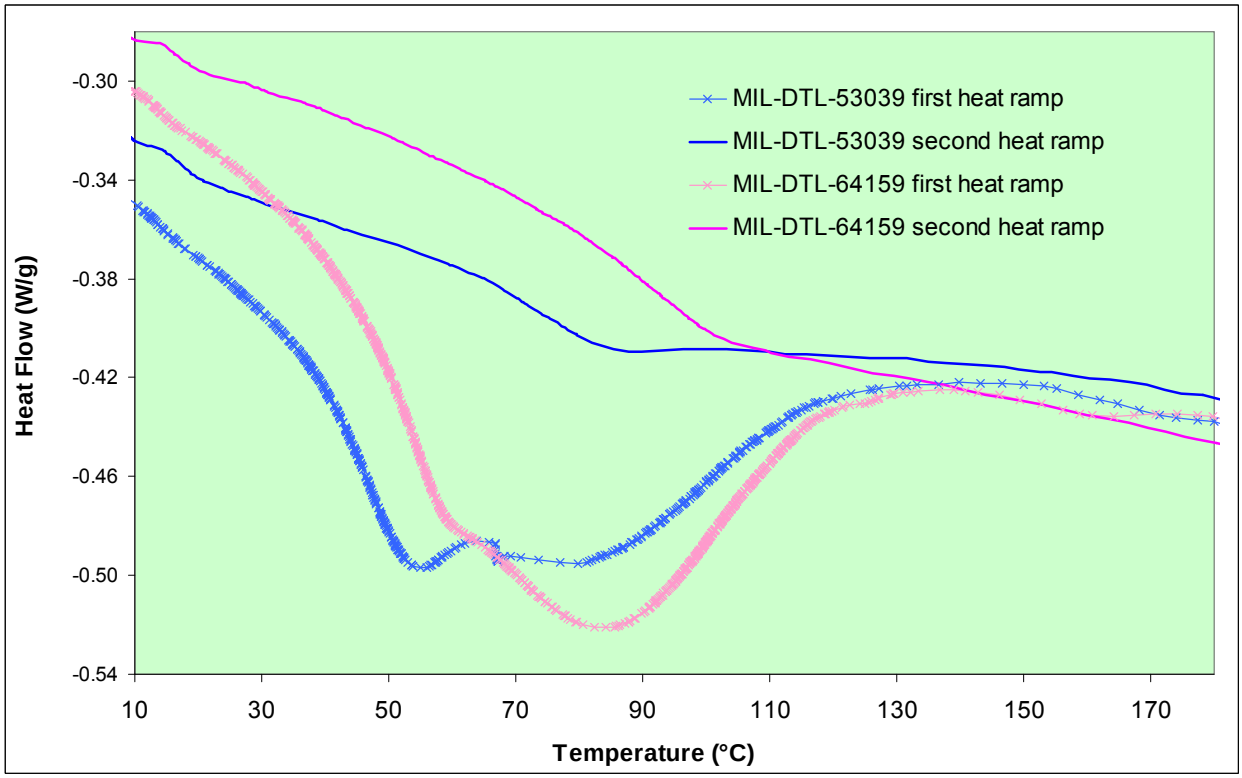

Figure 124: DSC curves for polyurethane systems

From the curves without the endotherms, the T_gs of the coatings are:

- Clear coat MIL-P-53022 ~82°C
- Clear coat MIL-DTL-53039 ~72°C
- Clear coat MIL-DTL-64159 ~90°C

Again, the MIL-DTL-64159 coating had the highest T_g. However, the T_gs measured with DSC were higher than that measured for DMA. This occurred because of the higher heating rates used for DSC. The higher T_g for MIL-P-53022 clear coat vs. MIL-DTL-53039 in DSC was opposite the trend for DMA results due to the sharper glass transition for 53022 coatings.

After preparing clear primers from the second stage of the study it was possible to compare various epoxy chemistries used by the Military. Figure 125 shows the heat flow curves obtained by DSC. All samples except for MIL-P-53022 were cycled from -50°C to 200°C at 10°C/minute. MIL-P-53022 was tested months earlier from -10°C to 200°C at 10°C/minute which may be part of the reason for the difference in the overall shape of the DSC curve. Future experiments will include retesting MIL-P-53022 at the lower temperature range. The key in Figure 125 has been arranged to list the products in order of lowest to highest glass transition temperature.

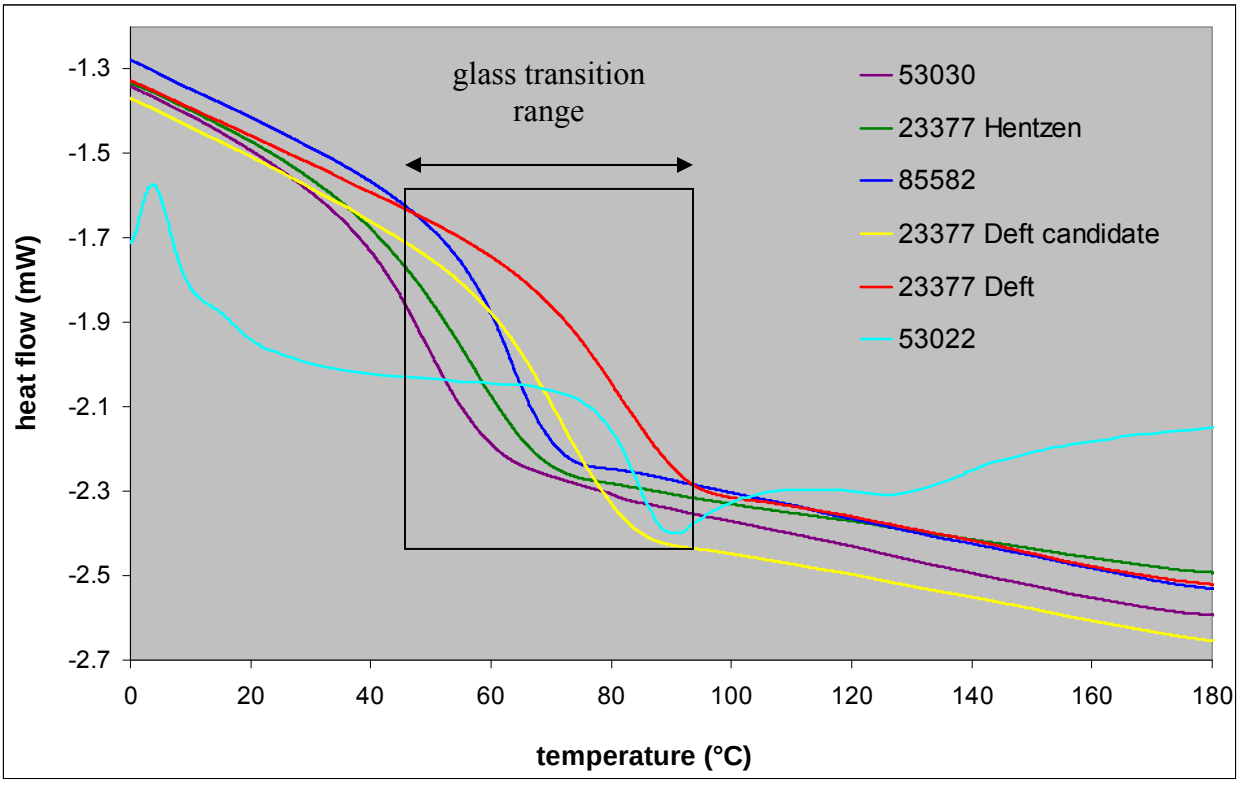

Figure 125: DSC curves for various clear military epoxy primer chemistries

It is clear to see that all epoxy primers are not the same. The range of glass transition from onset to endpoint spans more than 50°C. Additionally it should be noted that different products meeting the same performance specification can vary in chemistry and binder properties.

A similar comparison was made for the three polyurethane chemistries studied to date. The Air Force utilizes a fluorinated polyurethane and the Army employs both a 1K moisture-cure polyurethane and a 2K waterborne polyurethane. For this comparison, clear MIL-DTL-64159 was made by centrifuging commercial product as was done for the other products. Figure 126 compares the heat flow curves of these various chemistries. The unusual endotherm on the MIL-DTL-64159 curve seen near 118°C has been identified as a polyethylene wax melt transition.

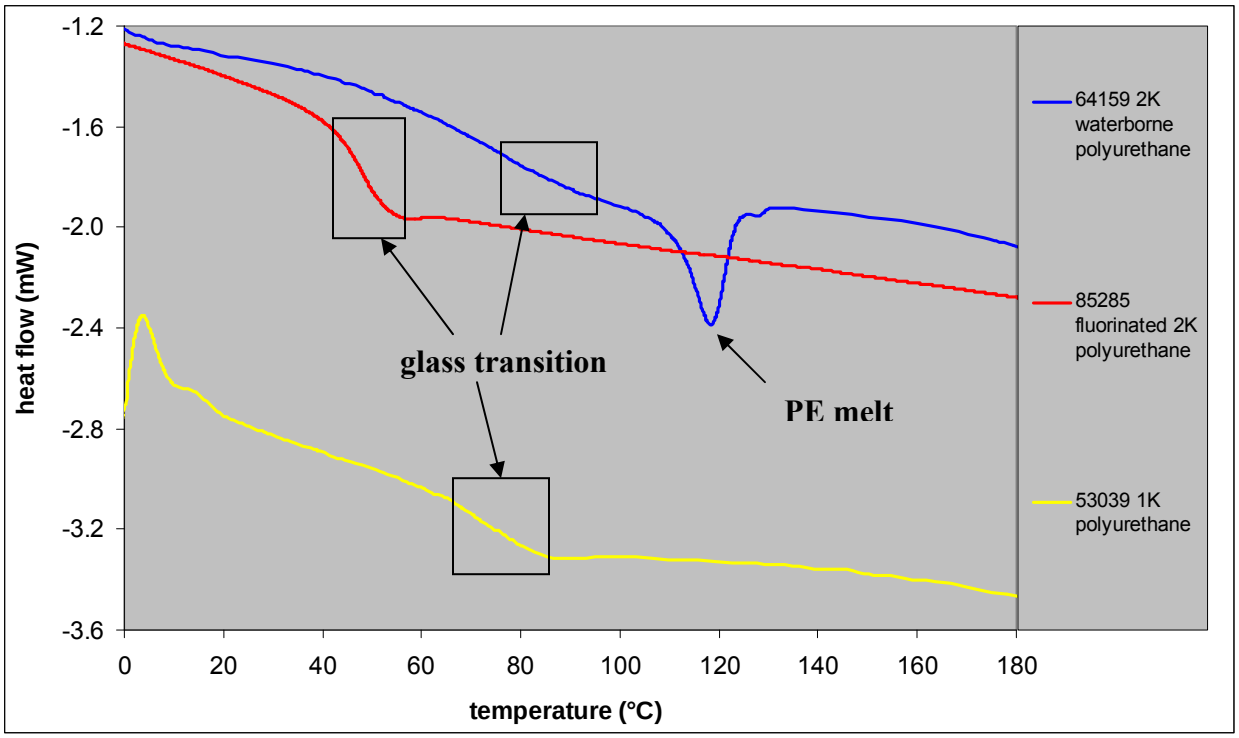

Figure 126: DCS of three types of clear military polyurethane coatings

From Figure 126 we can see that the fluorinated APC coating used by the Air Force has a significantly lower glass transition temperature than either Army polyurethane. This result is explored in more detail in 3.6.3.5 The Effect of Lumiflon FE-4400 in Clear MIL-DTL-64159.

TGA Analysis of Clear Resin Films

Figure 127 shows the TGA weight loss curves for the Army clear coats initially studied. Figure 128 shows the derivative sample weight curves for the same experiments. These results show that the thermal degradation of clear epoxy occurs more gradually than polyurethanes which exhibit sharper weight loss derivatives. Also, two-component polyurethane MIL-DTL-64159 is thermally more stable than the one-component polyurethane MIL-DTL-53039.

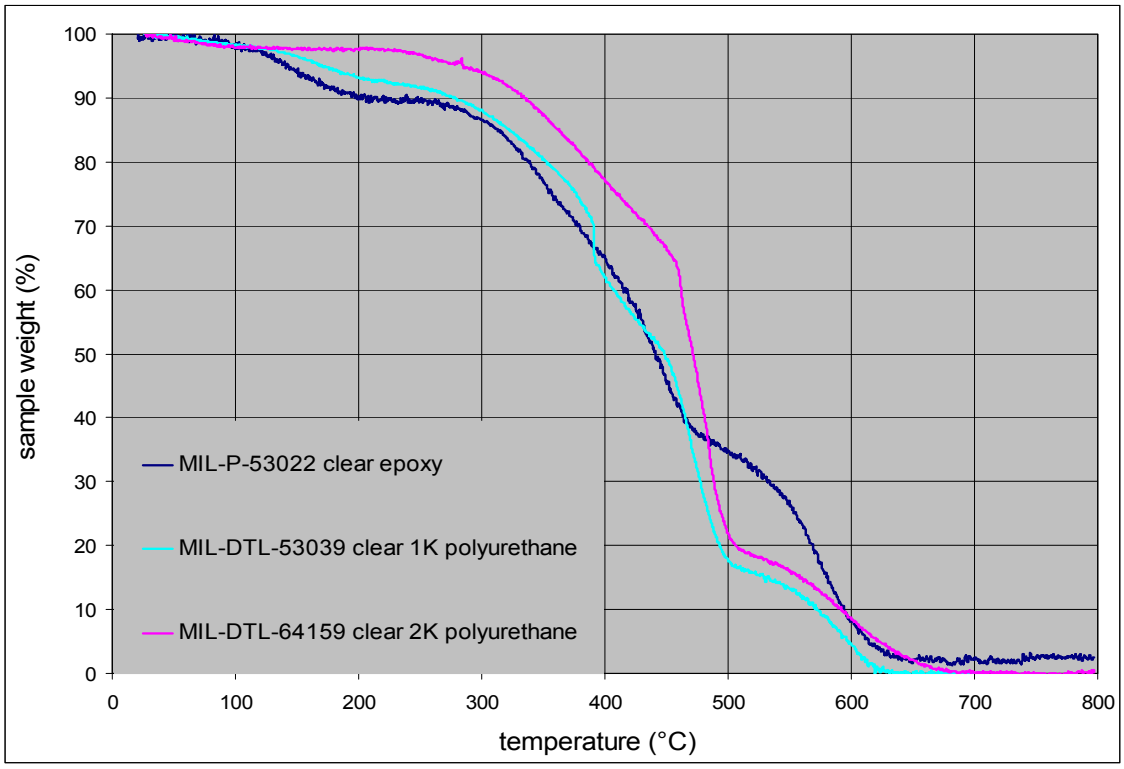

Figure 127: TGA weight loss of clear resin films

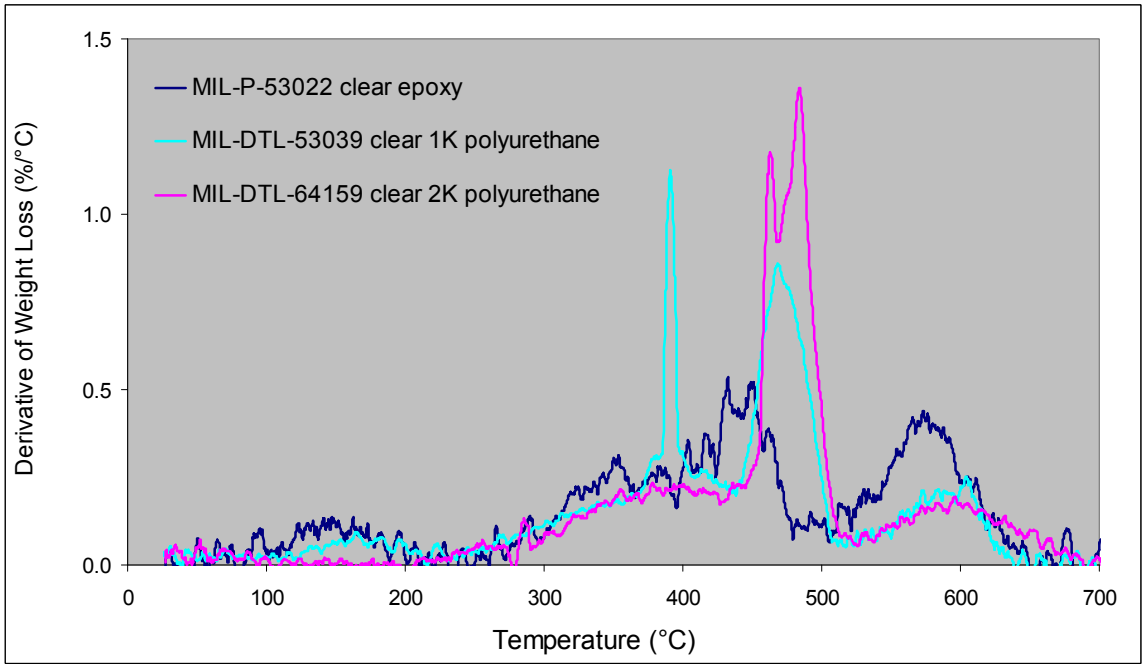

Figure 128: TGA derivative of sample weight for clear resin films

When comparing the range of clear epoxy resins, they generally appear similar. MIL-P-53022 stands apart as having a slightly different thermal degradation profile (Figure 129 and Figure 130).

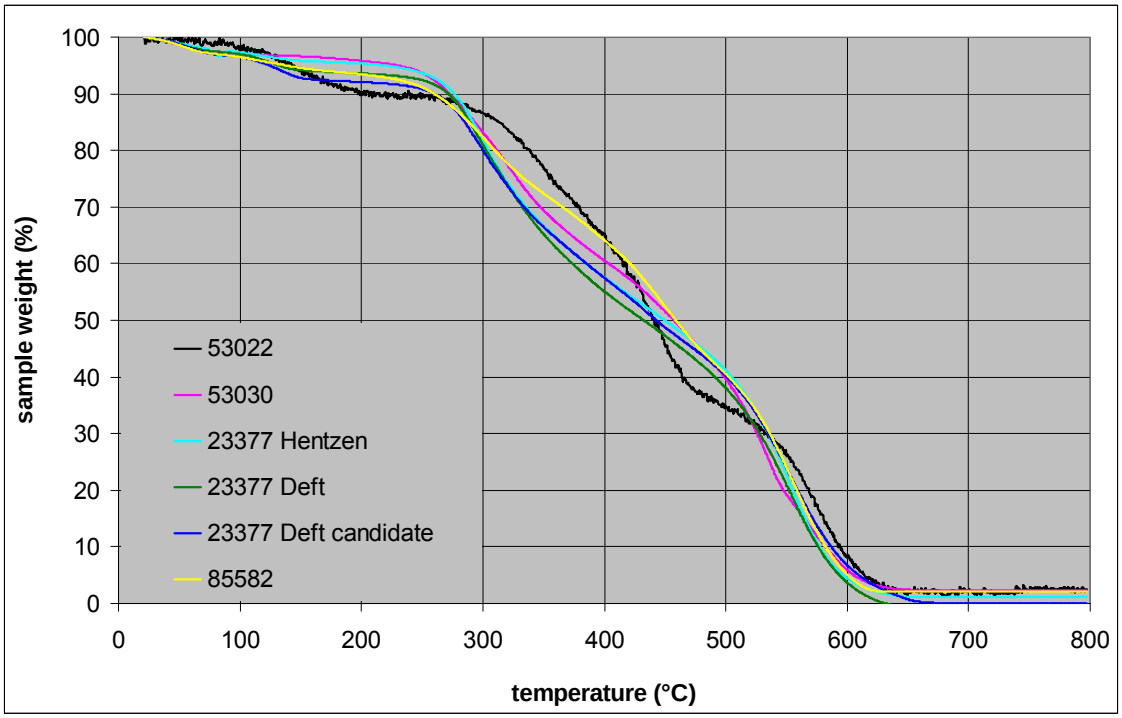

Figure 129: TGA weight loss of clear epoxy primer resins

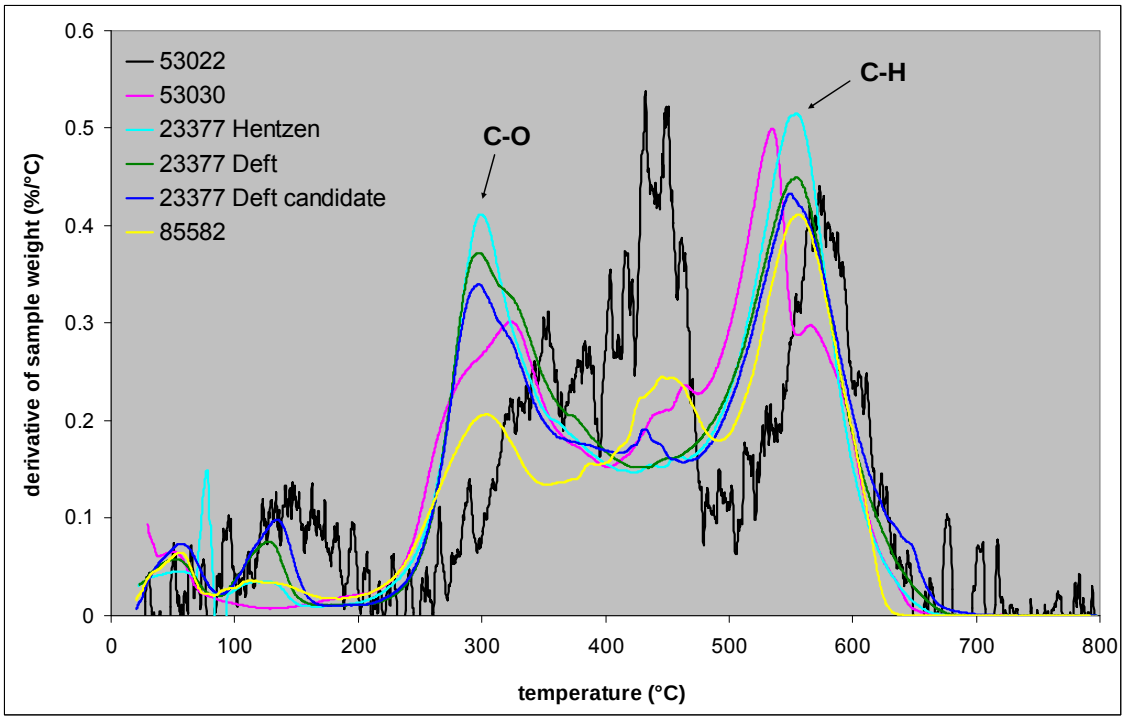

Figure 130: TGA derivative weight curves for clear epoxy primer resins

More samples of MIL-P-53022 will be analyzed due to the large amount of noise in the data relative to the other samples to confirm these differences.

TGA was also used to compare three types of polyurethane resin. Clear resin films from the Air Force fluorinated topcoat MIL-PRF-85285, the Army 1K moisture-cure MIL-DTL-53039 topcoat and the Army 2K waterborne MIL-DTL-64159 topcoat are depicted in Figure 131 and Figure 132.

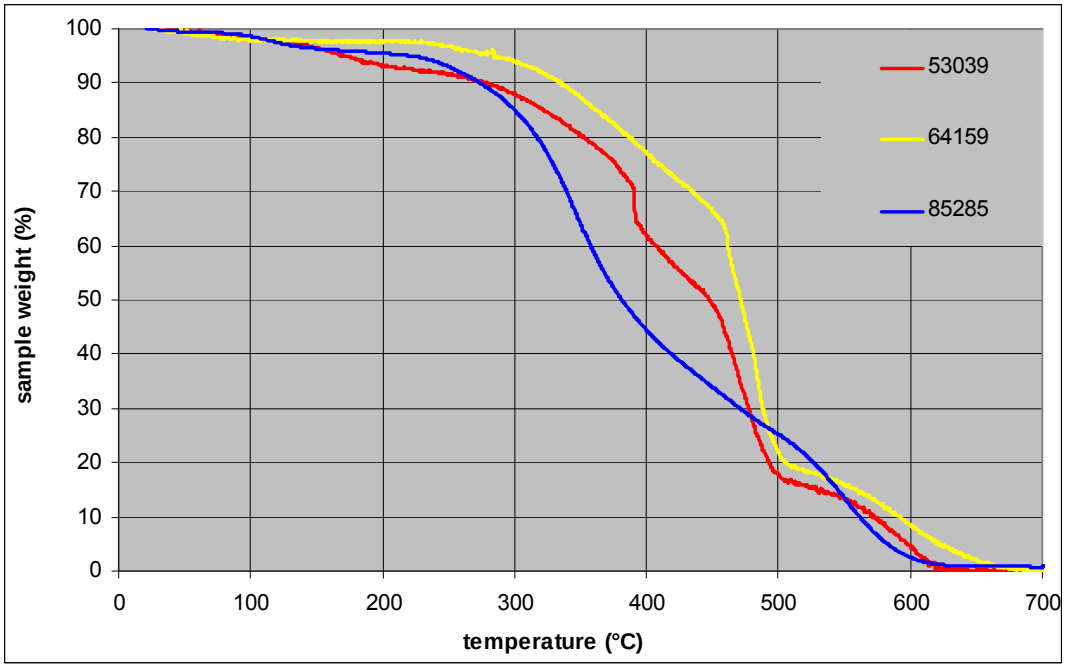

Figure 131: TGA weight loss curves for clear polyurethane topcoat resins

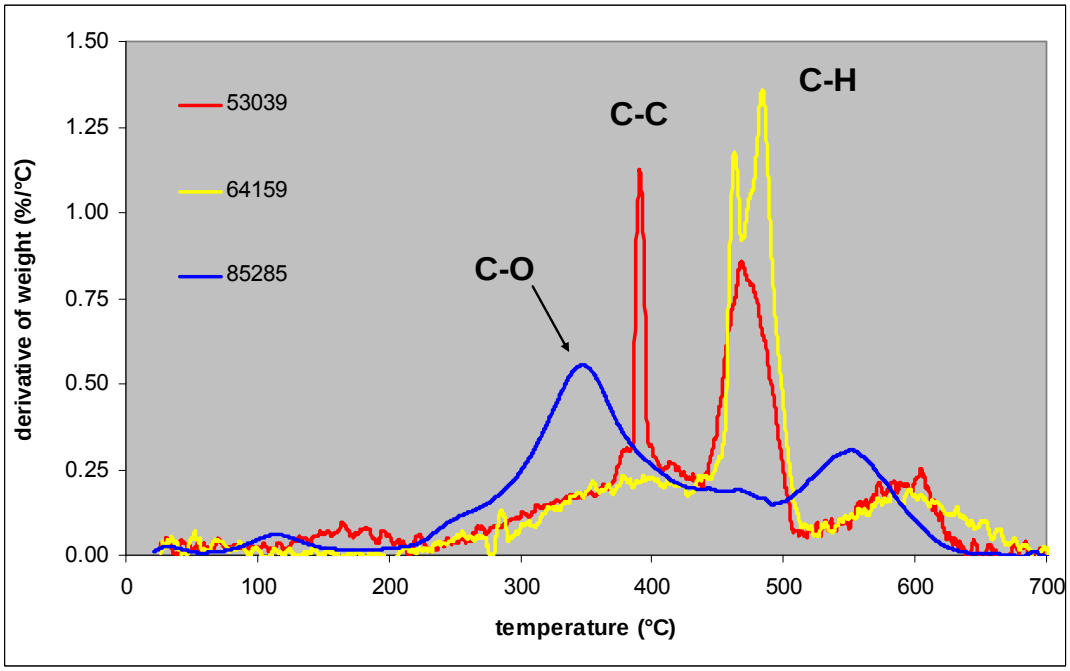

Figure 132: TGA derivative weight curves for clear polyurethane topcoat resins

These data would suggest that the fluorinated resin also contains a greater proportion of C-O bonds than the other materials and degrades more rapidly with heat relative to the other urethane resins. Of the three chemistries studied, the MIL-DTL-64159 appears to have the greatest thermal stability. MIL-DTL-53039 has a unique peak around 400°C which correlates to the temperature at which C-C bonds break, however, it is should be noted that all three polyurethane resins experienced rapid weight loss above 400°C. Although it is expected that the fluorinated APC topcoat would be flame retardant, as halogen radicals scavenge oxygen and hydrogen radicals in the flame.

3.6.3.5 The Effect of Lumiflon FE-4400 in Clear MIL-DTL-64159

Elemental Surface Analysis

The cured polyurethane films were examined by XPS at 90° at the air-polymer interface (front) and the glass-polymer interface (back), and the atomic percent of fluorine was measured for each formulation on each side of the cured films in order to determine if the fluoropolymer had indeed effectively segregated to the air interface. Based on our knowledge of Lumiflon FE-4400, the atomic percent fluorine of polymer solids should be approximately 17% [42]. The nominal percent Lumiflon added to the formulation is the weight percent of the polyol fraction. Because there is a large stoichiometric excess of isocyanate to hydroxyl groups, the atomic percent fluorine in samples with 10 wt. % Lumiflon, for example, is only approximately 0.35 %. The surface enrichment factor, S_F, is simply the ratio of the fluorine content measured at the top surface of the dried film, $F_{surface}$, to the calculated fluorine content in the dried polymer film given a uniform and random distribution, F_{bulk}:

$$S_F = F_{surface}/F_{bulk} \quad (7)$$

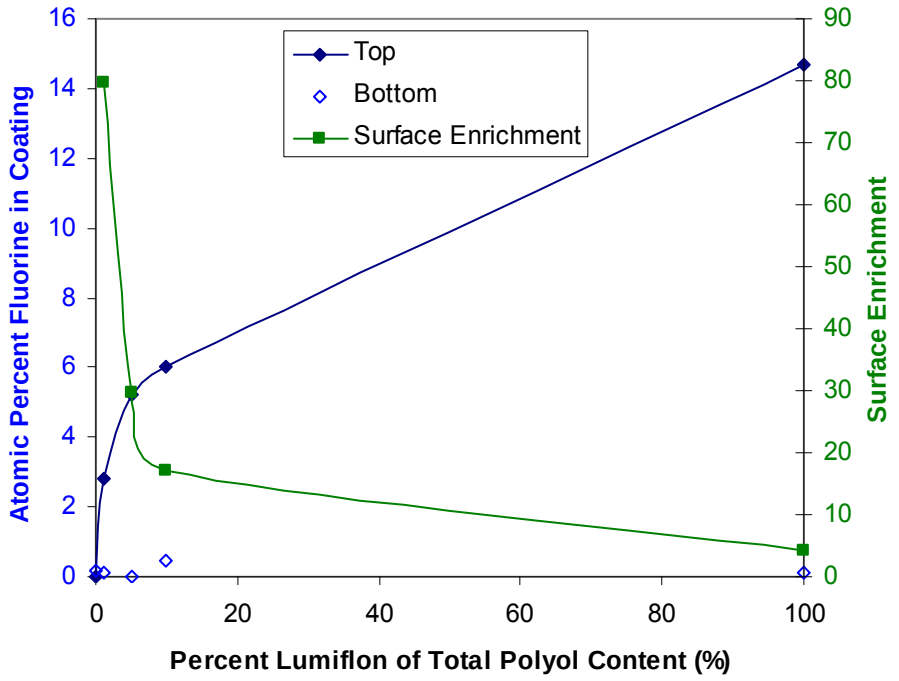

Figure 133: XPS results for fluorine content and surface enrichment of polyurethane films

The atomic percent fluorine and surface enrichment factor as a function of Lumiflon fraction are depicted in Figure 133. These data clearly illustrate the concentration of fluorine at the air interface. In each film containing fluorine groups, the front of the film contains significantly more fluorine vs. the back of the film. For the 10% Lumiflon, there is ~6% fluorine at the top surface while the bulk concentration was approximately 0.35% before surface segregation, resulting in a surface enrichment factor of 17. Thus, XPS analysis confirmed the migration of fluorine groups to the film surface. The concentration of fluorine at the back of the 10% Lumiflon film (0.44%) closely matched the bulk concentration, indicating the surface enrichment is simply a surface effect, rather than causing a gradient of fluorine concentration from the front to back of the film. In addition, there is a significant diminishing return of increasing Lumiflon content to deliver higher fluorine content to the film surface, as can be seen by the reduction in the surface enrichment factor with Lumiflon content. A five-fold increase from 1% to 5% less than doubles the fluorine content at the surface. A ten-fold increase of Lumiflon from 10% to 100% of the formula polyol increases the fluorine content at the surface by less than 2.5 times. The trace appearance of fluorine on the back of the control film suggests surface contamination of the glass was taken up by the film.

Contact Angle

Contact angle of the film surface with water should increase with increasing amounts of fluoropolymer, which is intended to increase film hydrophobicity. As seen in Figure 134, water contact angle increases approximately in a linear fashion with the surface fluorine concentration. Thus, as expected, hydrophobicity increased with increased surface fluorine concentration.

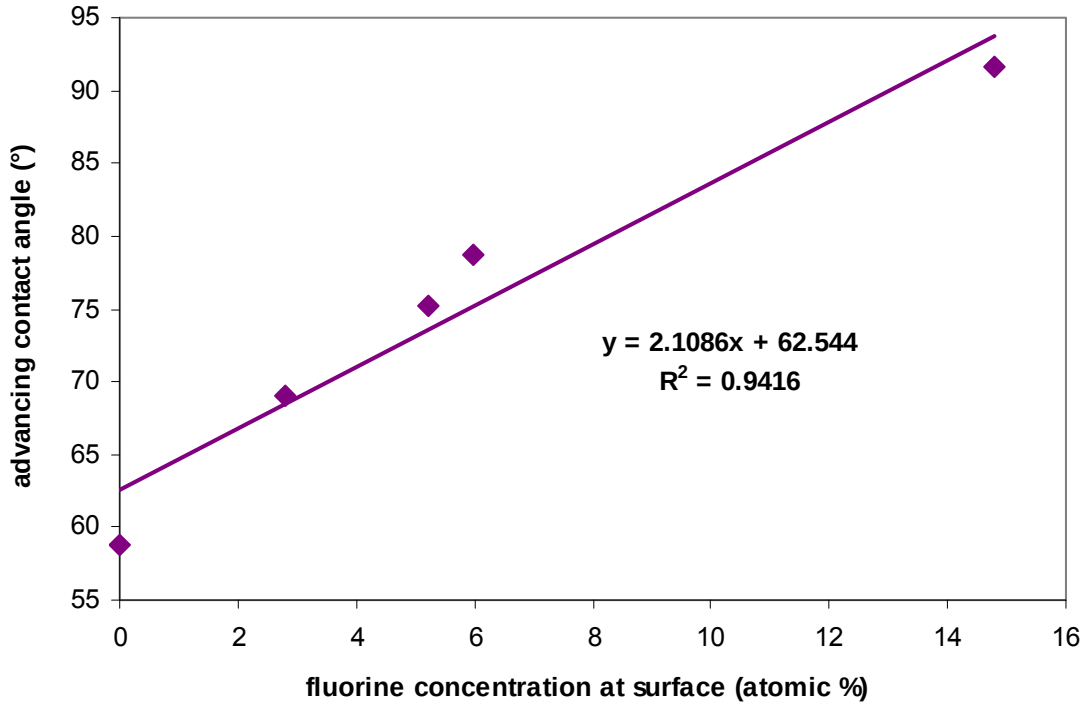

Figure 134: Contact angle with water as a function of surface fluorine concentration

Contact angle hysteresis is the difference between the advancing and receding contact angles. The magnitude of the hysteresis value is proportional to the heterogeneity of surface energy distribution arising from differences in the elemental composition across the surface being wetted [43]. Our results showed a relatively contsant hyteresis of 17.3° ± 1.8°, indicating that the the distribution of fluorine at the surface was relatively similar across all samples. This would suggest that additive levels of Lumiflon achieve a comparable distribution, albeit lower overall level, of surface fluorine as the 100% Lumiflon film.

Thermal Stability

The temperatures at which thermal degradation occurs (indicated by sharp sample weight loss) can give some insight to the types of chemical bonds within those materials. Some important bond energies and degradation temperatures have been provided (Table 49). The degradation temperature of carbon-oxygen bonds is expected to be less than 400 ºC because of its lower bond energy.

Table 49: Bond energies and degradation temperatures [44]

Bond	Bond Energy (kj/mol)	Temp (°C) degradation commences
C – F	443 – 450	> 500
C – H	390 – 436	> 500
C – C	330 – 370	400
C (aromatic) – Br	335	360
C – O	286	n/a
C – Br	285 – 293	290

The TGA derivative weight curves show comparable stability for films containing Lumiflon and the clear control MIL-DTL-64159 (Figure 135). For the most part, addition of Lumiflon FE-4400 had no effect on the thermal stability of cured clear films. The clear exception is the 100% Lumiflon film (shown in green). As previously discussed, it is known that Lumiflon FE-4400 is highly ethoxylated due to the presence of polyoxyethylene units on the vinyl monomer in order to better stabilize the polymer in an aqueous emulsion. This is evident in the appearance of a unique peak around 380 °C where one would expect a carbon-oxygen bond to decompose. It is not yet clear why there was a shift in degradation above 500°C for some films. This is most likely an artifact of experimental error as the sample size is relatively small as most of the material has been consumed between 300 and 500°C.

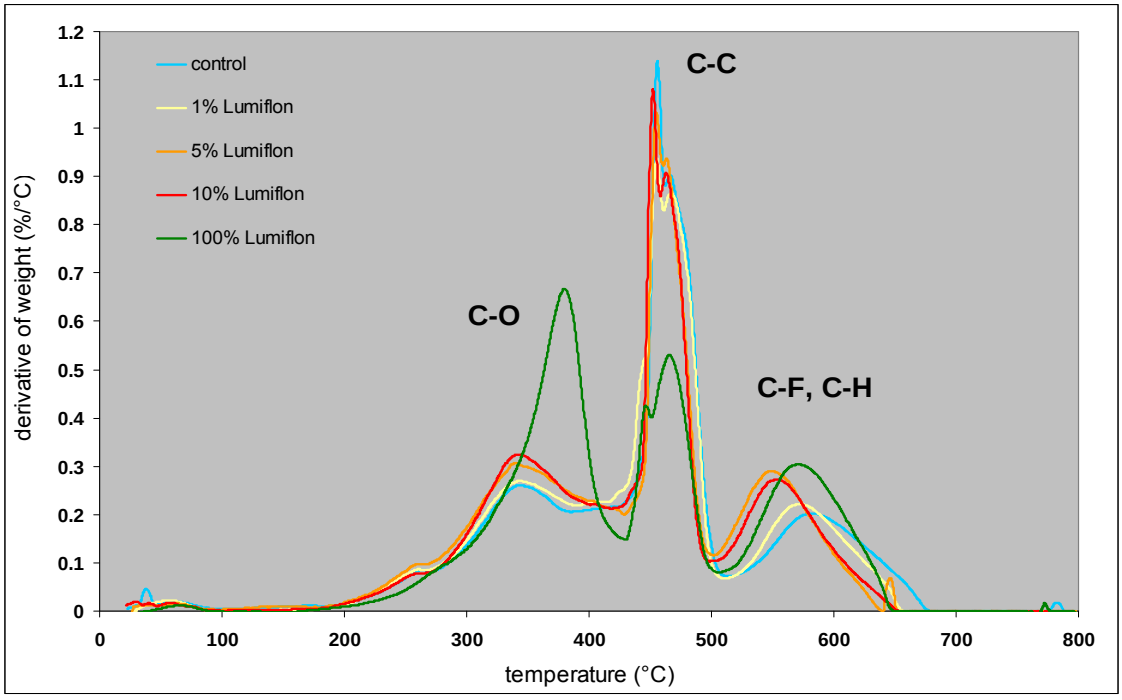

Figure 135: TGA derivative weight curves for clear MIL-DTL-64159 films

Glass Transition Temperature

Glass transition temperature (T_g) was determined by DMA and DSC. The maximum peak in the DMA loss modulus (E") is an easily read marker of glass transition. The baseline shift associated with glass transition on a DSC curve is a much more subtle inflection. The first DSC heating and cooling cycle was ignored to mitigate differences in thermal history between samples and residual solvent evaporation. In most cases, the first heat ramp produced a broad endotherm between 40 and 100°C as residual solvent and moisture was driven off obscuring the relatively small thermal changes from the glass transition. T_g values determined by DSC are generally slightly higher than those measured by DMA because the temperature ramp rate on DSC is 10°C/minute versus a 2°C/minute ramp rate for DMA. Post curing, or heating a sample above its glass transition temperature after room temperature curing has stopped in some cases produces films which are more highly crosslinked and have higher T_g. This effect would be observed in the DSC method where samples are heated to 200°C and cooled before the test data are collected. In addition to the RT cured films, a sample of each film was post cured for 2 hours at 105 °C and DMA was run to determine if T_g increased due to postcure.

The T_g results are graphed in Figure 136. Clearly 100% Lumiflon had a lower glass transition temperature, as T_g suppression begins to be evident in the RT cured films as low as 5% level of polyol replacement. This suppression of T_g may be a result of the ethoxylation of the Lumifon polyols, which may result in lower backbone stiffness and higher chain mobility relative to Bayhydrol 7110E polyol. Post curing the films produced slightly higher T_gs in most cases. The T_g determined by DSC was the highest of the three measurements except for the 100% Lumiflon sample. Perhaps the faster temperature ramp and lower sensitivity of this technique masks differences in the formulations as the control through the 10% Lumiflon samples all exhibited the same T_g as determined by DSC within experimental error. These results suggest that the DMA is a more accurate tool for determining glass transition of polymer films.

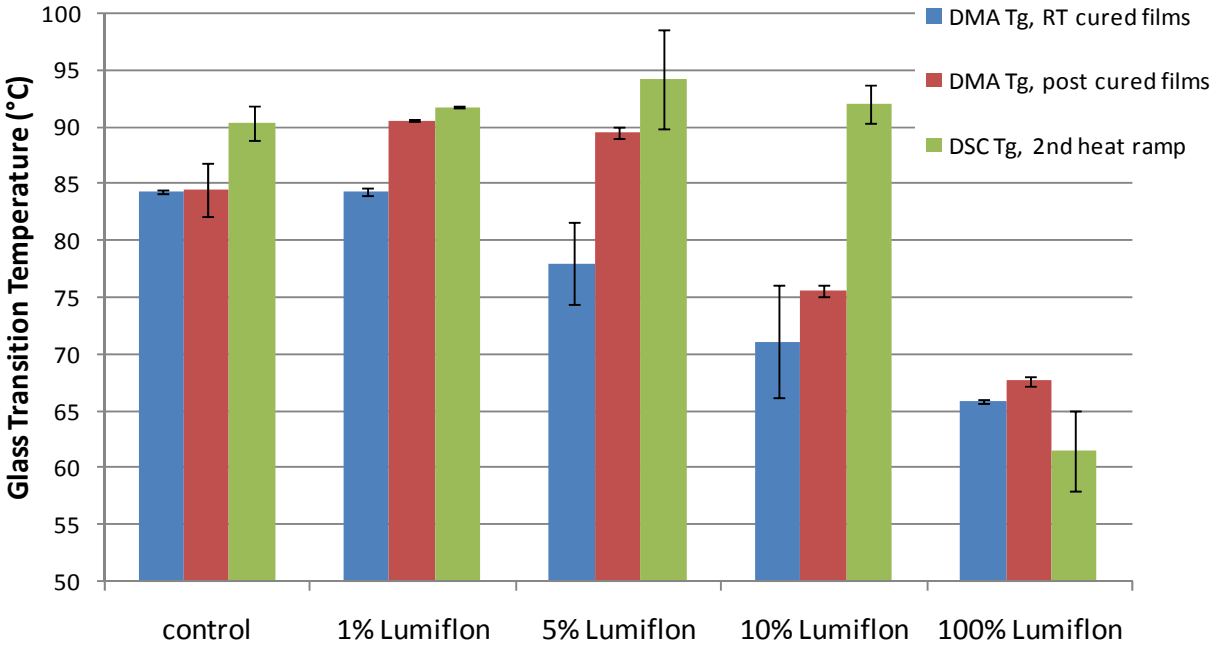

Figure 136: T_g determined by DSC and DMA

Storage Modulus

DMA was used to examine the effect of Lumiflon FE-4400 on film modulus for both RT cured and films post cured 2 hours at 105 °C. In these experiments the storage modulus achieved its highest value at -20°C, the lowest temperature in the test range. Modulus values continued to decline steadily as temperature increased. The glass transition can be seen as the temperature range experiencing the fastest decline of storage modulus (Figure 137). From these data it is clear that the 1% and 5% Lumiflon films had very similar mechanical properties to the control sample. Beginning at the 10% level of addition, the storage modulus dropped with increasing Lumiflon content. In particular, the storage modulus for 100% Lumiflon was lower than the other urethane system. Again, the ethoxylation of the Lumiflon polyol may result in lower backbone stiffness relative to Bayhydrol XP-7110E polyol causing this observed decrease in modulus for 10% and 100% Lumiflon films. The glass transition for 100% Lumiflon was sharper and occurring over a narrower range of temperature than the other films. It is believed that this result could arise from a tighter distribution of molecular weight for the Lumiflon polymer.

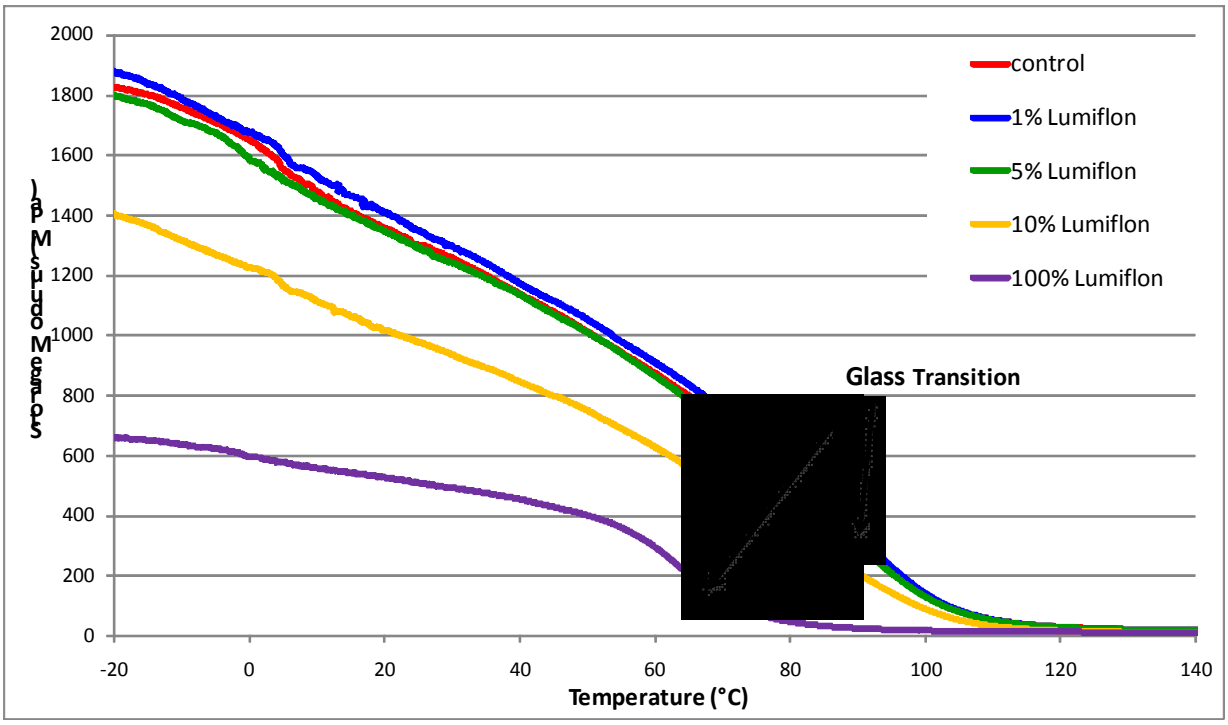

Figure 137: Storage modulus in the glassy region and glass transition for RT cured films

Molecular Weight Between Cross-links

Of key interest in the study of Lumiflon FE-4400 in MIL-DTL-64159 is the effect of the fluoropolymer on film crosslinking. Highly crosslinked binder systems have been directly correlated to better chemical agent resistance [45]. DMA data, specifically the storage modulus in the rubbery region, can provide a calculated value of the average molecular weight between cross links. M_c is inversely proportional to the more familiar parameter of cross-link density.

Lower M_c means a more highly cross-linked resin. The results clearly showed that Lumiflon FE-4400 had a much higher M_c than the control formula which suggests that it would not provide comparable resistance to chemical agents at the 10% level or above (Figure 138). The 1% and 5% Lumiflon films were equally cross-linked as the control. Post curing provided significant amounts of additonal cross-linking for only two samples, the control and 5% Lumiflon films.

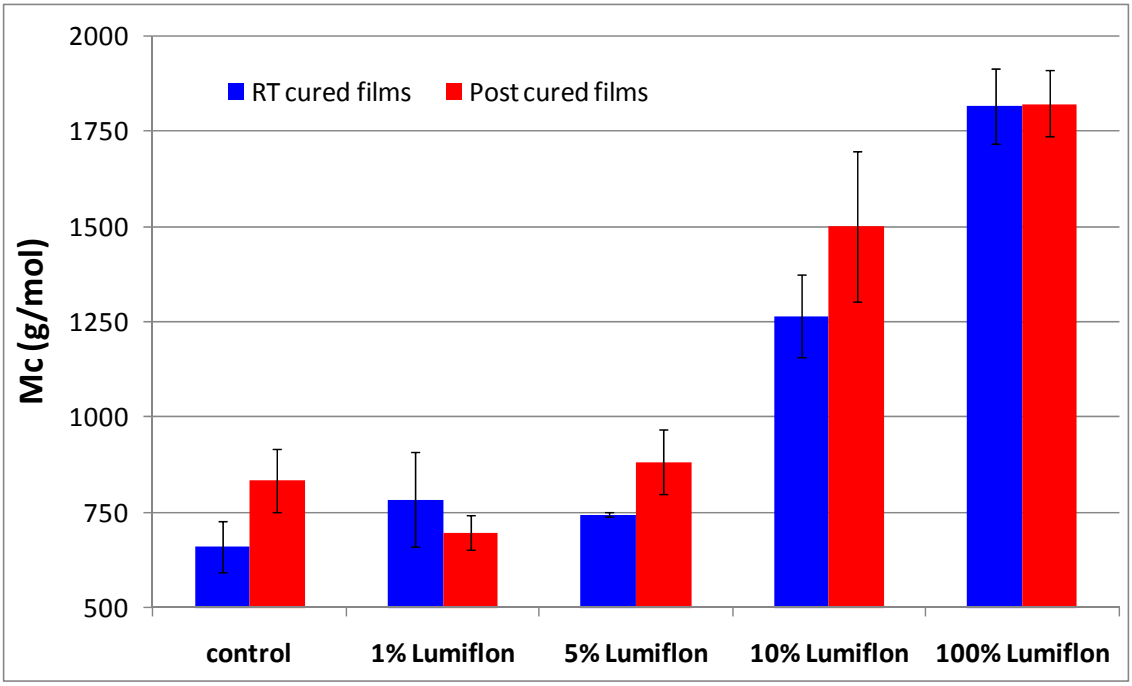

Figure 138: M_c for RT cured and post cured films at 180°C

Tensile Testing

Tensile testing of films provided a comparison of basic mechanical properties of modulus, ultimate tensile strength, elongation at break and material toughness. For many polymer systems there exist tradeoffs between flexibility and strength. More specifically, very stiff materials may exhibit greater strength but much higher brittleness, resulting in very low elongation and toughness. Results are reported in Table 50. Elongation measured was adjusted for toe compensation [17] which may result from slack or misalignment of the sample within the grips. Tensile strength and elastic modulus were relatively constant until the 10% Lumiflon level was reached, at which point strength and stiffness began to drop and declined sharply for the 100% Lumiflon sample. Percent elongation at break, and by extension, film toughness began to decline with 5% added Lumiflon. All of these material properties were lowest for the 100% Lumiflon film which may be partially a result of lower cross-link density as determined by DMA. In addition, the ethoxylation of the Lumifon polyols may result in lower backbone stiffness relative to Bayhydrol XP-7110E polyol. Samples post cured at 105°C for 2 hours were tested under the same conditions as the RT cured films. No clear trends for the effect of post curing on tensile properties emerged from the results. Post cured tensile data are not reported.

Table 50: Tensile testing data

	tensile strength (MPa)		adjusted elongation at break (%)		elastic modulus (MPa)		toughness (MPa)	
	Average	St. Dev.	Average	St. Dev.	Average	St. Dev.	Average	St. Dev.
Control	34.39	1.73	7.17	1.35	1091	32	1.74	0.48
1% Lumiflon	38.74	0.84	7.35	1.00	1204	27	2.01	0.35
5% Lumiflon	30.41	3.38	3.69	0.64	1158	50	0.67	0.21
10% Lumiflon	22.64	3.27	3.56	0.92	923	72	0.50	0.19
100% Lumiflon	6.64	0.72	2.11	0.31	425	15	0.08	0.02

Elastic modulus determined from tensile data and DMA should be fairly similar. In Figure 139 the data show strong correlation to each other. DMA modulus tracks slightly higher than that obtained from tensile testing because DMA samples are cooled to -20°C for the beginning of the test and may not be as relaxed by the time the furnace reads 25°C as the tensile samples which are stored and tested at room temperature.

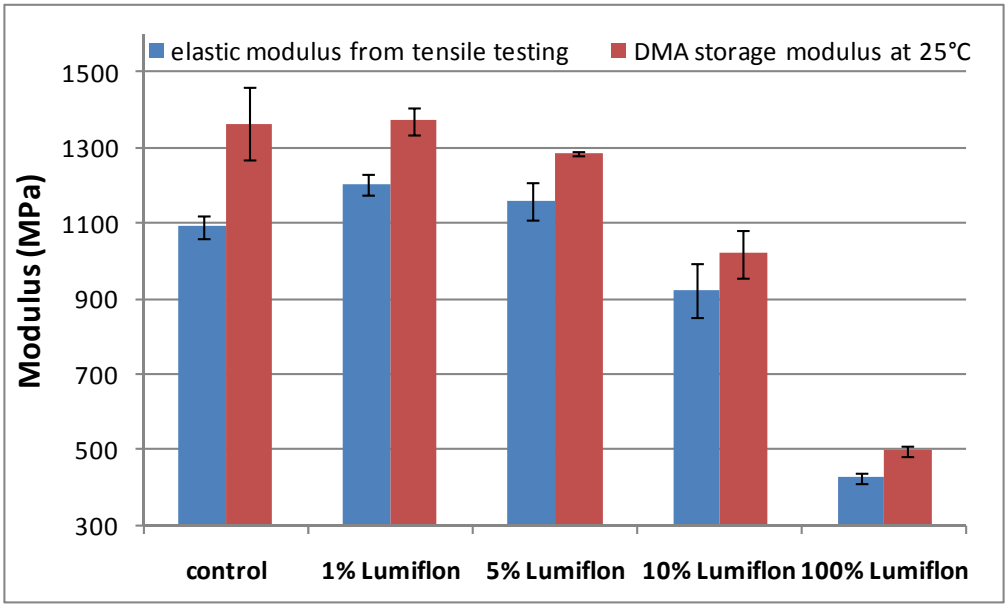

Figure 139: Comparison of DMA storage modulus at 25°C and elastic modulus from tensile testing

Solubility, Permeability and Diffusivity

The equilibrium solubility of water and DMMP in the test films at 35 °C was measured. The solubility results (Table 51) are expressed as percent weight gain of the film after submersion in liquid to the point of saturation. DMMP was on average seven times more soluble than water in these clear polyurethane films. Solubility of water was slightly higher as Lumiflon level increased but this trend was not considered significant. Film morphology is more likely to influence water uptake than the hydrophobicity of the surface as would be suggested by contact angle (Figure 134). In other words, once the submersion liquid wets the film surface and begins infusion into the film voids and the crosslink structure, the bulk properties of the film (chemistry and morphology) should have a greater effect on liquid solubility than the surface chemistry of the film. Surface chemistry should affect the rate at which saturation of the liquid in the film sample is reached; however surface chemistry should have little effect on the total amount of liquid absorbed by the film at saturation. DMMP uptake dropped significantly for the 100% Lumiflon samples, while it was fairly constant at 0-10 wt% Lumiflon added.

The permeability of water vapor and DMMP vapor at 35°C did not have a significant correlation with Lumiflon content. Two anomalous results (denoted by "n/a") were measured for the DMMP permeability through the 5% Lumiflon film and water permeability through the 100% Lumiflon film. Thus ignoring these anomalies, permeability appears not to be related to fluoropolymer content. The water and DMMP permeability values appear to be similar within experimental error; this was surprising given the vast difference in both vapor pressure at 35°C and molecule size.

Table 51: Permeability, solubility and diffusivity of water and DMMP through clear polyurethane films

	Permeability (g/h*m)		Solubility (% wt. gain)		Diffusivity (m^2/s)	
	Water	DMMP	Water	DMMP	Water	DMMP
Control	0.036	0.065	7.0	65.8	1.4E-10	2.7E-11
1% Lumiflon	0.081	0.097	9.0	63.4	1.1E-10	2.6E-11
5% Lumiflon	0.060	n/a	8.6	58.8	2.6E-10	n/a
10% Lumiflon	0.036	0.061	9.5	67.0	1.7E-10	2.6E-11
100% Lumiflon	n/a	0.064	11.1	47.0	n/a	1.9E-10

Diffusivity (m^2/s) can be related to permeability and solubility by equation 6:

$$D = P/S \quad (8)$$

where permeability is expressed in units of g/s·m and solubility is expressed as weight of solute uptake divided by film volume (g/m^3) [46]. Values for vapor diffusivity were caluculated for water and DMMP from the experimental data for permeability and solubility. Given that DMMP is seven times more soluble than water in these samples and that permeability was not remarkably different, we are left to conclude that DMMP diffused much more slowly through the films. The values in Table 51 show that diffusivity of DMMP was roughly 5 times lower than water.

An ideal paint film should be impervious to penetration by both water and chemical vapor. Permeability and solubility as determined by immersion studies are not controlled by surface effects and therefore do not relate to contact angle or surface concentration of fluorine. These are more likely influenced by film morphology and defects.

Clear Film Morphology

The effect of Lumiflon FE-4400 added to clear polyurethane formulations on film morphology was studied. In order to identify the underlying morphology in these clear films, a phase contrast microscope at 40 times magnification was used. Attempts were made to identify structures via traditional optical dark field microscopy, but the contrast was far too low to be of any use.

Figure 140 clearly shows that addition of Lumiflon affects the morphology of the polyurethane. The addition of fluorinated polyol resulted in the formation of structures in the film. As the fluorinated polyol content increased, the number of the structures increased. Due to the lack of stabilizers and other additives which promote formulation homogeneity, it can be surmised from these pictures that there is a broad range of structures and reaction products incorporated into the films. Given the relatively inconclusive solubility and permeability results, these structural differences do not seem to affect vapor sorption and diffusion through the films.

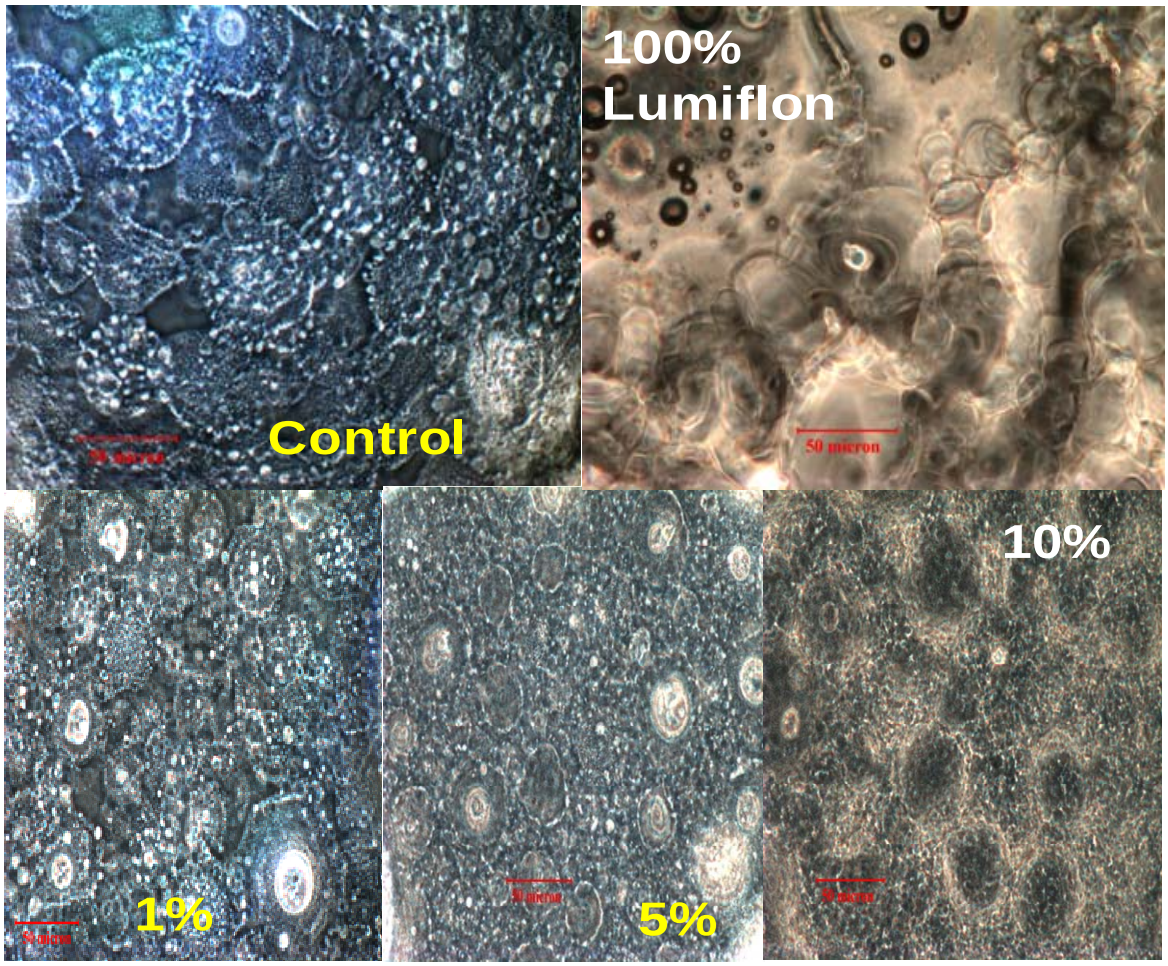

Figure 140: Phase contrast microscopy images of clear coat polyurethanes with increasing Lumiflon FE-4400 content. All images are the same level of magnification. Scale bar is 50 microns.

Resistance to Weathering

Gloss measurements at 60° and 85° angles of observation showed no appreciable change after QUV exposure for any of the coated panels. Color was measured after every 1000 hours of exposure in the QUV. The average change in chromaticity values are depicted in Figure 141. Chromaticity values (x, y) are numerical representations most closely related to value and hue of human color perception. Individual values were calculated for the distance $(\Delta x^2 + \Delta y^2)^{-1/2}$ between the chromaticity coordinates at time zero and after exposure. Based on these results Lumiflon FE-4400 actually degraded the weatherability of the coatings, as the coatings with Lumiflon added performed similarly or worse than the control for all Lumiflon contents and weathering durations. Interestingly, after 1000 hours and 1936 hours, the chromaticity was worst for the 1% samples and improved as the Lumiflon content increased, but was always worse than the control. After 3000 hours, the results showed a significant increase in chromaticity change as the Lumiflon content was increased from 0 to 10%. Although the exact trends are hard to

understand, it is clear that the addition of Lumiflon degrades the weathering performance of these coatings.

The enriched control, with 10% additional polyol and isocyanate, should, in theory, provide a more robust coating with higher binder content which should show greater resistance to UV degradation relative to the control. However, the chromaticity change after 3,000 hours would suggest that perhaps the UV absorbers and other formulation stabilizers included by the manufacturer were diluted through the addition of pure polyol and isocyanate to a point that harmed overall coating performance. This may further suggest that the admix method of preparing the pigmented formulas may not be a fair assessment of fluoropolymer resistance to weathering.

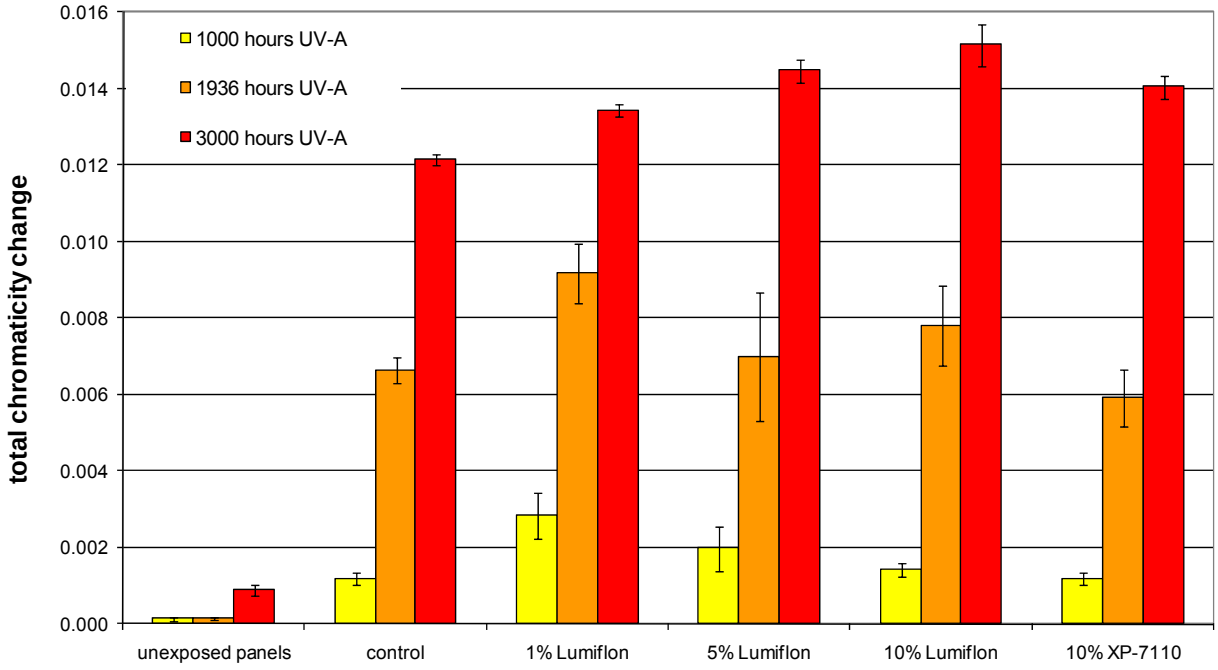

Figure 141: Average chromaticity change after QUV exposure

Chemical Agent Resistance

Table 52 shows that the Lumiflon additive reduced HD chemical agent resistance, but the formulation still produced a coating that passed specifications. GD chemical agent testing is currently in process. Lumiflon likely reduced the CAR because of the resulting morphology change (Figure 140).

Table 52: Chemical agent reistance of MIL-DTL-64159 sample with the addition of 5 wt% Lumiflon FE-4400 or an additional 5 wt% XP-7110 as a control

NOMENCLATURE	HD-PASS	GD-PASS
5% Lumiflon FE-4400	127.55	IN TESTING
CONTROL 5% XP-7110	<10.3	IN TESTING

NOTE: PASS/FAIL is 180 μg or less for HD and 40 μg or less for GD.

Conclusions

Lumiflon FE-4400 segregated to the film surface of clear coats of military polyurethane providing significant fluorine enrichment at the air interface. Increasing the level of Lumiflon FE-4400 had diminishing benefit to the surface fluorine concentration (i.e., 1% Lumiflon resulted in a surface enrichment of 79.5, while 10% Lumiflon resulted in a surface enrichment factor of only 17). Contact angle with water correlated very well to surface fluorine content determined by XPS. Addition of Lumiflon FE-4400 below 10% resulted in no significant change in film properties but at or above 10% of polyol fraction, the glass transition temperature, modulus, strength, toughness, molecular weight between cross-links, and weathering resistance were significantly reduced. The clustering morphology indicating phase separation of the components likely played a role in reducing the film properties. Weathering resistance was likely also reduced as a result of the ethoxylation of the fluorinated polyol which is necessary to make it water dispersible. Overall, it was demonstrated that the current ethoxylated FEVE resin emulsion does not provide the sought after benefits of better durability and greater resistance to water and chemical agents. However, because these fluorinated additives do improve some aspects of performance, ARL will pursue newer fluorinated polyols that are non-ethoxylated to improve weathering and cleanability.

3.6.3.6 Formulation of Zero VOC Topcoats

Zero VOC topcoats were formulated through the use of new polyols and VOC-exempt solvents. New polyols were used that did not require any N-methyl pyrolidinone to make a stable water dispersion with the isocyanate component. The isocyanate component was completely dissolved in tert-butyl acetate to reduce the VOC content in the coating to zero. The isocyanate to hydroxyl indexing was varied from 5:1 to 3:1. The following are the formulations that proved most successful:

50 grams –Polyester Urethane--- Part A Binder
12 grams – High Density Polyethylene additive – Enhance Mar Resistance and reduce viscosity
2.0 grams – Silane-coupling agent – Adhesion promoter, assist in binding inorganics (green pigment), enhances water resistance and other properties.
0.01gram – Proprietary defoamer

0.01 gram – Proprietary silane surface tension reducer
The appropriate amount of Polyisocyanate to obtain isocyanate:hydroxyl index from 5:1 through 3:1.

The resulting coatings were clear, uniform, and contained few bubbles or holes. The coatings are expected to be chemical agent resistant in nature, but further studies must be done to ensure this.

3.6.3.7 The Effect of Isocyanate:Hydroxyl Indexing on Clear Film Properties

A series of clear polyurethane films was made from an aqueous polyol dispersion and isocyanate thinned with exempt solvent t-butyl acetate. The difference between the sample formulations was the index or equivalent weight ratio between isocyanate groups to hydroxyl groups. A second set of films was prepared repeating the same indexing as the first set of formulations but using a lower molecular weight polyol. Films were cast on glass and cured at room temperature. Testing performed on these films revealed interesting results.

Crosslinking

Graphing the storage modulus data in the rubbery region from DMA showed that indexing had a significant effect on crosslink density (Figure 142). A higher index yielded higher modulus values above the glass transition which means a lower M_c or molecular distance between cross-links or a higher cross-link density. Figure 143 shows the average values calculated for M_c and some interesting trends emerged. The higher molecular weight polyol, XP-7110, appeared to follow a strong trend of decreasing Mc as indexing increases. At lower indexing, the M_c distribution was wider (denoted by larger error bars) which suggested that there could be a much broader range of structures and reaction products at lower indices. Competing side reactions with isocyanate become more significant as the amount of available isocyanate decreases. The lower molecular weight XP-2591 provided greater cross-linking than XP-7110 at lower indices. There also appeared to be no relationship of Mc to indexing for XP-2591 but the generally smaller error bars might indicate that maximum cross-linking can be achieved at lower indices while producing a more regular cross-linked polymer network.

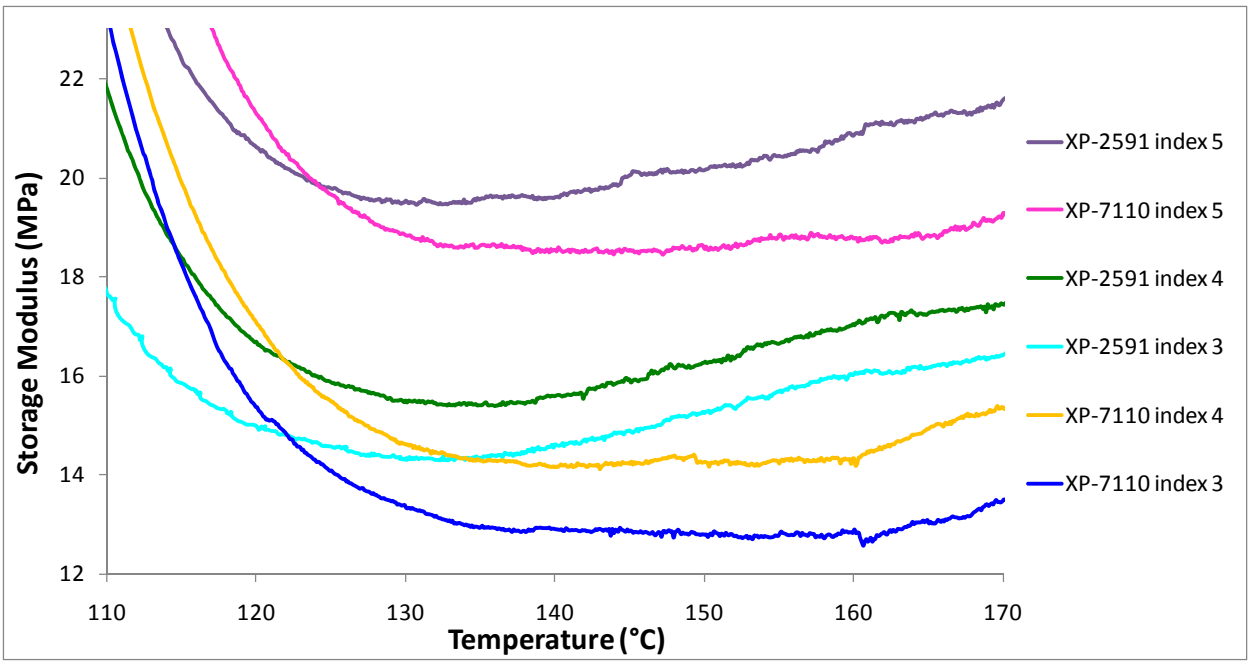

Figure 142: Rubbery modulus of XP-7110 and XP-2591 indexing series

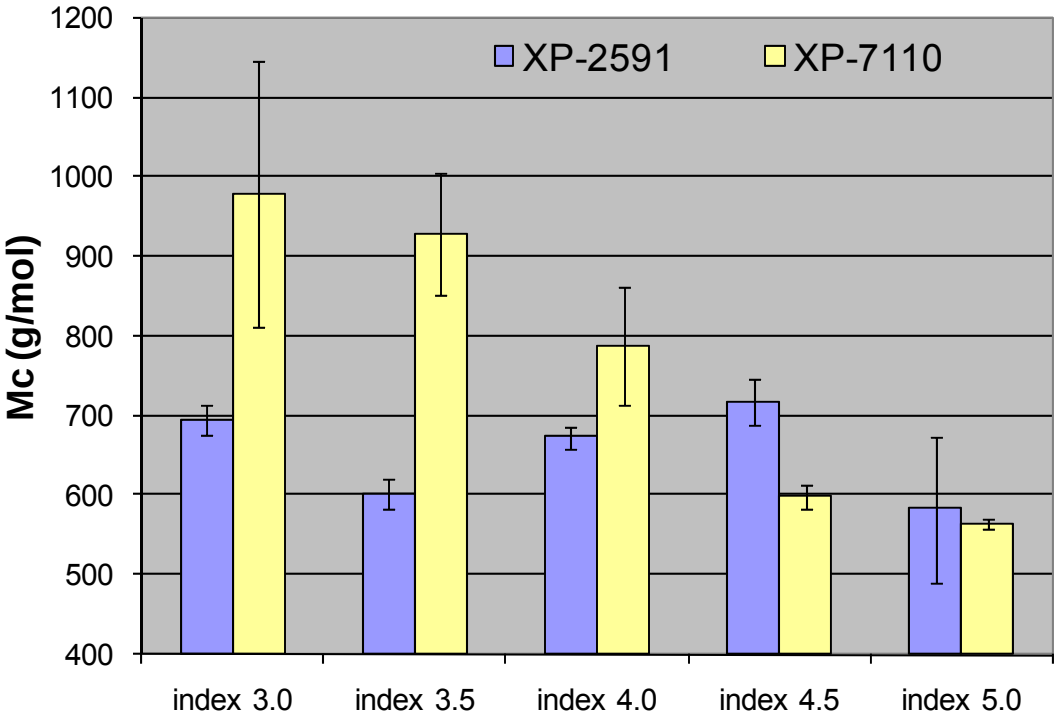

Figure 143: Molecular weight between cross-links for two indexing series

Glass Transition Temperature

DMA analysis revealed that the glass transition temperature (T_g) increased slightly at higher isocyanate to hydroxyl indexing (Figure 144). This trend was expected for samples with higher cross-link density. However, XP-2591 formed more highly cross-linked films than XP-7110 yet the XP-2591 films had lower T_g than XP-7110. Looking at the DMA loss modulus curves provides an explanation for this result (Figure 145). The broader loss modulus peaks for XP-7110 samples supports the conclusion that those films contain a broader range of structures, leading to a broader glass transition temperature range.

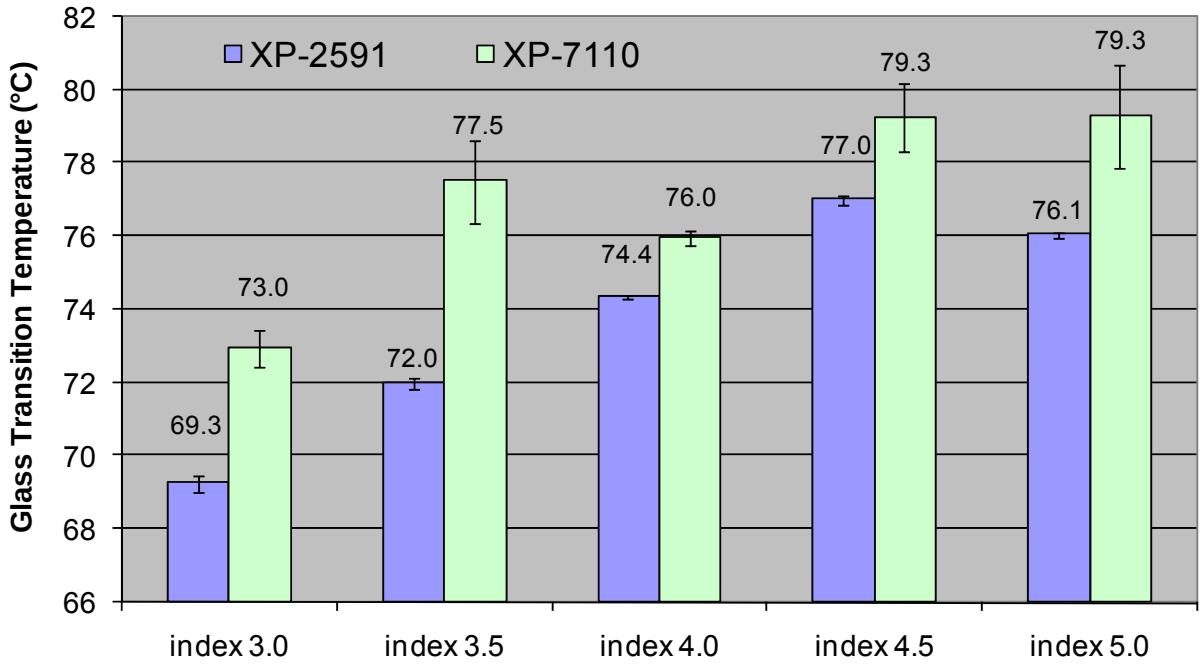

Figure 144: Glass transition temperature of indexing films determined by DMA

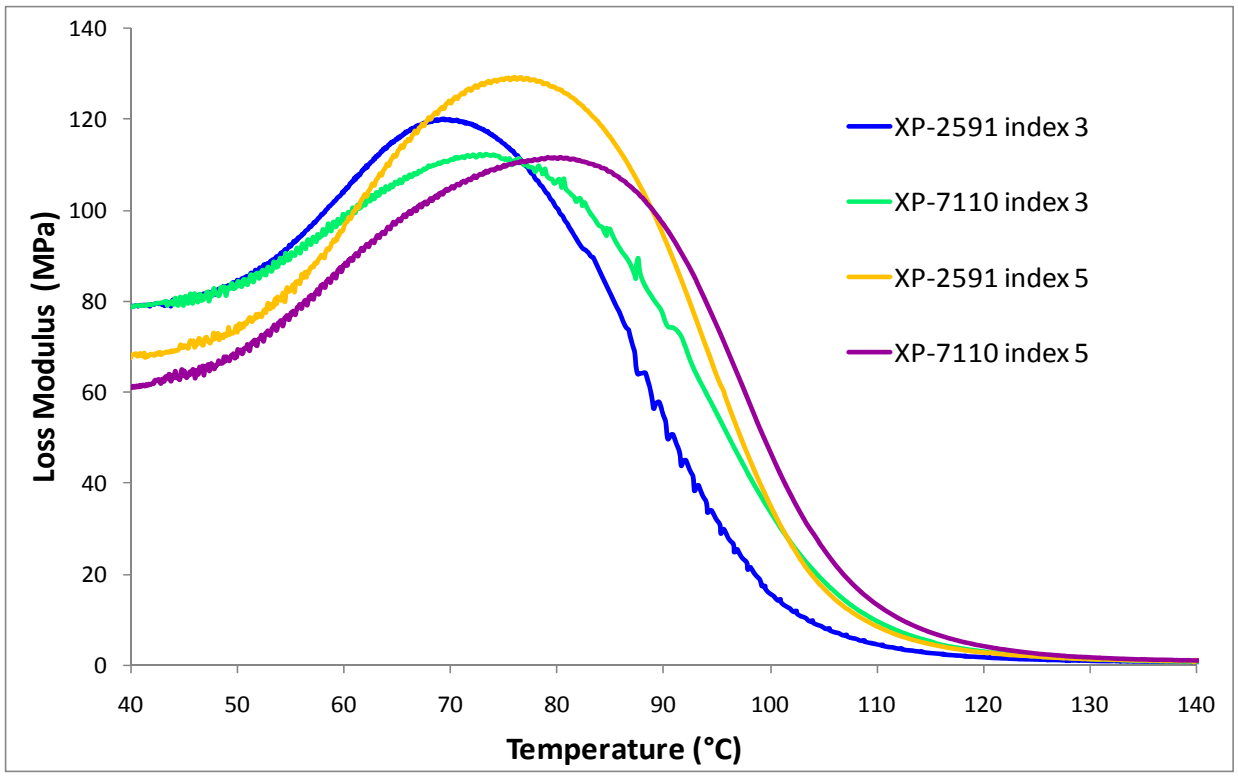

Figure 145: DMA loss modulus curves of indexing films

TGA analysis of the indexing samples revealed no significant difference in thermal stability. Figure 146 shows representative curves of sample weight loss as a function of temperature.

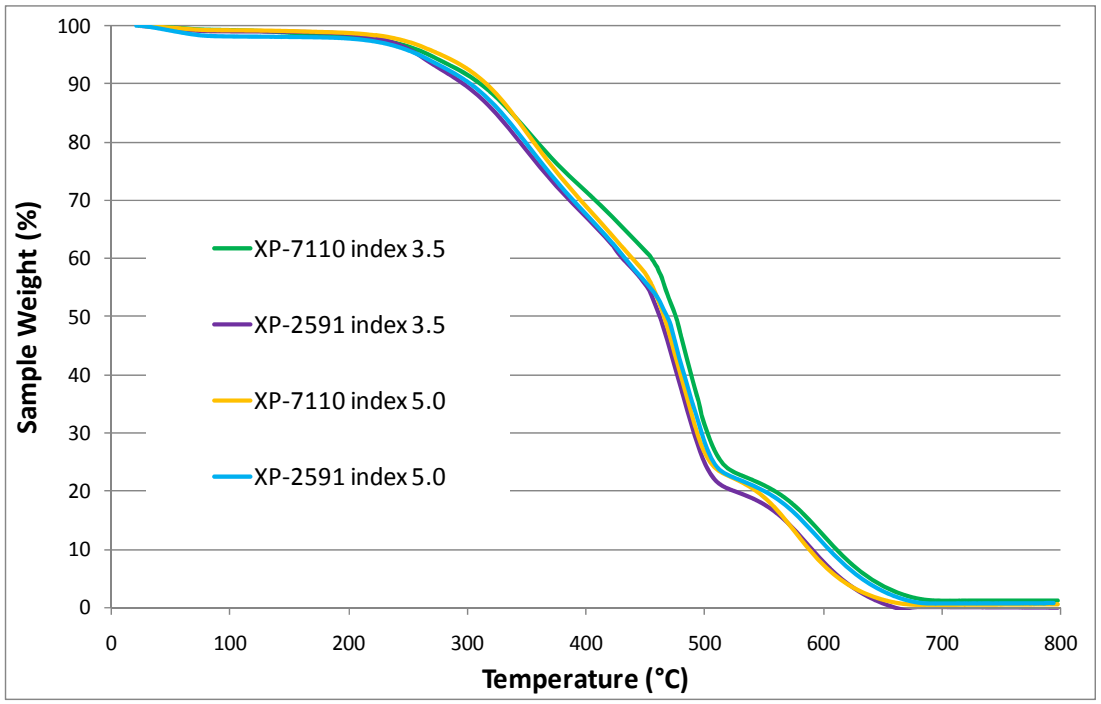

Figure 146: TGA weight loss curves for the indexing series

Phase contrast microscopy images were taken for selected indexing films. As indexing increased more structures could be seen for both polyols studied (Figure 147). It also appeared as if XP-2591 had a more defined and uniform structure than the analogous XP-7110 sample. Images are darker for the higher indices indicating that more light is diffracted as the film density increases.

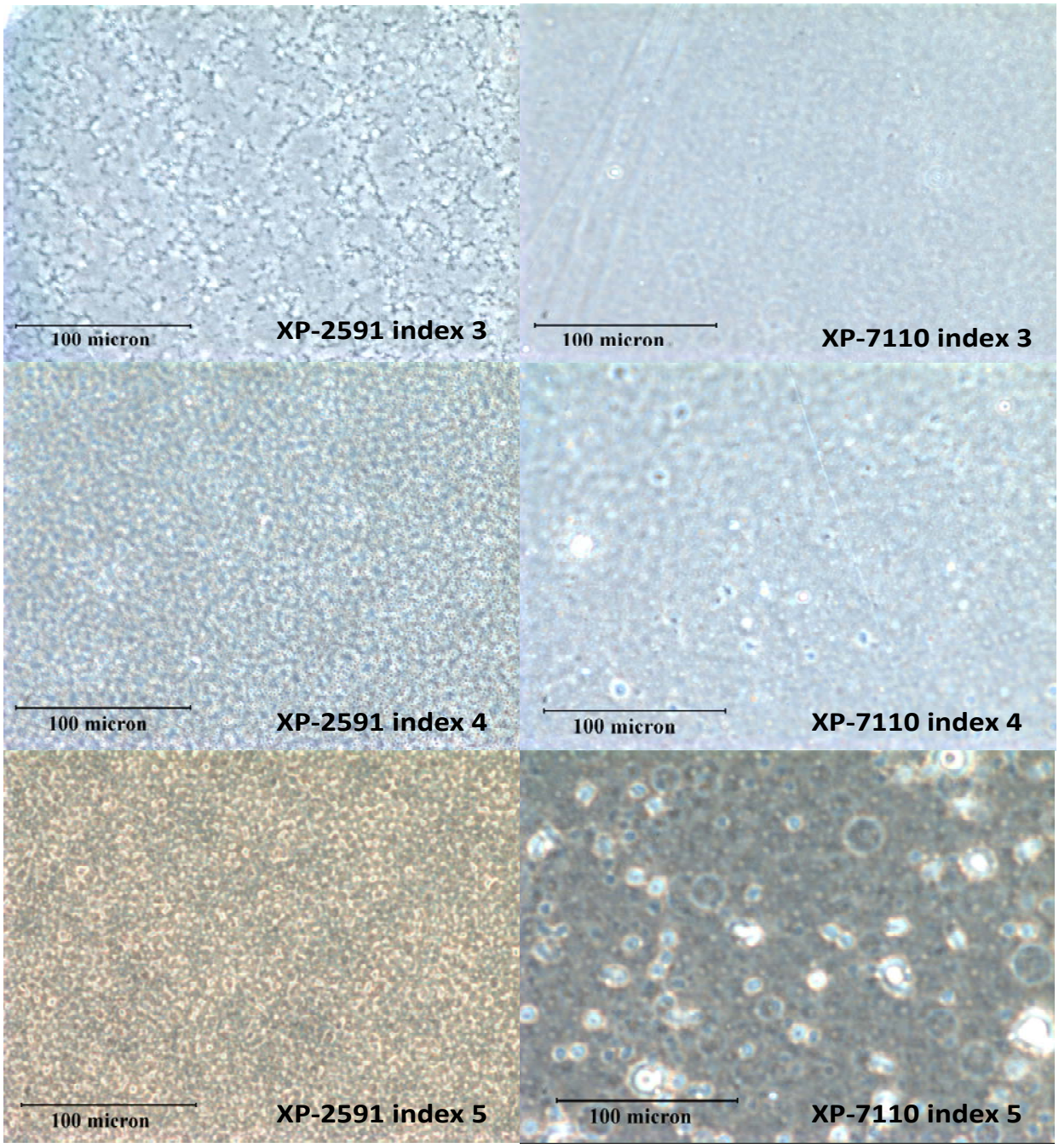

Figure 147: Phase contrast images of select indexing films

The Effect of Indexing on Permeability and Solubility of DMMP

DMMP is a simulant for the chemical warfare agent Sarin. Permeability and solubility of DMMP was measured for the indexing study to confirm a widely held belief that higher cross-link density will reduce the vapor transmission and solubility of liquids in contact with a coating, thus providing better chemical agent resistance and cleanability after contamination. Vapor transmission rate was measured and vapor permeability was calculated from these data (Figure 148). While there was no measurable difference between the lower and higher molecular weight polyols, both showed a decrease in permeability as indexing increase.

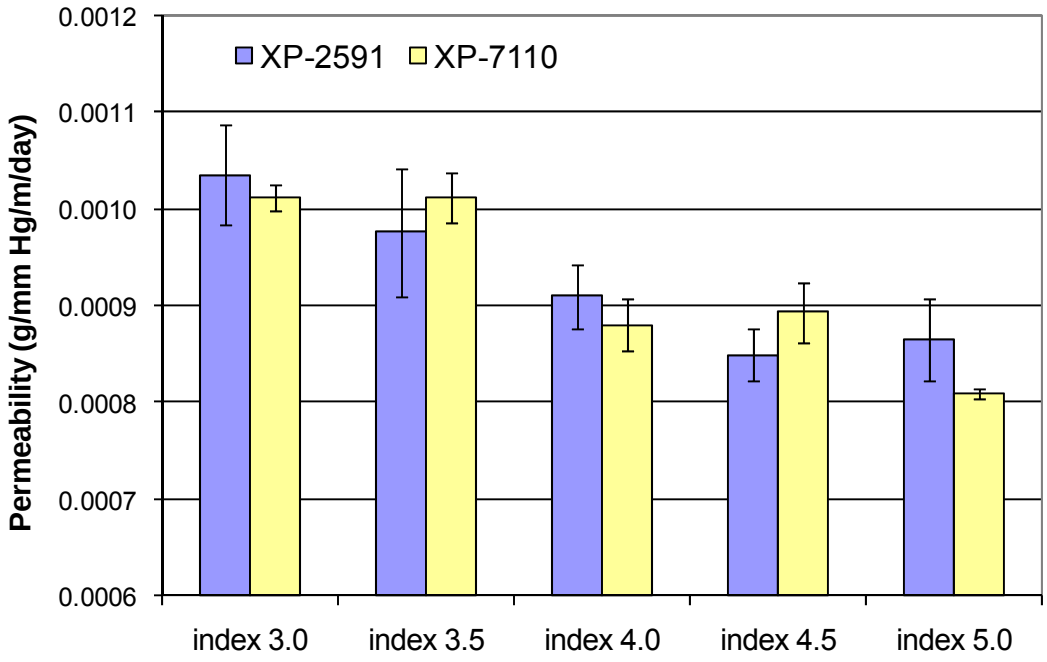

Figure 148: Permeability of DMMP through clear indexing films

Solubility of DMMP in the clear films was determined by percent weight uptake after immersion. The experiment was carried out until saturation was reached and the weight remained relatively constant. It was found that solubility of DMMP decreased as indexing increased for both polyols. This experiment showed that solubility of DMMP was greater in XP-2591 films than XP-7110 films for all indices measured (Figure 149).

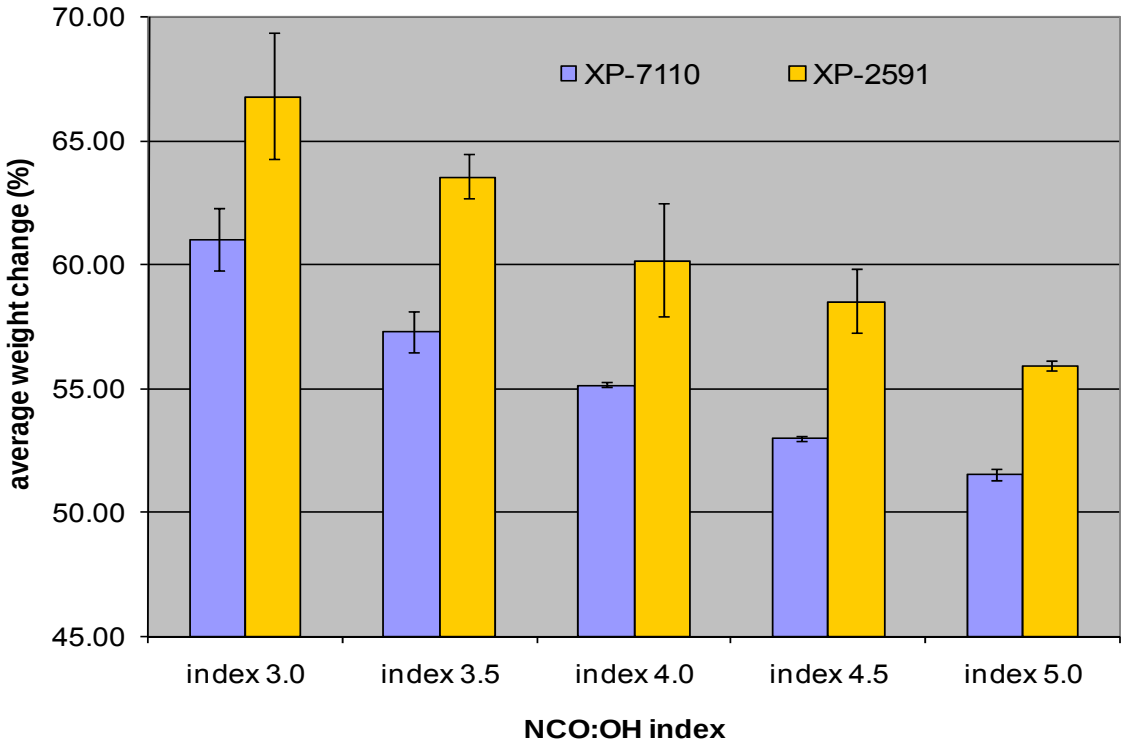

Figure 149: Solubility of DMMP in clear indexing films

4 Environmental Impact and Cost-Savings Analysis

4.1 Environmental Impact

The whole purpose of this project is to reduce the negative impact of military coatings on the environment. As such, we are developing pretreatments, primers, and topcoats that have reduced Cr(VI) and VOC content. Analysis of TCP shows that this pretreatment contains no Cr(VI) and uses no other dangerous heavy metals. The Army primers are already chrome-free. If the Navy class N primers prove effective on TCP pretreated surfaces, then the overall Cr(VI) content in military coatings would be zero and would therefore pass the 5 $\mu g/m^3$ OSHA exposure limit. The ultra low VOC topcoats would simply replace VOC and HAP solvents with water or VOC-exempt solvents, such as tert-butyl acetate. Therefore, the new formulations would reduce worker exposure to solvent vapors and improve general air quality. Fluorinated materials have been found to be environmentally pervasive, and as such partly fluorinated polyols may cause a negative environmental impact. However, at the moment, there is no evidence of any environmental damaging effect of the particular class of fluorinated material that is being used in this work. The new pigments and additives being examined for use in coatings contain no environmentally damaging compounds. Overall, the pallet of coatings being developed for the military in this project would reduce the negative impact of military coatings on the environment.

4.2 Cost Savings Analysis

4.2.1 PRETREATMENTS

TCP-S has already proven to be economically competitive with commercial Cr(VI) and commercial non-chrome pretreatments according to ESTCP PP-0025 [47]. The TCP variants are similar in chemical make-up and cost relative to TCP-S. Thus, similar economic analysis would occur. CFP is contains many of the same components as TCP does, but does not contain any Cr(III) and contains higher concentrations of the fluorozirconates. Again, the economic assessment is expected to be very similar for CFP relative to TCP and other commercially available pretreatments.

4.2.2 BINDERS

Preliminary economic analysis of binders shows that the current binders and new binders being tested for use are chemically similar and should result in similar economic cost-benefit analysis in the long-term. However, it is possible that initial costs will be higher due to the higher initial price point as industrial suppliers attempt to offset development and manufacturing start up costs for these new binders.

4.2.3 SOLVENTS

In order to make primers and topcoats with ultra low VOC content, we have substituted VOC solvents with exempt solvents. The exempt solvents cost more than the VOC solvents. Yet, many of the VOC and HAP solvents used are not common solvents, like N-methyl pyrolidinone and triethylamine, which cost more than tert-butyl acetate.

4.2.4 EXPERIMENTAL PIGMENTS/ADDITIVES

ARL is exploring variants in pigmentation to establish a new palette for the Army's basic woodland colors which will impart greater reflectance yet maintain similar visual appearance. This approach will permit extended UV exposure with minimal degradations to the coating. Listed below (Figure 150) are alternative formulations currently being evaluated for this effort and their relative costs. One key criterion for selection is that cost remains within an acceptable range relative to our standard pigment package. In summary, cost expenditures would be appropriate to move toward higher reflectance type pigmentation. Preliminary analysis shows that Z-VOC non-chrome primers use additives that have similar cost relative to the current additives used, and thus should have little impact on overall primer cost.

Formulations

Pigment	Standard Formulation	Formulation #1	Formulation #2	Formulation #3
Standard Pigment	40.5	0	0	0
Low Solar Loading Pigment #1	0	83	84	0
Low Solar Loading Pigment #2	0	0	0	98.2
Other Pigments	59.5	17	16	1.8

Relative Costs Per Pound

Pigment	Standard Formulation	Formulation #1	Formulation #2	Formulation #3
Standard Pigment	1			
Low Solar Loading Pigment #1		0.52	0.52	
Low Solar Loading Pigment #2				0.52
Other Pigments	0.23	0.266	0.273	0.2
Overall Relative Pigment Costs	**1.00**	**0.88**	**0.89**	**0.95**

Figure 150: Relative cost of low solar loading pigment formulation candidates

The attributes of these novel formulations will enable the United States to be independent from foreign sources for cobalt spinel pigments which have risen over 300% due to unstable foreign economies and governments. Also, the Army will eliminate cobalt in its camouflage formulation which directly supports the Environmental Protection Agency in the elimination of regulated non-volatile Hazardous Air Pollutants. This will be a significant benefit to all manufacturers, end-users and waste disposal efforts to eliminate a Hazardous Air Pollutant. Finally, based on reduction of repainting activities alone, due to enhanced coating system durability, a conservative Return on Investment (ROI) has been calculated and validated by the Office of Corrosion Policy and Oversight an office within the Secretary of Defense and appointed by the Deputy Secretary of Defense (Figure 151) [48]. A substantial cost saving of $101.5 Million in the first cycle of repainting has been calculated with the implementation of these new formulations. Currently, as the approving and validating authority for CARC, we have approved 2.3 million gallons of CARC since March of 2008. The ROI ratio of 77.97 was based on 1.6 million gallons. The impact of these formulations to the United States is very significant and continues to establish the Army in the forefront of technology and material advancement.

Investment Required			**940**
Return on Investment Ratio	**77.97**	**Percent**	**7797%**
Net Present Value of Costs and Benefits/Savings	**623,513**	**696,807**	**73,294**

A Future Year	B Baseline Costs	C Baseline Benefits/Savings	D New System Costs	E New System Benefits/Savings	F Present Value of Costs	G Present Value of Savings	H Total Present Value
1	132,000		145,000		135,517	123,367	-12,150
2	132,000		145,000		126,643	115,289	-11,354
3	132,000		145,000		118,364	107,752	-10,612
4	132,000		145,000		110,621	100,703	-9,918
5	132,000		145,000		103,385	94,116	-9,269
6	132,000		43,500	101,500	28,984	155,581	126,597

Figure 151: ROI calculation for low solar loading pigments.

4.3 Life Cycle Changes

In general, the non-chromate and ZVOC coatings developed are expected to achieve comparable service life relative to existing coatings systems. In some cases, like the low solar loading pigments used in CARC, we expect to increase the life cycle of these coatings, reducing the requirement for re-painting. On the other hand, non-chromate pretreatments and primers may have reduced performance in the field. Dem/Val efforts are currently underway to determine the life-cycle and performance of non-chrome primers and pretreatments for NAVAIR.

4.4 Life Cycle Analysis Conclusions

Although some non-chromate and ZVOC coating systems may have reduced life cycle or slightly increased costs, the results show that most coatings systems should have similar cost and life cycle relative to current coatings systems. In fact, some coatings will likely have reduced cost due to longer lifetimes.

5 Conclusions

Alternatives to hexavalent chromium-based coatings systems must be developed to reduce environmental and worker exposure to Cr(VI). The VOC content in military coatings systems must also be reduced to make the next generation of environmentally friendly coatings systems.

The trivalent chromium process (TCP), and to a lesser degree the non-chromium process (CFP) are the leading candidates to replace hexavalent chromium pretreatments in the military. Variants of TCP and CFP were tested and the results have shown that newer variants have improved performance. TCP has been used effectively on steel surfaces as a pretreatment.

Experiments have analyzed the elemental composition of the deposited TCP and CFP pretreatments. These have determined that Cr, Zn, and other metals are deposited onto the surface.

Various pretreatment solutions and pretreated panels were rigorously tested for the presence of Cr(VI). Alodine 1200S and 1600S had considerable contents of Cr(VI). On the other hand, no Cr(VI) was detected in TCP pretreatment solutions. Very low concentrations of Cr(VI) were detected on TCP coatings on aluminum, but were likely due to oxidation of Cr within the aluminum substrate.

Non-chromated primers have worked well with TCP and CFP pretreatments, although they were slightly inferior to the hexavalent chromium pretreatments. Ultra low VOC primers have had lower performance relative to higher VOC primers. Zero VOC powder coats have been very successful in reducing corrosion; however powder coats with cure temperatures low enough for aviation substrate applications as yet have not exhibited the same level of performance. As such, ARL is currently preparing a military specification for CARC primer powder coats. Yet powder coats must be baked at elevated temperatures before they can be used, limiting their usefulness for DoD applications.

Polymeric bead flattening agents are being incorporated into MIL-DTL-53039. This will increase the UV stability and mar resistance of these coatings, thus improving sustainability. A zero VOC one-component system was evaluated, but had poor UV stability. Zero VOC powder topcoats failed to meet gloss requirements. Potentially higher-performance partially fluorinated

topcoats have been prepared through the addition of fluorinated polyols and fluorinated hyperbranched polymers. These coatings have passed all military specification testing done so far.

Zero VOC chemical agent resistant topcoats have been formulated successfully using a novel polyol and isopheronediisocyanate. Properties of these formulations are excellent and similar to the current CARC topcoats. Low solar loading pigments have been effectively used to develop CARC topcoats with improved weathering. Small amounts of fluorinated polyols can be added to topcoats to largely affect the surface chemistry with little effect on bulk coating properties, but have detrimental effects on weathering properties.

Decreasing the isocyanate to hydroxyl indexing in polyurethanes increased the permeability of these coatings to water and chemical agent simulants, and decreased the cross-link density. Thus, it is unlikely that decreasing the indexing will be beneficial regarding chemical agent resistance.

Environmental analysis indicates that TCP pretreatments, class N primers, zero VOC primers, and zero VOC topcoats will reduce the negative impact of military coatings on the environment. Economic analysis shows that the new coatings will be competitive with current coatings systems. In fact, high performance pigments would actually reduce the cost of these coatings.

Overall, the program has been successful at both identifying critical DoD environmental needs and developing practical solutions to these requirements for reducing VOC emissions and hexavalent chromium content from military coatings systems. Future work must still be done to further demonstrate/validate these new coatings systems and make them widely applicable to DoD weapons platforms.

References

1. *Federal Register*, Vol. 69, No. 191, Oct. 10, 2004, Proposed Rules.

2. *Report to Congressional Committees*, GAO (General Accounting Office), Defense Management, Opportunities to Reduce Corrosion Costs and Increase Readiness, GAO-03-753, July 2003.

3. EPA ID # 2060-AM84

4. SERDP/ESTCP Metal Finishing Workshop Summary, SERDP/ESTCP, Washington, D.C., May 22-23, 2006.

5. Yushan Yan, "Zeolite Coating System for Corrosion Control to Eliminate Hexavalent Chromium for DoD Applications," SERDP PP-1342, 2004 Annual Report.

6. W. van Ooij, D. Scaheffer, G. Pan, T. Mugada, Y. Wang, "Superprimer: Chromate Free Coating System for DoD Applications," SERDP PP-1341, 2004 Annual Report

7. Paul C. Wynn, Craig V. Bishop, "Replacing Hexavalent Chromium in Passivations on Zinc Plated Parts," PF Online, November, 2005.

8. C.V. Bishop, Galvanotechnik, **71**, 1199 (1980).

9. U.S. Department of Commerce.,, Agency of Toxic Substances and Disease Registry Atlanta, PB93-182434 app., 1993.

10. D.J. Weinmann, K. Dangayach, C. Smith, "Amine-Functional Curatives for Low Temperature Cure Epoxy Coatings, *Resolution Performance Products tech paper SC:2357-01*, 2001 (www.resins.com).

11. R.W. Katz, "Low Volatile Organic (VOC) Chemical Agent Resistant Coating (CARC)," Final Report, SERDP PP-1056, April 2000.

12. J. Duncan, "Demonstration/Validation of Low Volatile Organic Compound (VOC) Chemical Agent Resistant Coating (CARC)," Final Report, ESTCP 200024, November 2003.

13. Zhang, X. M. *Yejin Fenxi*. **2001**, *21,* 67.

14 Methods for Chemical Analysis of Water and Wastes, EPA-600/4-82-055, December 1982, Methods 218.4 and 218.5.

15. The Chemistry of Polyurethane Coatings: A General Reference Manual. Bayer MaterialScience, 2006 http://www.bayermaterialscienceNAFTA.com.

16. Lumiflon: Fluoropolymer for Coating, AGC, Chemicals, Charlotte, NC, 2004.

17. ASTM D 882-02 Standard Test Method for Tensile Properties of Thin Plastic Sheeting.

18. E. Napadensky, Y.A. Elabd; Breathability and Selectivity of Selected Materials for Protective Clothing; ARL-TR-3235; July 2004.

19. D.B. Murphy, R. Oldfield, S. Schwartz, M.W. Davidson; "Phase Contrast Microscopy", 2004. http://www.microscopyu.com/articles/phasecontrast/phasemicroscopy.htm

20. General Motors Corporation. "Accelerated Corrosion Test" GM9540P, December 1997.Apparatus (Fluorescent UV-Condensation Type) for Exposure of Nonmetallic Materials." ASTM G 53, January 1996.

21. R.G. Buchheit, et. al, "Active Corrosion Protection and Corrosion Sensing in Chromate-Free Organic Coatings", Progress in Organic Coatings, 47 (2003), 174-182.

22. H. L. Archer, Jr, « Hexavalent Chromate Alternative for Propellant and Cartridge Actuated Devices », E213K-015-07, October 2007.

23. http://webbook.nist.gov/cgi/

24. Adriano Bigotto*, Barbara Pergolese, Journal of Raman Spectroscopy, 2001, 32.

25. Kikuchi, S.; Kawauchi, K.; Kurosawa, M.; Honjho, H.;Yagishita, T. Analytical Sciences, 2005, Vol. 21, 197-198.

26. Hughes, A. E.; Gorman, J.; Harvey, T. G.; McCulloch, D.; Toh, S. K. *Surface and Interface Analysis,* **2004**, 36, 1585-1591.

27. Chidambaram, D.; Clayton, C.; Halada, G.; *Electrochimica Acta*, **2006**, *51*, 2862-2871.

28. Zhao, J; Frankel, G; McCreery, R.; *Journal of Electrochemical Society*, **1998**, *145*(7), 2258-2264.

29. Kendig, M.; Jeanjaquet, S.; Addison, R.; Waldrop, J. *Surface and Coatings Technology*, **2001**, *140,* 58-66.

30. Dimitrov, N.; Mann, J.A.; Sieradzki, K. *J. of Electrochemical Society*, **1999**, *146* (1), 98-102.

31. Clark, W.; McCreery, R. *J. of Electrochemical Society*, **2002**, *149* (9), B379-B386.

32. Matzdorf, C. A.; Nickerson, W. C. Jr. Composition and process for preparing protective coatings on aluminum substrates, PCT Int. Appl., WO 2006088521, 2006.

33. Alodine 1200S-Technical Process Bulletin, Henkel, Surface Technologies, **1999**.

34. Clark, W.; McCreery, R. *J. of Electrochemical Society*, **2002**, *149* (9), B379-B386.

35. Pearlstein, F.; Agarwala, V.; Trivalent Chromium Solutions for Sealing Anodized Aluminum, US Patent 5374347, Dec 20 1994.

36. W.E. Kosik, "Mechanisms of Military Coatings Degredation," SERDP PP-1133 Final Report, August, 2003.

37. G. Woods, The ICI Polyurethanes Book, Wiley, New York, 1990.

38. G. Oertel, Polyurethanes Handbook, Hanser, New York, 1985.

39. P.B. Jacobs, P.C. Yu, Journal Coatings Technology 65 (1993).

40. GAO Report to Congressional Committees, Additional Measures to Reduce Corrosion of Prepositioned Military Assets Could Achieve Cost Savings, GAO-04-601, June, 2006.

41. J.A. Orlicki, M.S. Bratcher, W.E. Kosik, C.A. Winston, R.E. Jensen, S.H. McKnight, **"**Characterization of Modified Hyperbranched Polymer Migration and Transport Properties," ARL-TR-3296, 2004.

42. N. Sumi, I. Kimura, M. Ataku, T. Maekawa; "Fluoropolymer Dispersions for Coatings" presented at The Waterborne Symposium, Advances in Sustainable Coating Technologies, New Orleans, LA, U.S.A., Feb. 1, 2008.

43. D. Anton; Advanced Materials, Vol. 10, No. 15, 1998.

44. P. Georlette, J. Simons, L. Costa; *Fire Retardency of Polymeric Materials*, Grand, A. F., Wilkie, C. W., eds., Marcel Dekker, New York, pp. 257-260, 2000.

45. D. M. Crawford and J. A. Escarsega, Thermochimica Acta, 357-358 (2000) 161.

46. S. Manabe, Diffusion in Polymers, P. Neogi, ed., Marcel Dekker, New York, pp. 242-244, 1996.

47. B. Nickerson, Demonstration and Validation of Non-Chromate Aluminum Pretreatments, ESTCP PP-0025.

48. D.H. Rose and C.E. Grethlein, *The Amptiac Quarterly*, **7**, 12-14 (2003)